Sensors for *in vitro* Bone Tissue Engineering Applications

Johan Gustavsson

Doctoral Thesis
Biomedical Engineering Doctoral Programme

Supervised by Dr. Elisabeth Engel

Department of Materials Science and Metallurgy
Universitat Politècnica de Catalunya

Barcelona (Spain)
April 2011

This page is intentionally left blank

Till min morfar och mormor,
till min mor och min bror,
och till Laura.

This page is intentionally left blank

It has been said that I am interested in mountaineering. That's true. The qualities it requires are just those, which I feel we all need today. Perseverance and patience. A firm grip on realities. Careful, but imaginative planning. A clear awareness of the dangers, but also of the fact that faith is what we make it. And that the safest climber is he who never questions his ability to overcome all difficulties.

Dag Hammarskjöld

The wine is awful, the people without temperament, and even the sun radiates no warmth.

Jean Bernadotte, ex-monarch of Sweden

This page is intentionally left blank

Abstract

The field of tissue engineering (TE) aims to understand structure-function relationships in mammalian tissues and from there on develop biological substitutes that can restore, maintain, or improve tissue functions. To progress such efforts, research into fundamental biology should also be complemented with advances in engineering and manufacturing issues. New or improved enabling tools of predictive, producing, performing, and preserving character need to be invented, developed, and implemented. If correctly applied, enabling tools of performing character, such as different sensing and imaging modalities, could contribute to increased temporal and spatial control of the TE environment by providing indirect information on cellular metabolic activity, scaffold performance, and cell-biomaterial interactions. Along that line, this thesis has explored how ion sensors, when applied to standard *in vitro* bone tissue engineering environments, can provide information for both improved understanding and control of cellular and material activities.

First, commercial ion sensors were used to determine the influence of three different osteoblast-like cell models on their ionic extracellular environment (IEE). Rat-derived mesenchymal stem cells (rMSCs) and SAOS-2 cells expressed high or very high alkaline phosphatase (ALP) activity, and as a consequence they influenced the concentration of total inorganic phosphorus (P_i) in culture medium containing β-glycerophosphate. On the contrary, MG63 cells showed extremely low ALP activity and did not indfluence [P_i]. Moreover, cell-induced calcium deposition in the extracellular matrix was observed both in mature SAOS-2 and rMSC layers but not in MG63 layers, and was correlated with decreased concentration of calcium in the culture medium. Fluctuations in the bone tissue engineering IEE, mainly with respect to P_i, Ca^{2+}, and pH may therefore be indicative of specific osteoblastic activity.

Second, the nature of ion reactivity of calcium-deficient hydroxyapatite (CDHA), a scaffold candidate material for bone tissue engineering, was systematically investigated by exposing it during different time periods to standard culture media of different chemical composition. Traditional sorption models were used to describe experimental data, revealing for example significant sorption of calcium onto CDHA as well as acidification of the culture media. Slight variations in the chemical composition of culture medium were observed to provoke different ion reactivity with respect to total phosphorus (P_i). It was further shown that ion reactivity of CDHA was a function of material maturity as certain ion replacement processes were allowed to occur

during prolonged contact times. Taken altogether, evaluation of ionic concentrations of culture medium exposed to CDHA contributed to improved understanding of the underlying mechanisms of ion reactivity of CDHA.

Third, the effects of the dynamic IEE induced by CDHA on cellular behaviour were evaluated by growing osteoblast-like SAOS-2 cells in semi-permeable culture inserts placed in close proximity to CDHA. It was revealed that cells proliferated well and that their alkaline phosphatase activity was modified mainly in time rather than in absolute levels. However, while ALP activity of SAOS-2 cells grown in absence of CDHA easily created conditions for cell-induced calcium deposition in the extracellular matrix, presence of CDHA resulted in competition between cells and material for the calcium and phosphorus. The competition delayed calcium deposition in the cell layers, but as sorption of phosphorus onto CDHA gradually decreased with time, conditions for mineralisation were slowly created for SAOS-2 cells also when grown in presence of CDHA. Obtained results indicate that sorption of phosphorus rather than sorption of calcium was the main limiter for bone mineralisation around CDHA, and should be considered in development of osteogenic biomaterials.

Following above observations that the IEE can be significantly altered by the presence of standard bone tissue engineering components such as cells or scaffold materials, a generic setup for online potentiometric measurements of ionic concentrations and pH was fabricated. Traditional calcium-selective electrodes for measurements in small volumes (easily down to 0.1 mL) were fabricated in house, and were characterised in standard *in vitro* TE conditions. They exhibited a Nernstian response to calcium, and were little influenced by other major extracellular ions. Moreover, the electrodes resisted sterilisation through UV irradiation, did not induce any cytotoxic effects in contact with osteoblasts, and the electrode potential was subject only to minor drift during longer measurements. Ca^{2+}-electrodes were used to successfully monitor sorption of calcium onto calcium-deficient hydroxyapatite immersed in cell culture medium, as well as osteoblast-induced calcium deposition in the extracellular matrix during a time frame of 24 hours. Such proof-of-concept measurements demonstrate the potential of these instruments as enabling tools in TE processes.

Finally, all-solid-state potentiometric microelectrodes based on anodically grown films of iridium oxide were prepared for real-time monitoring of pH in traditionally inaccessible bone tissue engineering environments. In particularly, the great usefulness of these sensor was demonstrated by measuring

pH in the interior of hydrolysing α-tri calcium phosphate (an injectable bone cement), as well as at its immediate interface with extracellular fluid. In both these cases the pH sensors clearly indicated how the material initially provoked a very alkaline environment, which with time became more and more acidic. The absolute pH variation caused by the material was detected to be of such magnitude that it may influence its adjacent biological environment, and should be considered upon drug loading and/or implantation.

Taken altogether, the developed sensor setups (i.e. pH microelectrodes and ion-selective electrodes) are applicable to standard *in vitro* TE environments. Their small size allow to approach local environments previously neglected, and in that way they can contribute to improved temporal and spatial control of the TE environment, and so enhance reproducibility and efficiency of many TE processes.

This page is intentionally left blank

Acknowledgements

I am grateful to **Prof. Josep A. Planell** and **Dr. Elisabeth Engel** for hosting me as member in their research group and for having provided me excellent facilities to carry out this work. In a financial context I would also like to acknowledge support received from **Generalitat de Catalunya** and **IBEC**, as well as from **Fundación F. y M. Pehrzon** and **Exportradet**.

All members of the biomaterials group at UPC and the Bio/Non-bio group at IBEC, as well as former colleauges, have their share in this work. The mentorship initially provided by **Prof. George Altankov** was very important, and it contributed to find appropriate focus on my work. Among many colleagues, **Sergio del Valle**, **Roman Perez**, **Gemma Mestres**, **Pablo Sevilla**, **Edgar Montufar**, and **Dr. Montserrat Espanol** contributed with their experience on biomaterial preparation and characterisation. A special thanks goes to **Marta Pegueroles** for always being very helpful and kind.
A large part of this thesis was acheived thanks to helpful **Dr. Martin Arundell** who introduced me to **Prof. Danny O'Hare** and **Prof. Martyn Boutelle** at Imperial College, London. I appreciate enormously that they let me visit their laboratories where **Dr. Eleni Bitzou** and **Delphine Feuerstein** shared with me their knowledge on pH and ion sensors fabrication. I would also like to acknowledge **Dr. Monica Mir** at IBEC and **Dr. Jordi Colomer** at the Department of Physics (UB) for occasionally borrowing me equipment for electrochemical measurements. Also, **Philipp Schuler** deserves a very special mentioning for assisting me in the development of my own such equipment and for being a good friend.

One great experience gained during the development of this thesis was my participation in the educational program *Recerca a secundaria*. I would especially like to express my admiration for talented **Pablo Ruiz** whose work was very inspiring to take part of.

Family and friends, among them **Tamara** and **Marijn**, and **Simone** and **Lourdes**, helped me to put this work in a more appropriate perspective.

Last, but in principle the first, **Laura Orellana Ramirez** has been the outstandingly most important person behind me in this work. While your values and courage are true sources of inspiration, your faith in my seemingly endless efforts gave me strength when I needed it most.

Contents

Abstract **7**

Acknowledgements **11**

Contents **12**

List of Figures **18**

List of Tables **21**

List of Abbreviations **22**

1 Introduction **25**
1.1 Objective and Outline of the Present Thesis 26
1.2 Tissue Engineering 27
1.2.1 Definition 27
1.2.2 Evolution and Concepts 28
1.2.3 The Components of Tissue Engineering 32
1.2.3.1 Cells and the extracellular matrix 32
1.2.3.2 Biomaterials as scaffolds 34
1.2.3.3 Chemical and physical stimuli 36
1.2.4 Clinical Tissue Engineering - Can It Work? 38
1.2.5 Need For Critical Assessment 40
1.2.6 Enabling Tools for Tissue Engineering 43
1.3 Concluding Remarks 44
Bibliography 45

2 The Role and Use of Sensors for *in vitro* Tissue Engineering Applications **51**
2.1 What to Measure? 52
2.1.1 Relevant Cell Metabolites for TE Monitoring 52
2.1.1.1 Glucose 55

2.1.1.2 Lactate 56
2.1.1.3 Carbon dioxide 57
2.1.1.4 Oxygen 58
2.1.1.5 Glutamine 59
2.1.1.6 Ammonium 60
2.1.1.7 pH 60
2.1.2 Non-catabolic Cellular Events 63
2.1.2.1 The ionic extracellular environment 63
2.1.2.2 Cell death 64
2.1.3 Biomaterials Activity 66
2.2 How to Measure? 68
2.2.1 Where to Measure? 68
2.2.2 Sensors for Tissue Engineering Applications 70
2.2.2.1 Gas sensors 72
2.2.2.2 pH sensors 75
2.2.2.3 Ion sensors 76
2.2.2.4 Towards *in vivo* applications 78
2.3 Conclusions 79
Bibliography 79

3 The Osteoblastic Ionic Extracellular Environment 91
3.1 Introduction 91
3.1.1 Bone Tissue 91
3.1.2 Life of an Osteoblast 94
3.1.3 *In Vitro* Osteoblast-like Model Systems 99
3.1.3.1 Osteogenic medium 100
3.1.3.2 Assesment of *in vitro* mineralisaton 102
3.1.4 The Ionic Extracellular Environment 102
3.2 Objective and Strategy 104
3.3 Materials and Methods 105
3.3.1 Preparation of Osteoblastic Culture Media 105
3.3.2 Measuring Ions in Culture Medium 106
3.3.3 Measuring Total Phosphorus of Culture Medium 107
3.3.4 Ionic Profile of Cell Culture Media 107
3.3.5 Ionic Stability of Cell Culture Medium 108
3.3.6 Cell Sources and Standard Cell Maintenance 108
3.3.7 Osteoblast Cell Cultures 109
3.3.8 Alizarin Red Staining 110
3.3.9 Alkaline Phosphatase Activity 110
3.3.10 Influence of Cell Culture Medium on Osteoblast Activity 111
3.3.11 Cellular Influence on the IEE at Different Total Volumes 112

3.4 Results . . . 113
3.4.1 Ionic Composition of Osteoblastic Culture Media . . . 113
3.4.2 Stability of Cell Culture Medium With Time . . . 117
3.4.3 Ionic Levels of Cell Culture Media During Osteoblast Cultures . . . 119
3.4.4 Calcium Deposition in Extracellular Matrix . . . 128
3.4.5 Ionic signals as function of cell number and media volume 130
3.4.6 Alkaline Phosphatase Activity . . . 132
3.5 Discussion . . . 133
3.5.1 Cell Culture Media Characterisation . . . 133
3.5.2 Calcium Deposition Provoked by Osteoblast Activity . 134
3.5.3 Osteoblastic Activity Observed Through the Ionic Extracellular Environment . . . 135
3.5.4 Biological Significance of Cell-induced Calcium Deposition . . . 137
3.6 Conclusions . . . 138
Bibliography . . . 139

4 Ion Reactivity of Calcium- deficient Hydroxyapatite 147
4.1 Introduction . . . 147
4.1.1 In Search for the Ideal Bone Graft Material . . . 147
4.1.2 Calcium Phosphate Based Bone-graft Substitutes . . . 151
4.1.2.1 Calcium phosphate ceramics . . . 151
4.1.2.2 Calcium phosphate cements . . . 152
4.1.3 Bioactivity and Ionic Interactions . . . 154
4.2 Objective and Strategy . . . 155
4.3 Materials and Methods . . . 156
4.3.1 Fabrication of α-TCP powder . . . 156
4.3.2 Hydrolysis of α-TCP . . . 156
4.3.3 Cell culture media preparations . . . 158
4.3.4 Ion Exchange Processes between CDHA and Cell Culture Media . . . 158
4.3.5 Scanning Electron Microscopy . . . 160
4.3.6 Spectroscopic Analysis . . . 160
4.3.7 Statistics . . . 161
4.4 Results . . . 162
4.4.1 Cell Culture Medium Characterisation . . . 162
4.4.2 Short-term Ion Exchange Processes . . . 162
4.4.2.1 Pseudo-first-order kinetics . . . 163
4.4.2.2 Pseudo-second-order kinetics . . . 163
4.4.2.3 pH . . . 164

4.4.2.4 Sodium and potassium . . . 166
4.4.2.5 Calcium and phosphorus . . . 167
4.4.3 Long-term Ion Exchange Processes . . . 171
4.4.3.1 pH . . . 171
4.4.3.2 Sodium and potassium . . . 173
4.4.3.3 Calcium and phosphorus . . . 174
4.4.4 Surface Analysis . . . 176
4.5 Discussion . . . 178
4.5.1 Ionic Interaction Mechanisms . . . 178
4.5.1.1 Short-term kinetics . . . 179
4.5.1.2 Long-term kinetics . . . 182
4.6 Conclusions . . . 185
Bibliography . . . 185

5 Cellular Response to the Dynamic Ionic Environment Induced by Calcium-deficient Hydroxyapatite 191
5.1 Introduction . . . 191
5.1.1 Ionically Reactive CaP Compounds and its Possible Influnce on Osteoblast Behaviour . . . 191
5.2 Objectives . . . 193
5.3 Materials and Methods . . . 194
5.3.1 Calcium-deficient hydroxyapatite . . . 194
5.3.2 Cell Culture . . . 194
5.3.2.1 Cell culture media . . . 194
5.3.2.2 Cell seeding and handling . . . 195
5.3.3 Ion Measurements of Cell Culture Media . . . 196
5.3.3.1 Long-term measurements . . . 196
5.3.3.2 Short-term measurements . . . 196
5.3.4 Cell Proliferation . . . 196
5.3.5 Alkaline Phosphatase Activity and Total Protein . . . 197
5.3.6 Extracellular Calcium Deposition . . . 197
5.3.7 Statistics . . . 198
5.4 Results . . . 199
5.4.1 Cell Culture Media . . . 199
5.4.2 The Extracellular Ionic Environment . . . 199
5.4.2.1 Long-term experiments . . . 200
5.4.2.2 Short-term experiments . . . 201
5.4.3 Cell Proliferation . . . 209
5.4.4 Alkaline Phosphatase Activity and Total Protein . . . 210
5.4.5 Extracellular Calcium Deposition . . . 213
5.5 Discussion . . . 219

5.5.1 The Ionic Extracellular Environment 219
5.5.2 Cellular Response 221
5.6 Conclusions 224
Bibliography 224

6 Fabrication, Characterisation, and Application of Ion Sensors in Bone Tissue Engineering 229
6.1 Introduction 229
6.1.1 Potentiometric Ion Sensors 229
6.1.1.1 Ions in solution 231
6.1.1.2 Electrodes of first and second kind 233
6.1.2 Ion Selective Electrodes 235
6.1.2.1 Electrode bodies 235
6.1.2.2 Ion selective membranes 236
6.1.2.3 Response mechanism 238
6.1.2.4 Sensor characterisation 240
6.2 Objectives 242
6.3 Materials and Methods 243
6.3.1 Potentiometric Instrumentation 243
6.3.1.1 Hardware 243
6.3.1.2 Software 244
6.3.2 Ag/AgCl Reference Electrode 246
6.3.3 Calcium Selective Electrodes 249
6.3.3.1 ISE characterisation 251
6.3.4 Sensor Applications 252
6.3.4.1 Cl^--activity during α-TCP-hydrolysis 252
6.3.4.2 Ca^{2+}-activity of CDHA in cell culture medium 253
6.3.4.3 Ca^{2+}-activity during osteoblast mineralisation 253
6.4 Results 255
6.4.1 Potentiometric Instrumentation 255
6.4.2 Ag/AgCl Reference Electrode 255
6.4.3 Calcium Selective Electrode Characterisation 260
6.4.3.1 Standard characterisation 260
6.4.3.2 ISE characterisation in complex solutions . . 263
6.4.4 Sensor Applications 266
6.4.4.1 Cl^--activity during α-TCP-hydrolysis 266
6.4.4.2 Ca^{2+}-activity of CDHA in cell culture medium 267
6.4.4.3 Ca^{2+}-activity during osteoblast mineralisation 268
6.5 Discussion 273
6.5.1 On the Design of the Sensor Platform 273
6.5.2 Calcium selective electrodes 275

6.5.3 Sensors Applications . . . 276
6.5.3.1 Cl^--activity during setting of α-TCP . . . 276
6.5.3.2 Ca^{2+}-sensor . . . 277
6.6 Conclusions . . . 278
Bibliography . . . 278

7 pH Microelectrodes Applied in Bone Tissue Engineering 283
7.1 Introduction . . . 283
7.1.1 pH Detection . . . 283
7.1.2 Metal-Metal Oxide Electrodes . . . 284
7.1.2.1 Iridium oxide pH electrodes . . . 285
7.1.2.2 Microelectrodes . . . 286
7.2 Objectives . . . 286
7.3 Materials and Methods . . . 287
7.3.1 Solid-state Microelectrode Body . . . 287
7.3.2 Iridium Oxide Deposition . . . 288
7.3.3 pH Electrode Characterisation . . . 289
7.3.4 Sensor Applications . . . 289
7.4 Results . . . 291
7.4.1 Microelectrode Characterisation . . . 291
7.4.2 Iridium Oxide Deposition . . . 292
7.4.3 pH Electrode Characterisation . . . 293
7.4.4 Sensor Applications . . . 294
7.5 Discussion . . . 297
7.6 Conclusions . . . 300
Bibliography . . . 300

8 Conclusions and Future Work 303
8.1 Conclusions . . . 303
8.1.1 The Cells (Chapter 3) . . . 303
8.1.2 The Scaffold Material (Chapter 4) . . . 305
8.1.3 Cells and Scaffold Combined (Chapter 5) . . . 306
8.1.4 Ion Sensors for Online Monitoring (Chapter 6) . . . 308
8.1.5 Sensors for Local Measurements (Chapter 7) . . . 309
8.2 Perspectives . . . 310
8.3 Future Work . . . 311
Bibliography . . . 314

List of Figures

1.1 Outline of the present thesis 26
1.2 Concepts of tissue engineering 29
1.3 An illustrative proof of concept 30
1.4 Bioreactors 37
1.5 Prometheus, the symbol of TE 39

2.1 Schematic representation of the metabolic pathways 54
2.2 Intracellular potassium ion release 65
2.3 Sensing locations 69
2.4 The local and global TE microenvironments 70
2.5 Concept of chemical sensors 72
2.6 Oxygen sensors for TE applications 74
2.7 pH sensors for TE applications 76

3.1 Bone tissue 93
3.2 Osteoblastic cell functions with time 94
3.3 Fundamental requirements for mineralisation 96
3.4 Lineage potential of mesenchymal stem cells 99
3.5 Calcium distribution in serum 103
3.6 Experimental osteoblast cell culture model system 109
3.7 Colourimetric method for determination of total phosphorus . 114
3.8 Calibration curve for absorbance of inorganic phosphorus . . . 114
3.9 Ion concentration of osteoblastic cell culture media 115
3.10 Ionic stability of cell culture medium 118
3.11 Osteoblast morpholgy 120
3.12 The ionic extracellular environment of osteoblast cultures . . . 123
3.13 Quantitative calcium deposition in extracellular matrix 128
3.14 Early calcium deposition in extracellular matrix 129
3.15 Late calcium deposition in extracellular matrix 130
3.16 Calcium depostion using non-corresponding medium 131
3.17 Estimation of the osteoblastic influence on the ionic extracellular environment 131

3.18 Alkaline phosphatase activity 132

4.1 Bone tissue engineering 150
4.2 Calcium phosphate cement 153
4.3 Theoretical scheme on α-TCP hydrolysis 153
4.4 Fabrication steps of α-TCP and CDHA 157
4.5 Medium compositions 158
4.6 Scheme: experimental layor 159
4.7 Calculation of regression coefficient 161
4.8 Short-term CDHA/Culture Medium Interactions 165
4.9 Alternative view on Ca^{2+}-sorption 168
4.10 Kinetics of hydrolysis of β-GP 169
4.11 Ca/P sorption ratio 171
4.12 Long-term CDHA/culture medium interactions 172
4.13 Release kinetics of phosphorus from CDHA into DMEM . . . 175
4.14 SEM micrographs of CDHA exposed to cell culture medium . 176
4.15 FTIR of CDHA exposed to cell culture medium 177
4.16 Summary of CDHA ionic interactions with cell culture medium 179

5.1 Experimental setup to study the chemical influence of CDHA on cellular response 194
5.2 Medium compositions 195
5.3 Experiment layour 198
5.4 Ion concentration of osteoblastic cell culture media, 21 days . 203
5.5 Ion concentration of osteoblastic cell culture media, 48 hours . 206
5.6 Cell proliferation 209
5.7 Total protein 211
5.8 Alkaline phosphatase activity 212
5.9 Calcium depostion during long-term cell culture 214
5.10 Quantitative evaluation of calcium depostion 218

6.1 The potentiometric principle 230
6.2 Walther Hermann Nernst 231
6.3 Traditional ISE designs 236
6.4 The phase boundary potential 239
6.5 Interpretation of experimental ISE response 240
6.6 Experimental potentiometric setup 243
6.7 LabView flowcharts 245
6.8 Ag/AgCl reference electrode designs 247
6.9 Setup for deposition of AgCl 248
6.10 Calcium selective membrane components 249

6.11 Calcium selective electrode design 250
6.12 Setup for measuring Cl^- activity during setting of α-TCP . . 252
6.13 Setups for measuring Ca^{2+} in bone TE applications 254
6.14 User interface of sensor software 256
6.15 Micrographs of Ag/AgCl reference electrode 257
6.16 Potential response of Ag/AgCl electrode 258
6.17 Ag/AgCl electrode calibration curve 258
6.18 Stability of Ag/AgCl electrode 259
6.19 Calcium selective electrode: potential response 261
6.20 Calcium selective electrode: response time 261
6.21 Calcium selective electrode: selectivity 262
6.22 Calcium selective electrode: stability 262
6.23 Calcium selective electrode: UV sterilisation 264
6.24 Calcium selective electrode: drift 264
6.25 Calcium selective electrode: biofouling 265
6.26 Calcium selective electrode: cytotoxicity 265
6.27 Calcium selective electrode: cell proliferation 266
6.28 Cl^--activity during hydrolysis of α-TCP 267
6.29 Real-time Ca^{2+}-activity of culture medium exposed to CDHA 268
6.30 Calcium uptake by cells grown in DMEM with 3 mM β-GP . . 269
6.31 Calcium deposition in SAOS-2 cultures 270
6.32 Real-time monitoring of cellular influence on Ca^{2+}-activity . . 271
6.33 Aspect and viability of cells exposed to Ca^{2+}-sensors 272

7.1 Schematic view of pH microelectrode body 287
7.2 Setups for pH measurement of curing α-TCP and set CDHA . 290
7.3 Voltammograms of Au microelectrodes 291
7.4 IrO_2-deposition on Au microelectrodes 292
7.5 SEM of IrO_2 microelectrodes 293
7.6 Open-circuit potential response of IrO_2 electrodes. 294
7.7 Interior pH measurement during curing of α-TCP 295
7.8 Exterior pH measurement during curing of α-TCP 296
7.9 Exterior pH measurement of CDHA in cell culture medium . . 296
7.10 Calibration of IrO_2 electrodes in cell culture medium 297

8.1 Cell cultures directly onto CDHA 314
8.2 Setup for measurements in local environments 314
8.3 Local microenvironments around CDHA 315

List of Tables

1.1 The development of tissue engineering. 31
1.2 Scaffold materials commonly used in tissue engineering 36
1.3 Strategic priorities in TE. 42

2.1 Glutaminolysis 59
2.2 Cell metabolites for TE monitoring 61
2.3 Metabolic rates in mammalian cell cultures 62
2.4 Intra- and extracellular ionic levels 63
2.5 Performing enabling tools 71

3.1 The main components of bone tissue 98
3.2 Standard osteoblast culture models 100
3.3 Standard composition of osteogenic medium 101
3.4 Inorganic salts content of cell culture media 105
3.5 Cell culture medium formulations. 106
3.6 Characteristics of ion selective electrodes 107
3.7 Ionic levels of complete media used for cell cultures 119

4.1 Bone-graft substitutes 149
4.2 Heating protocol to obtain α-TCP. 156
4.3 Ion levels of fresh cell culture medium 162
4.4 Sorbate model data 170

5.1 Extinction coefficients of alamarBlue 197
5.2 Ionic levels of cell culture media 199
5.3 Total Protein, statistics 211
5.4 Alkaline phosphatase activity, statistics 212

6.1 Ion electrodes of first and second kind categories 235
6.2 Conductive polymers applied to solid-state ISEs 236
6.3 Traditional ion-selective membrane components 238
6.4 Calcium selective membrane composition 249
6.5 Sensitivity and stability of Ag/AgCl electrode 259

List of Abbreviations

Abbreviation	Details
AA	Ascorbic acid
aDMEM	advanced Dulbecco's Modified Eagle Medium
AIROF	Anodic iridium oxididation film
ARS	Alizarin red S
β-GP	β-glycerophosphate
CDHA	Calcium-deficient hydroxyapatite
CPC	Calcium phosphate cement
DAQ	Data aquisition
Dex	Dexamethasone
DMEM	Dulbecco's Modified Eagle Medium
ECM	Extracellular matrix
EGTA	Ethylene glycol-bis(2-aminoethylether)-N-N-N'-N'-tetraacetic acid
EMF	Electromotive force
FBS	Foetal bovine serum
FTIR	Fourier transform infrared
I	Ionic strength
IEE	Ionic extracellular environment
ISE	Ion selective electrode
ISFET	Ion selective field effect transistor
McCoy	McCoy's 5A medium modified
MMO	Metal-metal oxide
og	Osteogenic
P_i	Total inorganic phosphorus
PBS	Phosphate buffered saline
PEG	Poly(ethylene glycol)
rMSC	Rat-derived mesenchymal stem cell
SBF	Simulated body fluid
SEM	Scanning electron microscope
TCP	Tricalcium phosphate
TE	Tissue engineering

This page is intentionally left blank

This page is intentionally left blank

Chapter 1

Introduction

'If engineering is the making of things useful to the human race, then tissue engineering is the making of tissues useful in some way to us'. (Curtis & Riehle, 2001)

It has been estimated that one of five people reaching the age of 65 will benefit from some kind of tissue replacement therapy during their remaining life span (Vunjak-Novakovic & Kaplan, 2006). While these patients suffer or die every year waiting for a suitable transplant, medical doctors are facing two main problems: (1) limited availability of donors, and (2) counterproductive immunological reactions induced by allogenic transplants. To reduce the shortage of available organs, and to be able to custom-make transplants for patients, a new field of research called *tissue engineering* (TE) has emerged during the last decades.

The concept of replacing or regenerating lost tissue with personalised tissue grown *in vitro* has until recently only been possible in science fictional stories. However, the growing clinical need for "spare parts" to damaged or diseased tissue, in combination with the scientific challenges contained within it have recruited scientists from various disciplines such as medicine, biology, chemistry, materials science, and engineering, to produce revolutionary products for the full spectrum of biotechnology; from early diagnostic testing to advanced stages of therapy. The human value of these products has turned TE into a high impact life science discipline, and the efforts made so far have made it possible to launch on the health care market commercial products such as artificial skin, bladders, and cartilage. However, in the shadaw of its progress, the field of tissue engineering has also suffered many failures during its development, and should still today be considered a field in its infancy in need for improvements in all its aspects.

1.1 Objective and Outline of the Present Thesis

The ambition of this thesis was to explore how *sensors* can serve as *enabling tools* in tissue engineering, and how they can contribute to better understanding and increased efficiency of its processes. Particular focus is on bone tissue engineering and ion electrodes.

The content has been divided into eight chapters (Figure 1.1). The first two chapters are literature-oriented, while the following five ones cover the experimental part of the thesis. The final chapter is devoted to general conlusions and outlook for future advances.

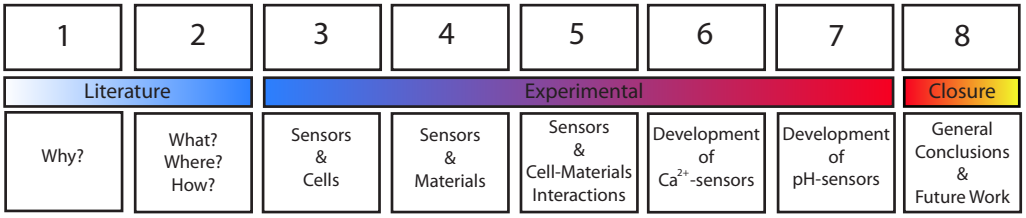

Figure 1.1: The outline of the present thesis.

The introductory chapter discusses the principles of tissue engineering from a conceptional point of view, as well as its evolution as a field of science. The objective is to identify its major challenges as well as to highlight the benefits of an appropriate use of enabling tools in TE processes.

The second chapter then reviews in detail how enabling tools of *performing* character can be used in TE. For this purpose it is initially discussed how the TE environment is influenced by its different components, and based on that discussion it is summarised the most relevant process parameters that may be obtained from this environment. The chapter finishes with a summary of the most interesting techniques for detection and monitoring of such parameters.

The following three chapters (3-5) are of experimental character, and they all concern aspects of bone tissue engineering. First it is investigated how osteoblast-like cells influence the extracellular ionic environment during growth and differentiation (Chapter 3). The same methods and principles are then used to study how a certain bioactive scaffold candidate, *calcium-deficient hydroxyapatite* (CDHA), influences the same ionic extracellular environment (Chapter 4). Following the results from Chapter 3 and Chapter 4, cells and materials are then combined to study the ionic effects of CDHA on osteoblast growth and function (Chapter 5).

The following two chapters (6-7) are devoted to the development of potentiometric sensors for real-time measurements of ions in the TE environment. It is described the development of an electronic setup for potentiometric measurements, as well as the fabrication and characterization of a biocompatible calcium-selective electrode (Chapter 6) and miniaturised pH sensor (Chapter 7). Both chapters contain experimental data obtained from the developed sensors when applied to specific bone tissue engineering environments.

1.2 Tissue Engineering

Considering the development of an embryo, *i.e.* the transformation from a single cell into a fetus with separate organs interconnected via the nervous system, reminds us that a single cell has to first aquire, and then process, information on how to organize itself into complex structures. The necessary information for such processes is contained both within the cell itself and in the extracellular environment. The importance of the extracellular environment for directing morphogenesis of cells into tissues is undisputed, but still far from understood (see for example Cowin (2000) and Nelson & Bissell (2006) for discussions on this topic).

Tissue formation can therefore be considered a process that involves complex interplays of cells, extracellular matrix, and signaling factors in both time and space. For tissue formation to proceed correctly, cells have developed refined methods for aquisition, interpretation, and processing of both biochemical and biophysical signals of different variety. Thus, in order to synthesize or regenerate tissue, it is not only required molecular and genetic tools for cell-cell communication issues, but also tools that create an appropriate extracellular environment that gives structure and allows for cells to process the information contained in its composition. This was the starting point for the pioneers of tissue engineering, and so it continue to be still today.

1.2.1 Definition

The invention of the term *tissue engineering* was recently discussed in an editorial by Lysaght & Crager (2009). According to them, the first documented use of the expression was a press release issued in 1982 by two American medical firms. It was however not until a couple of years later that the term appeared for the first time in a scientific paper (Wolter & Meyer, 1984). The topic of that paper was related to the effects of long-term implantation of Teflon knee protheses, and it contained the following paragraph:

"Nature impresses us with a great variety of reactive possibilities in the adaptation of its tissues to new conditions and substances. Sound progress in medicine is easiest when we work along with the physiological currents of beneficial reaction and adaptation. To understand the direction and the limits of nature's reactions is always the first step toward progress in ***tissue engineering****."*

Although not a scientific milestone itself, the paper by Wolter & Meyer correctly highlighted the need for dynamic adaptive tissue replacements. That was also what would become the direction and the comprehensive strategy of tissue engineering, which a few years later, was defined by Skalak *et al.* (1988) as:

"The application of principles and methods of engineering and life sciences toward fundamental understanding of structure-function relationships in normal and pathological mammalian tissues and the development of biological substitutes to restore, maintain, or improve tissue functions."

Even though above definition is not unambiguously agreed on and applied by everyone working in the field of TE, it benefits from its clear emphasis on the overall goal of TE, namely to **develop biological substitutes that restore, maintain or improve tissue function**. No matter the exact definition, both today and in the very earliest days of TE, it was clear that such an ambitious goal required new ways of thinking, new methods, and a truly interdisciplinary approach.

1.2.2 Evolution and Concepts

The National Science Foundation (NSF, America) considered in a report that the concept, character, and direction of TE had underwent three different phases[1]:

1984-1989: Imagination of the possibility of designing replacement tissue.

1989-1997: Wide-spread use of the term TE in abstracts and titles, referring to work concerning all the main organs closely connected to tissue engineering: bone, cartilage, blood vessels, liver, skin, neurons and also to biomedical materials.

[1]The Emergence of Tissue Engineering as a Research Field,
Available at: `http://www.nsf.gov/pubs/2004/nsf0450/start.htm`

1998-2003: Growth in number of core papers fundamental to tissue engineering.

When analyzing the evolution of the field of TE from the perspective of the private sector, Lysaght *et al.* (2008) explain how things went very wrong between 2001 and 2003. They even refer to this period as the "worst of times" for TE due to failed product launches, disappointing results from clinical trials, and bankruptcies for several leading TE firms. Since then the field has recovered and now it seems even more versatile due to major technological advances. The standard *top-down* approach, in which cells are supposed to populate a pre-fabricated scaffold with adequate geometry and then create an apropriate extracellular matrix and microarchitecture is lately complemented by the reverse *bottom-up* approach, also referred to as modular tissue engineering (Figure 1.2). In the bottom-up approach smaller strucutres are assembled and organised in different ways into larger modules to finally reach the size of the desired tissue (see for example Tysseling-Mattiace *et al.* (2008) and Nichol & Khademhosseini (2009)). Technological advances and improved understanding of biological interactions have also provoked a gradual conceptual change within the field of TE and the current ideology among tissue engineers is that *"rather than attempting to recreate the complexity of living tissues ex vivo, the aim should be to develop synthetic materials that establish key interactions with cells in ways that unlock the body's innate powers of organization and self-repair"* (Place *et al.*, 2009).

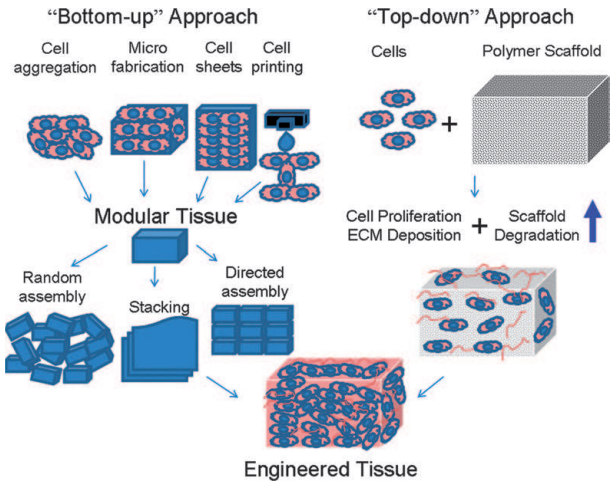

Figure 1.2: The tissue engineering concept can be either of top-down or bottom-up character. Adapted from Nichol & Khademhosseini (2009).

During the period that NSF consider as the third phase of development it also appeard new research branches intimately related to TE. New terms such as *regenerative medicine* and *synthetic biology* were introduced to distinguish and specify different approaches and techniques nowadays used by life scientists dedicated to understand structure, growth, and development of biological tissue. While both regenerative medicine and tissue engineering have the same ultimate objective of providing functional tissue and organs for patients, it is generally accepted that tissue engineering provides a set of tools that can be used to perform regenerative medicine, while regenerative medicine attempts to engage innate physiological processes to rebuild organs through endogenous recruitment or exogenous delivery of appropriate cells, biomolecules, and supporting structure (Andersson & Lendahl, 2009). Synthetic biology, following recent developments in whole-genome sequencing and synthesis, has been defined as the design and construction of new biological parts, devices, and systems, and the redesign of existing, natural biological systems for useful purposes (Sia *et al.*, 2007). While there is significant overlap in these evolving fields, regenerative medicine focus on cure rather than treatment and by permitting *in vivo* regeneration of whole organs and tissues, regenerative medicine will ultimately replace tissue engineering (Ratner & Bryant, 2004). Nevertheless, tissue engineering has to be considered as the first properly organised field of science dedicated to the study of above mentioned topics, and promises to increase our knowledge and understanding of essential working elements of life, and at the same time provide useful biomedical technologies with potential to revolutionize medical implants.

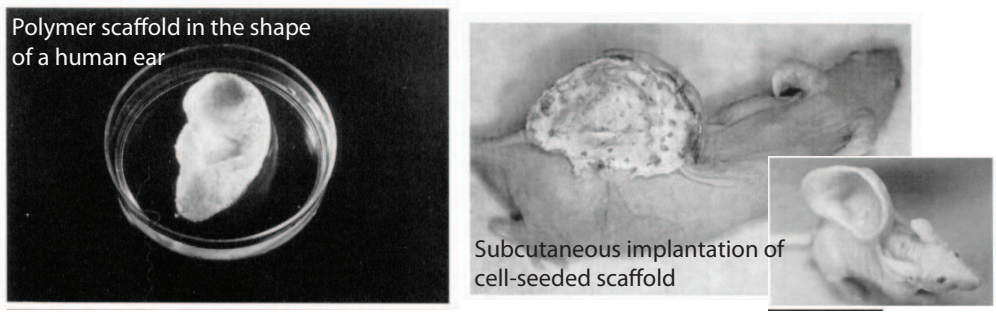

Figure 1.3: An illustrative, but ethically unacceptable, proof of concept of top-down tissue engineering. Adapted from Cao *et al.* (1997).

Year	**Event**	**Reference**
1917	First application of a free tissue graft for bladder replacement	Neuhof (1917)
1930s	Efforts to maintain organs in vitro for use as replacement body parts	Carrel & Lindberg (1938)
1940s	Exceptional treatments for skin regeneration	Sir Archibald McIndoe
1961	The first genetic evidence that stem cell exist	Till & McCulloch see Becker *et al.* (1963)
1967	First transplantation of a live heart into a patient with heart failure	Christiaan Barnard see Cooper (2001)
1968	First bone marrow transplantation	Robert A. Good
1970s	Intention to generate cartilage by culturing chondrocytes on bone fragments and then implantingthe construct in mice	Dr. Green
1970s	Strategies for in vitro reproduction of skin, glandular tissue, and blood vessels	Eugene Bell
1970-1980s	Linking biological response to physico-chemical properties of biomaterial surfaces	Buddy Ratner Jim Anderson Allan Hoffman
1983	Living skins equivalent	Bell *et al.* (1983)
1985, 1987	First attempts to commercialize off-the-shelf TE products	
1985	The word Tissue Engineering appears for the first time in the scientific literature	see Lysaght & Crager (2009)
1993	The concept of TE is presented to a broad scientific community: 3D polymer scaffolds	Langer & Vacanti (1993)
1997	Successful regeneration of cartilage by mouse subcutaneous implantation of synthetic biodegradable scaffolds seeded with chondrocytes	Cao *et al.* (1997)
1998	FDA approves Apligraf, first allogenic TE product	
2000s	Use of nanotechnology and self-assembly to create artificial extracellular matrix components	Stupp *et al.* (1997)
2000s	Focus on smart biomaterials	
2000s	Increased efforts in regenerative medicine	

Table 1.1: Some important events and trends during the development of the field of tissue engineering.

1.2.3 The Components of Tissue Engineering

Repair and regeneration of tissue is a multi-level process of physical, chemical, biological, and engineering character. The minimal set of material required are the appropriate types of cell, but it is also common to use non-living substrata that can provide structure for tissue development. Also, drugs to induce cellular activity as well as bioreactors that control the cellular microenvironments, facilitate mass transport to the cells, and that provide the necessary biochemical and biophysical signals are commonly applied in tissue engineering (Radisic *et al.*, 2008). These four components, (1) *cells and extracellular matrix*, (2) *biomaterials*, (3) *drugs*, and (4) *bioreactors*, are interdependent as each component and its intrinsic parameters have to be choosen based on the other components. Therefore it is important to understand the role of each one of them.

1.2.3.1 Cells and the extracellular matrix

Being the architect of tissue, cells are the functional and fundamental elements of tissue science. They can be recruited from the patient itself (autologous) or be supplied from an external source (allogenic, or xenogenic if comes from a different species). In a few cases, controling cells is all that may be needed for a successful TE application, but the complete understanding of the process by which cells self-assemble into tissue and organs still remains as the main challenge for the TE field. Although specific functional properties of cells vary from tissue to tissue, tissue engineers heavily rely on cells capability to *proliferate*, *differentiate*, *migrate*, and *communicate*.

The proliferative capacity of cells, *i.e.* when one cell divides into two daughter cells, is controlled by the extracellular environment and the state of cell differentiation. With other words, there are no single genes or molecular switches that control cellular proliferation, but this process is rather controlled by interactions with several extracellular regulatory molecules. These extracellular factors include stimulatory and inhibitory cytokines, the extracellular matrix (ECM) or substratum which cells make contact to, as well as the type and degree of proximity of neighboring cells. Very often, these same factors are also important regulators of differentiation (Oshima & Campisi, 1991).

The understanding of cell functions means understanding of cell-cell and cell-ECM communication mechanisms (Rosso *et al.*, 2004). While cell-cell interactions largely happens through transmembrane glycoproteins (cadherins),

cell-ECM interactions happen either via receptor-mediated signaling or via mobilization of growth or differentiation factors from the ECM. The ECM, which is composed of a great variety of molecules (*e.g.*, proteins, glycosamineoglycans, proteoglycans, and adhesive glycoproteins) provides structure, localization, and guidance for cells. Many of the ECM molecules also play critical roles during development and postnatal tissue repair as they bind to receptors in the cell membrane to induce cytoskeletal deformations that activate second-messenger systems that can alter gene expression, adhesion, migration, proliferation, growth and cell death. Thus, much of the secret to control tissue formation under controlled laboratory conditions relies on providing conditions for creation of an ECM that can send appropriate signals to cells.

The field of tissue engineering reclaims much of its potential to stem cells (Bianco & Robey, 2001), which are cells that can (1) self-renew, and (2) given the appropriate physical and chemical signals be induced to differentiate into one or more committed descendants, including fully functional mature cells (L.Weissman *et al.*, 2001). Since long time it has been known that skin, other epithelia, and the bone marrow host stem cell populations that persist throughout life, but except these locations it was believed that most stem cells die out during tissue development. However, during the last ten years it has been demonstrated that many tissues of the adult body actually continue to host stem cells (Verfaillie, 2002), and that it therefore exist sources of cells with considerable potential for differentiation and multiplication, which makes stem cells an ideal candidate for use in tissue and regenerative medicine.

Based on its origin one distinguishes between *embryonic* and *adult* stem cells, which have different capacity for self-renewal and differentiation. Embryonic cells are obtained from the inner cell mass of early embryons or the blastocyst, and they are able to proliferate in long-term cultures while maintaining capacity to form almost any cell type, and as such they are referred to as *totipotent* or *pluripotent* stem cells.

On the other hand, stem cells obtained from adult tissues are more accesible than embryonic stem cells, but they can also be more difficult to expand in culture, and they are usually also more limited in their differentiation capacity only giving rise to a few specific cell types. The most common source of adult stem cells is the bone marrow which contains two types of stem cells: *hematopoietic* and *mesenchymal* cells. While hematopoietic cells are committed to differentiate only into mature blood cells, stromal mesenchymal stem cells have the ability to differentiate into a variety of adult mesenchymal tissues such as bone, cartilage, adipose, and muscle cells both *in vivo*

and *in vitro*. This plasticity renders mesenchymal stem cells potential for use in several clinical treatments.

Despite the advantage of using intrinsic stem cells for tissue repair, there still exist many fundamental biological and engineering challenges, as well as ethical concerns, that must be overcome before clinical use (Weissman, 2000). It has to be aquicerd knowledge on how to control the microenvironment and signalling pathways leading to efficient differentiation and self-renewal of stem cells. It also has to be resolved how to perform *in vivo* delivery and integration to the host milieu. And finally there is the critical question whether one will be able to grow large enough populations from a patient rapidly enough when needed.

1.2.3.2 Biomaterials as scaffolds

When damaged tissue is to be repaired (either *in situ* or *ex vivo*) it is of greatest concern that the structure and biological function of native extracellular matrix and environment is mimicked as much as possible both in terms of chemical composition and physical properties. Since initially the volume of cells and intercellular material is likely to be considerably less than that of the mature tissue, a supporting substrate that provides temporary mechanical properties will in general be necessary. Such non-living structural device, that on one hand is supposed to define the geometry of the replacement tissue, and on the other hand provide environmental cues to promote tissue regeneration, is referred to as the *scaffold*. At a minimum, the ideal scaffold for engineered tissue should (see for example Hutmacher (2001); Chen & Boccaccini (2008)):

- posses adequate mechanical properties,
- posses interconnecting pores of appropriate scale to favour supply of nutrition, cellular infiltration, tissue integration, vascularization, as well as removal of cellular waste products,
- be made from material with controlled biodegradability or bioresorbability, so that the scaffold is replaced in such a way and at such a rate that the mechanical strength of the tissue remains constant,
- have appropriate surface chemistry for cellular attachment, differentiation and proliferation,
- be easily handled and fabricated into a variety of shapes and sizes.

In addition one obviously anticipates proper *biocompatibility* of the scaffold material itself, *i.e.* that the material does not exert a toxic effect on its environment, nor provoke any immunological or foreign body reaction (Williams, 2008). To ensure this issue, the scaffold is made from *biomaterials* that provide stable interactions with biological systems. The TE concept has gradually shifted focus of biomaterials research to extend from rigid prostheses to nowadays include materials that fulfill more than only one action. Nevertheless, the research activity and knowledge obtained from many decades of biomaterials development (*e.g.*, hip implants, knee replacements, intraocular lenses, cardiovascular implants, etc) is of greatest importance also in tissue engineering, and it contributes to deeper understanding of how materials interact with the body on a cellular and molecular level. Therefore, the need for standard biomaterials can be well envisioned throughout at least this century (Ratner & Bryant, 2004).

There is no such biomaterial that is capable of meeting with all criteria necessary for successful application towards engineering many tissues. Rather, the choice of biomaterial(s) to fabricate the scaffold depends on the particular type of tissue it will help to regenerate. In order to meet with the spatial and temporal constraints imposed by growing tissue, scaffold materials with tuned physico-chemical properties and biomimicking architectures have been developed to provide cells with the appropriate physical, chemical, and biological cues. The main materials studied and used can be divided into two main categories: *synthetic* or *natural* materials. Further classifications can be based on whether the material is organic or inorganic, inert or bioactive, durable or subject to remodeling, etc. Engineering solutions have been offered to obtain composite materials that can provide a wide array of properties in which the cellular niche can be tailored to guide tissue development. Table 1.2 provides a brief summary of some common materials used to produce scaffolds for different kinds of tissue (also see Hubbell (1995)).

POLYMERS
poly(lactic acid), poly(glycolic acid), poly(lactic acid-co-glycolic acid), poly(caprolactone) poly(urethane)
NATURAL MATERIALS
Collagen, elastin, silk, chitosan, alginate
HYDROGELS
poly(HEMA), poly(ethylene glycol), gelatin, agar, fibrin
CERAMICS
Calcium phosphate, hydroxyapatite, bioglass, corals
COMPOSITES
Polymer/bioglass
FABRICS
Gore-Tex

Table 1.2: Main classes and some examples of scaffold biomaterials used in tissue engineering.

1.2.3.3 Chemical and physical stimuli

The environment where cells and scaffold are brought together to produce functional tissue is subject to many external parameters with significant importance for proper tissue development. Since tissue organisation is a process known to depend on adequate biomechanical and biochemical signalling in both space and time (Wang & Thampatty, 2006), it is necessary to provide cells with an appropriate physicochemical environment. This becomes especially evident when translating the biological models of two dimensional cell cultures into three dimensions. While traditional 2D-cell cultures rely on simple diffusion of gases and molecules for nutrient supply and metabolic activity, bigger and more complex tissue structures will require more sophisticated and efficient routes for supply and removal of metabolites. Considering that the distance between cells and blood capillaries ranges from 20 to 200 μm *in vivo*, distances which are largely overriden *in vitro*, together with the poor diffusion capacity and solubility of oxygen in aqueous solutions, hypoxia becomes one of the main limiting factors to obtain 3D cultures *in vitro* (Volkmer *et al.*, 2008).

One of the technical means to partly overcome such obstacles and to provide suitable physicochemical environments is the use of *bioreactors*, which are devices where biochemical processes can develop under closely monitored

and tightly controlled conditions. Bioreactors are nowadays considered a fundamental component in the *ex vivo* tissue growth process, as it provides dynamics to the cell culture. In short, bioreactors have had three main applications in TE (Butler *et al.*, 2000):

- Improving seeding efficiency and cell distribution of 3D scaffolds by convection or perfusion of the cell suspension.
- Enhancing tissue quality throughout the full scaffold geometry by reducing negative concentration gradients within the construct through improved supply of nutrient and oxygen.
- Applying defined regimes of physical forces to yield construct with regulated and improved strength and/or functionality.

To meet with these purposes different bioreactor designs have been developed (Bilodeau & Mantovani, 2006), among which can be distinguished perfusion systems, rotating systems, and systems for mechanical loading (Figure 1.4). It is also possible to combine two or more systems.

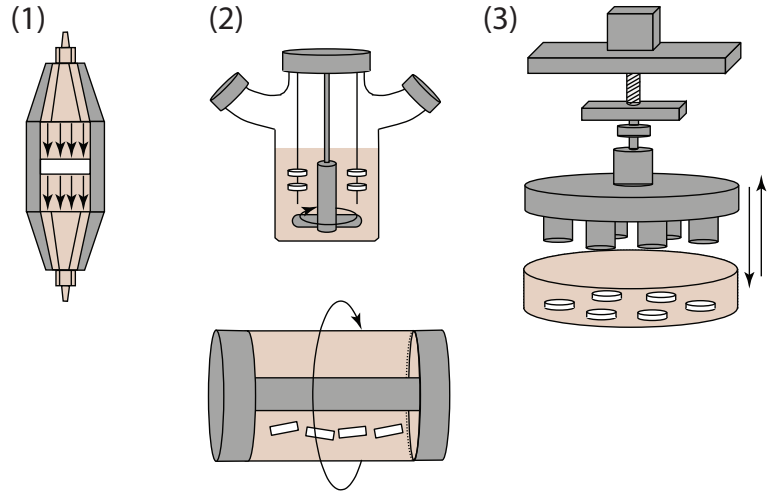

Figure 1.4: Different types of bioreactors; (1) perfusion systems, (2) rotating systems, (3) systems for mechanical loading. Adapted from Martin *et al.* (2004).

Perfusion systems allow cell culture medium to flow directly through a porous scaffold, and is used to both seed and maintain cell cultures in a 3D environment. The perfusion of medium is mainly supposed to avoid diffusional limitations and to help maintain cell viability and homogeneity

throughout the whole construct, and not only in the periphery which often happens during static cultures. Obviously, the effects of direct perfusion is dependent on medium flow-rate and the maturation stage of the constructs. Therefore, optimizing a perfusion bioreactor for the engineering of 3D tissues must address a careful balance between the mass transfer of nutrients and waste products to and from cells, as well as the retention of newly synthesised extracellular matrix components within the constructs (Martin *et al.*, 2004). Also it has to be taken into account the fluid-induced shear stresses within the scaffold pores, and that the fluid flows along paths of least resistance and therefore do not solve the problem of heterogenity in tissue outcoumes (Lovett *et al.*, 2009). Typically, and compared to static cultures, direct perfusion enhance growth, differentiation, and matrix production (e.g. Fassina *et al.* (2005)).

As bioreactor designs continue to improve, and as one learns more on how mechanical forces can translate into biological response, bioreactors will not only provide improved physicochemical conditions for tissue development, but will also significantly contribute to make the TE process more reliable and to produce reproducable outcomes with decreased contamination risks (Martin *et al.*, 2009).

1.2.4 Clinical Tissue Engineering - Can It Work?

The capacity to auto-regenerate severely damaged tissue has been described for a few species, for example newt and zebra fish, but is absent or suppressed in almost all human organs. One well-known exception is the human liver which indeed regenerates even after significant loss or injury (Ankoma-Sey, 1999), and which was described already in the classical drama *Prometheus* (Wolfson, 2006). Prometheus, a titan in Greek mythology, was punished for bringing the powers of the Gods to the people, and for this he had his liver torn out by an eagle (Figure 1.5). When regenerated, the liver was repeatedly torn out again by the eagle. Mythological stories apart, and until it is revealed if the body possesses unleashed innate powers to regenerate other tissues than the liver, clinicians will basically have to rely on TE approaches.

It is not until recently that tissue engineered products actually has turned into an alternative in clinical situations. Place *et al.* (2009) recently summarised the products commercially available, and this revealed a dominance in areas of skin, bone, and cartilage regeneration but the clinical basis extends beyond these common tissues. Below two particular cases illustrate how the top-down TE approach has been successfully implemented in clinical situations.

Figure 1.5: The sculpture *Prometeo Engadenat* by Josep Campeny i Santamaria is exposed in Igualada, Catalonia. It represents the story of how Prometheus has his liver eaten by an eagle.

Example 1: A tissue-engineered bladder
Using a top-down TE approach, Atala *et al.* (2006) successfully treated young patients suffering from end stage bladder disease. The aim was to decrease intravesical pressure and improve bladder compliance and continence, and for this purpose surgeons obtained autologous urothelial and muscle cells from bladder biopsies (1-2 cm^2) from each patient. The cells were cultivated and expanded during several weeks to obtain large quantities that could be seeded on a biodegradable scaffold made from polyglycolic acid and collagen. The scaffolds had been designed specifically for each patient using templates based on CT scans. The initial size of the scaffold was 70-150 cm^2, with a total thickness of about 2 mm, and it was seeded with about 7×10^8 cells of each type. First the smooth muscle cells were seeded on the exterior of the scaffold, then a couple of days later the urothelial cells were seeded on the interior part. The seeded construct was then incubated for about four days before wrapped with omentum, which is commonly used in reconstructive surgery to enhance vascularization thanks to its rich blood supply, before implanted in the patients.

The patients were followed up during a period of several years, and it was generally observed that the TE construct improved bladder function. The engineered bladder did not only show an adequate structural architecture and phenotype, it also reduced the leak point pressure. Neither was observed any negative metabolic consequences nor urinary calculi formation. The bowel function returned rapidly after implantation.

Example 2: A tissue-engineered allograft airway
A young woman suffering from severe difficulties to breathe due to an obstructed airway caused by prolonged tuberculosis was treated by Macchiarini *et al.* (2008) using a tissue-engineered human trachea. In detail, a 7 cm tracheal segment was obtained from a 51-year-old female who had died of cerebal haemorrhage. The trachea was subsequently decellularised during a period of six weeks, before the graft was inserted in a bioreactor. A biopsy from the patient was done to isolate chondrocytes and epithelial cells respectively. The outside of the scaffold was seeded with chondrocytes while the interior was lined with epithelial cells as the construct rotated around its own longitudinal axis in the bioreactor. The total period of bioreactor culture was 96 hours, and the adherence to the matrix was estimated to be near 100%. The bioreactor phase was then followed by implantation.
The patient recovered rapidly after operation. Lung-function tests done two months after implantation were all within normal range, and the patient has been able to return to normal life. Follow-up measurements interestingly showed a healthy, adjacent microvascular bed suggesting proper vascularization.

1.2.5 Need For Critical Assessment

Expectation on the field of TE has been huge from both the public and private sector of healthcare. The business sector entered the field in an early stage, attracted by the potential market for TE products. For example, it has been estimated that the demand for tissue engineering as a consequence of loss and/or failure of tissues will account for as much as half of all medical-related problems in the United States, and taking into account that by 2040 as much as 25% of the US GDP is expected to be related to healthcare, translating this technology into clinical use is associated with enormous financial reward (Boehrs *et al.*, 2008). But so far TE therapies have far from achieved the commercial goals, and the majority of launched TE products is related to acellular products where the regenerative response is due to either the biomaterial itself or the delivery of bioactive agents from biomaterials. The question to ask therefore is, *why have the expectations not been lived up to yet?*

One has to understand that the tissue engineering treatment is an entity that spans widely separate phases such as cell recovery and manipulation to grafting. Although a great deal of new knowledge has been accumulated, and even some new therapies and treatments have been brought into practice, it is obvious that the field is still in its infancy with major limitations. Undoubtedly, a main problem is the limited mass transfer into the newly cre-

ated tissue. While most cells in our body are in close vicinity of capillaries that supplies oxygen and nutrients, all engineered tissue of today lack instant blood supply, and therefore engineered structures remain very primitive in relation to what is required. There exist a variety of strategies to circumvent the problem of vascularization (Lovett *et al.*, 2009), but even if successful, still will remain the sub-sequent problem of integration to the host vascular system *in vivo*.

To achieve clinical success, continued interdisciplinary efforts are required, and alliences between industry and academia need to continue to promote innovative, cost-effective, and high quality research (Pangarkar & Hutmacher, 2003). Organisations with the purpose to unite tissue engineers play important roles by providing community platforms and as well as strategic directions. One such organisation, MATES-IWG[2] which includes representatives from several American agencies (FDA, NIH, NASA, NSF, etc), published in 2007 a strategic plan[3] for investments in tissue science and engineering that identified four overreaching goals that needs to be developed for clinical success to be reached:

1. **Understanding and controlling the cellular response**. How do cells receive and respond to information from their local environment in establishing and maintaining tissues?

2. **Formulating biomaterial scaffolds and the tissue matrix environment**. To better understand the biology underlying the relationship between scaffold properties and cell fate.

3. **Developing enabling tools**. Complex, multiparametric inputs are required to assess the state of a tissue and the cells within it. This information will be supplied by improvements in high-throughput assays and instrumentation, imaging modalities, fabrication technologies, computational modeling, and bioinformatics. Additionally, tissue preservation technologies and bioreactors will facilitate the generation of tissues of demand.

4. **Promoting scale-up, translation, and commercialization**. Establishing protocols and instruments that contribute to increase reproducibility, robustness, and user-friendliness that can enable broad distribution of products.

[2]Multi-Agency Tissue Engineering Society Interagency Working Group
[3]Available at `http://www.tissueengineering.gov/welcome-s.htm`

In parallel to the MATES-IWG plan, Johnson *et al.* (2007) assessed the field's strategic directions by interviewing 24 key international leaders in tissue engineering, to determine the best path towards the goal of clinical success by year 2021. This study confirms that the international community is thinking along a similar line as the MATES group does, and that there is a demand for better insight into basic mechanisms in order to obtain good strategies for control of more complex processes. In Table 1.3 are listed the strategies/priorities proposed by the MATES report on one hand, and Johnson *et al.* (2007) on the other hand.

Although a great deal of work has yet to be done before for example angiogenic systems can be created, or stem cells can be differentiated into a desirable outcome in space and time, or that all of our scale-up needs are reached, one can fortunately find comfort in that developments in any area of TE are likely to positively impact the field as a whole.

Priority	**MATES-IWG**	**Johnson *et al.* (2007)**
1	Understanding the cellular machinery	Angiogenic control
2	Identifying and validating biomarkers and assays	Stem cell science
3	Advancing imaging technologies	Molecular biology / systems biology
4	Defining cellenvironment interactions	Cell sourcing and characterization
5	Establishing computational modeling systems	Clinical understanding
6	Assembling and maintaining complex tissue	Immunological understanding and control
7	Improving tissue preservation and storage	Manufacturing / scale up
8	Facilitating effective applications development and commercialization	Regulatory transparency
9	-	Standardised models
10	-	Enhanced biomaterial functionality
11	-	Multidisciplinary understanding
12	-	Expectation management
13	-	Pharmacoeconomic/commercial pathway
14	-	Multilevel funding

Table 1.3: Strategic priorities in TE

1.2.6 Enabling Tools for Tissue Engineering

Obtaining more viable commercial TE products will not only require improved understanding, handling, and manipulation of the biological part, but will also require improvement of the engineering and manufacturing issues releated to the fabrication process. This standpoint is explicitly stressed in the MATES-IWG report which recommends further development of different *enabling tools* for assessment of the state of tissue and the cells within it, as well as tools for improved preservation of produced tissue. Also the survey presented by Johnson *et al.* (2007) attach great importance to new methods that can handle the manufacturing and scale-up issues for TE products.

To get a clearer overview on how and where such enabling tools might play important roles in the TE process, Pancrazio *et al.* (2007) divided them in four different classes: (1) *predictive*, (2) *productive*, (3) *performing*, and (4) *preserving* tools.

Predictive tools are supposed to answer key questions regarding cell, tissue, and ultimately organ behaviour using *a priori* data. The main purpose is to correctly manage and interpret data, to convert it into accurate models that can be used to simulate behaviour in complex three-dimensional environments. One of the key enabling features of predictive computational methods in TE is to do testing of new constructs and scaffolds and to develop strategies to identify optimal therapy for individual patients (Semple *et al.*, 2005). Improved predictive tools will be based on more efficient algorithms, better computational frameworks, and access to experimental data for validation of rules underlying the models. Advances in this area also include development of instruments that allow access to huge data streams, such as multiarrays to study cellular interactions with other molecules, or even with material topographies to predict certain cell-material interactions (van Blitterswijk *et al.*, 2008).

Among the productive tools are the bioreactors (Section 1.2.3.3) as well as different technologies to precisely fabricate scaffolds. Such fabrication tools include 3D rapid prototyping, 3D printing, and micro- and/or nanotechnologies, such as self-assembly and lithography, to imprint scaffolds with appropriate topography and surface chemistry.

To be able to assess the state of developing tissue without damaging it will require non-invasive performing tools. Such tools will not only increase the control and permit adjustment of the growth process by providing information on performance of key parameters, but will also contribute positively on the cost and time-efficiency of the full process by reducing the need for additional controls. Key parameters of interest are commonly related to

biochemical cellular processes (metabolic activity), but could also be cell number and potency, or many other physical and chemical properties of the cell culture environment. To obtain such information, two main classes of performing tools can be identified: *imaging* and *sensing modalities*. These will be discussed more in detail in Chapter 2.

Finally, there are the preserving tools, supposed to maintain fabricated tissue in a ready-to-use state whenever needed. Once again, sensors could be considered such an enabling tool monitoring storage conditions. Otherwise, the preserving tools are generally considered to be biochemical processes such as cryopreservation using different preserving agents, or dry storage technologies.

1.3 Concluding Remarks

From this introductory chapter it follows that tissue engineering is a field of research that resides at the interface of life and physical sciences. So far it has offered promising approaches towards its goal of creating biological custom-made replacement tissue which not only would decrease the need of available and compatible donors, but also could serve as reliable model systems, providing insight into relationships in normal and pathological conditions, and with possible commercial applications in for example drug screening.

The collective efforts of investigators from various disciplines have clarified several aspects of the complex process of induced organ regeneration, and many of the principles required to achieve the goal are known and already applicable for simpler tissues such as skin and cartilage. The number of commercial products and firms grow at a slow but steady pace. Still the TE field is in its infancy and is decades away from creating more complex structures such as kidney, liver, heart, or pancreas tissues. A number of issues and challenges in all the various aspects have to be solved before the full potential of TE is realised.

First and foremost, researchers need to continue to learn about interactions and the interdependence between cells and extracellular matrix, as well as the role of other environmental parameters of physical and chemical character in space and time. This is a present process at full speed which is further accelerated by invention of new biotechnological means, improved methods for data handling and interpreation, and discoveries of new biological pathways. Deeper understanding and insights into basic mechanisms will lead to more accurate strategies of control, which will then lead to desired new therapies.

Among the most cruical technical challenges related to sustainable TE

processes are the issues concerning cell sourcing, vascularization, and smart scaffolding. While the considerable development of stem cell biology presents huge potential for using human-originated adult or embryonic stem cells as sources for *in vitro* generation of tissues, the other two issues will partly depend on further development of enabling tools. Therefore, to progress and to continue develop the field of TE, research into fundamental biology has to be complemented with advances in engineering and manufacturing issues. New or improved enabling tools of predictive, producing, performing, and preserving character need to be invented, developed, and implemented. As part of such effort, this thesis aims to explore how sensors can be applied in tissue engineering in general, and in bone tissue engineering in particular.

Bibliography

Andersson, E. & Lendahl, U. (2009). *Journal of Internal Medicine,* **266** (4), 303–310.

Ankoma-Sey, V. (1999). *News in Physiological Sciences,* **14**, 149–155.

Atala, A., Bauer, S. B., Soker, S., Yoo, J. J., & Retik, A. B. (2006). *The Lancet,* **367**, 1241–1246.

Becker, A., McCulloch, E., & Till, J. (1963). *Nature,* **197**, 452–454.

Bell, E., Sher, S., Hull, B., Merrill, C., Rosen, S., Chamson, A., Asselineau, D., Dubertret, L., Coulomb, B., Lapiere, C., Nusgens, B., & Neveux, Y. (1983). *Science,* **81**, S2–S10.

Bianco, P. & Robey, P. G. (2001). *Nature,* **414**, 118–121.

Bilodeau, K. & Mantovani, D. (2006). *Tissue Engineering,* **12** (8), 2367–2383.

Boehrs, J., Zaharias, R. S., Laffoon, J., Ko, Y. J., & Schneider, G. B. (2008). *Journal of Prosthodontics,* **17**, 517521.

Butler, D. L., Goldstein, S. A., & Guilak, F. (2000). *Journal of Biomechanical Engineering,* **122**, 570–575.

Cao, Y., Vacanti, J. P., Paige, K. T., Upton, J. M., & Vacanti, C. A. (1997). *Plastic and Reconstructive Surgery,* **100** (2), 297–302.

Carrel, A. & Lindberg, C. (1938). *The Culture of Organs.* Medical Book Department of Harper & Brothers.

Chen, Q.-Z. & Boccaccini, A. R. (2008). In: *Encyclopedia of Biomaterials and Biomedical engineering*, (Wnek, G. E. & l. Bowlin, G., eds) pp. 142–151. Informa Healthcare.

Cooper, D. (2001). *The Journal of Heart and Lung Transplantation,* **20** (6), 599–610.

Cowin, S. C. (2000). *Journal of Biomechanical Engineering,* **122**, 553–569.

Curtis, A. & Riehle, M. (2001). *Phys. Med. Biol.* **46**, R47–R65.

Fassina, L., Visai, L., L.Asti, Benazzo, F., Speziale, P., Tanzi, M., & Magenes, G. (2005). *Tissue Engineering,* **11** (5/6), 685–699.

Hubbell, J. A. (1995). *Biotechnology,* **13**, 565–576.

Hutmacher, D. W. (2001). *Journal of Biomaterials Science, Polymer Edition,* **12** (1), 107–123.

Johnson, P. C., Mikos, A. G., Fisher, J. P., & Jansen, J. A. (2007). *Tissue Engineering,* **13** (12), 2827–2837.

Langer, R. & Vacanti, J. P. (1993). *Science,* **260** (5110), 920–926.

Lovett, M., Lee, K., Edwards, A., & Kaplan, D. (2009). *Tissue Engineering Part B: Reviews,* **15** (3), 353–370.

L.Weissman, I., Anderson, D. J., & Gage, F. (2001). *Annual Review of Cell and Developmental Biology,* **17**, 387–403.

Lysaght, M. J. & Crager, J. (2009). *Tissue Engineering Part A,* **15** (7), 1449–1450.

Lysaght, M. J., Jaklenec, A., & Deweerd, E. (2008). *Tissue Engineering: Part A,* **14** (2), 305–315.

Macchiarini, P., Jungebluth, P., Go, T., Ansnaghi, M. A., Rees, L. E., Cogan, T. A., Dodson, A., Martorell, J., Bellini, S., Parnigotto, P. P., Dickinson, S. C., Hollander, A. P., Mantero, S., Conconi, M. T., & Birchall, M. A. (2008). *The Lancet,* **372**, 2023–2030.

Martin, I., Smith, T., & Wendt, D. (2009). *TRENDS in Biotechnology,* **27** (9), 495–502.

Martin, I., Wendt, D., & Heberer, M. (2004). *TRENDS in Biotechnology,* **22** (2), 80–86.

Nelson, C. M. & Bissell, M. J. (2006). *Annual Review of Cell and Developmental Biology,* **22**, 287–309.

Neuhof, H. (1917). *Surgery, Gynecology and Obstetrics,* **25**, 383.

Nichol, J. W. & Khademhosseini, A. (2009). *Soft Matter,* **5**, 1312–1319.

Oshima, J. & Campisi, J. (1991). *Journal of Dairy Science,* **74**, 2778–2787.

Pancrazio, J. J., Wang, F., & Kelley, C. A. (2007). *Biosensors and Bioelectronics,* **22**, 2803–2811.

Pangarkar, N. & Hutmacher, D. W. (2003). *Tissue Engineering,* **9** (6), 1313–1322.

Place, E. S., Evans, N. D., & Stevens, M. M. (2009). *Nature Materials,* **8**, 457–470.

Radisic, M., Marsano, A., Maidhof, R., Wang, Y., & Vunjak-Novakovic, G. (2008). *Nature Protocols,* **3** (4), 719–736.

Ratner, B. D. & Bryant, S. J. (2004). *Annual Review of Biomedical Engineering,* **6**, 41–75.

Rosso, F., Giordano, A., Barbarisi, M., & Barbarisi, A. (2004). *Journal of Cellular Physiology,* **199**, 174–180.

Semple, J. L., Woolridge, N., & Lumsden, C. J. (2005). *Tissue Engineering,* **11**, 341–356.

Sia, S. K., Gilette, B. M., & Yang, G. J. (2007). *Birth Defects Research (Part C),* **81**, 354–361.

Skalak, R., Fox, C., & Fung, B. (1988). *Tissue Engineering* chapter Preface, p. 1. Alan R. Liss, Inc.

Stupp, S., LeBonheur, V., Walker, K., Li, L., Huggins, K., Keser, M., & Amstutz, A. (1997). *Science,* , **276**, 384–389.

Tysseling-Mattiace, V. M., Sahni, V., Niece, K. L., Birch, D., Czeisler, C., Fehlings, M. G., Stupp, S. I., & Kessler, J. A. (2008). *The Journal of Neuroscience,* , **28** (14), 3814–3823.

van Blitterswijk, C., Stamatialis, D., Unandhar, H., Papenburg, B., Rouwkema, J., Truckenmuller, R., van Apeldoorn, A., Wessling, M., & de Boer, J. (2008). *Tissue Engineering Part A,* , **14** (5), 796.

Verfaillie, C. M. (2002). *Trends in Cell Biology,* , **12** (11), 502–508.

Volkmer, E., Drosse, I., Otto, S., Stangelmayer, A., Stengele, M., Kallukalam, B. C., Mutschler, W., & Schieker, M. (2008). *Tissue Engineering,* , **14** (8), 1331–1340.

Vunjak-Novakovic, G. & Kaplan, D. L. (2006). *Tissue Engineering,* , **12** (12), 3261–3263.

Wang, J.-C. & Thampatty, B. (2006). *Biomechanics and Modelling in Mechanobiology,* , **5**, 1–16.

Weissman, I. L. (2000). *Science,* , **287**, 1442–1446.

Williams, D. F. (2008). *Biomaterials,* , **29**, 2941–2953.

Wolfson, W. (2006). *Chemistry & Biology,* , **13**, 233–234.

Wolter, J. & Meyer, R. (1984). *Transactions of the American Ophtalmological Society,* , **82**, 187.

This page is intentionally left blank

Chapter 2

The Role and Use of Sensors for *in vitro* Tissue Engineering Applications

'Much of the information is not missing, just not used'
(Vunjak-Novakovic & Kaplan, 2006)

One of the keys for future clinical success in tissue engineering (TE) will be the production of consistent and reproducible cell-based products of high quality and high yield. To accomplish such products, the production process needs to be extremely precise and preferably adjusted continuously to the changing demands imposed by the developing tissue. As of today, the general TE process is still essentially manual, which often leads to sub-optimal productivity. Therefore, development and application of performing enabling tools, for example different *sensing modalities*, that provide quantitative information on product fate, is highly acknowledged.

Performing enabling tools can be beneficial to the TE process in two ways. First, since tissue growth/regeneration evolves with time, any TE application would benefit from real-time monitoring. In that way, important parameters such as growth and different bioreactions can be controlled, just as well as early indications of catastrophic events, such as contamination or cessation of growth, can be obtained. Second, performing enabling tools could provide information from TE environments crucial for proper tissue development but which are normally inaccessible for standard measuring technologies. With other words, properly designed and applied performing enabling tools could contribute with both *spatial* and *temporal* information on many TE processes that until today have been overlooked, or even impossible to obtain.

2.1 What to Measure?

The tissue engineering environment is complex by nature, and complexity increases since each type of tissue requires its specific environment for adequate development and function.

The standard *in vitro* TE environment is composed of cells and scaffold materials usually contained in some kind of bioreactor. Each of these standard components (i.e., cells, materials, bioreactor) can by themselves influence the environment they reside in. For example, cellular activity influences total biomass, consumption of nutrients, and production of bioproducts (matrix); scaffold materials are often designed to be either biodegradable or bioactive, resulting in changing material composition with time; bioreactors are commonly used to establish a stable environment (e.g., temperature and gas levels) but they can also induce changes in flow rates, mechanical stresses, or chemical gradients. It is therefore of greatest importance to know the activity of each of these standard components to be able to predict possible synergistic or agonistic effects that may be induced when different TE components are combined in one and the same environment.

In the following sections it is discussed how activity of cells (Section 2.1.1-2.1.2) and materials (Section 2.1.3) may influence the final *in vitro* TE environment. Basically this environment is an aqueous solution containing all the essential molecules for proper cell function. It is often designed to mimick the *in vivo* biological environment with respect to parameters such as osmolarity, pH, gas levels, vitamin, amino acid and protein content. Between these parameters and any standard TE component may arise reactions that can be directly and/or indirectly indicative of specific TE events, and that could be advantageously measured by correctly applied performing enabling tools. However, monitoring a specific parameter should be considered worthwhile only if that parameter (1) has importance for the TE construct development, (2) is produced/consumed at such amount that the initial concentration is significantly changed, and (3) that the rate of activity is neither too fast nor too slow to be detected.

2.1.1 Relevant Cell Metabolites for TE Monitoring

Cellular metabolic activity drives the conversion of energy stored in carbon-containing fuels to *adenosine triphosphate* (ATP), which is a versatile source of chemical energy that can be used for production of complex molecules needed for construction, restoration, and maintenance of tissues and organs within the body. In presence of oxygen, cells derive their ATP mainly through cellular respiration (2.1):

$$C_6H_{12}O_6(aq) + 6O_2(g) \rightarrow 6CO_2(g) + 6H_2O(l) + 36ATP \quad (2.1)$$

The cellular respiration oxidises glucose into carbon dioxide, and releases free energy stored as ATP. But what appears as a straight-forward and efficient energy-transfer (2880 kJ per mole of glucose is obtained) involves an intricate series of chemical transformations before the full amount of ATP is harnessed:

1. *Glycolysis*, an anaerobic process which mainly transfers the chemical energy of glucose into pyruvate, but also creates a small amount of ATP (see Section 2.1.1.1).

2. *Pyruvate oxidation*, which converts glycolytic pyruvate into acetyl-CoA (see Section 2.1.1.3).

3. *Citric acid cycle*, which converts acetyl-CoA into CO_2, with the creation of additional ATP (see Section 2.1.1.3).

4. *Respiratory chain*, where finally the energy stored in different transfer molecules is harvested and large amount of ATP is created, and which the cells can use for anabolic reactions (see Section 2.1.1.4).

Each of above sub-reactions influences, and is influenced by, the instantaneous composition of both the intra- and extracellular environment, and therefore also the TE environment. In addition to above reactions, there also exist alternative or complementary metabolic routes for cells to produce energy. One of these pathways is *fermentation* which is anaerobic production of ATP following the glycolytic pathway (see Section 2.1.1.2). Another is the *glutaminolytic* pathway which can contribute with moderate levels of ATP derived from glutamine (see Section 2.1.1.5-2.1.1.6). All these main metabolic pathways are discussed below, and they are also schematically illustrated in Figure 2.1.

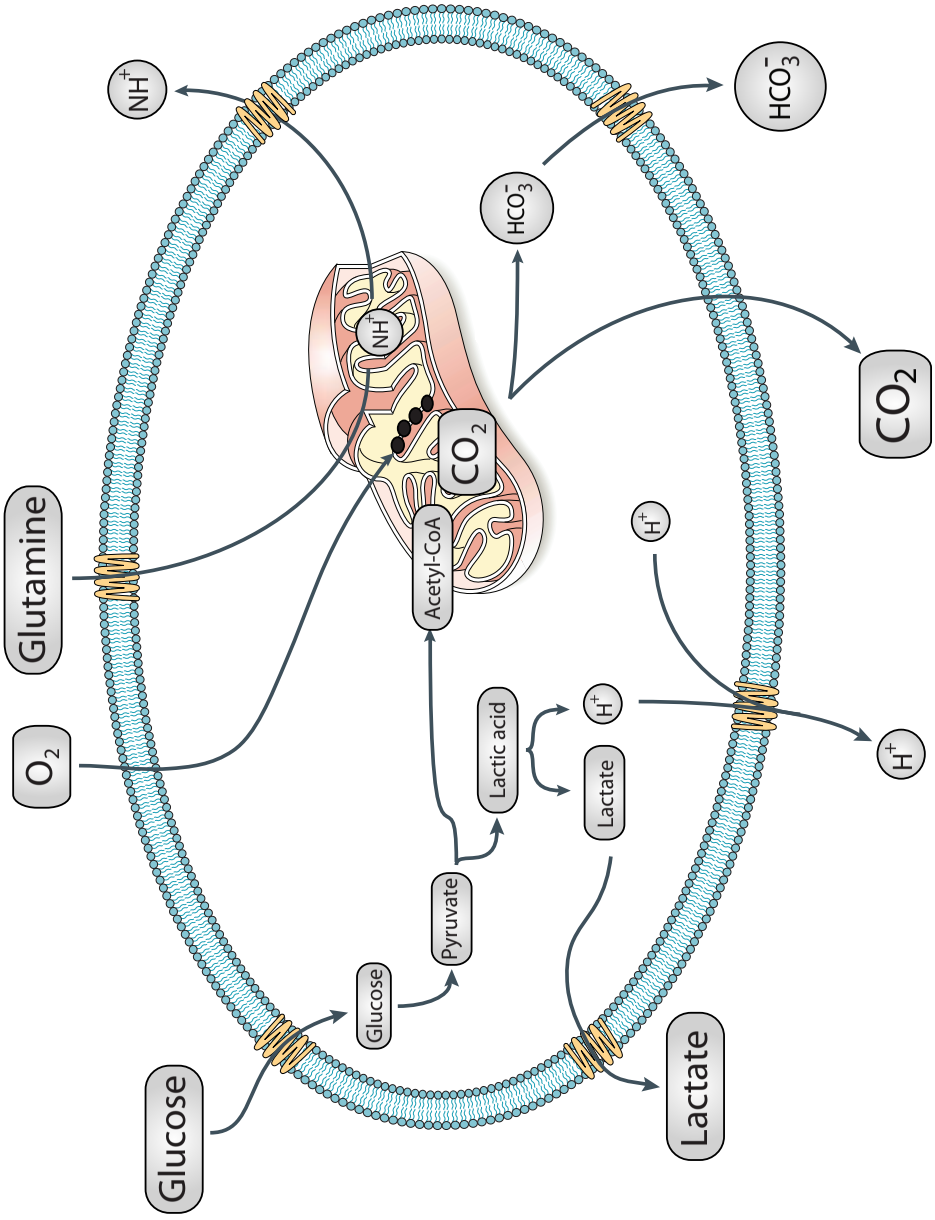

Figure 2.1: Schematic representation of the main metabolic pathways in mammalian cells.

2.1.1.1 Glucose

Glucose serves the metabolic demands for survival, growth, proliferation and function in most mammalian cells. After entering the cell through specific transport membrane proteins, the molecule is subject to several sequent enzyme reactions. First, the glucose molecules gain a phosphate group derived from ATP, and is cleaved into two identical sub-compounds. Each of these sub-compounds binds phosphate while NAD^+ is reduced to NADH + H^+,[1]. The bound phosphate is later transferred to ADP to form ATP. Finally, the remaining structure is dehydrated andconverted into two molecules of pyruvate (which is the anion of pyruvic acid, $C_3H_4O_3$). Thus, the net reaction of glycolysis can be written as in (2.2):

$$C_6H_{12}O_6 + 2NAD^+ + 2P_i \rightarrow 2\text{pyruvate} + 2NADH + 2H^+ + 2ATP + 2H_2O \quad (2.2)$$

Although the energetic yield from glucolysis only contributes with about 5% of total ATP-yield from the complete glucose catabolism, glycolysis can by itself account for a major part of energy production. For example, both neutrophils and myoblasts derive up 95% of their energy from glycolytic activity (Wiley & Beeson, 2002; Gaitain *et al.*, 1997). Therefore, glucose consumption is a highly relevant indicator of cellular capacity to produce fuel for cellular work. However, metabolic consumption rate of glucose ($q_{glucose}$) varies with cell phenotype and also between species (see Table 2.3), as was clearly demonstrated by Schop *et al.* (2009) who studied mesenchymal stem cells obtained from human, rat, and goat, respectively. Even more important is that the glucose consumption rate varies with level of cell differentiation. Komarova *et al.* (2000) measured $q_{glucose}$ of osteoblasts throughout a period of 14 days, and they observed fluctuations between about 0.2-0.5 μmol h^{-1} / 10^6 cells, with the higher glycolytic activity detected in highly mature osteoblast cultures producing nodule mineralization. In a similar way, Collins *et al.* (1998) observed that glycolytic activity increased its role in energy production as haemopoietic cells matured. On the contrary, Tsao *et al.* (2005) observed that consumption rate of glucose was higher in the beginning of ovary cell cultures in suspension when cells were still actively growing.

Taken together, glucose consumption is indicative of cellular metabolic activity, but its rate cannot be expected to be constant over time. Therefore no direct relationship between glucose consumption and cell growth can be clearly established.

[1] NAD^+, nicotinamide adenine dinucleotide, is a coenzyme that works as a major redox carrier and universal energy intermediate in cells.

2.1.1.2 Lactate

Glycolysis is a completely anaerobic process, which to continue requires constant access to NAD^+. In an anaerobic cellular ambient (e.g., muscle tissue), NAD^+ can be regenerated through incomplete oxidation of glucose. In that case, pyruvate is reduced by lactate dehydrogenase to lactic acid (2.3). At physiological pH, lactic acid is dissociated into lactate and H^+ (Gladden, 2004), with the former being extruded to the extracellular environment via monocarboxylate carriers (Poole & Halestrap, 1993) and anion exchange proteins.

$$\text{pyruvate} + \text{NADH} + \text{H}^+ \rightarrow \text{lactate} + \text{NAD}^+ \tag{2.3}$$

In strictly anaerobic conditions all consumed glucose will be converted to lactate, and the molar ratio of produced lactate to utilised gluose ($Y_{Lac/Glu}$) reaches 2. However, under aerobic conditions lactate production is normally a secondary process for cells to obtain energy and to regenerate NAD^+, and $Y_{Lac/Glu}$ naturally decreases to levels below 2. The yield coefficent $Y_{Lac/Glu}$ therefore can be used as a preliminary indicator of which metabolic routes cells use to produce energy (Obradovic *et al.*, 1999; Komarova *et al.*, 2000; Schop *et al.*, 2009).

The cellular lactate production rate ($q_{lactate}$) can vary with many parameters, among them oxygen pressure, cell type and differentiation level, and due to environmental influence on $q_{lactate}$, lactate production does not directly relate to cell growth. However, in cases where lactate can be converted back to pyruvate (which is the case for mammalian cells that undergo the metabolic Cori cycle), Tsao *et al.* (2005) demonstrated experimentally the direct relationship at any given timepoint (t) between the integral of viable cells and the cumulated amount of glucose and lactate (Q_{GL}) calculated according to Equation 2.4;

$$Q_{GL} = (G_0 + L_0) - (G_t + L_t) \tag{2.4}$$

where G_0 and L_0 represent initial glucose and lactate concentrations, respectively.

In most mammalian cells, lactate will however not regenerate pyruvate, but rather accumulate in the extracellular environment where it can reach significant levels (>30 mM). Accumulation of lactate has been mentioned to be responisble for toxic/inhibitory effects on cell growth (Chen *et al.*, 2009), but since lactate production is associated with decreased pH, it has been

debated which of the two effects is the main responsible for the provoked effects. Among others, Patel *et al.* (2000) demonstrated that lactate accumulation without lowering the pH has less influence on cell growth than the combined effect of lactate accumulation and pH decrease.

2.1.1.3 Carbon dioxide

Reaching the mitochondrion, pyruvate can be enzymatically converted to acetyl-coenzyme A (acetyl-CoA). The reaction also produces CO_2 and it reduces NAD^+ to NADH and H^+ (2.5);

$$\text{pyruvate} + NAD^+ + \text{CoA} \rightarrow \text{AcetylCoA} + \text{NADH} + H^+ + CO_2 \tag{2.5}$$

The produced acetyl-CoA is then the main input for a series of cyclic reactions known as the *citric acid cycle* (or the *Krebs cycle*, or the *tricarboxylic acid cycle*) that completes the conversion of glucose (as well as other carbon-containing fuels such as fatty acids and certain amino acids) to CO_2 and electron carrier molecules such as NADH and $FADH_2$, and with the additional creation of a small amount of ATP (2.6);

$$\begin{aligned} &\text{AcetylCoA} + 3NAD^+ + FAD + ADP + P_i + 2H_2O \\ &\rightarrow \text{CoASH} + 3\text{NADH} + 3H^+ + FADH_2 + \text{ATP} + 2CO_2 \end{aligned} \tag{2.6}$$

In its gaseous state CO_2 is a higly labile molecule that rapidly reacts with water to form carbonic acid (H_2CO_3), which further dissociates into hydrogen and bicarbonate ions (HCO_3^-) (see equilibrium reaction 2.7).

$$CO_2(g) \rightleftharpoons CO_2(aq) + H_2O \rightleftharpoons H_2CO_3 \underset{K_1}{\rightleftharpoons} HCO_3^- + H^+ \underset{K_2}{\rightleftharpoons} CO_3^{2-} + H^+ \tag{2.7}$$

At physiological conditions (temperature 37°C, pH 6.8, ionic strength 0.1M), Goudar *et al.* (2007) estimated the equilibrium constants to be $K_1 = 10^{-6.07}$, and $K_2 = 10^{-10.04}$, which would mean that carbon dioxide produced by cells exists as combination of HCO_3^- (about 84%) and CO_2 and H_2CO_3 (together about 16%). While the presence of CO_2 in the atmosphere is extremely low (ppm), *in vitro* cultures are normally done at 5-7% CO_2 to reflect levels *in vivo* (about 5.3%), and to act as a buffer (Csete, 2005).

As gaseous CO_2 diffuses freely across cell membranes, and since HCO_3^- can enter or leave the cell through specific transport membrane proteins,

which mainly are different types of Cl^-/HCO_3^- exchangers (Cordat & Casey, 2009; Sterling & Casey, 2002), cellular CO_2 production can be considered as an indicator of metabolic activity and mitochondrial function. However, information on cellular CO_2 production rates is still relatively scarce. Goudar *et al.* (2007) reported the CO_2 production rate of BHK cells in a perfusion bioreactor to be 8 pmol/cell-day, while Yang & Balcarcel (2004) measured it to $\approx 1.2 \times 10^{-10}$ mmol/cell-h for fibroblast cells, which resulted in an increase of CO_2(aq) from 0.1 to 1.2 mM during ten hours in a sealed volume of 0.5 mL. Important to notice is that accumulation of extracellular CO_2 has been shown to inhibit both growth and cellular production in large-scale cultures from several cell lines (deZengotita *et al.*, 1998).

2.1.1.4 Oxygen

In presence of oxygen, acetyl-CoA emerging from glycolytic pyruvate is used to fuel additional cellular energy-producing reactions. In addition to the ATP generated in the Krebs cycle, large amounts of energy has also been trapped in the carrier molecules NADH and $FADH_2$. To liberate and convert this energy to ATP, and to regenerate NAD^+ and FAD which are necessary to maintain catabolic activity, the transferred electrons of these carrier molecules are harnessed through the reactions of *oxidative phosphorylation*. Briefly, electrons carried by NADH + H^+ and $FADH_2$ are transferred to molecular oxygen through a chain of reactions involving electron transfer molecules located in the inner mitochondrial membrane. Oxygen is converted into H_2O, and driven by a proton gradient, free protons return to the interior of the mitochondrion through specific proton channels, ATPsynthase, inducing a conformational change in the active site of this enzyme which favours the creation of ATP from ADP and P_i (Pedersen, 1994). In total, 32 molecules of ATP are created in the respiratory chain for every molecule of glucose entering the glycolytic pathway, making cellular respiration highly efficient compared to other catabolic routes.

Lack of oxygen (hypoxia) can inhibit ATP production and maintainence of essential cellular functions (Malda *et al.*, 2007; Maria *et al.*, 2009), whereas excess of oxygen (hyperoxia) can result in generation of reactive oxygen intermediates which can damage the cells (Kazzaz *et al.*, 1996), and which indicates that cellular oxygen concentration ought to be tightly regulated within a physiological range. *In vivo* the oxygen level varies drastically between different tissues (2-20 mmHg), with a mean P_{O_2} = 0.03-0.05 atm (Atkuri *et al.*, 2007). Nevertheless, most *in vitro* studies are done at atmospheric oxygen levels, i.e. at P_{O_2} = 0.21 atm. In those cases when P_{O_2} has been

varied *in vitro*, effects on both cellular proliferation and differentiation has been observed (Utting *et al.*, 2006). Especially stem cell function has been demonstrated to be P_{O_2}-sensitive (Csete, 2005).

The specific oxygen uptake rate (q_{O_2}, or OUR) has been determined for a multitude of mammalian cells (for a review, see Ruffieux *et al.* (1998)), and is a good measure on how well the cell is able to carry out respiration. However, it is important to remember that q_{O_2} may vary significantly with time and cell maturation. Nevertheless, several authours, among them Janssen *et al.* (2006b), have successfully used cellular oxygen consumption as a parameter to estimate viable cell number in tissue engineering applications during specific phases of growth.

2.1.1.5 Glutamine

Cells with high energy demand (in particular rapidly dividing cells, or cells producing large amounts of proteins) can in presence of oxygen produce additional energy through the *glutaminolytic* pathway that converts glutamine, which is a labile amino acid rich in nitrogen, and in abundance in blood plasma as well in cell culture medium, into ATP. The glutamine is uptaken by dividing cells through specific transporter proteins, and the molecule further propagates to the mitochondrion where it is first enzymatically hydrolysed to yield glutamate and ammonium (route 1, Table 2.1). The glutamate is then further degraded to α-ketoglutarate either enzymatically yielding another ammonium (2a) or through transamination (2b). Finally, before α-ketoglutarate enters the citric acid cycle where it can be either partially or completely oxidised to yield energy (3a-d).

Route	**Reaction**	**Type**	**ATP yield**
1	glutamine → glutamate + NH_4^+		-
2a	glutamate → α-ketoglutarate + NH_4^+	Enzymatic	-
2b	glutamate → α-ketoglutarate	Transamination	-
3a	α-ketoglutarate → oxaloactate → aspartate	Partial oxidation	9
3b	α-ketoglutarate → malate → pyruvate → lactate	Reduction	9
3c	α-ketoglutarate → malate → pyruvate → alanine	Transamination	9
3d	α-ketoglutarate → CO_2	Complete oxidation	27

Table 2.1: Metabolic pathways and energy yield of glutamine degradation. ATP yield is given as moles of ATP formed by mol of glutamine consumed.

Partial oxidation of α-ketoglutarate produces 9 moles of ATP for each mole of glutamine, while complete oxidation to CO_2 yields 27 moles of ATP per mole of glutamine (Schneider *et al.*, 1996). Although the latter route is three times more energy efficient, Aledo (2004) speculates that partial oxida-

tion offers important kinetic advantages with respect to complete oxidation, and that the energy derived from glutaminolysis mainly is used for amino acid transport across the cell membrane, which in turn could favour cell division.

Glutamine is present in most cell culture media at concentrations of 2-6 mM, a concentration that is much higher than for other amino acids. It should be noted that glutamine is unstable in aqueous solutions at physiological pH, where it spontaneously breaks down to pyrrolidonececarboxylic acid and ammonia in an irreversible manner. Its half-life depends on parameters such as pH, concentration of ammonia, temperature, and presence of serum, but has been reported to be in the range 6-20 days (Schneider *et al.*, 1996).

2.1.1.6 Ammonium

Amino acid metabolism, mainly that of glutamine, results in production of ammonium (NH_4^+) within the mitochondrion. In aqueous solution, and depending on pH, NH_4^+ can convert into ammonia (NH_3).

$$pH = pK + \log \frac{NH_3}{NH_4^+} \tag{2.8}$$

However, with pK = 9.3 at 37°C, about 99% of all ammonia exist as ammonium ions at physiological pH, and can be extruded from the cell via active transport proteins in the cell membrane. While *in vivo* ammonia can be metabolised to urea, *in vitro* it rather accumulates in the extracellular environment as ammonium (Obradovic *et al.*, 1999), and it has been observed to limit cell growth and affect the quality of cultured cells already at relatively low concentrations (> 2-3 mM) (Schneider *et al.*, 1996; Genzel *et al.*, 2005).

2.1.1.7 pH

While blood pH is normally around 7.40, pH of the extracellular fluid is subject to complex gradients depending on metabolic activity of cells and their distance from the nearest capillary, and can therefore be significantly lower. In general, metabolic activity acidifies the extracellular environment, and among the catabolic pathways that, either directly or indirectly, contribute to this *acidosis*, the glycolytic pathway produces the largest amount of "H^+" per ATP (Hafner, 2000). Additional acidification of the cellular environment is caused by other catabolic pathways, such as incomplete oxidation of glucose to lactic acid, pyruvate oxidation, the Krebs cycle, and glutaminolysis.

Accumulation of "H^+" within the cell is detrimental to many physiological processes, and acidosis has been observed to affect a variety of cells. For example, and only with respect to bone tissue engineering, low extracellular pH may inhibit matrix production (Frick *et al.*, 1997; Frick & Bushinsky, 1998), as well as alkaline phosphatase activity and mineralisaton (Brandao-Burch *et al.*, 2005). Furthermore, and as pointed out by Brown *et al.* (2007), apoptotic effects related to hypoxia are only evident if acidosis also occur.

Cells have several control mechanisms for regulation of pH. The most effective mean to eject "H^+" out of the cell is by the exchange for external Na^+ by specific proteins ubiquitously expressed in the plasma membrane as well as in the inner mitochondrial membrane (Orlowski & Grinstein, 1997). Other common ways to extrude "H^+" is by V-ATPase (Beyenbach & Wieczorek, 2006), or by carbonic anhydrase which catalyses hydration of CO_2 to HCO_3.

Below, in Table 2.2, are listed the main extracellular parameters that are influenced by cellular catabolic activity, and that may be used as indicator of cell activity within the TE environment. In Table 2.3 are further specified experimental consumption and production rates of some of these parameters for a variety of cell types obtained from different species.

Cell Metabolite	**Metabolic pathway**	**Influence**	**Typical range**
Glucose, $C_6H_{12}O_6$	Glycolysis	↓	0-55 mM
pH, H^+	Glycolysis Pyruvate oxidation	↓	6-8
Lactate	Glycolysis	↑	0-30 mM
Carbon dioxide, CO_2	Pyruvate oxidation Krebs cycle Glutaminolysis	↑	5%
Oxygen, O_2	Cellular respiration	↓	0-20%
Glutamine	Glutaminolysis	↓	0-6 mM
Ammonium, NH_4^+	Glutaminolysis	↑	0-5 mM

Table 2.2: Common cell metabolites, and their variation in the extracellular environment during cellular metabolic activity.

Metabolite	Cell type	Species	Rate (μmol h^{-1}/ 10^6 cells $^{(*)}$	Reference
Glucose	Bone marrow stromal cells	Human	0.38	Schop *et al.* (2009)
		Mouse	0.25	
		Goat	0.11	
	Bone marrow cells	Mouse	0.015	Gaitain *et al.* (1997)
	Granulocytes	Mouse	0.066	
	Hepatocytes (HEPG2)	Human	1.125	Mishra & Starly (2009)
	Myoblast	Rat	0.093	Wiley & Beeson (2002)
	Osteoblasts	Rat	0.2-0.5	Komarova *et al.* (2000)
Lactate	Blood mononuclear cells	Human	$\approx$ 15	Patel *et al.* (2000)
	Cartilage	Bovine	0.095	Obradovic *et al.* (1999)
	Osteoblasts	Rat	0.3 - 0.65	Komarova *et al.* (2000)
Carbon dioxide	Fibroblasts	Mouse	0.12	Yang & Balcarcel (2004)
	Kidney cells (BHK cell line)	Hamster	0.33	Goudar *et al.* (2007)
Oxygen	Bone marrow	Murine	0.01-0.04	Collins *et al.* (1998)
	Bone marrow mononuclear cells	Human	0.005-0.038	Peng & Palsson (1996)
	Granulocyte/Macrophage	Human	0.017-0.12	Collins *et al.* (1998)
	Hepatocytes (HEPG2)	Human	1.08 - 3.24	Mishra & Starly (2009)
	Hybridoma cell lines	Various	0.05-0.46	Ruffieux *et al.* (1998)

Table 2.3: Reported metabolic rates of the common cell metabolites for some different cell types, and species. (*) For easier overview, metabolic rate values obtained from indicated articles have in some cases been converted in order to express them with one common unit.

2.1.2 Non-catabolic Cellular Events

About 30% of the total cellular energy obtained from catabolic activity is used to pump ions through the cell membranes to maintain membrane potentials (Alberts *et al.*, 2002, p.357). Another 18-20% is accounted for by protein synthesis (Brown, 1992). The remaining energy need is related to cell motility and mechanical work. This anabolic cellular activity, not only depends on, but may also influence the TE environment.

2.1.2.1 The ionic extracellular environment

Homeostasis of major inorganic cations (Na^+, K^+, Ca^{2+}, Mg^{2+}, and H^+) and anions (Cl^-, phosphate, and bicarbonate) is fundamental to all cells, and is carefully controlled through passive and active transport of ions via specific channels and transporters located within the cell membrane. Cells may also respond to ionic disturbances through changing their physical volume (Koivusalo *et al.*, 2009).

The ionic cellular milieu, principally characterised by high extracellular sodium levels and high intracellular potassium levels (see Table 2.4) directly determines the cell membrane potential, and it also has significance for macromolecular conformation, protein and enzyme function (Stasio, 2004), as well as water structure.

Ion	**Intracellular** (mmol dm^{-3})	**Extracellular** (mmol dm^{-3})
Na^+	5-15	145-153
K^+	140	4.4-5.0
Ca^{2+}	10^{-4}	1-2
Mg^{2+}	0.5-0.7	1-2
pH	7.2	7.4
Cl^-	1-15	110-112
HCO_3^-	8-12	24
Phosphate	85-100	2.2
Sulfates	17-22	1

Table 2.4: Typical cellular ionic levels ((Alberts *et al.*, 2002, p.157 and p.942), Stasio (2004), and Despopoulos A (2003)). Exception to these values occur for cells that reside in non-typical extracellular fluid, e.g., chondrocytes (see Hopewell & Urban (2003)).

Beside establishing cell membrane potentials, many of the ions also act as important biochemical molecules that transmit information from the exterior to the interior of the cell, or assist in co-transport of other molecules across the cell membrane. While for example both chloride (Duran *et al.*, 2010),

phosphate (Beck, 2003), and magnesium (Walker, 1994; Romani, 2007) are known to influence different cellular events, calcium is undoubtedly the ion with highest documented influence on cellular life. Calcium acts both as a secondary messenger to influence intracellular Ca^{2+} concentration (through the actions of calcium channels, exchangers and pumps in the cellular membrane), as well as a first messenger through membrane-located Ca^{2+}-receptors (Hofer, 2005). Via further intracellular processing cellular functions such as spreading (ONeill & Galasko, 2000), proliferation and differentiation (Eklou-Kalonji *et al.*, 1998), apoptosis (Lin *et al.*, 1998; Lorget *et al.*, 2000), matrix production (Nakade *et al.*, 2001), hormone regulation (Ahlstrom *et al.*, 2008), bone tissue development (Dvorak *et al.*, 2004), and angiogenic events (Aguirre *et al.*, 2010) can be regulated.

Although ionic strength of the cell culture environment is normally maintained constant, single ionic activity can still be subject to local significant changes during tissue development. For example, in Chapter 3 and 6 of this thesis it is investigated how extracellular concentrations of calcium and phosphorus are subjected to osteoblast activity. Disturbance of homeostasis may also be used as an indicator of catastrophic cellular events, as is discussed in the following section.

2.1.2.2 Cell death

As a consequence of cell death, metabolic activity is ceased and the cellular membrane looses its permselective properties. Therefore, upon cell death, both the intra- and extracellular ionic environment will be disturbed. The major change in the extracellular environment would be an increase of both potassium and phosphorus. This increse, $\Delta[X]_o$, where $[X]$ is either K^+ or P_i, would depend on the extent of damage (i.e., number of damaged cells, N) as well as the total volume of the cell culture environment (V, dm^{-3}), and could be roughly estimated with Equation 2.9:

$$\Delta[X_o] = [X_{new}] - [X_{bkg}] = \frac{NV_{cell}[X]_i + V[X]_{bkg}}{NV_{cell} + V} - [X_{bkg}] \tag{2.9}$$

where V_{cell} is the volume of one single cell, $[X]_i$ is the intracellular ion concentration of X, and $[X]_{bkg}$ is the standard background extracellular concentration.

In Figure 2.2(a) it is visualised how the extracellular potassium concentration is affected by release of intracellular potassium for different number of damaged cells ($0 < N < 10^7$) in different cell culture volumes ($0 < V < 10$ cm^{-3}). The background potassium concentration was set to 5.5 mM and

$[K^+]_i$ to 140 mM, and V_{cell} was set to 1.0×10^{-12} dm^{-3} which would correspond to a radius of 6.2 μm for a perfectly spherical cell.

The validity of Equation 2.9 was tested experimentally with a fixed sample volume ($V = 0.30\times10^{-3}$ dm^{-3}), and by lysing different numbers of SAOS-2 osteoblast cells grown on tissue culture polystyrene with 0.1% Triton-X diluted in phosphate buffered saline solution. The concentration of potassium was then measured using a commercial potassium-selective electrode [2], and $[K^+]_{bkg}$ of the lysis solution was determined to 2.49 ± 0.04 mM. Experimental data confirmed that potassium was released, and that the release could be well correlated to number of lysed cells (Figure 2.2(b)).

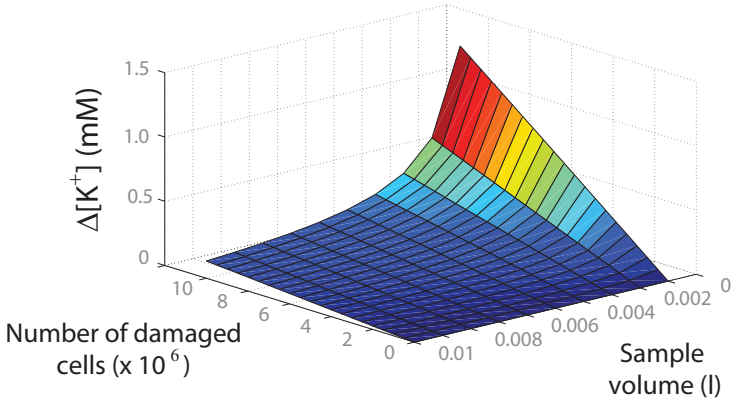

(a) Potassium release due to membrane damage as a function of cell number and culture volume.

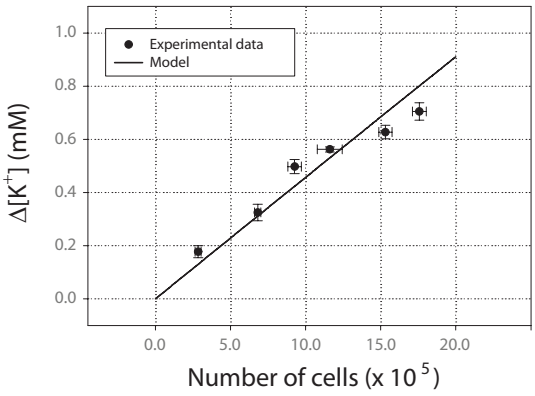

(b) Experimental data compared to model data for V_{sample} = 0.3 ml. Data is mean ± standard deviation, n = 4.

Figure 2.2: Damage to the cellular membrane causes release of intracellular K^+.

[2]See Section 3.3.2 for details on ion measurements.

2.1.3 Biomaterials Activity

The general concept behind the use of biomaterials in tissue engineering is to support cells with an appropriate environment that favours cellular growth and function. To some extent it is possible to control such cellular response through biomaterials properties. For example, it is well established that material properties such as *elasticity*, *wettability*, and *topography* play very important roles and are known to influence events such as cell attachment, contractility, motility, spreading, protein adsoprtion, and cell differentiation (Discher *et al.*, 2005; Bao & Suresh, 2003; Vogler, 1998; Dalby *et al.*, 2007). In addition to such physical materials properties, many biomaterials also interact (bio)chemically with the TE environment, and doing so they can provide (or deplete) the environment with soluble factors that cells metabolise or use as messenger molecules. One of the main material classes in TE is polymeric materials, which are often designed to degrade through one or another mechanism as new tissue is formed (Woodruff & Hutmacher, 2010). Biodegradability is not necessarily restricted only to polymers, but can also be prescribed certain metals (Yun *et al.*, 2009). In brief, these materials are degraded through hydrolysis or corrosion reactions to produce monomeric components that can be removed by natural pathways (but not always).

Antoher major category of chemical interaction that can be induced by certain biomaterials is through *ionic substitution/exchange* which causes ions to be either released into the extracellular environment or absorbed by the material. Among materials that induce such interaction are the ceramics, bioglasses, and apatitic materials, as well as composites containing any of these materials as one of its components. Materials that release or absorb ions to and from the TE environment has been reported for a variety of ions of different biological relevance; e.g. calcium and phosphorus (Engel *et al.*, 2008), magnesium (Yang & Zhang, 2009), strontium (Qiu *et al.*, 2006), zinc (Storrie & Stupp, 2005), copper (Barralet *et al.*, 2009), and fluoride (Itota *et al.*, 2004).

A third approach to tune the biochemical properties of a biomaterial is to load it with drugs or other promotor molecules that are then released upon implantation or during *in vitro* cell culture prior to implantation (Cartmell, 2009; Lee & Shin, 2007). Local release improves efficiency by delivering higher concentrations and can also decrease systemic toxicity and possible side effects of the molecule released. Materials popularly used as delivery vehicles are polymers (Luo & Prestwich, 2001), proteins (Friess, 1998), or ceramics (Ginebra *et al.*, 2006) since these materials possess inherent properties (such as biodegradability or that they favour ionic exchange) that can facilitate controlled release of molecules previously bound/trapped/encapsulated

to the scaffold. This approach has been explored both to deliver antibiotics to the implant site to impede bacterial infections (Jiang *et al.*, 2010), as well as bioactive molecules to accelerate extracellular matrix production and tissue integration (Porter *et al.*, 2009). An alternative approach to suppress bacterial infections in the vicinity of implanted biomaterials is through material-induced release of nitric oxide (NO) from polymeric and sol-gel coatings (Gupta & Kumar, 2008).

Monitoring and characterisation of biomaterials activity (let it be either through degradation, ionic exchange, or release mechanisms) distinguishes as an important sub-field in biomaterials research. Independent of the mechanism of interaction, any biomaterial designed to interact with its environment should do so at favourable rate and magnitude. While the rate of reaction is principally determined by the actual reaction mechanism, the magnitude of reaction is commonly an equilibrium between amount of unreacted material and amount of reactor material at any time, implying that the chemical activity of a biomaterial often can vary with its mass and exposed surface area. Furthermore, external physical parameters such as pH, temperature, and ionic strength, may significantly influence the reactivity. Moreover, the biological milieu with which the biomaterial is supposed to interact is usually of compex nature containing proteins, inorganic salts, vitamins, amino acids, and other cells. That imposes difficulties to precisely predict *a priori* the biochemical response of the biomaterial upon implantation, as only slight variations in the chemical composition of the aqueous environment may provoke completely different interaction responses (see further Chapter 4). As a consequence, characterisation of biochemical activity of biomaterials should ideally be done in conditions that simulate the *in vivo* environment as much as possible, and it is emphasised once for all that the biochemical activity of any material always should be put in perspective of the environment in which it has been characterised. Finally, it is desirable that the chemical characterisation also provides information on spatial differences of the material reactivity. The latter can be provoked either by the material itself (e.g. changing porosity) or for example through cell-material interactions (e.g. biofilm-coating). Until today, limited information about local microenvironments created around the cell-material interace have and can be obtained. Yet, this is the particular zone where the chemical activity of the biomaterial must be optimised in order to provide adequate cellular response. This issue will be further discussed in Section 2.2.1, and is also illustrated in Figure 2.4.

2.2 How to Measure?

When knowing which parameters that are of interest to measure, the next decision that has to be taken is *how* to detect them. This decision is however dependent on *where* in the TE environment the detection is to be done.

2.2.1 Where to Measure?

Traditionally, four different detection approaches, or *sensing locations*, have been described in literature (Figure 2.3): (1) invasive sensing, (2) non-invasive sensing, (3) sampling or shunt sensing, and (4) differential measurements (Rolfe, 2006).

While methods (1)-(3) are direct measurements of the TE environment, differential measurements are of indirect character as they measure the parameter of interest as a difference at the inlet and the outlet of the TE environment during medium flow. From such measurements the amount of biomass, $C_x(t)$, is determined according to Equation 2.10:

$$\frac{F}{V}([X]_{in} - [X]_{out}) = C_x(t)q_0 \tag{2.10}$$

where F is the flow rate of the medium, V is the volume of the environment, $[X]_{in}$ and $[X]_{out}$ are the concentrations or partial pressures of the parameter of interest at the inlet and the outlet respectiviely, and q_0 is the consumption or production rate of the parameter of interest (Janssen *et al.*, 2006b). Difference between $[X]_{in}$ and $[X]_{out}$ indicates activity from any of the TE components included in the volume V.

Normally all four sensing locations mentioned above provide representative information on the average, or the *global*, extracellular tissue engineering environment, and they are appropriate when the environment is homogenous. However, increased complexity in cellular cultures (e.g., co-cultures) and materials designs (e.g., porosity, topography, degradation, etc) provokes that the global environment becomes less and less representative of the infinite numbers of microenvironments created immediately adjacent to cells growing in proximity to another TE component (Figure 2.4). Examples of local TE microenvironments are the interiors of porous scaffolds and interfaces between cells and the surface of scaffold materials. These local environments are exceptionally small (approaching size and volume of individual cells) and may therefore be subject to higher influence from changes caused by any TE component. For example, the distance between cells attached to a solid material is of the order of 5-30 nm (Curtis, 2001), thus creating a volume of *nl*-μ*l*

between cells and the surface of the material where signals crucial for cell survival and functioning are transmitted and received.

Measurement of local environments is important because these are the environments that cells experience and that decide cellular fate, and it can provide information on the spatial variations in the TE environment. Obviously, getting access to these microenvironments require not only sophisticated techniques, but also an increased number of measuring points to obtain representative data. Therefore, in addition to the decision on the actual sensing location, it is also important to determine the appropriate number and exact position of the sensors to effectively monitor the culture parameters and to obtain information-rich data (Lim *et al.*, 2007, 2008).

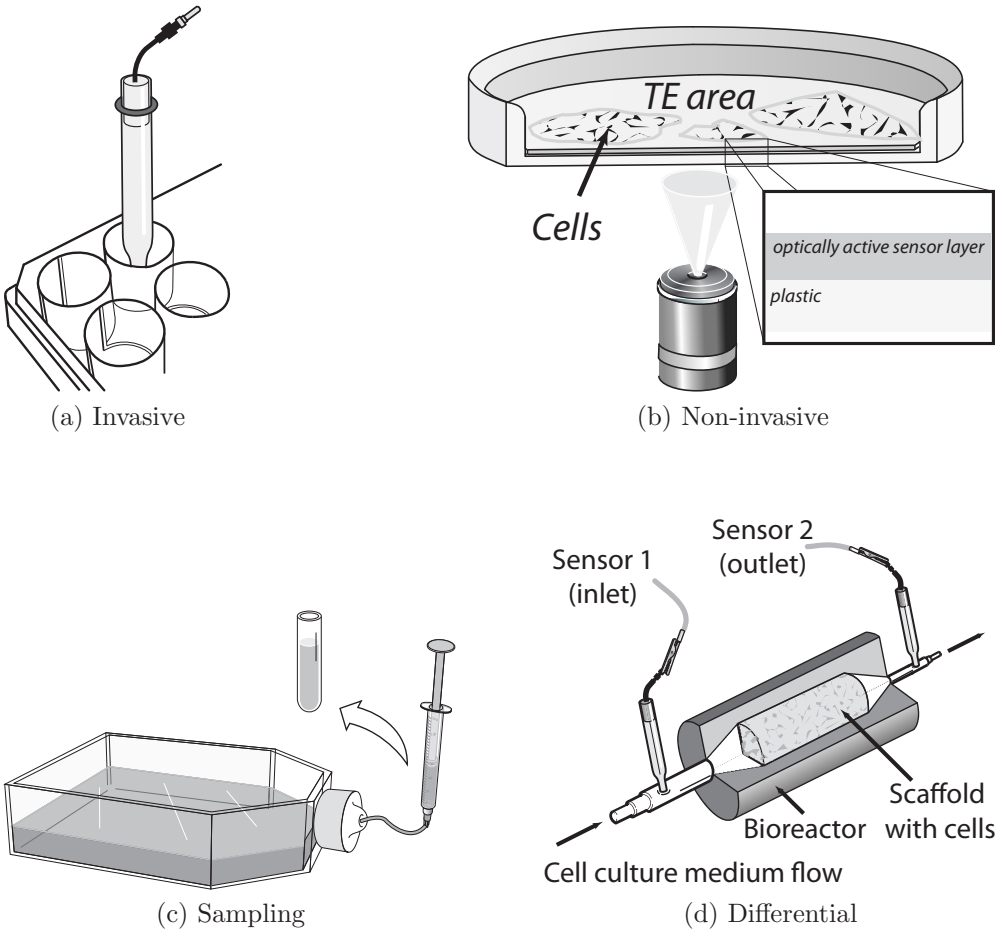

(a) Invasive

(b) Non-invasive

(c) Sampling

(d) Differential

Figure 2.3: Different sensing locations.

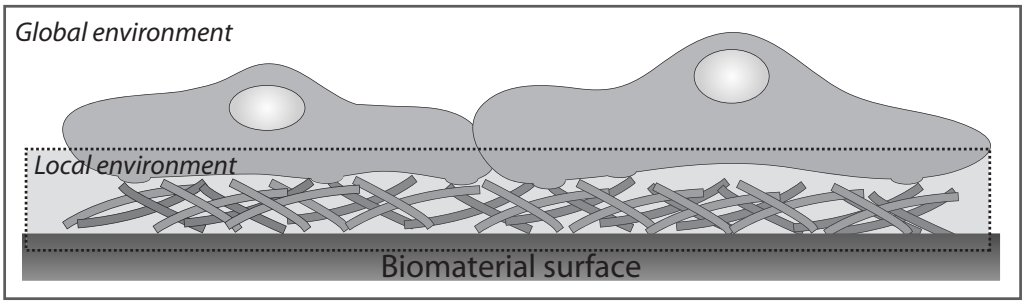

Figure 2.4: Two different TE environment can be defined; the global and the local environments.

2.2.2 Sensors for Tissue Engineering Applications

A multitude of techniques, among them different *imaging* and *sensing* modalities, can be used to assess the TE environment at different levels (see Table 2.5, and reviews by Vojinovic *et al.* (2006), Starly & Choubey (2007), Mason & Hoare (2007), Lim *et al.* (2007), and Mather *et al.* (2007)). Ideally, such techniques or tools should (1) possess adequate sensitivity, specficity, and stability towards the analyte of interest, (2) not interfere with any of the TE components, (3) allow for real-time monitoring of data, and (4) be possible to combine in order to obtain multi-parametric data on the TE process.

Most sensors rely on a common principle (Figure 2.5); a chemical reaction between analyte and recognition element (receptor) that produces a signal that can be transduced and detected with for example electrochemical or fibre optics methods (Marazuela & Moreno-Bondi, 2002). The heart of the sensor is obviously the receptor which should (1) react only with the analyte of interest, bind the analyte (2) irreversibly, and (3) at a concentration that corresponds to the range of interest. Commonly used receptors are based on biological components such as proteins, enzymes, antibodies, lipid bilayers, liposomes, DNA, whole cells, or even intact organs or tissue. In such cases the sensor is referred to as a *biosensor* (Kissinger, 2005). Non-biological receptor elements include synthetically derived ionophores, different metal oxides, fluorophores, and phosphorescent molecules.

In Sections 2.2.2.1 - 2.2.2.3 it is discussed the major sensor classes, and their possible application in the field of tissue engineering.

Parameter	Enabling tool	Detection technique	Reference
Glucose	Enzyme-based sensors	Ampereometry	Wang (2008)
	Nano-particles	Fluorescence	Billingsley *et al.* (2010)
Lactate	Enzyme-bases sensors	Ampereometry	Romero *et al.* (2010)
CO_2	Severinghaus electrode	Potentiometry	Zhao & Cai (1997)
	Optical film sensors	Fluorescence	Ge *et al.* (2003)
O_2	Clark electrode	Ampereometry	Andreescu & Sadik (2005)
	Microparicles	Fluorescence	Acosta *et al.* (2009)
	Thin film sensors	Optical	Thomas *et al.* (2009)
pH	ISFET	Potentiometry	Poghossian *et al.* (2009)
	MMO electrodes	Potentiometry	Glab *et al.* (1989)
	ISE	Potentiometry	
Ions	ISE	Potentiometry	Radomska *et al.* (2008)
	Optodes	Fluorescence	Hisamoto & Suzuki (1999)
Amino acids and proteins	Porphyrin-tailored electrode	Optical absorbance	Awawdeh *et al.* (2003)
	Cu-tailored electrodes	Ampereometry	Luque *et al.* (2007)

Table 2.5: Parameters of interest for TE monitoring, and corresponding performing enabling tools.

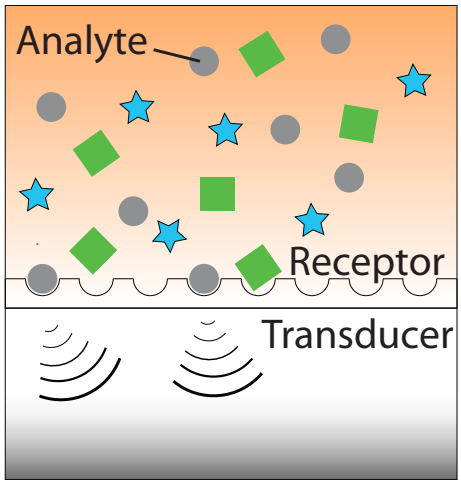

Figure 2.5: The concept of chemical sensors.

2.2.2.1 Gas sensors

On-line gas analysis is an attractive method to monitor cultivation of growing cells, and it can also be used as the basis for changing medium or as indicator of contamination.

The most common means for measurement of dissolved oxygen and carbon dioxide are the *Clark* and the *Severinghaus* electrodes, respectively, which both have been described in detail by, for example, Hahn (1980). These electrodes contain a gas-permeable membrane that separates the site of detection from the sample subject to investigation. When gas passes the permeable membrane of the Severinghaus electrode it encounters a buffer of bicarbonate solution which pH obviously is under influence of CO_2. As the pH of the buffer solution is *potentiometrically* measured by an internal pH electrode, an indirect measurement of the concentration of CO_2 is obtained.

In the Clark electrode, the detection mechanism is based on reduction of oxygen at a cathode (normally made from platinum) which is negatively polarised against a reference electrode. As oxygen that passes the permeable membrane is reduced (Equation 2.11), a current flow in the circuit and a linear relationship between current and P_{O_2} can be established.

$$O_2 + 2H_2O + 4e^- \rightarrow 4OH^- \tag{2.11}$$

A consequence of the Clark electrode detection mechanism is that oxygen is consumed by the electrode during operation, and this can potenially alter the oxygen concentration in culture.

Although the underlying detection principle of both the Clark and the Severinghaus electrodes limit their use to be of either invasive or differential character, still they can be miniaturised down to a few micrometers which could allow for measurements in extremely small volumes (Lee *et al.*, 2007; Zhao & Cai, 1997; Suzuki *et al.*, 1999), as well as high-troughput applications (Andreescu & Sadik, 2005).

Both sensors have been applied in bioprocess monitoring, and to some extent also in tissue engineering applications. For example, Janssen *et al.* (2006a,b) demonstrated the usefulness of the Clark oxygen electrodes to monitor cell growth inside a closed perfusion bioreactor designed to produce bone tissue for clinical applications. For this purpose they applied low-consuming electrodes in a differential-mode, and from Equation 2.10 they could obtain accurate data on cell growth within the bioreactor during the exponential growth phase.

An alternative mean to measure gases is based on quenching of fluorescence or phosphorescence. In that case, *gas sensitive luminophores* (commonly variants of phosphorescent metal-porphyrin dyes or fluorescent ruthenium(II) complexes for oxygen, and 8-hydroxypyrene-1,3,6-trisulfonic acid, HPTS, for carbon dioxide) are incorporated either within (1) an optically transparent and gas-permeable matrix which is directly deposited onto an optical sensor, or (2) microparticles that are suspended in the TE environment. In both cases, the emission of the luminescent dye is quenched by the gas at a rate dependent upon gas concentration. Commonly optical gas sensors contain an additional reference dye which is independent of gas concentration, and so the intensity (I) of the luminescence is calculated as the ratio of luminescence obtained from the indicator dye (I_{ind}) and the reference dye (I_{ref}), and which further obey the *Stern-Volmer equation* (Equation 2.12),

$$I = \frac{I_{ind}}{I_{ref}} = \frac{I_0}{1 + K_{sv}[\mathrm{Q}]} \tag{2.12}$$

where I_0 is the intensity of fluorescence in absence of gas at partial pressue [Q] (atm), and K_{sv} is the Stern-Volmer quenching constant (atm^{-1}). Often, when the luminophore is embedded in a polymeric support its response deviates from the Stern-Volmer equation, and corrections for this has to be taken into account.

Optical gas electrodes have been proven successful candidates for long-term continuous monitoring in cell culture conditions. For example, Gao

et al. (2004) reported how optical oxygen sensors applied in a differential-mode could provide information on cellular respiration for a period of at least 180 days. A second major advantage of optical oxygen sensors is that they may provide conditions for essentially non-invasive measurements of the TE environment. In that sense, gas sensors based on thin-films have been affixed as patches on transparent sections of bioreactor walls (Ge *et al.*, 2005) or at the bottoms of culture wells (Thomas *et al.*, 2009). According to the latter principle, Kellner *et al.* (2002) achieved non-invasive, high-resolution P_{O_2} mesaurements over cross-sections of cutlivated tissue (see Figure 2.6a).

Optical oxygen sensors have successfully been modified to allow for measurements in cellular microenvironments (Lin *et al.*, 2009). Acosta *et al.* (2009) reported the development and characterisation of such non-cytotoxic oxygen-sensitive microparticles (see Figure 2.6b). The particles were made from silica-gel onto which were bound an oxygen-sensitive fluorophore as well as a reference fluorophore. The particles, 5-40 μm in diameter, were finally embedded in poly(dimethylsiloxane). Such microparticle sensors are possible to suspended in TE environments, and if the environment (i.e., the scaffold and bioreactor) is transparent this method may provide information on local oxygen concentrations and gradients.

These examples demonstrate well how sensors can be used to obtain both temporal and spatial information on the TE process, as well as how tissue development in local microenvironments of the TE construct can be followed.

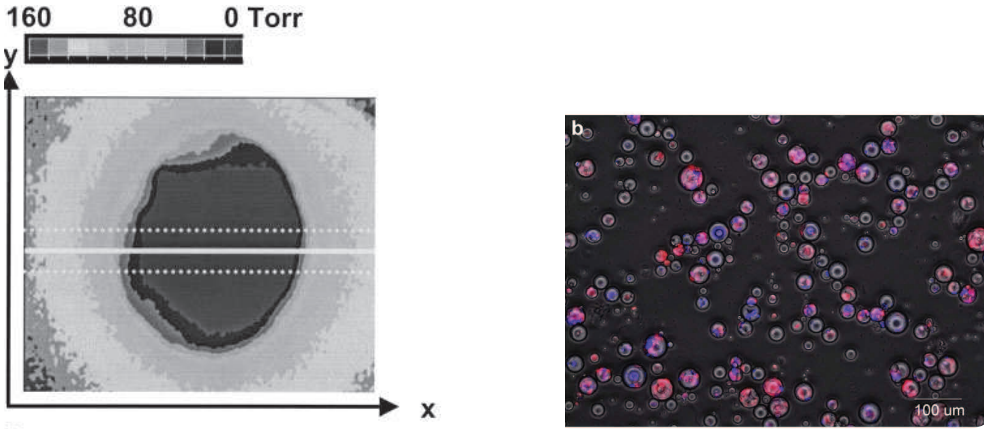

(a) *In situ*, cross-sectional mapping of oxygen tension in tissue engineered cartilage (size). Adapted from Kellner *et al.* (2002).

(b) Microparticles for O_2-sensing containing oxygen indicator dye (red) and reference dye (Nile blue). Adapted from Acosta *et al.* (2009).

Figure 2.6: Optical oxygen sensors for tissue engineering applications.

2.2.2.2 pH sensors

The two major classes of pH sensors are the *optical* and the *electrochemical* sensors. Electrochemical pH sensors are discussed more in detail in Chapter 7, but briefly they comprise the standard glass electrode, ion-selective electrodes (see further Section 2.2.2.3), ion-selective field-effect transistors (ISFET), and metal-metal oxide (MMO) electrodes, which all provide linear relationship between pH and sensor potential (Kurzweil, 2009).

The ISFET is a microelectronic transistor device with the gate as its pH-sensitive area (Bergveld, 2003). Typically the gate material is made of silicon dioxide (SiO_2) or silicon nitride (Si_3N_4), which beside giving the sensor its pH-sensitive properties also is biocompatible and thus allows the sensor to be used in cellular applications (Gustavsson *et al.*, 2008). To operate an ISFET, a potential is applied between the *drain* and the *source* of the transistor. The resulting drain current, I_d, is under certain external conditions directly influenced by the gate potential, which can be controlled through electronic circuitry.

Compared to ISFETs, MMO electrodes present a principally simpler construction and operation having the active sensing layer (typically hydrated iridium oxide (IrO_x), antimony, or palladium) deposited directly on top of the electrode (Glab *et al.*, 1989). IrO_x electrodes have been demonstrated to be extremely durable (Wang *et al.*, 2002), stable (Hendrikse *et al.*, 1998), and are possible to use in physiological conditions (O'Hare *et al.*, 2006).

The ISFET and MMO electrodes are both small in size, and have been used to measure metabolic activity of cells in volumes down to sub-nanolitres (Lehmann & Baumann (2005); Maharbiz *et al.* (2004); Ges *et al.* (2007)). Nevertheless, use of electrochemical sensors limits the measurement to be of invasive character, and as always, presence of proteins in the test solution may hamper the sensor behaviour (Wisniewski & Reichert, 2000). These problems can to some extent be counteracted using optical sensors where typically pH-sensitive dyes or fluorophores are either deposited/bound onto a fiber-optic-based detector or incorporated into carrier capsules which can be dispersed into the test solution and observed under a microscope. The latter approach provides *mobile* pH sensors that reaches microenvironments normally inaccessible to other sensors (Figure 2.7). Typically such sensors have been based on micro- and nano-particles from colloidal particles (Zhang *et al.*, 2010) or multifunctional polymer particles prepared by layer-by-layer methods (Sukhorukov *et al.*, 2007). The properties of these particles can be tuned, and has allowed for preparation of mobile biocompatible pH sensors (Hornig *et al.*, 2008).

Other approaches that have been proposed for online monitoring of pH

in complex physiologicl solutions are pH hologram sensors (Medlock *et al.*, 2007), as well as optical absorption measurements of phenol red contained in culture medium (Wu *et al.*, 2009), which to some extent has been used to extract information on pH gradients in engineered tissue (Brown *et al.*, 2007).

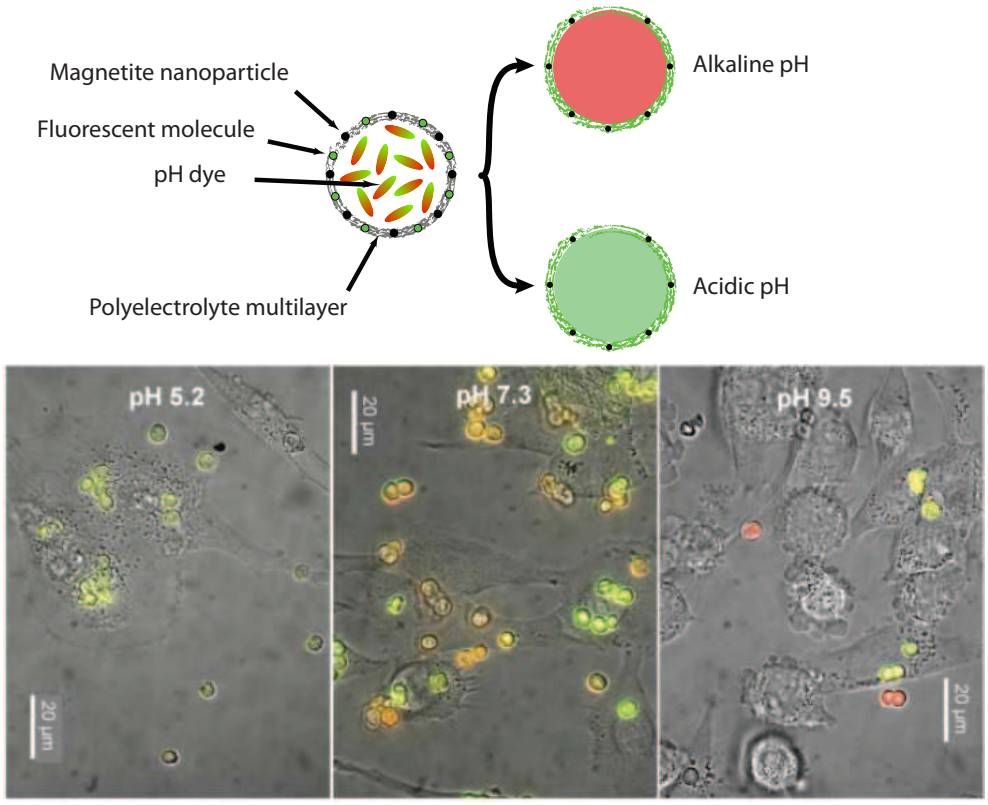

Figure 2.7: Principle and application of optical mobile pH sensors. The small size make these pH sensors an attractive approach for use in tissue engineering microenvironments. Images are adapted from Kreft *et al.* (2007).

2.2.2.3 Ion sensors

Online measurements of ionic activity is achieved by ion-selective *potentiometric* sensors (Bobacka *et al.*, 2008) or ion-selective *optodes* (Johnson & Bachas, 2003).

The principle of potentiometric ion sensors is discussed in detail in Chapter 6, but briefly, and according to the general sensor concept described in Section 2.2.2 and Figure 2.5, the receptor of an ion-sensor is the *ionophore*

which complexes with the analyte ion. Ionophores are commercially available for almost any cation, including the hydrogen ion for detection of pH, but are less common for anions (Antonisse & Reinhoudt, 1999). To dectect the ion complexation, the ionophore is typically incorporated into a polymeric membrane, preferentially made from plasticised poly(vinyl chloride), which contacts (directly or indirectly) with the electrode. Other materials. such as different sol-gels, have also been applied to produce the sensing element (Marxer & Schoenfisch, 2005). No matter the choice of membrane matrix material, the ion activity (a) of the sample is related to the sample-membrane potential (E) of the ion-selective electrode according to the *Nernst equation* (2.13):

$$\mathrm{E} = \text{constant} \pm 2.303\frac{RT}{nF}\log a \tag{2.13}$$

where R is the gas constant (8.313 J K^{-1} mol^{-1}), T is the absolute temperature (K), n is the charge number of the analyte ion, and F is the Faraday constant (96487 C mol^{-1}). Applying these numbers to the Nernst equation, at 37°C a change in potential of 1.0 mV corresponds to a change of 3.8% in activity for monovalent ions, and 7.8% for divalent ions.

Beside the high selectivity and the low detection limit (down to nanomolar range) that can be achieved with potentiometric ion-selective electrodes, one additional major advantage is that these sensors can be fabricated in a multitude of shapes and sizes, and thus can be adapted to different measurement situations, including microenvironmental ones (Guenat *et al.*, 2006). All these advantages were taken benefit of to develop ion-selective electrodes for detection of potassium efflux from necrotic cells (Generelli *et al.*, 2008). Relying on the same detection principles, and using ion-selective micro-electrodes, Berger *et al.* (1999) could study calcium release induced by osteoclast activity cultured on cortical bone fragments. In that study, real-time data was obtained during a time period of a few hours.

A persistent challenge that still remains is to make ion-selective electrodes resist both degradation and/or leakage of membrane components during long mesurement periods, as well as biofouling when exposed to complex protein-containing solutions. One successful approach to overcome the latter problem was presented by Radomska *et al.* (2008) who developed anti-fouling ion-selective membrane based on PEG, poly(ethylene glycol). In that way they could significantly improve the sensor behaviour and were able to monitor ammonia levels in mammalian cell cultures performed in a bioreactor during a period of at least one week.

One step towards non-invasive ion measurements can be taken, just as in the case with gas and pH sensors, by using optical detection methods. While more or less the same elements used in potentiometric ISEs also are used in ion-selective optodes, the detection mechanism is slightly different as cation-selective optodes often are based on exchange systems. For this purpose, an additional component, a chromoionophore that works as a pH-indicator and which is not selective to the analyte, is incorporated into the polymeric membrane. As the analyte cation is complexed by the ionophore, a positive charge in the form of a hydrogen ion is released into the test solution. Consequently, the bulk pH of the sensing film is changed and the optical properties of the chromoionophore are changed.

From this principle has been developed ion-selective nano-optodes (also known as PEBBLEs) with potential use for both intra- and extracellular measurements of major cations (Lee *et al.*, 2009) . Methods for tuning biocompatibility (Dubach *et al.*, 2007) and anti-fouling properties (Baxamusa *et al.*, 2008) have been reported.

2.2.2.4 Towards *in vivo* applications

Although this chapter is devoted to sensor applications *in vitro*, the aim of tissue engineering is towards *in vivo* applications. With respect to performing enabling tools, and particularly electrochemical sensors, its application *in vivo* has previously been reviewed by Wilson & Gifford (2005) and Li *et al.* (2007). Undoubtedly, *in vivo* glucose monitoring distinguishes as the most reputable application with its extensive record of implantation studies (Wang, 2001; Koschwanez & Reichert, 2007). A rather distinct application, but which demonstrates the wide usefulness of electrochemical sensors as enabling tools in biomaterials and tissue engineering research, was developed by Karp *et al.* (2008) who studied foreign body response of sensors upon implantation. More recent progress towards successful integration of electrochemical sensors *in vivo* include development of new materials that can host the electronic circuitry of electrochemical sensors while being both biocompatible and biodegradable (Kim *et al.*, 2010), as well as materials that reduce biofouling when implanted (Yu *et al.*, 2008).

Compared to electrochemical sensors, optical sensors reduce the need for electronic circuitry, and thus provide increased possibility for non-invasive measurements. Within this context it is explored how transfecting cells with reporter genes such as green fluorescent protein or luciferase can contribute to improved efficiency and control of the TE process (Blum *et al.*, 2004). Such approaches have lately been used to study cell viability and hypoxia in TE constructs when implanted in vivo (Logeart-Avramoglou *et al.*, 2010;

Liu *et al.*, 2010). Even more interesting are the non-invasive strategies that avoid transfection of cells. These include optical nano-sensors, and their development and applicability to monitor glucose concentration *in vivo* was recently demonstrated by Billingsley *et al.* (2010). Although it is not clear the effect of injecting nanoparticles *in vivo* on a long-term, similar devices hold much promise for future use in complex tissue engineering constructs, and their development is highly encouraged.

2.3 Conclusions

As a field of science, tissue engineering has hitherto proceeded to a great extent from methods based on trial and error, and it is greatly acknowledged that more systematic approaches are adopted. However, to be able to develop more solid theories and methodologies, increased understanding of almost any TE process is required. For this purpose, development and improvement of enabling tools of mainly predictive and performing character are highly asked for.

If correctly applied, enabling tools of performing character, such as different sensing and imaging modalities, could contribute to both increased temporal and spatial control of the TE environment by providing information on cellular metabolic activity, scaffold properties and performance, and cell-biomaterials interactions. As discussed in this chapter, the general concepts of such technologies are well established, but the compositional and spatial complexity of the TE environment require precise, and sometimes modified, use of these tools to make full use of them and to obtain the desired information. Important to notice is that recent advances in sensor technology (e.g. biocompatible microparticle sensors and improved anti-fouling sensor properties) demonstrate that an increased research interaction between tissue engineers and sensor developers could be beneficial for both fields of research, and together they could better answer the fundamental, and related, questions emphasised in this chapter: *what*, *where*, and *how* to measure.

Bibliography

Acosta, M. A., Ymele-Leki, P., Kostov, Y. V., & Leach, J. B. (2009). *Biomaterials,* **30**, 3068–3074.

Aguirre, A., Gonzalez, A., Planell, J., & Engel, E. (2010). *Biochemical and Biophysical Research Communications,* **393**, 156–161.

Ahlstrom, M., Pekkinen, M., Riehle, U., & Lamberg-Allardt, C. (2008). *Bone,* **42**, 483–490.

Alberts, B., Johnson, A., Lewis, J., Raff, M., Roberts, K., & Walter, P. (2002). *Molecular Biology of the Cell.* Garland Science (Taylar & Francis Group), 4th edition.

Aledo, J. C. (2004). *BioEssays,* **26**, 778–785.

Andreescu, S. & Sadik, O. A. (2005). *Methods,* **37**, 84–93.

Antonisse, M. M. & Reinhoudt, D. N. (1999). *Electroanalysis,* **11** (14), 1035–1048.

Atkuri, K. R., Herzenberg, L. A., Niemi, A.-K., Cowan, T., & Herzenberg, L. A. (2007). *PNAS,* **104** (11), 4547–4552.

Awawdeh, M. A., Legako, J. A., & Harmon, H. J. (2003). *Sensors and Actuators B,* **91**, 227–230.

Bao, G. & Suresh, S. (2003). *Nature Materials,* **2**, 715–725.

Barralet, J., Gbureck, U., Habibovic, P., Vorndran, E., Gerard, C., & Doillon, C. J. (2009). *Tissue Engineering: Part A,* **15** (7), 1601–1609.

Baxamusa, S. H., Montero, L., Dubach, J. M., Clark, H. A., Borros, S., & Gleason, K. K. (2008). *Biomacromolecules,* **9**, 2857–2862.

Beck, G. R. (2003). *Journal of Cellular Biochemistry,* **90**, 234–243.

Berger, C., Horrocks, B., & Datta, H. (1999). *Electrochimica Acta,* **44**, 2677–2683.

Bergveld, P. (2003). *Sensors and Actuators B,* **88**, 1–20.

Beyenbach, K. W. & Wieczorek, H. (2006). *The Journal of Experimental Biology,* **209**, 577–589.

Billingsley, K., Balaconis, M. K., Dubach, J. M., Zhang, N., Lim, E., Francis, K. P., & Clark, H. A. (2010). *Analytical Chemistry,* **82**, 3707–3713.

Blum, J. S., Temenoff, J. S., Park, H., Jansen, J. A., Mikos, A. G., & Barry, M. A. (2004). *Biomaterials,* **25**, 5809–5819.

Bobacka, J., Ivaska, A., & Lewenstam, A. (2008). *Chemical Reviews,* **108**, 329–351.

Brandao-Burch, A., Utting, J. C., Orriss, I. R., & Arnett, T. R. (2005). *Calcified Tissue International,* **77**, 167–174.

Brown, D. A., MacLellan, W. R., Wu, B. M., & Beygui, R. E. (2007). *Annals of Biomedical Engineering,* **35**, 1885–1897.

Brown, G. C. (1992). *Biochemical Journal,* **284**, 1–13.

Cartmell, S. (2009). *Journal of Pharmaceutical Sciences,* **98**, 430–441.

Chen, T., Zhou, Y., & Tan, W.-S. (2009). *Cell Biology and Toxicology,* **25**, 573–586.

Collins, P. C., Nielsen, L. K., Papoutsakis, S. D. P. A. T., & Miller, W. M. (1998). *Biotechnology Progress,* **14**, 466–472.

Cordat, E. & Casey, J. R. (2009). *Biochemical Journal,* **417**, 423–439.

Csete, M. (2005). *Annals of the New York Academy of Sciences,* **1049**, 1–8.

Curtis, A. (2001). *eCells & Materials Journal,* **1**, 59–65.

Dalby, M. J., Gadegaard, N., Tare, R., Andar, A., Riehle, M. O., Herzyk, P., Wilkinson, C. D., & Oreffo, R. O. (2007). *Nature Materials,* **6**, 997–1003.

Despopoulos A, S. S., ed (2003). *Color atlas of physiology.* New York: Thieme.

deZengotita, V. M., Kimura, R., & Miller, W. M. (1998). *Cytotechnology,* **28**, 213–227.

Discher, D. E., Janmey, P., & li Wang, Y. (2005). *Science,* **310**, 1139–1143.

Dubach, J. M., Harjes, D. I., & Clark, H. A. (2007). *Journal of the American Chemical Society,* **129**, 8418–8419.

Duran, C., Thompson, C. H., Xiao, Q., & Hartzell, H. C. (2010). *Annual Review of Physiology,* **72**, 95–121.

Dvorak, M. M., Siddiqua, A., Ward, D. T., Carter, D. H., Dallas, S. L., Nemeth, E. F., & Riccardi, D. (2004). *PNAS,* **101** (14), 5140–5145.

Eklou-Kalonji, E., Denis, I., Lieberherr, M., & Pointillart, A. (1998). *Cell and Tissue Research,* **292**, 163–171.

Engel, E., del Valle, S., Aparicio, C., Altankov, G., Asin, L., Planell, J. A., & Ginebra, M. P. (2008). *Tissue Engineering,* **14**, 1341–1351.

Frick, K. & Bushinsky, D. (1998). *American Journal of Physiology,* **275** (5), F840–F847.

Frick, K., Jiang, L., & Bushinsky, D. (1997). *American Journal of Physiology,* **272** (5), C1450–1456.

Friess, W. (1998). *European Journal of Pharamceutics and Biopharmaceutics,* **45** (2), 113–136.

Gaitain, S., Escribano, S., Sancho, P., Cuenllas, E., & Tejero, C. (1997). *British Journal of Haematology,* **96**, 559–565.

Gao, F. G., Jeevarajan, A. S., & Anderson, M. M. (2004). *Biotechnology and Bioengineering,* **86** (4), 425–433.

Ge, X., Kostov, Y., & Rao, G. (2003). *Biosensors and Bioelectronics,* **18**, 857–865.

Ge, X., Kostov, Y., & Rao, G. (2005). *Biotechnology and Bioengineering,* **89** (3), 329–334.

Generelli, S., Jacquemart, R., de Rooij, N. F., Jolicoeur, M., Koudelka-Hep, M., & Guenat, O. T. (2008). *Lab on a Chip,* **8** (7), 1210–1215.

Genzel, Y., Ritter, J. B., Konig, S., Alt, R., & Reichl, U. (2005). *Biotechnology Progress,* **21**, 58–69.

Ges, I. A., Ivanov, B. L., Werdich, A. A., & Baudenbacher, F. J. (2007). *Biosensors and Bioelectronics,* **22**, 1303–1310.

Ginebra, M., Traykova, T., & Planell, J. (2006). *Journal of Controlled Release,* **113**, 102–110.

Glab, S., Hulanicki, A., Edwall, G., & Ingman, F. (1989). *Critical Review in Analytical Chemistry,* **21** (1), 29–47.

Gladden, L. (2004). *The Journal of Physiology,* **558** (1), 5–30.

Goudar, C. T., Matanguihan, R., Long, E., Cruz, C., Zhang, C., Piret, J. M., & Konstantinov, K. B. (2007). *Biotechnology and Bioengineering,* **96** (6), 1107–1117.

Guenat, O. T., Generelli, S., de Rooij, N. F., 2, M. K.-H., Berthiaume, F., & Yarmush, M. L. (2006). *Analytical Chemistry,* **78** (21), 7453–7460.

Gupta, R. & Kumar, A. (2008). *Biomedical Materials,* **3** (3), 1–15.

Gustavsson, J., Altankov, G., Errachid, A., Samitier, J., Planell, J. A., & Engel, E. (2008). *Journal of Materials Science - Materials in Medicine,* **19** (4), 1839–1850.

Hafner, F. (2000). *Biosensors & Bioelectronics,* **15**, 149–158.

Hahn, C. (1980). *Journal of Physics E: Scientific Instruments,* **13**, 470–482.

Hendrikse, J., Olthuis, W., & Bergveld, P. (1998). *Sensors and Actuators B,* **53**, 97–103.

Hisamoto, H. & Suzuki, K. (1999). *Trends in analytical chemistry,* **18** (8), 513–524.

Hofer, A. M. (2005). *Journal of Cell Science,* **118** (5), 855–862.

Hopewell, B. & Urban, J. P. (2003). *Biorheology,* **40**, 73–77.

Hornig, S., Biskup, C., Grafe, A., Wotschadlo, J., Liebert, T., Mohr, G. J., & Heinze, T. (2008). *Soft Matter,* **4**, 1169–1172.

Itota, T., Carrick, T. E., Rusby, S., Al-Naimi, O. T., Yoshiyama, M., & McCabe, J. F. (2004). *Journal of Dentistry,* **32**, 117–122.

Janssen, F., Hofland, I., van Oorschot, A., Oostra, J., Peters, H., & van Blitterswijk, C. (2006a). *Journal of Biomedical Materials Research Part A,* **79A** (2), 338–348.

Janssen, F. W., Oostra, J., van Oorschot, A., & van Blitterswijk, C. A. (2006b). *Biomaterials,* **27**, 315–323.

Jiang, P.-J., Patel, S., Gbureck, U., Caley, R., & Grover, L. M. (2010). *Journal of Biomedical Materials Research Part B: Applied Biomaterials,* **93** (1), 51–58.

Johnson, R. D. & Bachas, L. G. (2003). *Analytical and bioanalytical chemistry,* **376**, 328–341.

Karp, F. B., Bernotski, N. A., Valdes, T. I., Bhringer, K. F., & Ratner, B. D. (2008). *IEEE Sensors Journal,* **8**, 104–112.

Kazzaz, J. A., Xu, J., Palaia, T. A., Mantell, L., Fein, A. M., & Horowitz, S. (1996). *The Journal of Biological Chemistry,* **271** (25), 15182–15186.

Kellner, K., Liebsch, G., Klimant, I., Wolfbeis, O. S., Blunk, T., B.Schulz, M., & Gpferic, A. (2002). *Biotechnology and Bioengineering,* **80**, 73–83.

Kim, D.-H., Viventi, J., Amsden, J. J., Xiao, J., Vigeland, L., Kim, Y.-S., Blanco, J. A., Panilaitis, B., Frechette, E. S., Contreras, D., Kaplan, D. L., Omenetto, F. G., Huang, Y., Hwang, K.-C., Zakin, M. R., Litt, B., & Rogers, J. A. (2010). *Nature Materials,* **9**, 511–517.

Kissinger, P. T. (2005). *Biosensors and Bioelectronics,* **20**, 2512–2516.

Koivusalo, M., Kapus, A., & Grinstein, S. (2009). *The Journal of Biological Chemistry,* **284** (11), 6595–6599.

Komarova, S. V., Ataullakhanov, F. I., & Globus, R. K. (2000). *American Journal of Physiology - Cell Physiology,* **279**, C1220–C1229.

Koschwanez, H. E. & Reichert, W. M. (2007). *Biomaterials,* **28**, 3687–3703.

Kreft, O., Javier, A. M., Sukhorukov, G. B., & Parak, W. J. (2007). *Journal of Materials Chemistry,* **17**, 4471–4476.

Kurzweil, P. (2009). *Sensors,* **9**, 4955–4985.

Lee, J.-H., Lim, T.-S., Seo, Y., Bishop, P. L., & Papautsky, I. (2007). *Sensors and Actuators B,* **128**, 179–185.

Lee, S.-H. & Shin, H. (2007). *Advanced Drug Delivery Reviews,* **59**, 339–359.

Lee, Y.-E. K., Smith, R., & Kopelman, R. (2009). *Annual Reviews Analytical Chemistry,* **2**, 57–76.

Lehmann, M. & Baumann, W. (2005). *Experimental Cell Research,* **305**, 374–382.

Li, C. M., Dong, H., Cao, X., Luong, J. H., & Zhang, X. (2007). *Current Medicinal Chemistry,* **14**, 937–951.

Lim, M., Ye, H., Drakakis, E. M., Yue, X., Cass, A. E., Panoskaltsis, N., & Mantalaris, A. (2008). *Biochemical Engineering Journal,* **40**, 1–7.

Lim, M., Ye, H., Panoskaltsis, N., Drakakis, E. M., Yue, X., Cass, A. E., Radomska, A., & Mantalaris, A. (2007). *Biotechnology Advances,* **25**, 353–368.

Lin, K.-I., Chattopadhyay, N., Bai, M., Alvarez, R., Dang, C. V., Baraban, J. M., Brown, E. M., & Ratan, R. R. (1998). *Biochemical and Biophysical Research Communications,* **249**, 325–331.

Lin, Z., Cherng-Wen, T., Roy, P., & Trau, D. (2009). *Lab on a Chip,* **9**, 257–262.

Liu, J., Barradas, A., Fernandes, H., Janssen, F., Papenburg, B., Stamatialis, D., Martens, A., van Blitterswijk, C., & de Boer, J. (2010). *Tissue Engineering: Part C,* **16** (3), 479–485.

Logeart-Avramoglou, D., Oudina, K., Bourguignon, M., Delpierre, L., Nicola, M.-A., Bensidhoum, M., Arnaud, E., & Petite, H. (2010). *Tissue Engineering: Part C,* **16** (3), 447–458.

Lorget, F., Kamel, S., Mentaverri, R., Wattel, A., Naassila, M., Maamer, M., & Brazier, M. (2000). *Biochemical and Biophysical Research Communications,* **268**, 899–903.

Luo, Y. & Prestwich, G. D. (2001). *Expert Opinion on Therapeutic Patents,* **11** (9), 1395–1410.

Luque, G. L., Ferreyra, N. F., & Rivas, G. A. (2007). *Talanta,* **71**, 1282–1287.

Maharbiz, M. M., Holtz, W. J., Howe, R. T., & Keasling, J. D. (2004). *Biotechnology and Bioengineering,* **85** (4), 376–381.

Malda, J., Klein, T. J., & Upton, Z. (2007). *Tissue Engineering,* **13** (9), 2153–2162.

Marazuela, M. D. & Moreno-Bondi, M. C. (2002). *Analytical and bioanalytical chemistry,* **372**, 664–682.

Maria, C. A. D., Bogoyevitch, M. A., McKitrick, D. J., Arnolda, L. F., Hool, L. C., & Arthur, P. G. (2009). *Journal of Molecular and Cellular Cardiology,* **47**, 49–56.

Marxer, S. M. & Schoenfisch, M. H. (2005). *Analytical Chemistry,* **77**, 848–853.

Mason, C. & Hoare, M. (2007). *Tissue Engineering,* **13** (2), 301–311.

Mather, M. M., Morgan, S. P., & Crowe, J. A. (2007). *Regenerative Medicine,* **2** (2), 145–160.

Medlock, K., Harmer, H., Worsley, G., Horgan, A., & Pritchard, J. (2007). *Analytical and bioanalytical chemistry,* **389**, 1533–1539.

Mishra, A. & Starly, B. (2009). *Microfluidics and Nanofluidics,* **6**, 373–381.

Nakade, O., Takahashi, K., Takuma, T., Aoki, T., & Kaku, T. (2001). *Journal of Bone and Mineral Metabolism,* **19**, 13–19.

Obradovic, B., Carrier, R. L., Vunjak-Novakovic, G., & Freed, L. E. (1999). *Biotechnology and Bioengineering,* **63** (2), 197–205.

O'Hare, D., Parker, K. H., & Winlove, C. P. (2006). *Medical Engineering & Physics,* **28**, 982–988.

ONeill, C. A. & Galasko, C. S. B. (2000). *Calcified Tissue International,* **67**, 53–59.

Orlowski, J. & Grinstein, S. (1997). *The Journal of Biological Chemistry,* **272**, 22373pp.

Patel, S. D., Papoutsakis, E. T., Winter, J. N., & Miller, W. M. (2000). *Biotechnology Progress,* **16**, 885–892.

Pedersen, P. L. (1994). *Current Biology,* **4** (12), 1138–1141.

Peng, C. & Palsson, B. (1996). *Annals of Biomedical Engineering,* **24** (3), 373–381.

Poghossian, A., Ingebrandt, S., Offenhusser, A., & Schning, M. (2009). *Seminars in Cell & Developmental Biology,* **20**, 41–48.

Poole, R. & Halestrap, A. (1993). *American Journal of Physiology,* **264** (4 Pt 1), C761–C782.

Porter, J. R., Ruckh, T. T., & Popat, K. C. (2009). *Biotechnology Progress,* **25** (6), 1539–1560.

Qiu, K., Zhao, X. J., Wan, C. X., Zhao, C. S., & Chen, Y. W. (2006). *Biomaterials,* **27**, 1277–1286.

Radomska, A., Singhal, S., Ye, H., Lim, M., Mantalaris, A., Yue, X., Drakakis, E. M., Toumazou, C., & Cass, A. E. (2008). *Biosensors and Bioelectronics,* **24**, 435–441.

Rolfe, P. (2006). *Measurement Science and Technology,* **17**, 578–583.

Romani, A. (2007). *Archives of Biochemistry and Biophysics,* **458**, 90–102.

Romero, M. R., Ahumada, F., Garay, F., & Baruzzi, A. M. (2010). *Analytical Chemistry,* **82**, 5568–5572.

Ruffieux, P.-A., von Stockar, U., & Marison, I. W. (1998). *Journal of Biotechnology,* **63**, 85–95.

Schneider, M., Marison, I. W., & von Stockar, U. (1996). *Journal of Biotechnology,* **46**, 161–185.

Schop, D., Janssen, F. W., van Rijn, L. D., Fernandes, H., Bloem, R. M., de Bruijn, J. D., & van Dijkhuizen-Radersma, R. (2009). *Tissue Engineering Part A,* **15**, 1877–1885.

Starly, B. & Choubey, A. (2007). *Annals of Biomedical Engineering,* **36** (1), 30–40.

Stasio, E. D. (2004). *Biophysical Chemistry,* **112**, 245–252.

Sterling, D. & Casey, J. R. (2002). *Biochemistry and Cell Biology,* **80**, 483–497.

Storrie, H. & Stupp, S. I. (2005). *Biomaterials,* **26**, 5492–5499.

Sukhorukov, G. B., Rogach, A. L., Garstka, M., Springer, S., Parak, W. J., Munoz-Javier, A., Kreft, O., Skirtach, A. G., Susha, A. S., Ramaye, Y., Palankar, R., & Winterhalter, M. (2007). *Small,* **3** (6), 944–955.

Suzuki, H., Arakawa, H., Sasaki, S., & Karube, I. (1999). *Analytical Chemistry,* **71**, 1737–1743.

Thomas, P. C., Halter, M., Tona, A., Raghavan, S. R., Plant, A. L., & Forry, S. P. (2009). *Analytical Chemistry,* **81**, 9239–9246.

Tsao, Y.-S., Cardoso, A., Condon, R., Voloch, M., Lio, P., Lagos, J., Kearns, B., & Liu, Z. (2005). *Journal of Biotechnology,* **118**, 316–327.

Utting, J., Robins, S., Brandao-Burch, A., Orrissa, I., Behar, J., & Arnett, T. (2006). *Experimental Cell Research,* **312**, 1693–1702.

Vogler, E. A. (1998). *Advances in Colloid and Interface Science,* **74**, 69–117.

Vojinovic, V., Cabral, J., & Fonseca, L. (2006). *Sensors and Actuators B,* **114**, 1083–1091.

Vunjak-Novakovic, G. & Kaplan, D. L. (2006). *Tissue Engineering,* **12** (12), 3261–3263.

Walker, G. M. (1994). *Critical Reviews in Biotechnology,* **14** (4), 311–354.

Wang, J. (2001). *Electroanalysis,* **13** (12), 983–988.

Wang, J. (2008). *Chemical Reviews,* **108**, 814–825.

Wang, M., Yao, S., & Madou, M. (2002). *Sensors and Actuators B,* **81**, 313–315.

Wiley, C. & Beeson, C. (2002). *Analytical Biochemistry,* **304**, 139–146.

Wilson, G. S. & Gifford, R. (2005). *Biosensors and Bioelectronics,* **20**, 2388–2403.

Wisniewski, N. & Reichert, M. (2000). *Colloids and Surfaces B: Biointerfaces,* **18**, 197–219.

Woodruff, M. A. & Hutmacher, D. W. (2010). *Progress in Polymer Science,* **Article in press**, Corrected Proof.

Wu, M.-H., Lin, J.-L., Wang, J., Cui, Z., & Cui, Z. (2009). *Biomed Microdevices,* **11**, 265–273.

Yang, L. & Zhang, E. (2009). *Materials Science and Engineering C,* **29**, 1691–1696.

Yang, Y. & Balcarcel, R. R. (2004). *BioTechniques,* **36**, 286–295.

Yu, B., Wang, C., Ju, Y. M., West, L., Harmon, J., Moussy, Y., & Moussy, F. (2008). *Biosensors and Bioelectronics,* **23**, 1278–1284.

Yun, Y., Dong, Z., Lee, N., Liu, Y., Xue, D., Guo, X., Kuhlmann, J., Doepke, A., Halsall, H. B., Heineman, W., Sundaramurthy, S., Schulz, M. J., Yin, Z., Shanov, V., Hurd, D., Nagy, P., Li, W., & Fox, C. (2009). *Materials Today,* **12** (10), 22–32.

Zhang, F., Ali, Z., Amin, F., Feltz, A., Oheim, M., & Parak, W. J. (2010). *ChemPhysChem,* **11**, 730–735.

Zhao, P. & Cai, W.-J. (1997). *Analytical Chemistry,* **69**, 5052–5058.

This page is intentionally left blank

Chapter 3

The Osteoblastic Ionic Extracellular Environment

3.1 Introduction

3.1.1 Bone Tissue

Bone tissue is the great mineral reserve of our bodies, constituting 98% of all calcium in the body. While its most obvious function is to form and shape the body by providing mechanical strength and leverage for motion, it also has an important heamopoietic role, as the bone marrow contains pluripotent stem cells able to differentiate into a variety of blood cells (Herzog *et al.*, 2003).

Bone, like all other tissue, is composed of cells and extracellular matrix, which both play important and specific roles to maintain the bone tissue healthy and functional. This is accomplished by complex and dynamic processes that constantly degrade and rebuild our skeleton. For example, it is estimated that in an adult of 20 to 30 years, about 10% of the total bone mass is completely renewed every year (Manolagas, 1999). With time, the equilibrium of creation and destruction is skewed, resulting in a loss of bone mass every year.

Simplified, the mission of bone cells is to fabricate an extracellular matrix with mechanical strength as high as possible while the weight of the matrix is maintained as low as possible. This is achieved by bone cellular production of large amounts of organic material, mainly collagen type 1, but also some ground substance (being mainly proteoglycans). Individual collagen monomers are rapdily polymerised to form collagen fibers, and their localisation within the matrix along the lines of tensile force provide strength.

Their mechanical properties are further improved by crystalline salts, principally composed of calcium and phosphate, which precipitate on the surface of the collagen fibers to add hardness. These precipitates first appear at intervals along each collagen fiber, forming minute nidi that rapidly grow over a period of weeks into the finished product which is hydroxyapatite (HA), $Ca_{10}(PO_4)_6(OH)_2$. Hydroxyapatite can then conjugate other ions to its crystal, among them magnesium, sodium, potassium, and carbonate to reinforce itself (Porter *et al.*, 2008). The combination of directed, pliable collagen fibers and hard mineral provide bone tissue with mechanical properties to withstand great forces of all kinds: pression, torsion, and flexion (Burger *et al.*, 2008).

The major cell types present in bone tissue are: *osteoblasts*, *osteocytes*, and *osteoclasts*. Between these cells exists a complex relationship which allows the skeleton to be continuously remodelled throughout life via the breakdown of older osteons (see Figure 3.1) and the replacement with new ones.

- **Osteoblasts** are of mesenchymal origin, arising primarily from stromal cells found in the bone marrow, which under appropriate influence of growth factors and other stimuli, evolve into more differentiated osteoblasts (see Aubin & Triffitt (2002)). They are fusiform, cuboidal, polyhedral, or spherical cells located at the surface of a forming bone (see Figure 3.1) where they are involved in bone deposition through an ordered expression of genes that control synthesis, deposition, and mineralisation of the organic matrix of bone. These cells are polarised with the basolateral plasma membrane facing the bone marrow and the apical plasma membrane facing the forming bone.

  The phenotypical characterisics of osteoblasts include synthesis and expression of collagen type I, bone sialoprotein, osteopontin, osteonectin, osteocalcin, and cell membrane enzymes and receptors such as alkaline phosphatase and vitamin D receptor (Triffitt, 2002). After fulfilling their secretory activity, osteoblasts undergo either apoptosis (about 80%) or terminal differentiation to osteocytes (about 20%). *In vivo* the osteoblast pool is normally replaced continuously through differentiation of pre-osteoblasts.

- **Osteocytes** are quiescent osteoblasts encased in mineralised matrix that communicate with each other by cytoplasmic processes within interconnecting channels (canaliculi) in the matrix (see Figure 3.1). They maintain the osseaous matrix, participate in extracellular ex-

changes and are involved in the mechanotransduction (Marks & Popoff, 1988). Morphologically, osteocytes resemble osteoblasts in every respect, and biochemically they produce the same proteins as fully mature osteoblasts. However, as more mineral is laid down and osteocytes become encased deeper within the matrix, biochemical and morphological changes gradually occur that distinguish them from their precursors. As a result of the decreased synthetic capacity and cytoplasmic volume, the nuclei become the most prominent ostecytic cellular feature.

- **Osteoclasts** are the only cells known to resorb bone. They are large, multinucleated cells formed by the fusion of precursor cells which are derived from the same hematopoietic lineage as monocytes (Asagiri & Takayanagi, 2007). As the only cells truly embedded in the bone ECM, they reside in the mineralizing bone matrix during the process of bone formation (Burger *et al.*, 2008). To fulfill their purpose, i.e. to dissolve HA, acidification of their local environment is a key requirement, which is achieved by secretion of HCl (Leinonen, 2008). Extracellular pH may thus be regarded as a major osteoclast activation factor (Arnett, 2008).

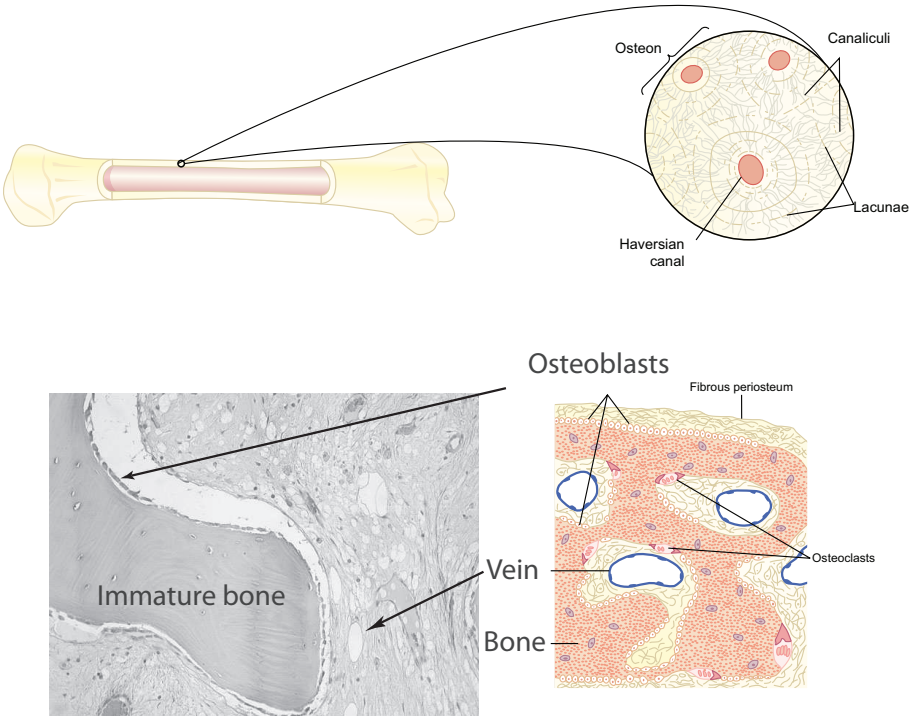

Figure 3.1: Schematic and histological view of bone tissue. Illustrations adapted from Guyton & Hall (2005), and histological image provided by Patrica Paz.

3.1.2 Life of an Osteoblast

The osteoblast differentiation process spans over several weeks, terminating with an induction of biological mineralisation. The molecular and cellular events required to produce mineralised bone are only partially known, and the temporal and spatial coordination of these events is even less understood. Nevertheless, the process is generally divided into three distinct stages: (1) *proliferation*, (2) *matrix maturation*, and (3) *mineralisation* by formation of hydroxyapatite (Figure 3.2). During this period, a number of genes are expressed for discrete periods of time, producing different proteins and biochemical signals that together provide conditions for mineralisation to occur.

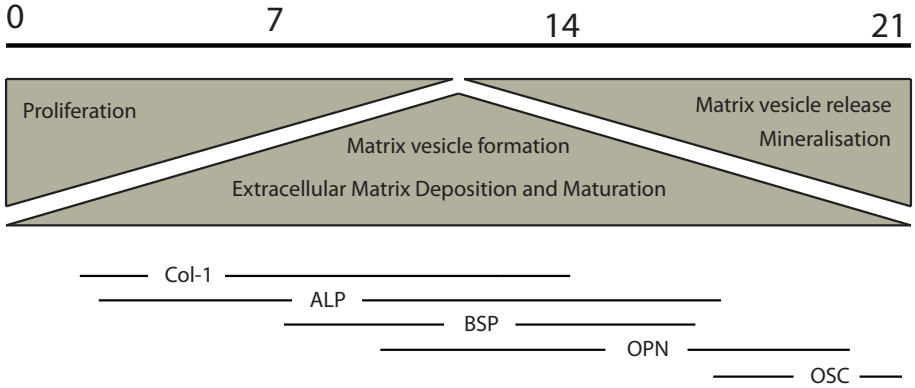

Figure 3.2: Osteoblastic cell functions with time. Image adapted from Beck (2003).

In the early phase of *in vitro* osteoblast culture systems, cells strive to become confluent and proliferation-associated markers (e.g. H4 histone) are expressed (Arnett & Henderson, 1998, p.10). Osteoblasts rapidly start to secrete collagen that accumulates in the extracellular matrix, and it is not until the very end of the differentiation process (beyond day ≈20), that collagen production is significantly downregulated (McQuillan *et al.*, 1995). In parallel to collagen production, the activiy of alkaline phosphatase (ALP) quickly rises in the early phase. ALP is a membrane bound enzyme situated so that the catalytic subunit is extracellular, but it can also be secreted into the matrix via small membrane-derived vesicles (Morris *et al.*, 1992). ALP expression is furthermore correlated with cell cycle as it increases during G_1 and S, and decreases during G_2/M or G_0, which indicates that when cells do not proliferate any more, ALP activity ceases (Fedarko *et al.*, 1990). Since its discovery in 1923, the function of this enzyme in osteoblast differentiation has been somewhat debated, and numerous functions of it have been proposed

(Bilezikian *et al.*, 2008). It is well established that ALP can hydrolyse organic phosphate (such as β-glycerophosate, β-GP) into inorganic phosphate (P_i) and thereby provide a source of phosphate that can be used for cellular mineralisation events (Chung *et al.*, 1992). As pointed out by Beck (2003), the ability of inorganic phosphate to substitute for both ALP activity and β-GP supplementation in the mineralisation process argues that one critical function is to locally increase inorganic phosphate levels.

During the middle stages of the differentiation process, but before mineralisation occurs, osteoblasts also starts to express various bone-specific proteins, among them bone sialoprotein (BSP) and osteopontin (OPN). Both BSP and OPN contains the amino acid sequence of Arg-Gly-Asp (RGD) which binds to the vitronectin-type intergrin receptor of osteoblasts (Baht *et al.*, 2008; Allori *et al.*, 2008b), and which proposes that these proteins may have roles in mediating cell attachment to bone matrix. Both proteins may influence the regulation of hydroxyapatite crystal growth, either as inhibitor (Boskey *et al.*, 1993) or promotor (Hunter & Goldberg, 1993).

To advance to the final stage of the osteoblast differentiation process three fundamental conditions have to be fulfilled (Figure 3.3). One of these is the presence of collagen to act as the structural framework for mineral deposition. Another requirement is the presence of phosphate (Murshed *et al.*, 2005), which normally is not a problem since bone ECM is supersaturated on both calcium and phosphate (Neuman & Neuman, 1958, Ch.2). The ECM however contains many mineralisation inhibitors (Boskey, 1996), among them inorganic pyrophosphate (PP_i) which is known to bind rapidly to newly formed mineral crystals and thereby prohibit further incorporation of phosphate ions into the crystal. PP_i further upregultes OPN expression, and inhibits ALP activity (Addison *et al.*, 2007). ALP is capable of ezymatic removal of PP_i (Terkeltaub, 2001), and for mineralisation to occur the balance between nucleation inhibitors and promoters must favor mineralisation.

When above conditions are fulfilled, mineralisation of the osteoid takes place. Nevertheless, the exact pathway through which ions are translocated from blood serum to the site of deposition in the extracellular matrix is not fully clear. Distinct modes of action have been proposed. In one of them, matrix vesicles (MVs) are released from osteoblasts into the ECM to act as initial sites of hydroxyapatite mineral formation. Those MVs, which range from 30 to 300 nm in diameter, may be found in both cartilage and bone tissue, and contains many different proteins, among them annexins and peptidases (Xiao *et al.*, 2007). The biogenesis of them is poorly understood. It has been suggested that amorphous calcium phosphate is formed inside the vesicles in a protected environment (Wu *et al.*, 1997). More recently it has

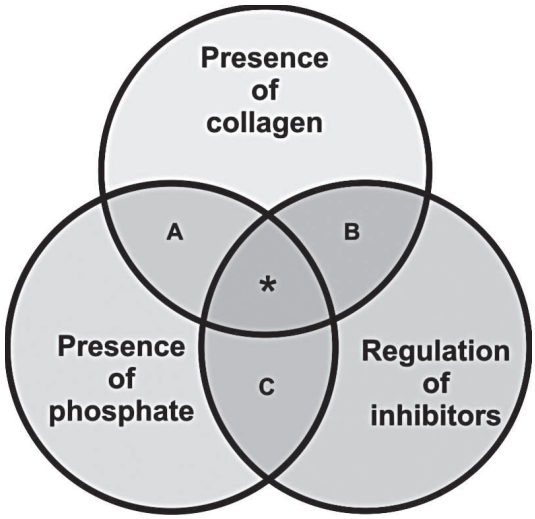

Figure 3.3: The fundamental factors for mineralisation to occur. Image adapted from Allori *et al.* (2008a).

been proposed that cellular mechanisms gradually enrich the phosphate-rich vesicles with calcium (Mahamid *et al.*, 2011). After being released from the cells, and once the crystals have reached a certain size, the vesicle membrane is ruptured and the crystals grow out into the extracellular matrix. It has been shown that these MVs origin from microvilli from the apical plasma membrane in hypertrophic chondrocytes (Hale & Wuthier, 1987), as well as in osteoblasts (Thouverey *et al.*, 2009).

The initial calcium salts to be deposited in the ECM are normally not hydroxyapatite crystals but rather amorphous compounds (noncrystalline), typically a mixture of $CaHPO_4$ x $2\,H_2O$, $Ca_3(PO_4)_2$ x $3\,H_2O$, and others (Guyton & Hall, 2005, Ch.79). Then by a process of substitution and addition of atoms, or reabsorbtion and reprecipitation, these salts are converted into hydroxyapatite crystals over a period of weeks or months. However, a few per cent remain permanently in the amorphous form which can be rapidly absorbed when there is need for extra calcium in the extracellular fluid.

After the onset of mineralisation, osteoblasts continue to express bone-specific proteins. One such protein is osteocalcin (OCN) which is characterised by its γ-carboxyglutamic acid residues, and also known as bone Gla protein. OCN is both released into circulation, and incorporated into the bone matrix. In presence of calcium, the γ-carboxyglutamic acid residues allow specific conformational changes in the protein, which in turn promotes osteocalcin to bind to bone minerals with consequent accumulation in the matrix (Chenu *et al.*, 1994; Fassina *et al.*, 2005). Its exact function is un-

known at present, and although the OCN-gene only has been identified in osteoblasts, the protein is not an absolute requirement for mineralisation, but should rather be considered as a late marker of mature osteoblasts. *In vitro* experiments however show that osteocalcin has chemotactic activity for a number of cells, including monocytes which are known to be related to osteoclast precursor cells, and it has been proposed that OCN has a potential role in the induction of bone resporption (Mundy & Poser, 1983; Chenu *et al.*, 1994).

Another bone-related protein synthesised by mature cells of the osteoblastic lineage is osteonectin (ON), or SPARC. This protein is 10000 times more abundant in bone tissue than in other connective tissue. Osteonectin was given its name (osteonectin = bone connector) due to its strong affinity for both collagen, hydroxyapatite, and calcium (Kelm *et al.*, 1994). Its specific function is still unknown, and it has been shown to act both as a promotor and inhibitor of mineralisation (Romberg *et al.*, 1986; Boskey, 1996).

In Table 3.1 are summarised the main components of mammalian bone tissue.

CELLS		
Osteoblasts	Synthesis and regulation of bone ECM deposition and mineralisation.	
Osteocytes	Calcification of the osteoid matrix. Blood-calcium homeostasis.	
Osteoclasts	Bone resorption.	
ORGANIC MATERIAL		
Fibrinous proteins $\approx$ 90%	Collagen type I	Provide tensile strength Framework for skeletal structure
Non-fibrinous proteins $\approx$ 10%	Bone sialoprotein (BSP)	Adhesion; Constituent of cement line
	Osteopontin (OPN)	Adhesion Constituent of cement line Involved in bone remodelling
	Osteocalcin (OCN)	Inhibitor of nucleation Involved in bone remodeling
	Osteonectin (ON)	Enhance mineral deposition Binds Ca^{2+} and collagen
	Fibronectin (FN)	Adhesion, mechanochemical signaling
	Matrix Gla Protein (MGP)	Inhibitor of nucleation
Proteoglycans	Chondroitin sulfate Hyaluronic acid Dermatan sulfate Byglican	Compressive strength
Enzymes	Alkaline phosphatase (ALP)	$\uparrow$ P_i Regulate inhibitor
	Matrix metalloproteinases (MMPs)	
Growth factors	Tumour Growth Factor-β (TGF-β) Bone morphogenic protein (BMP)	
Cytokines		
INORGANIC MATERIAL		
Mineral	Hydroxyapatite (HA) HA-precursors	Mechanical resistance

Table 3.1: The main components of bone tissue. Partly adapted from Salgado *et al.* (2004).

3.1.3 *In Vitro* Osteoblast-like Model Systems

Osteoblast-like culture model systems fall into two main categories: *primary* cell cultures, or cloned *cell lines* (Table 3.2). Primary osteoblast models can be derived from different sites (typically trabecular bone or calvariae) and from different species, among which the most common ones include rat and human (Table 3.2). A major part of *in vitro* cell culutres are however performed with cloned cell lines. On one hand, this may be considered as a step away from the *in vivo* state, but on the ohter hand, commercially available and established cell lines derived from normal or malignant cell cultures often exhibit a similar pattern and time frame of gene expression as compared to the fully mature osteoblastic phenotype. In addition, the heterogenous character and maturity of primary cells is avoided, which improves the phenotypic stability and reproducibility of the results. However, when working with cell lines one should be aware that marked differences between cell lines of the same phenotype may exist.

Osteoblasts can also be obtained by inducing differention of mesenchymal stem cells (MSCs). MSCs reside as adult stem cells at various sites in the body, for example in adipose tissue, blood, dermis, trabecular bone, and periosteum. The most common host and source of MSCs is however the bone marrow (Tuan *et al.*, 2002). As adult stem cells, MSCs have the potential to differentiate into a great variety of phenotypes, including chondrocytes, adipocytes, fibroblasts, and osteoblasts, all being of mesodermal lineage (Figure 3.4). Interestingly, transdifferentiation into phenotypes of endoderm and enctoderm lineages has also been achieved. (Jiang *et al.*, 2002).

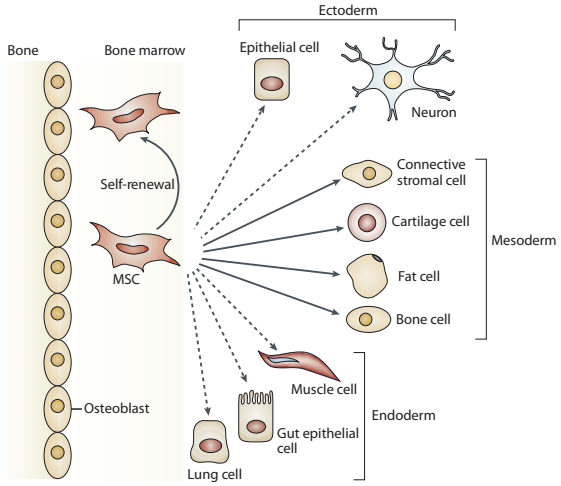

Figure 3.4: Lineage potential of mesenchymal stem cells. Image is adapted from Uccelli *et al.* (2008).

Primary culture models		
Human		Yamanouchi *et al.* (1997); ONeill & Galasko (2000) Beloti & Rosa (2005); Jones *et al.* (2007)
Pig		Eklou-Kalonji *et al.* (1998)
Rat		Chang *et al.* (2000); Dvorak *et al.* (2004) Hempel *et al.* (2004); Valerioa *et al.* (2004)
Cell lines		
Human	HOS TE-85	Clover & Gowen (1994); Habel & Glaser (1998)
	MG-63	Jukkola *et al.* (1993); Takamizawa *et al.* (2004) Gregory *et al.* (2004); Takagishi *et al.* (2006) Kim *et al.* (2007)
	OHS-4	Fournier & Price (1991)
	SAOS-2	Hale *et al.* (2000); Fassina *et al.* (2005) Ayers *et al.* (2006); Orimo & Shimada (2008) Thouverey *et al.* (2009)
	U2-OS	Abed & Moreau (2007)
Mouse	MC3T3-E1	Fratzl-Zelman *et al.* (1998); Balint *et al.* (2001) Beck (2003); Nakano *et al.* (2007) Xiao *et al.* (2007); Addison *et al.* (2007)
Rat	ROS 17/2.8	Mikami *et al.* (2007)
	UMR 106.06	Stanford *et al.* (1995); Hale *et al.* (2000)

Table 3.2: Examples of osteoblast-like cells (of different origins) that are commonly used to study cell differention (see indicated references). It is important to be aware of that slight differences in cellular behaviour may exist between these models.

3.1.3.1 Osteogenic medium

Both primary cells and established cell lines usually require specific *osteogenic* growth medium to be able to execute the full osteoblast differentiation program. This is especially true for MSCs which are severely dependent on the addition of certain osteogenic factors in order to develop towards the osteoblastic lineage (Tuan *et al.*, 2002). Among the most common osteogenic supplements are organic phosphate, ascorbic acid (AA), and dexamethasone. Other factors with demonstrated effect on osteoblast function include bone morphogenetic protein (BMP) and vitamin D (Arnett & Henderson, 1998).

Ascorbic acid is a water-soluble vitamin that has been observed to promote collagen maturation, influence cell growth and stimulate differentiation of osteoblasts and MSCs (Takamizawa *et al.*, 2004; Choi *et al.*, 2008). Being

a cofactor for the hydroxylation of proline and lysine residues of collagen, AA excerts a direct effect on the deposited matrix rather than affecting osteoblastic gene expression.

The use of dexamethasone, a synthetic glucocorticoid, as a supplement to induce osteoblast differentiation is somewhat contradictory as this agent is known to cause severe bone loss (osteoporosis) *in vivo* (Reid, 1997). However *in vitro*, dexamethasone has been demonstrated to possess both positive and negative effect on osteoblast differentiation and mineralisation, depending on the level of cell maturity or cell density. For example, dexamethasone promotes phenotypic markers of osteoblast differentiation, such as alkaline phosphatase (ALP), osteopontin (OPN), osteocalcin (OC), and bone sialoprotein (BSP) (Yamanouchi *et al.*, 1997). Also, Mikami *et al.* (2007) demonstrated that *Runx2* transcriptional activity was increased in osteoblasts upon treatment with dexamethasone, and they speculated that this may be followed by activation of specific osteoblast genes.

While common rich growth media (such as DMEM, α-MEM, RPMI, McCoy's, etc) containing serum provide conditions for osteoblasts in long-term cultures to proliferate and progressively develop collagen matrix and express bone-specific proteins, *in vitro* mineralisation does not occur spontaneously. The failing component in this case is lack of phosphate (recall Figure 3.3). Therefore, osteogenic medium is elaborated to contain an additional source of phosphate, typically 5-10 mM of β-glycerophosphate (β-GP), which is hydrolysed by alkaline phosphatase into inorganic phosphate (P_i) and glycerol.

$$\beta - \text{glycerophosphate} + H_2O \rightarrow P_i + \text{glycerol} \tag{3.1}$$

Supplement	**Abbreviation**	**Working concentration**
β-glycerophosphate	β-GP	5-10 mM
Ascorbic acid	AA	50 μg/mL
Dexamethasone	Dex	1-100 nM

Table 3.3: Typical composition of osteogenic medium (Arnett & Henderson, 1998)

3.1.3.2 Assesment of *in vitro* mineralisaton

Mineralisation, the final stage of osteoblastic differentiation, can be assessed by a number of means. The fastest and most easy way is to evaluate calcium deposition in the extracellular matrix. An alternative would be to assay inorganic phosphate deposition but this approach is less adopted. Evaluation of calcium distribution in the ECM is routinely done by methods such as von Kossa staining (Fratzl-Zelman *et al.*, 1998), Alizarin red S (ARS) incorporation (Stanford *et al.*, 1995), o-cresolphthalein complexone method (Fujita *et al.*, 2001; Takagishi *et al.*, 2006), or through fluorescent calcein binding (Hale *et al.*, 2000). ARS staining is considered particularly versatile in the sense that the dye can be extracted from the stained monolayer and then quantified (Gregory *et al.*, 2004). Also fluorescence analyses of calcein bound to calcium phosphate can allow for direct quantitation of extracellular matrix mineral content in monolayer cultures of bone-forming cells.

Precise stoichiometric evaluation of calcium salts is however only achieved by more sophisticated techniques, e.g. Fourier-transform infrared (FTIR) spectroscopy, atomic adsorption spectroscopy (Chang *et al.*, 2000), energy-dispersive X-ray (EDX) spectroscopy, and micro-Raman spectroscopy (Gentleman *et al.*, 2009). Beside providing detailed information on chemical composition, the latter technique is also non-destructive and therefore can be applied to living cells and tissue.

3.1.4 The Ionic Extracellular Environment

From Section 3.1.2 it follows that the composition of the ionic extracellular environment (IEE) is important for osteoblasts to fully execute its differentiation program. Among the many ions that constitute the IEE, calcium and phosphate undoubtedly accentuate as the most fundamental ones in the bone formation process.

In blood serum there is about 2.5 mM of total calcium. This amount is distributed in three forms: *ionised*, *protein bound*, and *complexed* when united to citrate, phosphate, bicarbonate, or other anions. The ionised calcium is diffusible, the citrate calcium is not ionised but is also diffusible, while the calcium chelated to proteins (mainly albumin and globulin) is neither ionised nor diffusible (Figure 3.5). In the end, the free ionised calcium of blood serum is maintained at a very constant level ($\approx$ 1.4 mM).

The calcium-protein interaction is complex, depending on pH, temperature, protein structure, as well as the concentration of phosphate, carbonate, citrate, etc. Regarding pH, the calcium binding of proteins (albumin) in-

creases almost linearly with incresing pH up to about pH 8 as the carboxyl groups of proteins are being ionised and thus the electrostatic interaction is increased (Neuman & Neuman, 1958).

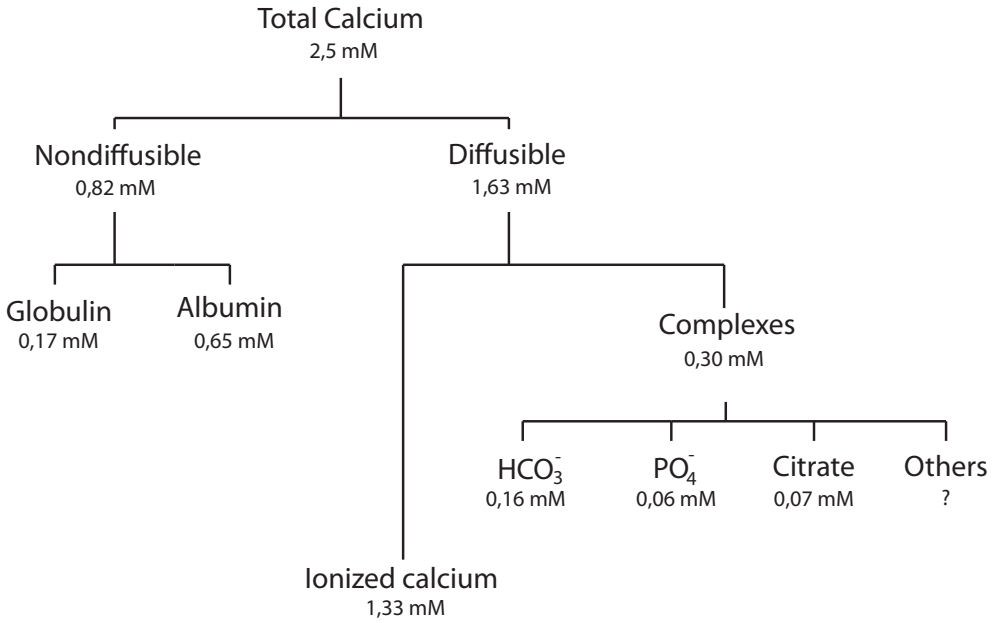

Figure 3.5: Calcium distribution in serum. Adapted from (Neuman & Neuman, 1958).

The distribution of inorganic phosphate in serum is less complicated than that of calcium. Protein-binding is negligible and except for a small fraction complexed by divalent ions ($\approx 12\%$) all the inorganic phosphate is ionised (Behari, 2009, p.26). Phosphorus exists in aqueous solutions in different forms of orthophosphate (3.2), and their distribution is pH dependant.

$$H_3PO_4 \leftrightarrow H_2PO_4^- \leftrightarrow HPO_4^{2-} \leftrightarrow PO_4^{3-} \tag{3.2}$$

While $H_2PO_4^-$ prevails in acidic conditions and ${HPO_4}^{2-}$ is more predominant under basic conditions, at a neutral pH both forms are present. In human serum, the relative distribution of orthophosphate is estimated to be 20% $H_2PO_4^-$ and 80% ${HPO_4}^{2-}$, but unlike serum calcium, it is difficult to precisely specify a normal value for the total inorganic phosphate of human serum as the phosphate concentration varies a great deal with age and metabolic state particularly. Normal variation is from 1-2 mmol/l.

3.2 Objective and Strategy

The objective of the work presented in this chapter was to understand how the *in vitro* ionic extracellular environment (IEE) might be influenced by osteoblast-like cell activity. For that purpose, it was used culture system comprised of three different osteoblast-like cell models: human osteosarcoma cell lines SAOS-2 and MG63 respectively, and mesenchymal stem cells derived from rat bone marrow. Each cell model was maintained in its specific cell culture medium, and the extracellular concentrations of Na^+, K^+, Ca^{2+}, and total inorganic phosphorus (P_i), as well as pH, were evaluated every second day during a period of three weeks.

The steps taken to characterise osteoblastic influence on the IEE were the following:

1. characterisation of the initial ionic composition of the three cell culture media used in the study,
2. evaluation of how different storage and preparation conditions influenced the ionic stability of the cell culture medium with time,
3. characterisation of the IEE of osteoblast cell cultures throughout a time range that covered cellular proliferation and differentiation events.

3.3 Materials and Methods

3.3.1 Preparation of Osteoblastic Culture Media

Three different basal cell culture media commonly used for osteoblast cultures have been used in this study: (1) Dulbecco's Modified Eagle's Medium (**DMEM**; Invitrogen 11960), (2) advanced Dulbecco's Modified Eagle's medium (**aDMEM**; Invitrogen 12491), and (3) McCoy's 5A Modified Medium (**McCoy**; Sigma, M8403). These media present differences in their chemical composition with respect to amino acid, vitamin, and glucose content. And as shown in Table 3.4, also the inorganic salt composition of McCoy and the both DMEMs is different.

McCoy's 5A		**DMEM & aDMEM**	
	[g/L]		[g/L]
$CaCl_2 \cdot 2\,H_2O$	0.132	$CaCl_2$ (anhydrous)	0.2
$MgSO_4$ (anhydrous)	0.098	$MgSO_4$ (anhydrous)	0.098
KCl	0.4	KCl	0.4
$NaHCO_3$	2.2	$NaHCO_3$	3.7
NaCl	6.5	NaCl	6.4
NaH_2PO_4 (anhydrous)	0.504	$NaH_2PO_4 \cdot H_2O$	0.125

Table 3.4: Inorganic salts content of the three different basal media, McCoy's and DMEMs respectively. For the record, the growth media also contain organic material, e.g. amino acids, vitamins, and glucose.

For optimal cell growth each medium was further supplemented with additional components according to Table 3.5; l-glutamine (Invitrogen, 25030-024), penicillin and streptomycin (Invitrogen, 15140-122), sodium pyruvate (Invitrogen, 11360-039), and foetal bovine serum (FBS) (Invitrogen, 10270-106). This preparation was based on previous experience and protocols derived in our own laboratory.

For induction of bone differentiation, osteogenic medium was prepared by supplementing abovementioned cell culture media with 50μg/mL ascorbic acid (AA; Sigma, A4034), 10 mM β-glycerophosphate (β-GP; Sigma, G9891), and 10^{-8} M dexamethasone (Dex; Sigma, D8893). AA was dissolved in ultrapure water (5.0 mg/mL), Dex in 2% ethanol (5.2×10^{-5} M), and β-GP in Phosphate Buffered Saline (PBS) (1 M). The solutions were filtered (0.22 μm) before being diluted into the cell culture medium to yield the desired concentrations (see Table 3.5).

Component	**DMEM**	**aDMEM**	**McCoy**
Base media	97%	98%	96.25%
l-glutamine	1%	1%	0.75%
Penicillin/Streptomycin	1%	1%	1%
Sodium pyruvate	1%	-	2%
FBS	10%	15%	15%
Ascorbic acid	$\leftarrow$ 50 μg/mL $\rightarrow$		
Dexamethasone	$\leftarrow$ 10^{-8} mol dm^{-3} $\rightarrow$		
β-GP	$\leftarrow$ 10^{-2} mol dm^{-3} $\rightarrow$		

Table 3.5: Cell culture medium formulations.

3.3.2 Measuring Ions in Culture Medium

Ion-selective electrodes being part of an automated and temperature controlled analyser (ILyte Na/K/Ca/pH, Instrumentation Laboratory), especially designed for flow-through measurements of serum, plasma, and whole blood were used to analyse ionic composition of cell culture medium and supernatants of osteoblast cell cultures.

Each analysis required approximately 100 μL of sample, and took about one minute to perform. The analyser was equipped with four separate electrodes (see Table 3.6) plus one common reference electrode, and applied a comparative method of measurement. First, the analyser measured the potential developed when the sample was pumped through the electrodes. Thereafter a standard solution was automatically pumped through the electrodes and the difference between the two potentials was related logarithmically to the concentration of ions in the sample according to the Nernst equation [1].

To assure proper readings, the analyser was calibrated daily using separate buffer solutions provided by the manufacturer. Also, three standard test solutions with *low*, *high*, and *normal* levels of each ion were used to confirm the correct functioning of each electrode (Standard solutions, Instrumentation Laboratory). After finishing a series of measurements, the instrumentation was cleaned using a solution containing protelytic enzymes (Calcium rinse solution kit, ME002118, Instrumentation Laboratory).

[1]For details on potentiometric ion measurements, see Chapter 6.

Ion	Selective element	Detection range	Resolution
Na^+	Glass	20 - 200 mmol/L	0.1 mmol/L
K^+	Valinomycin	0.2 - 40 mmol/L	0.01 mmol/L
Ca^{2+}	Neutral carrier	0.1 - 6.0 mmol/L	0.01 mmol/L
pH	Glass	6.0 - 8.0 units	0.005 units

Table 3.6: Characteristics of ion selective electrodes used for assessment of ions in cell culture medium.

3.3.3 Measuring Total Phosphorus of Culture Medium

Determination of total inorganic phosphorus (P_i) in cell culture medium samples was done using the method developed by Chen *et al.* (1956), which allows for orthophosphate to react with molybdate to form phosphomolybdic acid ($PMo_{12}O_{40}{}^{3-}$) which is an anion with α-Keggin structure. The $PMo_{12}O_{40}{}^{3-}$ can be further reduced to form a phosphomolydate complex, $PMo_{12}O_{40}{}^{7-}$ (reaction 3.3), which has a blue-coloured β-Keggin structure. The amount of reduced phoshomolybdate complex in the sample is directly proportional to the amount of total orthophosphate present in the assayed sample, and can be measured colourimetrically.

$$PMo_{12}O_{40}^{3-} + \text{reducing agent} \rightarrow PMo_{12}O_{40}^{7-} \tag{3.3}$$

In detail, cell culture medium samples were diluted in distilled water 15 or 30 times before mixed (1:1) with a reagent consisting of one volume $6N$ sulphuric acid (H_2SO_4), 2 volumes of ultrapure water, 1 volume of 2.5% ammonium molybdate ($(NH_4)_6Mo_7O_{24}{\cdot}4\,H_2O$, Sigma 13301), and finally 1 volume of 10% ascorbic acid to work as reducing agent of the formed phosphomolybdic acid. After mixed, the samples were incubated at 37°C during two hours before phosphate concentrations were determined by molecular absorption spectrophotometry (UV-Vis Spectrophotometer Shimadzu, 820 nm, path length 1 mm). Standards prepared from NaH_2PO_4 or Na_2HPO_4 solutions in the concentration range 1.67×10^{-6} to 1.0×10^{-3} M were used to produce a calibration curve.

3.3.4 Ionic Profile of Cell Culture Media

The procedure of medium preparation was as follows. Samples of fresh medium that came from unopened bottles were aliquoted in Eppendorf tubes (1.5 mL), and supplemented with l-glutamine, pen/strep, sodium pyruvate, and FBS according to Table 3.5.

The aliquots were assayed for Na^+, K^+, Ca^{2+}, and pH under normal atmospheric conditions and at room temperature immediately after preparation using the method described in Section 3.3.2. Samples were then stored at -20°C and were, the day after, assayed for inorganic phosphorus according to Section 3.3.3.

3.3.5 Ionic Stability of Cell Culture Medium

To optimise conditions for long-term stability of cell culture medium with respect to its content of inorganic ions, it was evaluated how preparation and storage conditions influenced the ionic concentrations of the medium with time.

For this purpose, McCoy's 5A modified media was supplemented with l-glutamine, penicillin/streptomycin, and sodium pyruvate according to Table 3.5. One group of these samples was also supplemented with 15% FBS. Sterile aliquots of these two medium preparations (i.e. with and without FBS) were prepared in Eppendorf tubes and filled to its full volumetric capacity to avoid air inside the tube (500 μL). These aliquots were then stored either at 4°C or in a cell culture incubator with an atmosphere of 5% CO_2 and a temperature of 37°C. Then during a period of 15 days, three aliquots of each group were assayed every second day for Na^+, K^+, Ca^{2+}, pH and P_i.

3.3.6 Cell Sources and Standard Cell Maintenance

Three different osteoblast-like cell models have been used in this study; two human osteoblast-like cell lines (**SAOS-2** and **MG63**), and mesenchymal stem cells derived from rat (**rMSC**). The two cell lines, MG63 and SAOS-2, are both derived from osteosarcoma and were obtained from ATCC. Upon receive, these cells were treated in an identical manner, only difference being the cell culture media used. While MG63 cells were cultured in complete DMEM, SAOS-2 cells were cultured in complete McCoy's 5A media (see Figure 3.6).

Mesenchymal stem cells had previously been derived from bone-marrow from the long bones of young Lewis rats (2-4 weeks old). Harvested cells had been grown to confluency in 6-well tissue culture plates, and after that subcultured in T75-flasks using complete advanced DMEM before cryopreserved at passage 2. None of these steps were performed by the author of this thesis.

For any experiment, cryopreserved cells were thawed and subcultured at least one passage before used. Cells were initially plated into T25 or T75 culture flasks using complete medium of corresponding type. When

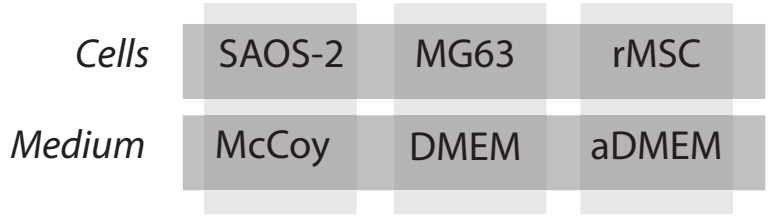

Figure 3.6: Throughout this thesis, each cell type has been consistently maintained in its corresponding medium if not otherwise mentioned.

reaching confluence, cells were incubated with a minimal volume of TrypLE Express (Gibco 12605) for five to ten minutes before the trypsin reagent was inactivated adding an equal amount of FBS plus another significant volume of supplemented media. The resulting volume was centrifuged during five minutes at 900 rpm before the supernatant was discarded and the cells were resuspended in fresh and complete medium. Cells were then counted using a Neubauer chamber to be resuspended for experiments at desired concentration.

3.3.7 Osteoblast Cell Cultures

To evaluate the influence of osteoblast activity on the composition of the ionic extracellular environment, MG63, SAOS-2, and rMSCs were grown in separate 24-well tissue culture wells during 21 days. Cells were seeded at a density of 30 000 cells per sample (=15 656 cells/cm^2) in 1.0 mL of complete medium that corresponded to the each cell type (Fig 3.6). The cell culture medium was renewed after about 24 hours from seeding, and from then on renewed every second day until the end of experiment. After five days in culture, one set of samples was provided osteogenic medium.

Upon medium renewal, 0.50 mL of supernatant was collected for ion analyses according to Sections 3.3.2-3.3.3. As a control, medium incubated under identical conditions but in absence of cells, was also collected and analysed. After assaying Na^+, K^+, Ca^{2+}, and pH, supernatants were frozen at -20°C before assayed for P_i (which was normally done within one or two days).

To assure stable initial ionic levels of cell cutlure media throughout the experiments, fresh base medium from unopened bottles was supplemented with basic factors (i.e., l-glutamine, pen/strep, and sodium pyruvate in the case of DMEM and McCoy, and l-glutamine and pen/strep in the case of aDMEM) the day before cell seeding. At that moment the prepared medium was aliquoted in 50 mL tubes and stored in the cell culture incubator at 5% CO_2 and at 37°C. To assure proper ionic composition throughout the full

experiment, new aliquots were prepared in the same way after about seven days. At the beginning of the experiment it was also prepared 15 mL-aliquots of FBS that were frozen at -80°C, as well as aliquots of β-glycerophosphate (1M), ascorbic acid (5 mg/mL) and dexamethasone (20 μg/mL) that were stored at -20°C until used. Addition of FBS and osteogenic factors was done just before addition to cell cultures. To be sure that the medium was well prepared, its ionic composition was analysed in conjunction with preparation.

3.3.8 Alizarin Red Staining

Calcium deposition in the extracellular matrix was detected using Alizarin red S (ARS) staining following the protocol proposed by Stanford *et al.* (1995). Briefly, after repeated rinsing with PBS, fixation of cell layers was done using ice-cold (absolute) ethanol at -20°C during at least one hour. For staining of calcium within fixed cell layers, a solution of 40 mM ARS (Sigma, A5533) was prepared in distilled H_2O, and its pH was adjusted to 4.1 by addition of concentrated NH_3. Rinsed cell layers were then incubated with ARS at room temperature for 10 minutes under gentle shaking. After incubation, cells were excessively, but carefully, rinsed repeatedly with dH_2O for removal of unincorporated dye.

Images of stained cell layers were taken using phase contrast or epifluorescence filter G-2A (excitation 510-560 nm, emission >590 nm) with an inverted microscope (Nikon TE200+, Olympus DP72). Quantification of incorporated ARS into the cell layers was done by extraction of ARS under moderate shaking during one hour in a solution of 10% cetylpyridinium chloride monohydrate (Sigma, C0732) which had been dissolved in 10 mM NaH_2PO_4 of pH of 7.1. Absorbance of the obtained solution was measured at 570 nm using a multi-plate spectrophotometer (BioTek PowerWave XS). The obtained data was expressed as a ratio between amount of extracted dye in cell layers provided osteogenic medium and amount of extracted dye in cell layers provided normal medium.

3.3.9 Alkaline Phosphatase Activity

Alkaline phosphatase (ALP) activity of cultured cells was assayed using the standard procedure of colourimetric evaluation of enzymatic conversion of p-nitrophenyl phosphate into p-nitrophenol (reaction 3.4). Although p-nitrophenyl phosphate is colourless, upon splitting off the phosphate group, the yellow salt of p-nitrophenol is liberated, and hence can be used as an indicator of the amount of splitting due to ALP activity.

$$\mathrm{p-nitrophenyl\ phosphate} + \mathrm{alkaline\ phosphatase} \rightarrow \mathrm{p-nitrophenol} \quad (3.4)$$

ALP activity was evaluated in SAOS-2, rMSC, and MG63 cells after nine days in culture (i.e., after four days with osteogenic medium). At that time, cells were rinsed with PBS, and then lysed during five minutes using a mammalian protein extraction reagent (M-PER, Thermo Scientific, 78501). The obtained lysis solution (200 μL) was collected and centrifuged for five minutes at 14000 rcf before stored at -20°C until further analysis.

To quantify ALP activity, samples were thawed and diluted in an alkaline buffer solution of 1.5M (Sigma, A9226). After addition of the phosphatase substraste (Sigma P5994), samples were incubated at 37°C during a time period of 5-30 minutes depending on the ALP activity of the sample. Colourimetric measurements were done at 405 nm and were repeated three times for one and the same sample, before compared to a calibration curve prepared from p-nitrophenol (Sigma, N7660) in the range of 0.06-1.0 mM. High ALP activity from SAOS-2 required dilution of samples ($\times$200).

Finally, from the same lysis solution, the amount of total protein was evaluated using the BCA^{TM} Protein Assay Kit (Pierce 23227). Basically, the samples were mixed (1:8) with the kit working reagent which allow for the biuret reaction (i.e. reduction of Cu^{2+} to Cu^{1+} by protein in an alkaline medium). Samples were incubated during two hours at 37°C before absorbance was measured at 562 nm. Obtained data was converted to amount of protein by comparing it to a standard curve prepared from albumin standards (0.025-2.0 mg/mL). This data was used to calculate the ALP activity, expressed in units of μmol min^{-1} (mg protein)$^{-1}$.

3.3.10 Influence of Cell Culture Medium on Osteoblast Activity

To decide the role of cell culture medium composition on osteoblast activity, MG63 cells and SAOS-2 cells were seeded in 24-well plates at a density of 30 000 cells/sample in their corresponding medium (Figure 3.6). However, after one day in culture the cell culture medium was renewed, and one set of samples with MG63 cells were from then on maintained in McCoy medium while another set continued to be cultured in DMEM medium. The same was done with SAOS-2 cells, i.e. SAOS-2 cultures were performed in either McCoy medium or in DMEM medium.

After five days in culture, one set of samples of MG63 and one set of samples of SAOS-2 in each medium were provided osteogenic factors in their

medium. At day eleven cell layers were fixed and stained with Alizarin Red according to Section 3.3.8.

3.3.11 Cellular Influence on the IEE at Different Total Volumes

To estimate the relative influence of osteoblast activity on the cell culture environment, this was measured varying the total volume of the environment. In detail, SAOS-2 cells were grown on porous polycarbonate membranes attached to specific inserts (Nunc, 137052). The inserts (10 mm diameter, pore size 0.4 μm) were initially located in separate wells of a standard 24-well culture plate, and were cared for as was described earlier in Section 3.3.7. However, at day 20 inserts were moved from the culture plate and placed in plastic tubes (15 mL). Each tube was filled with a different volume of osteogenic media (3-13 ml). The tap of the tube was loosely attached to allow for gas exchange, and cells were incubated for another 20 hours before 0.50 mL of supernatant was harvested and assayed according to Sections 3.3.2 and 3.3.3.

3.4 Results

3.4.1 Ionic Composition of Osteoblastic Culture Media

While concentrations of Na^+, K^+, Ca^{2+}, and pH of cell culture medium were measured using ion-selective electrodes, concentrations of inorganic total phosphorus was evaluated using the colourimetric molybden-ascorbic acid method (Figure 3.7). The calibration curve used to translate absorbance units to concentration of P_i is shown in Figure 3.8, and it reveals a linear relationship between the two units in the range 0.01 mM to 1.0 mM. This applied for both PO_4^{3-} and PO_4^{2-} ions. For example, with PO_4^{3-} ions, $y = 2.6064[P_i] + 0.0048$ with $R^2 = 0.999$ and $n = 12$.

The ionic composition of the different cell culture media is presented in Figure 3.9(a-c). Considering only the base media, i.e. without any supplements, it was observed that the ionic composition of DMEM and aDMEM was similar with respect to all investigated ions. The only marked differences were observed for calcium and phosphorus levels which were slightly higher in DMEM than in aDMEM. Much greater variation was however observed between the both DMEMs and McCoy medium. First, concentration of sodium was significantly lower in McCoy medium than in DMEMs (134.3 ± 1.1 mM in McCoy while 152.8 ± 0.55 mM in DMEM and 152.1 ± 0.16 mM in aDMEM). Second, concentration of calcium was more than halfed in McCoy medium compared to DMEM (0.64 ± 0.07 mM in McCoy, 1.46 ± 0.07 mM mM in DMEM, 1.35 ± 0.05 mM in aDMEM). And third, concentration of P_i was more than four times higher in McCoy medium than in DMEMs (4.49 ± 0.21 mM in McCoy, while 0.93 ± 0.07 mM in DMEM, and 0.82 ± 0.04 mM in aDMEM).

Among the different supplements added to cell culture medium it was FBS that induced the major changes in the ionic composition. In summary, upon adding supplements to any of the three base media it was observed an increase in potassium concentration (+19.7% in complete McCoy, +6.5% in complete DMEM, and +11.1% in complete aDMEM), and a strong decrease in total phopshorus (-57.2% for complete McCoy, -40.3% for complete DMEM, and -54.2% for complete aDMEM). For McCoy medium it was also observed how both sodium and calcium concentrations increased when adding FBS (+4.1% and +38.5%, respectively). The same effect was not observed in any of the both DMEM media. Rather the sodium concentration decreased upon addition of FBS, while the concentration of calcium maintained the same.

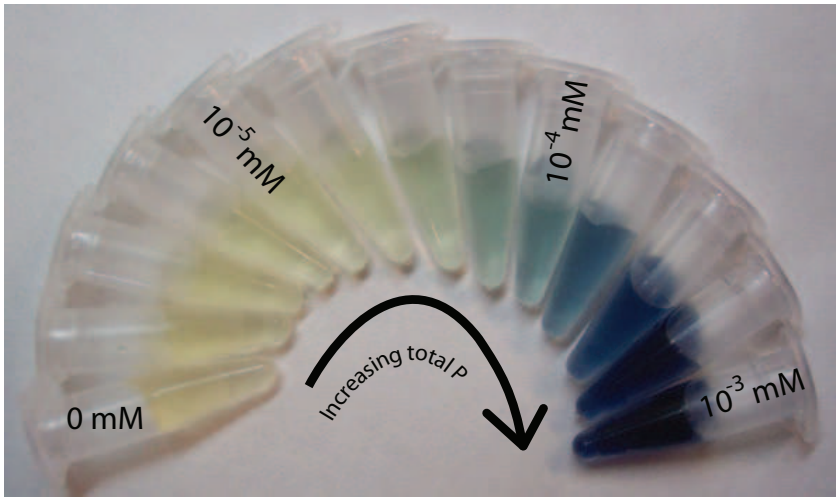

Figure 3.7: Colourimetric method for determination of total phosphorus.

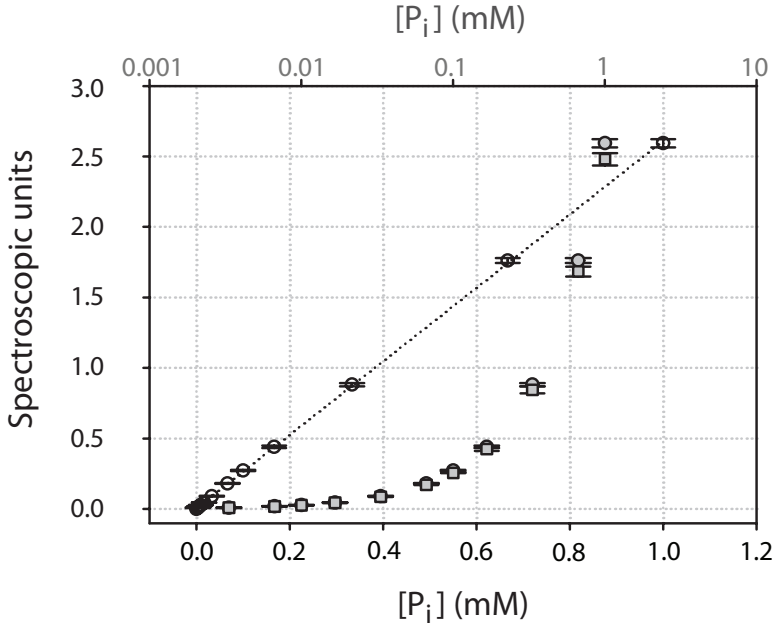

Figure 3.8: Calibration curve for quantification of total inorganic phosphorus using NaH_2PO_4 (∘) and Na_2HPO_4 (□). The data for NaH_2PO_4 is visualised twice: on a linear scale (empty ∘, bottom x-axis) and on a logarithmic scale (filled ∘, upper x-axis).

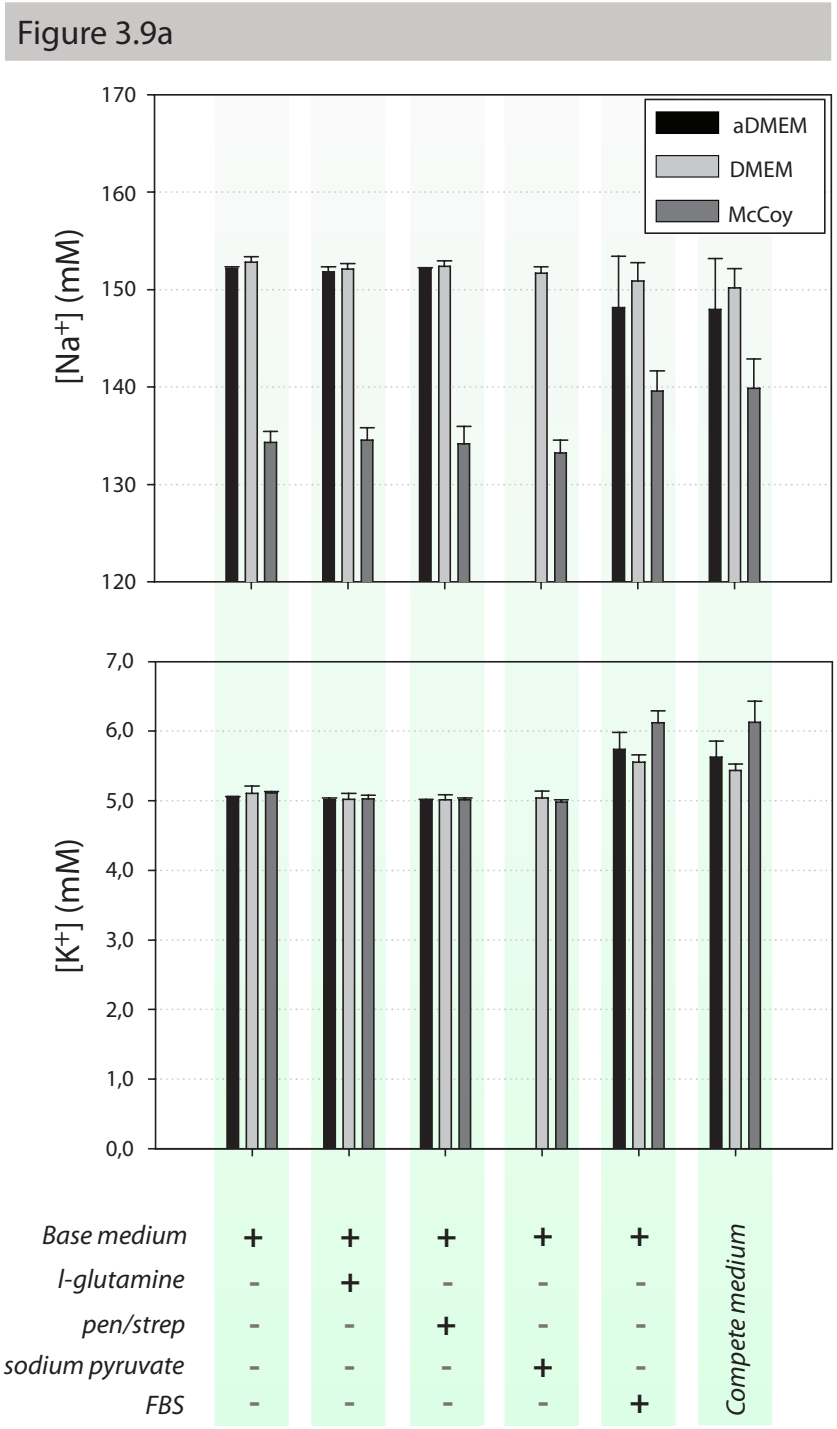

Figure 3.9: (a) Na^+ and K^+ concentration of osteoblastic cell culture media.

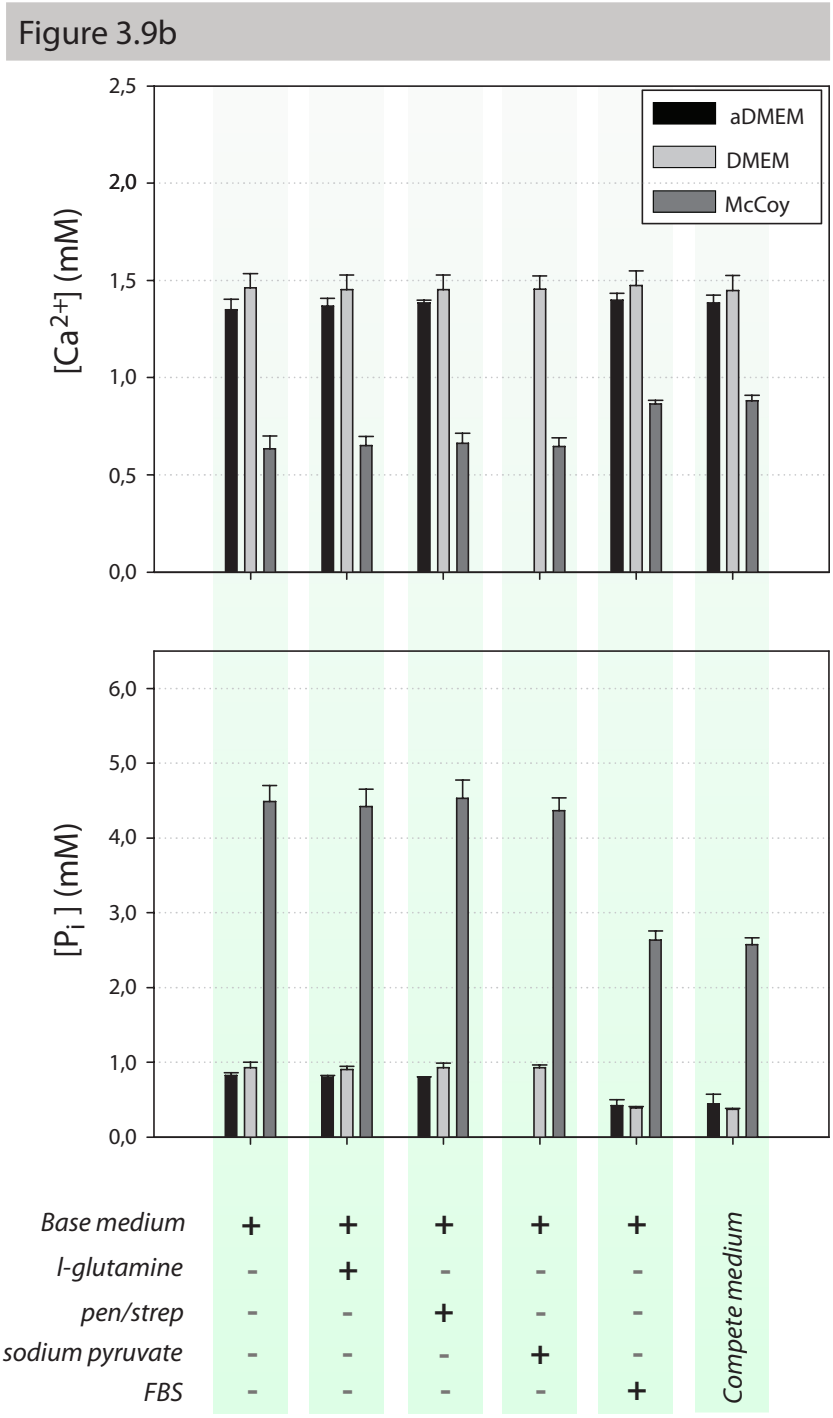

Figure 3.9: (b) Ca^{2+} and P_i concentration of osteoblastic cell culture media.

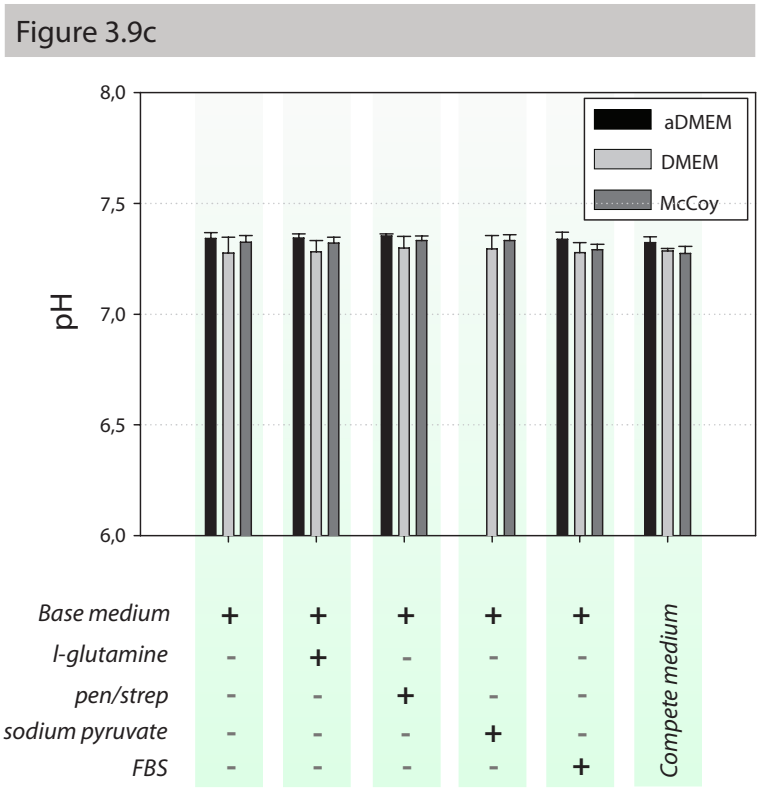

Figure 3.9: (c) pH levels of osteoblastic cell culture media.

3.4.2 Stability of Cell Culture Medium With Time

Concentrations of Na^+, K^+, Ca^{2+}, pH, and inorganic phosphorus of supplemented McCoy's 5A modified media with or without FBS, and stored either at 4°C (fridge) or at 37°C with 5% CO_2 (cell culture incubator), were repeatedly evaluated during a period of 15 days. The results are presented in Figure 3.10.

While medium stored at 37°C presented slightly higher concentrations of both Na^+ and K^+ than medium stored at 4°C, it was generally observed that both $[Na^+]$ and $[K^+]$ maintained relatively stable during 15 days, no matter if the medium contained FBS or not. In contrast, concentration of Ca^{2+} in FBS-containing medium stored at 37°C decreased gradually after seven days until the end of the experiment. Also when stored at 4°C FBS influenced $[Ca^{2+}]$ as the standard variation was observed to increase with time beyond day seven. However, in absence of FBS the concentration of calcium was preserved over the full length of experiment in both storage conditions.

Moreover, it was observed that storage of medium at physiological temperature and at controlled gas levels stabilised the pH of the medium while medium stored in the fridge was subject to drastic increases in pH. Finally, preparation and storage condition had no important influence on the concentration of total phosphorus.

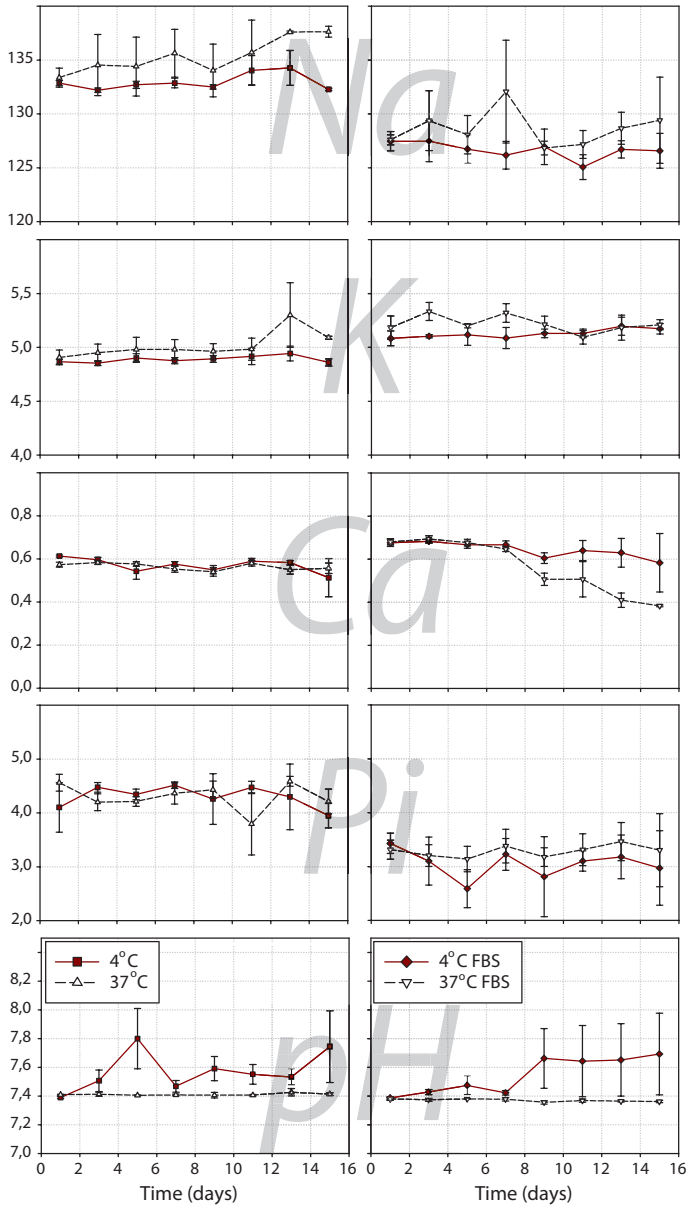

Figure 3.10: Ionic stability of supplemented McCoy cell culture medium without and with FBS (left and right column, respectively) at 4°C (black symbols) and 37°C (white symbols). Concentrations are expressed in units of mM.

3.4.3 Ionic Levels of Cell Culture Media During Osteoblast Cultures

Cell cultures of MG63, SAOS-2, and rat-derived mesenchymal stem cells (rMSCs) lasted for 21 days and were performed in polystyrene 24-well plates. Cells were maintained in one of the following media: complete DMEM (MG63), advanced DMEM (rMSC), or McCoys 5A media (SAOS-2). The different cell types all attained a similar aspect marked by an extended, triangular shape when adhered to the substrate. MG63 cells appeared slightly larger than both SAOS-2 and rMSC, with the latter cell type being recognised as slightly thinner and more elongated (Figure 3.11).

After one day in culture, and from then on every second day, the cell culture medium was exchanged for fresh media. After five days in culture, one set of each cell type was provided osteogenic media instead of normal media. The ionic composition of fresh media was monitored before addition to cells throughout the full length of the experiment (Table 3.7). Upon medium renewal, harvested supernatants were assayed for ionic and total phosphorus concentrations. The data is presented in Figure 3.12(a-e), where the ion concentrations of fresh medium given in Table 3.7 are drawn as dashed lines in red (normal media) or dotted lines in green (osteogenic media). Each one of Figure 3.12(a-e) is organised in three rows and two columns. Rows present data obtained from a different cell phenotype: SAOS-2 (top), MG63 (middle), and rMSC (bottom), respectively. Left columns show data obtained from cells maintained in normal medium throughout the full length of experiments, while right columns contain data obtained from cells maintained in osteogenic medium. Each graph also contains data on ionic concentration of cell culture medium both in presence and in absence of cells.

	$\mathbf{Na^+}$	$\mathbf{K^+}$	$\mathbf{Ca^{2+}}$	**pH**	$\mathbf{P_i}$
DMEM	149.0 ± 1.18	5.30 ± 0.03	1.41 ± 0.03	7.42 ± 0.03	0.36 ± 0.01
DMEM osteogenic	156.9 ± 1.02	5.10 ± 0.02	1.17 ± 0.03	7.49 ± 0.03	0.45 ± 0.01
aDMEM	151.2 ± 2.02	5.73 ± 0.10	1.44 ± 0.03	7.41 ± 0.02	0.46 ± 0.01
aDMEM osteogenic	159.8 ± 2.54	5.49 ± 0.11	1.17 ± 0.02	7.49 ± 0.03	0.44 ± 0.01
McCoy	132.9 ± 1.70	5.51 ± 0.06	0.77 ± 0.04	7.37 ± 0.03	2.77 ± 0.05
McCoy osteogenic	140.7 ± 1.35	5.29 ± 0.04	0.64 ± 0.03	7.43 ± 0.02	2.91 ± 0.04

Table 3.7: The ionic levels of each medium type (supplemented and with FBS) was measured before it was provided to cells. The values (expressed in units of mM, except for pH) are given as mean ± standard deviation. For osteogenic media $n = 8$, otherwise $n = 11$.

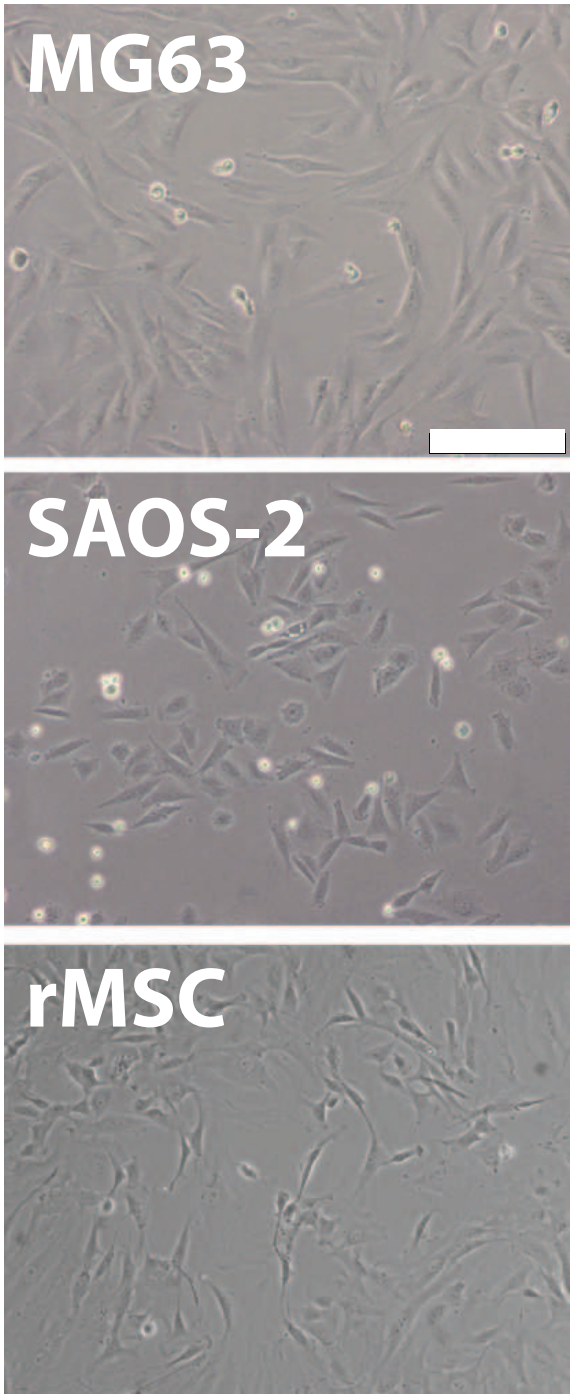

Figure 3.11: Representative images of the different osteoblast models used in this study were obtained after one day in culture when cells still had not reached confluency. Scale bar represents 200 μm, and applies to all three images.

As is shown in Figure 3.12(a & b), levels of Na^+ and K^+ followed similar trends for all three cell types in both normal and osteogenic medium. Incubated media presented increased concentrations of both Na^+ and K^+ compared to initial concentrations of these ions. While the levels of Na^+ increased about 2-8 mM between measurements, K^+ levels normally increased 0.1-0.2 mM. These changes represent increases of about 1-2%, and were due to evaporation of medium during the incubation period[2]. Beside the evaporation effect, the most important observation was that no difference in neither $[Na^+]$ nor $[K^+]$ was observed between cell culture medium that had been in contact with cells and cell culture medium not in contact with cells, except for MG63 cells maintained in osteogenic DMEM.

In contrast to the concentrations of sodium and potsasium, extracellular concentration of calcium in cell culture medium was influenced by osteoblast cultures (Figure 3.12c). After five days in culture and until the end of experiment $[Ca^{2+}]$ decreased in both MG63 and rMSC cultures when maintained in normal medium. The decreases corresponded to about 0.10-0.13 mM (7-9%) for MG63 cells, and about 0.05-0.10 mM (3-7%) for rMSC cells. This effect was however not observed in SAOS-2 cells maitained in normal McCoy medium.

When exposing cells to osteogenic medium, a massive decrease in $[Ca^{2+}]$ of cell culture medium was observed in both SAOS-2 and rMSC cultures, but not in MG63 cultures. At the same time osteogenic medium prepared from any of the three basal media maintained its calcium concentration level constant in absence of cells. The decrease in calcium in presence of SAOS-2 cells was about 0.17 mM ($\approx$ 24%) between day 5 and day 7, and then increased to about 0.4 mM ($\approx$ 60%) between day 7-9, 9-11, 11-13, and 13-15. After that, the decrease in $[Ca^{2+}]$ continued, but at a gradually slower rate. More or less the same tendency was observed for rMSC. Initially (i.e. day 5-7), the decrease in $[Ca^{2+}]$ was small, but then it gradually increased and beyond day 9 it reached about 0.75 mM ($\approx$ 65%).

Like $[Na^+]$ and $[K^+]$, concentrations of total phosphorus remained unchanged in cell cultures maintained in normal medium (Figure 3.12d). However, unlike normal medium without cells, osteogenic medium without cells repeatedly increased its $[P_i]$. In osteogenic McCoy medium $[P_i]$ raised on average 1.7 mM ($\approx$ 58%), while in osteogenic DMEM and aDMEM, $[P_i]$ in-

[2]It was observed that evaporation was higher in wells located at the border of the multi-well plate (data not shown). To compensate for the evaporation effect, samples and controls were always placed symmetrically in the culture plate.

creased 1.75 mM ($\approx 390\%$) and 2.44 mM ($\approx 550\%$), respectively. In addition to this spontaneous increase of $[P_i]$, which was presumably due to hydrolysis of β-GP by alkaline phosphatse present in FBS, presence of SAOS-2 cells and rMSC caused additional increases of $[P_i]$. In the case of SAOS-2 cells, $[P_i]$ initially reached about 8 mM (day 5-7), and from then on was maintained close to 10 mM until the end of the experiment. In rMSC cultures, $[P_i]$ reached a maximum about day 9 ($\approx$ 9 mM). Thereafter $[P_i]$ continued to raise in rMSC cultures compared to medium without cells.

In great contrast to both SAOS-2 and rMSC cultures, MG63 cells did not induce any increase of $[P_i]$ at all. Rather, at an initial stage (day 5-7) presence of cells actually lowered the concentration of inorganic phosphorus compared to medium without cells.

Finally, pH of cell culture medium was highly influenced by presence of cells. In all cell models, and in both normal and osteogenic medium, pH decreased with time as an effect of metabolic activity. In absence of cells, both DMEM and aDMEM increased their pH while being incubated during two days (about 0.x pH units). This effect was not observed in McCoy medium, making the cellular metabolic influence from SAOS-2 cells more pronounced than by either MG63 or rMSC cultures.

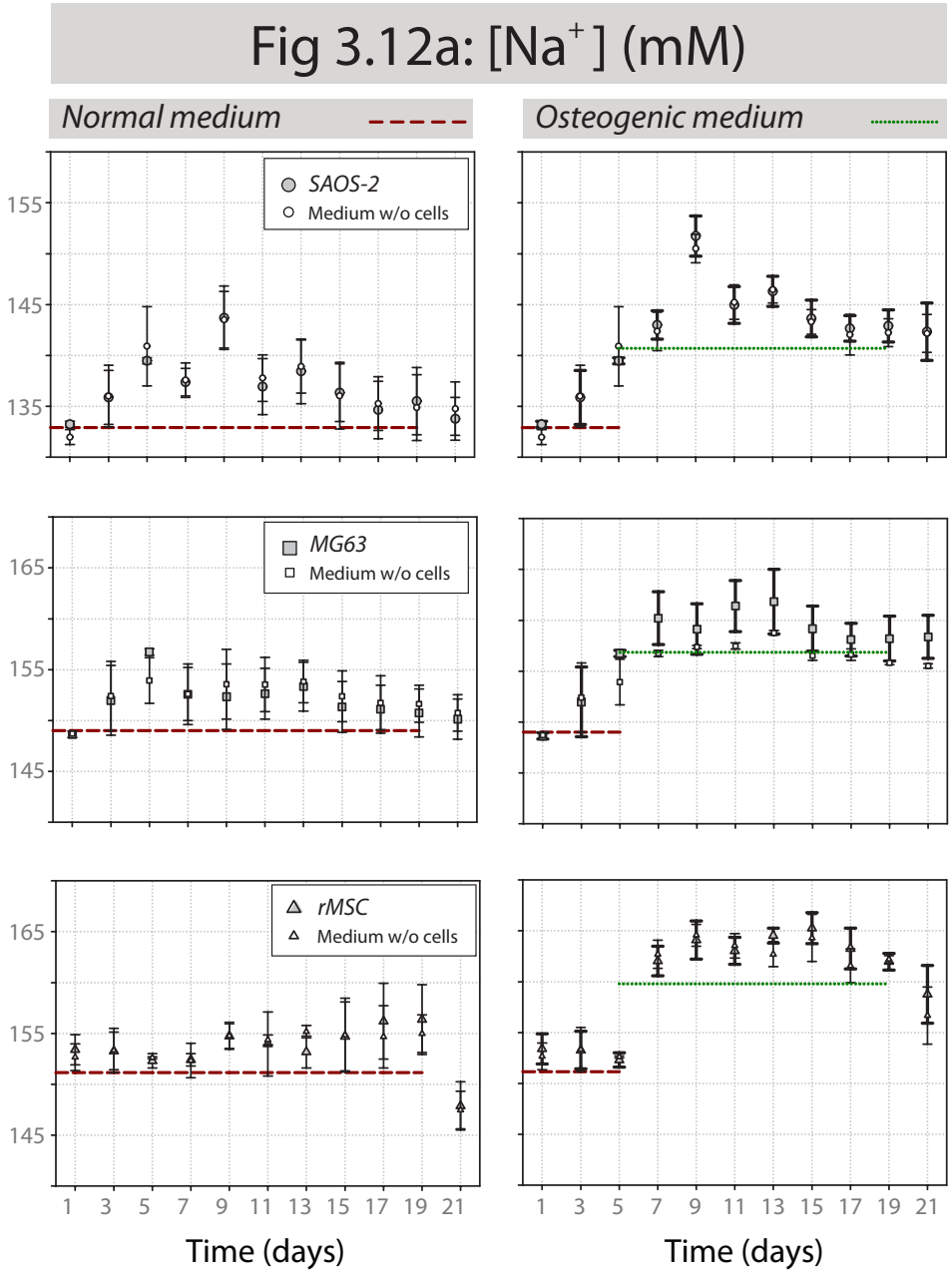

Figure 3.12: (a) Sodium concentration (mM) of cell culture medium in absence (empty symbols) and presence of cells (filled symbols): top row SAOS-2 (○), middle row MG63 cells (□), and bottom row rMSCs (△). Horizontal dashed and dotted lines correspond to initial concentration of normal and osteogenic medium, respectively.

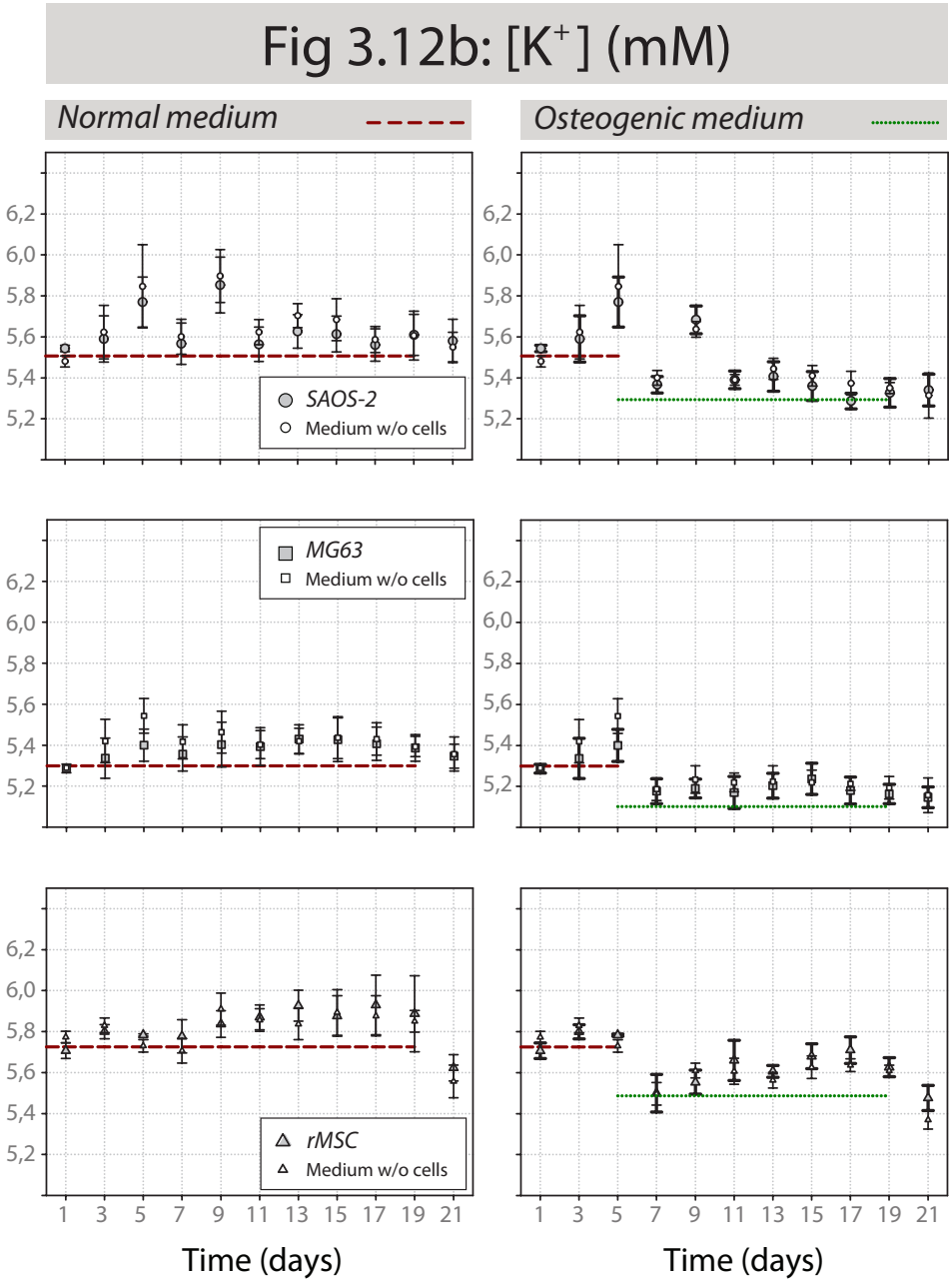

Figure 3.12: (b) Potassium concentration of cell culture media during cell growth. Symbols and organisation as described in Figure 3.12a.

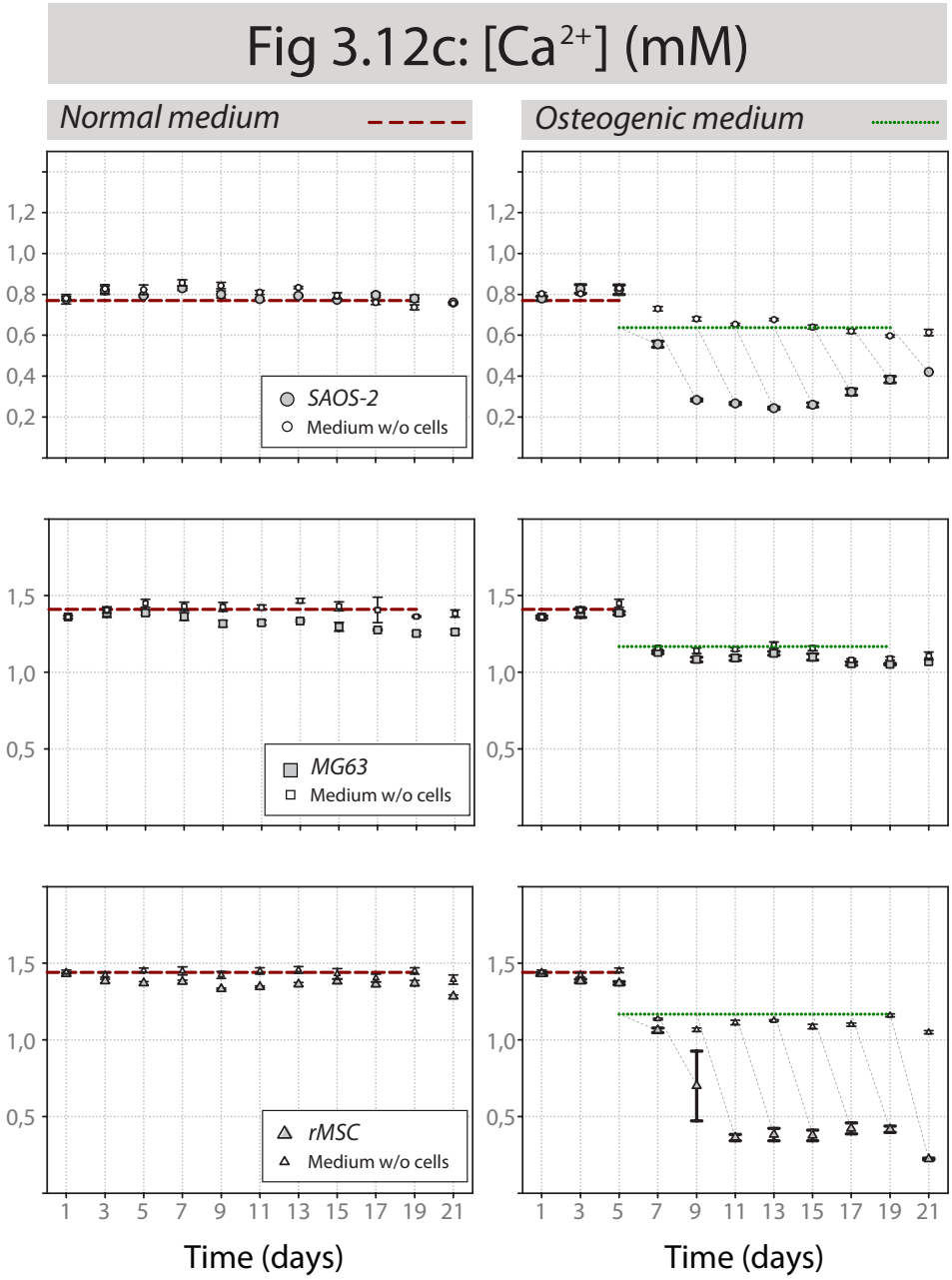

Figure 3.12: (c) Calcium concentration of cell culture media during cell growth. Symbols and organisation as described in Figure 3.12a.

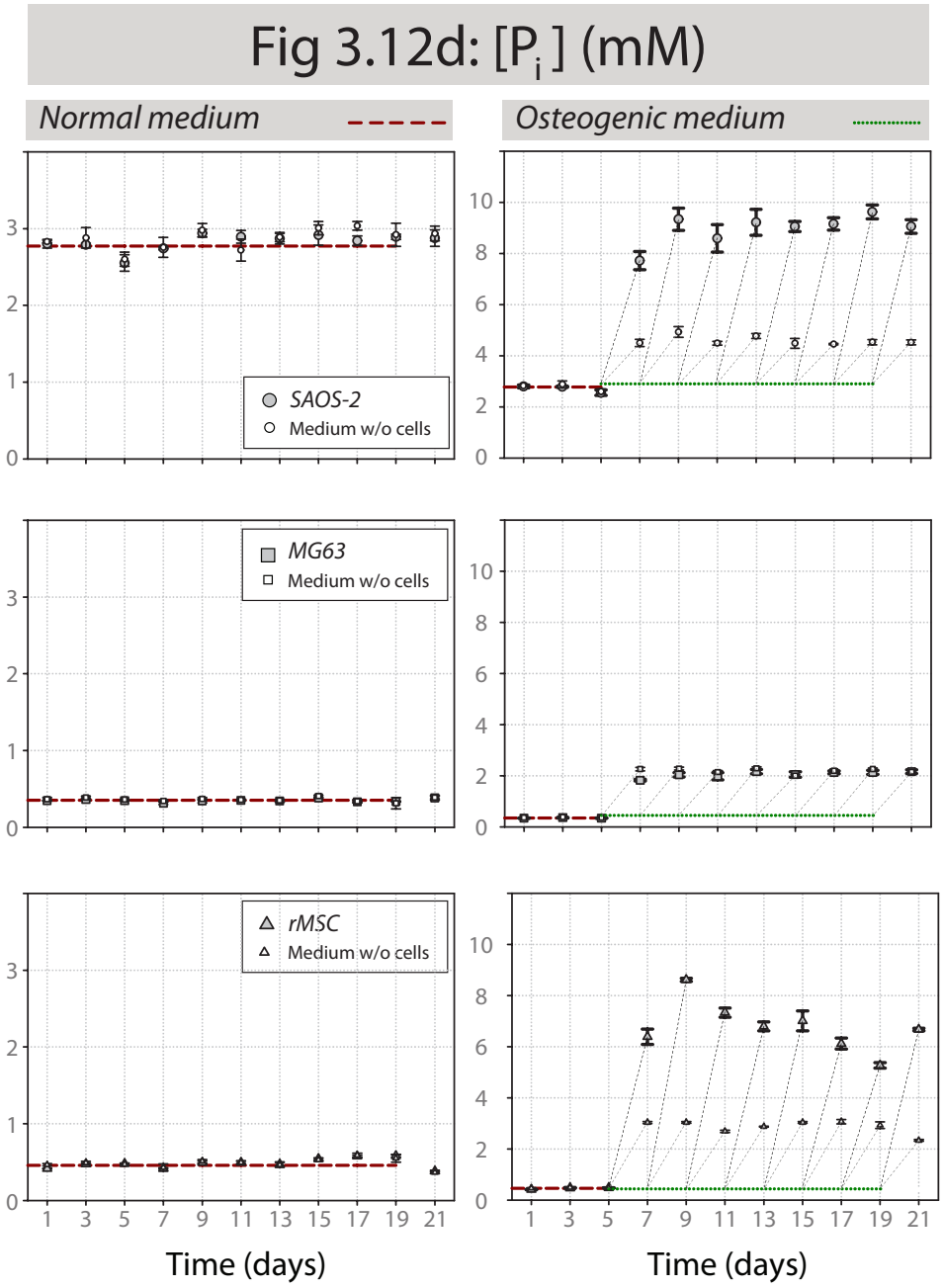

Figure 3.12: (d) Inorganic phosphorus concentrations of cell culture media during cell growth. Symbols and organisation as described in Figure 3.12a.

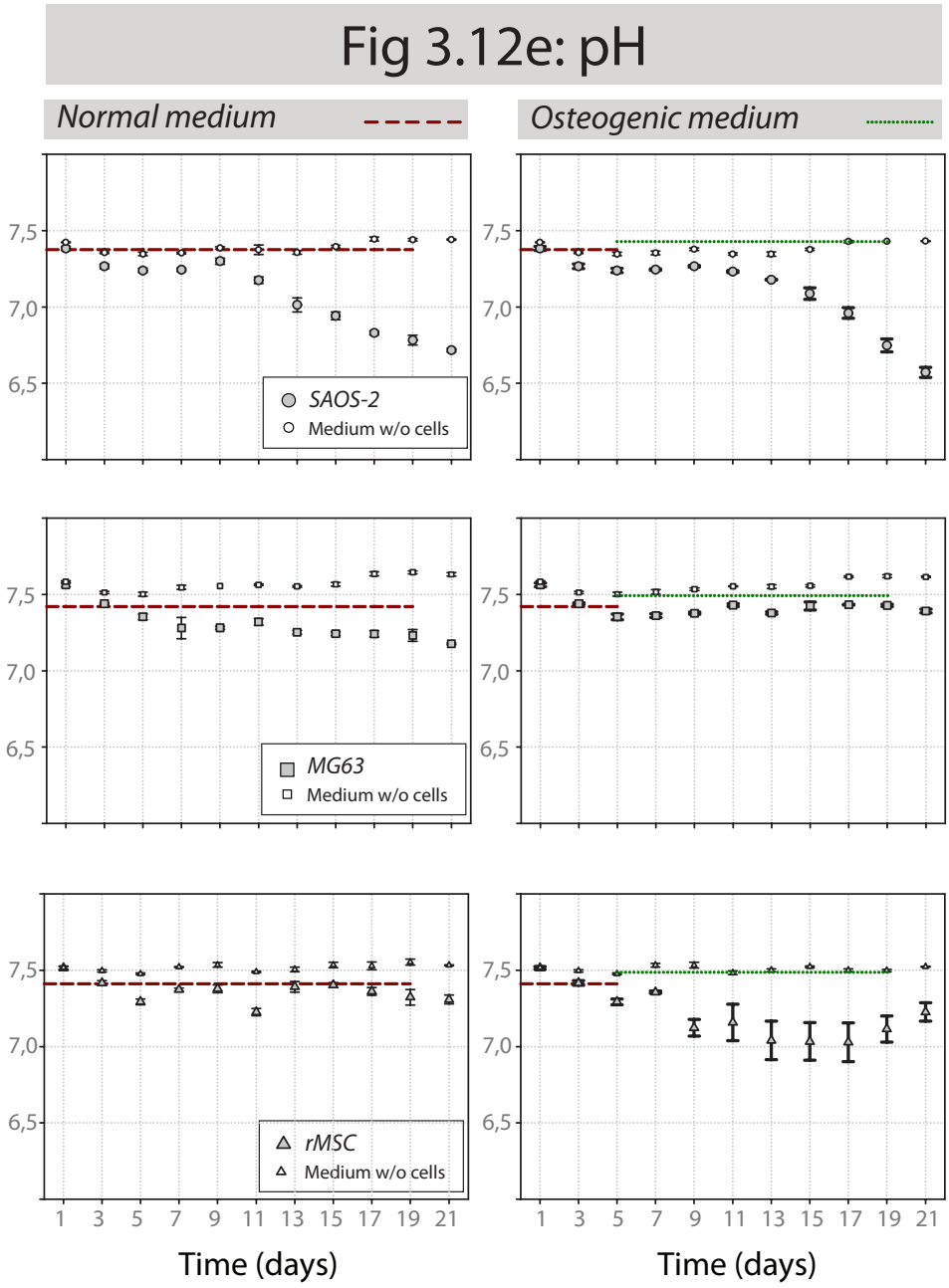

Figure 3.12: (e) pH of cell culture media during cell growth. Symbols and organisation as described in Figure 3.12a.

3.4.4 Calcium Deposition in Extracellular Matrix

Calcium deposition in the extracellular matrix was evaluated by Alizarin Red staining of fixed cell layers. At the end of experiment, i.e. after 21 days in culture, cell layers were stained with Alizarin Red. The amount of incorporated dye was quantitatively evaluated after extraction using CPC. The fold increase of calcium in the extracellular matrix was calculated as the ratio of calcium in cell layers grown in osteogenic medium compared to cells maintained in normal medium. The data is presented in Figure 3.13, and which shows that no calcium deposition occurred in MG63 layers while calcium deposition in SAOS-2 and rMSC cell layers had increased six to seven times.

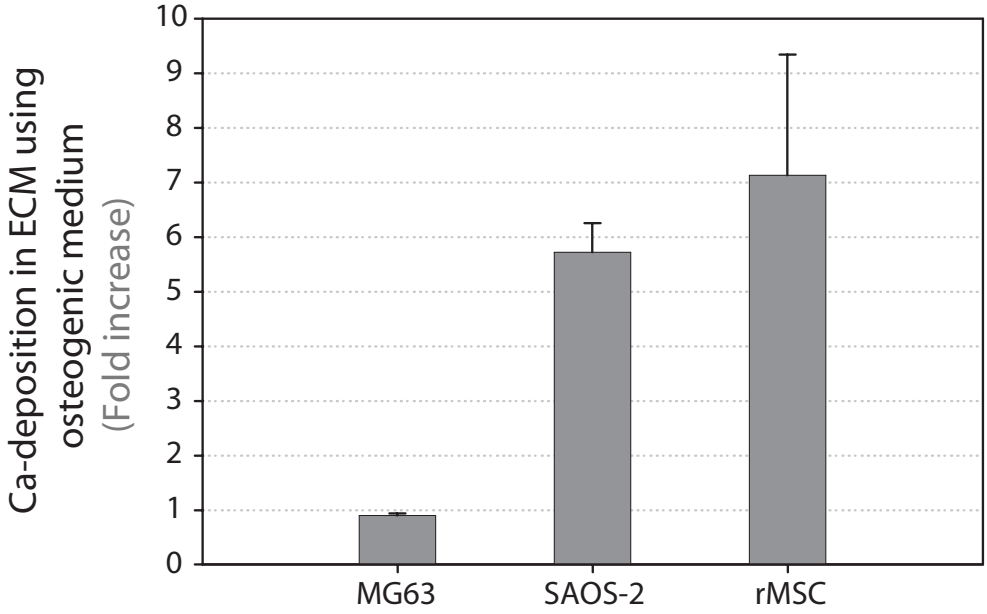

Figure 3.13: Quantitative calcium deposition in extracellular matrix. Fold increase of calcium in the extracellular matrix using osteogenic medium after 21 days in culture (n=6)

Representative images of stained cell layers were taken after nine days in culture are presented in Figure 3.14(a-i). Cells maintained in normal medium did not show any incorporation of Alizarin Red (a-c). However, when using osteogenic medium both SAOS-2 (e,h) and rMSC (f,i) cultures demonstrated large areas of calcium deposition distributed throughout the samples. In contrast, no calcium deposition was detected in MG63 cultures at this time point using osteogenic medium.

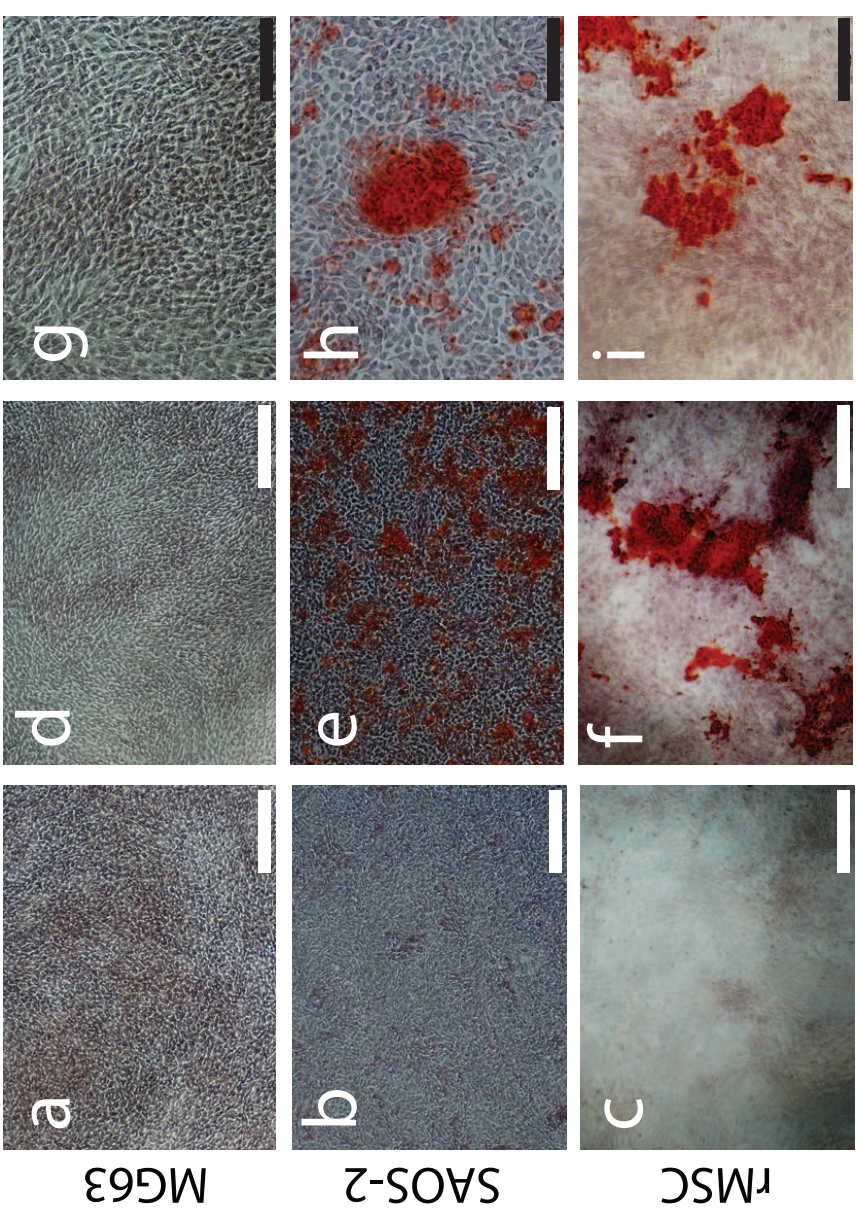

Figure 3.14: Alizarin Red staining of calcium in MG63 (top row), SAOS-2 (middle row), and rMSc (bottom row) cell layers after nine days in culture. Left column (a-c) show ARS stained cells maintained in normal medium. Middle (d-f) and right (g-i) columns show cells cultured in osteogenic medium. Scale bars represent 500 μm (white) and 200 μm (black), respectively.

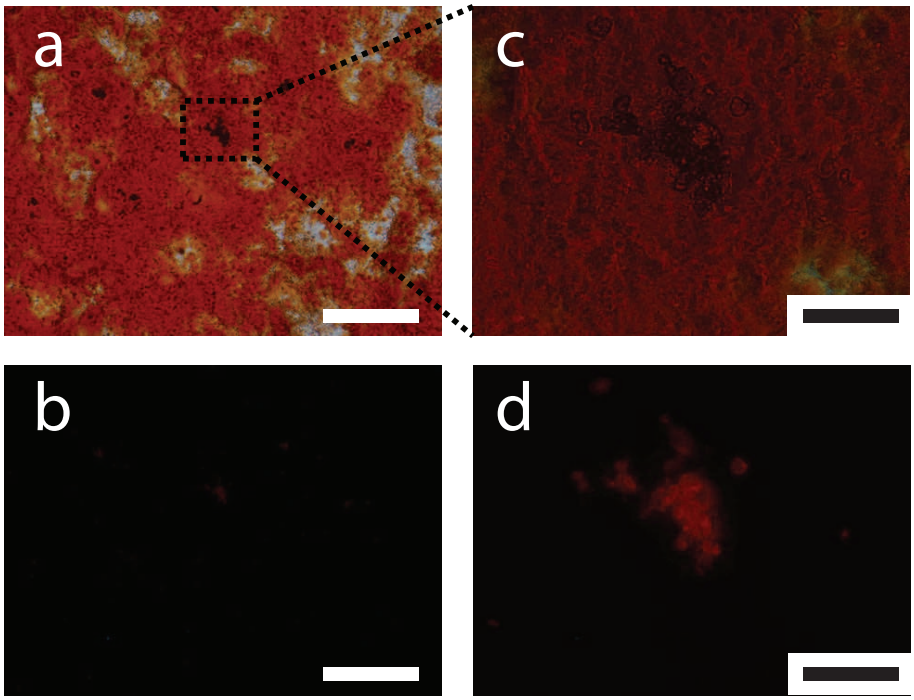

Figure 3.15: (a,c) Phase contrast images of Alizarin Red stained SAOS-2 cell layers cultured for 16 days. (b,d) Epifluorescent images (excitation 510-560 nm, emission >590 nm) of the same locations as in (a) and (c), respectively. Scale bars represent 500 μm (white) or 200 μm (black).

To elucidate the role of medium composition on calcium deposition, SAOS-2 cells and MG63 cells were cultured in either McCoy or DMEM media. As is shown in Figure 3.16, MG63 cells did not induce calcium deposition in any of the two medium compositions.

3.4.5 Ionic signals as function of cell number and media volume

Any change of the ionic extracellular environment induced by cells will depend on the experimental conditions, and ultimately on the ratio between amount of cells and the total cell culture volume. In Figure 3.17 it is demonstrated how the induced change on the extracellular ionic environment from SAOS-2 cell activity during 20 hours varied with total cell culture volume.

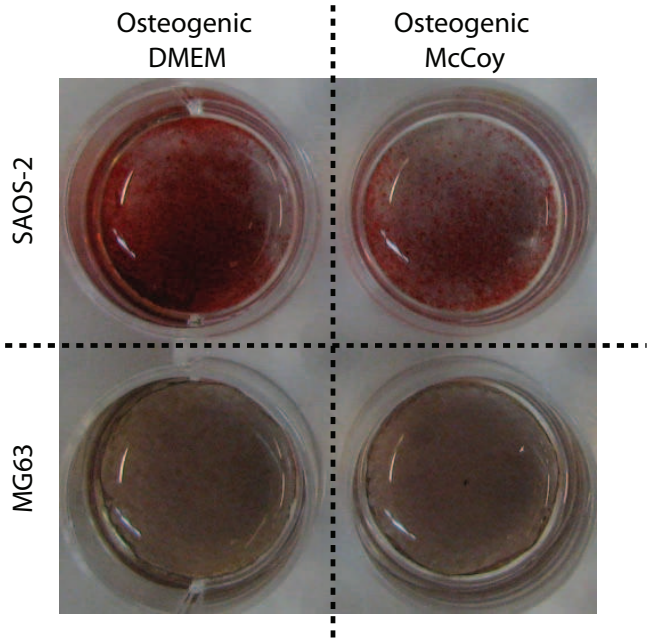

Figure 3.16: Alizarin Red staining of SAOS-2 and MG63 cells grown in both corresponding and non-corresponding medium. Images taken after eleven days in culture.

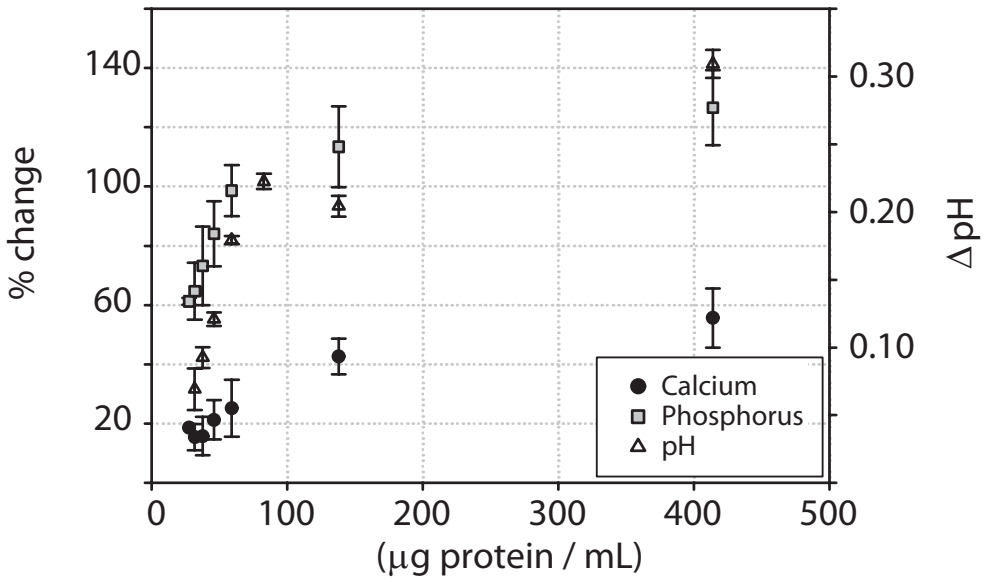

Figure 3.17: Double Y-axis. Estimation of SAOS-2 influence on the ionic extracellular environment in osteogenic medium.

3.4.6 Alkaline Phosphatase Activity

ALP activity of cell cultures was measured after nine days in culture, and at that time point great differences between the three different culture models were observed (Figure 3.18). Highest ALP activity was detected in SAOS-2 cells, while the lowest activity was observed in MG63 cells. The differences in ALP activity between SAOS-2 cells and rMSCs was in the order of about two magnitudes. More or less the same difference was then observed between rMSCs and MG63 cells.

In all cell models, osteogenic medium had a positive influence on ALP activity. The effect was more pronounced in MG63 cells (267.6 ± 45.3%), than in rMSCs (97.8 ± 38.1%) and in SAOS-2 cells (24.8 ± 9.7%).

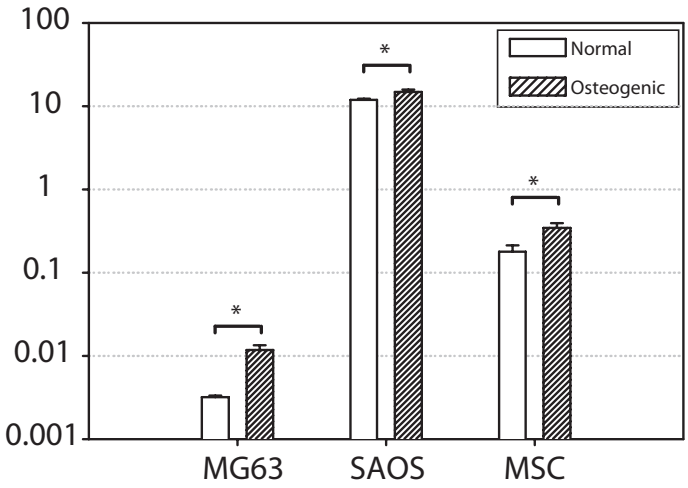

Figure 3.18: Alkaline phosphatase activity of MG63, SAOS-2 and rMSC cells grown in normal medium and osteogenic medium. ALP activity was measured after nine days in culture, and is expressed in units of μmol p-nitrophenol min^{-1} $(\text{mg protein})^{-1}$

3.5 Discussion

For proper cell growth and tissue development, cells depend on receiving the appropriate cues and information from their extracellular environment. Among the many signals actuating in that environment, ions are known to play an important role. They not only contribute to establish the cellular membrane potential, but also function as essential messenger and transporter molecules. Some ions, like calcium and phosphates, may also be fundamental building blocks for tissue development, especially in bone tissue.

In this chapter it has been studied how the ionic extracellular environment is influenced by osteoblast-like cellular activity. The reason behind this study was two-folded. First, the desire was to investigate if fluctuations in any of the extracellular inorganic ions could be considered as an indirect parameter of tissue development or cellular activity. Second, since in more complex bone tissue engineering situations one may also anticipate intervention of bioactive scaffold materials that by themselves interact with the ionic extracellular environment (see Chapter 4 and 5), our ambition was first to clarify to what extent osteoblast-like cells alone influence that specific environment.

3.5.1 Cell Culture Media Characterisation

Studies of the ionic extracellular environment initially required that appropriate measurement methods were established. Throughout this work ion-selective electrodes have been used as a reference method for cation analysis, while the colourimetric molybden-ascorbic acid method was used for phosphate analyses. The usefulness of these two techniques was clearly demonstrated through the cell culture media analysis in Section 3.4.1 where the compositional differences between the three cell culture media used in this study were reproduced; low levels of calcium and high levels of phosphate in McCoy medium, and high levels of calcium but low levels of phosphate in both DMEM and aDMEM. Furthermore, both methods produced consistent and reproducible results, and they could detect fluctuations in physiological ranges.

Beside the actual compositional differences between the different cell culture media, the most important findings regarding medium composition was the effect of FBS on the stability of ionic levels, and how to best store the medium throughout long-term experiments. In Section 3.4.2 it was demonstrated that ionic stability, mainly that of calcium, was better preserved in serum-free medium. Furthermore, if stored at 37°C and with 5% CO_2, the pH of the medium was stabilised over a much longer time period. The most likely explanation of the observed calcium instability of FBS-containing medium

would be spontaneous precipitation of calcium phosphate induced by alkaline phosphatase present in FBS. This explination is further supported by the fact that the decrease is faster at 37°C than at 4°C, where enzymatic activity is lower. One possible way to confirm this would be to centrifuge the medium samples, and analyse or stain the precipitated material for calcium and phosphorus.

The results presented in Sections 3.4.1-3.4.2 demonstrate the importance of appropriate preparation and storage of cell culture medium when studying the ionic extracellular environment, and this applies to studies both in absence and presence of cells.

3.5.2 Calcium Deposition Provoked by Osteoblast Activity

Using osteogenic factors it was demonstrated that both SAOS-2 cells and rMSCs provoke significant calcium deposition in the extracellular matrix (Section 3.4.4). As opposed to SAOS-2 and rMSCs, but under identical conditions, MG63 cell layers did not show any sign of calcium deposition.

The documented observations agree well with previous studies on similar systems and under similar conditions. SAOS-2 cells are relatively stable cells (Hausser & Brenner, 2005) known to undergo the entire osteoblastic differentiation program, including production of a collagenous extracellular matrix (McQuillan *et al.*, 1995), an extremely high ALP enzymatic activity (Rodan *et al.*, 1987; Stinson *et al.*, 1993), as well as spontaneous release of mineralisation-competent matrix vesicles (Thouverey *et al.*, 2009). Furthermore, an extractable bone-inducing agent (BIA) is present in lysates of SAOS-2 (Anderson *et al.*, 1998). As a result, calicum deposition in SAOS-2 layers has been commonly reported when using osteogenic medium (e.g. Fassina *et al.* (2005); Thouverey *et al.* (2009)). In a similar way, many studies have demonstrated the *in vitro* mineralisation potential of adult, marrow-derived mesenchymal stem cells (Ohgushi *et al.*, 1996; Nauman *et al.*, 2003; Shimko *et al.*, 2004; Maeda *et al.*, 2007).

Recalling Figure 3.3, the absent calcium deposition in MG63 cell layers could be due to inappropriate culture medium ionic composition, inadequate alkaline phosphatase activity, defect collagen production, or a combination of each of these factors. In this study, any influence of medium composition was discarded as it was observed that MG63 cells failed to deposit calcium also when grown in osteogenic McCoy medium (Figure 3.13). In addition, the ionic composition of DMEM was close to identical to that of aDMEM,

which in turn was successfully used to induce calcium deposition by rMSCs. Instead, a more important factor was that MG63 cells expressed extremely low levels of ALP activity (Figure 3.18), a fact previously described by other authors (Clover & Gowen, 1994). One plausible reason for the absent calcium deposition by MG63 cells could be its abnormal extracellular matrix which contains significant amounts of collagen type III, a protein normally absent in osteoblast cultures but rather present in fibroblast-like cultures (Jukkola *et al.*, 1993). Consequently, the likely reason for absent calcium deposition in MG63 cultures may be a combination of low ALP activity, and a defect osteoblast-matrix.

Although literature clearly emphasises that behaviour of MG63 cells deviates from standard osteoblast-like cells, still one can find a few studies where these cells are used as a model of osteoblast mineralisation. Gregory *et al.* (2004) reported mineral deposition in MG63 cell layers after 21 and 28 days in culutre. Calcium deposition by MG63 cells (referred to as mineralisation) was also reported by Takagishi *et al.* (2006) and Kim *et al.* (2007). However, for calcium deposition to occur at all, Takagishi *et al.* (2006) had to force it by adding exogenous calcium at non-physiological levels (8 mM). In the study by Kim *et al.* (2007), glucosamine sulfate was provided to cells in combination with β-GP, and induced an almost three-fold increase of mineralisation after already seven days in culture compared to their control. In another study, Sun *et al.* (2009) reported faint Alizarin Red staining of MG63 cell layers maintained in non-osteogenic medium for up to 12 days.

Taken altogether, MG63 cells seem to be a less appropriate cell model to use for studies of typical osteoblastic differentiation processes such as alkaline phosphatase activity and mineralisation events.

3.5.3 Osteoblastic Activity Observed Through the Ionic Extracellular Environment

By careful preparation and storage of cell culture medium it was possible to study the effects of cellular activity on the ionic extracellular environment (Section 3.4.3).

For all three cell models, as well as in both normal and osteogenic medium, cellular metabolic activity caused acidification of the cell culture medium already at early stages of the culture period. McCoy medium used for SAOS-2 cultures maintained its pH stable in absence of cells, and therefore a clear effect of cellular respiration could be observed in both normal and osteogenic McCoy medium from around day 13. Interestingly, pH of SAOS-2 cultures continued to decrease until the end of the experiment, indicating that cells

either continued to proliferate throughout the full experiment, or that the metabolic rate increased with stage of differentiation.

More or less the same effect was observed in rMSC cultures maintained in osteogenic aDMEM medium. However, in normal aDMEM, the pH-decrease was less pronounced. Rather than an effect of drastic changes in metabolic activity, this observation could be ascribed to an expermintal artefact. Upon reaching confluency, two-dimensional rMSC cultures in normal medium tended to detach from the culture substrate and collapse into a three-dimensional, ball-like structure. It is not known whether cells continued to be alive within this structure, but with time the empty culture surface was repopulised by proliferating cells not engaged to the collapsed structure. Using osteogenic medium, the cell layer maintained much better anchored to the culture substrate. It is possible that rMSC cultures exposed to osteogenic medium reinforce their matrix both through specific protein production and through calcium deposition.

In both DMEM media the pH spontaneously became more basic during incubation in absence of cells. Taken this effect into account, pH of DMEM in presence of cells clearly indicated cellular respiration. MG63 cells maintained in normal DMEM acidified the culture medium to a higher degree than cells maintained in osteogenic medium, indicating that osteogenic medium slowed down either the proliferation rate or the metabolic activity.

It was further demonstrated that cell-induced calcium deposition in the extracellular matrix was related to significant alterations in concentrations of both calcium and inorganic phosphorus in osteogenic medium. SAOS-2 cells and rMSCs both responded to osteogenic medium by hydrolysing β-GP which in turn increased the concentration of inorganic phosphorus. The hydrolysation was highly efficient in SAOS-2 cultures, reaching a turnover efficiency of about 90% already after a few days with osteogenic medium, and this was maintained until the end of the experiment. This data is in agreement with the study of Chung *et al.* (1992) who reported that 80% of 10 mM β-GP was hydrolysed by osteoblastic activity within 24 hours. In rMSC cultures, βGP-hydrolysation reached a maximum at early stages of cultures (around day 9) and then stabilised or slowed down, indirectly indicating decreased total ALP activity with time.

In parallel to the increased levels of inorganic phosphate, calcium concentration decreased in both SAOS-2 and rMSC cultures. In both cases, the decrease was relatively small during the first days, coinciding with the lower βGP-hydrolysation rate observed at this time point. Thereafter, the magnitude of calcium decrease stabilised in rMSC cultures throughout the full experiment, while in SAOS-2 cultures the calcium uptake was observed to

decrease during the last days of culture.

Although no calcium deposition was detected in the extracellular matrix of MG63 or rMSC cultures maintained in normal medium, still it was observed a slight decrease in extracellular calcium. This suggests that some of the ionised calcium was bound by soluble proteins produced by these cells, or accumulated intracellularly. Exactly which those proteins could be requires further investigation.

3.5.4 Biological Significance of Cell-induced Calcium Deposition

βGP-mediated induction of calcium and phosphate deposition in the extracellular matrix is widely used as an indicator of bone tissue differentiation *in vitro*. However, it should be clarified once for all that its use and relevance as a biological model system has been debated. Basically, the question is if mineralisation occurring only in presence of high concentrations of exogenous organic phosphate can be considered physiological, and not mainly being a consequence of spontaneous mineral precipitation. The latter observation has been documented by several authors (Khouja *et al.*, 1990; Chung *et al.*, 1992; Beresford *et al.*, 1993; Hamlin & Price, 2004), but is in many studies not even considered.

In this study it was observed that hydrolysis of 10 mM βGP occurs in both presence and absence of cells, as indicated by increased concentrations of P_i. In medium without cells, concentration of P_i increased presumably due to endogenous alkaline phosphatase activity of FBS, as has been described by Khouja *et al.* (1990). However, FBS-induced hydrolysis of βGP was not sufficient to form mineral precipitation in any of the three medium compositions used, as evident by maintained calcium concentrations. On the contrary, in presence of ALP-active cells mineral precipitation could be observed already after nine days in culture (of which four was done with osteogenic medium). Considering that bone differentiation is a process that takes several weeks, this has to be considered as very early. Still, extremely rapid mineralisation response *in vitro* has previously been described (Stanford *et al.*, 1995). In this study, the deposited calcium within mineralising cell cultures was initiated as separated areas being uniformly distributed over the sample. With time, and with continued exposure to β-GP, Alizarin Red staining observed through light microscopy revealed a rather homogenous distribution of calcium within the extracellular matrix. However, when observing the same samples through a narrower wavelength region, positive ARS staining was only observed as clearly separated nodules. Gentleman *et al.* (2009) applied

this method to identify mineralised foci of osteoblast cultures, which were later chemically characterised to be of hydroxyapatite or non-hydroxyapatite nature depending on the source of osteoblasts. Also other authors have reported different chemical character of calcium-phosphate minerals induced by β-GP in osteoblast cultures (see review by Hoemann *et al.* (2009)). Therefore, taking into account that mineralised nodules only was detected at later stages of the culture period, but that significant calcium deposition was apparent already at early stages, only a certain part of the calcium deposition was associated to nodule-forming mineralisation. This observation should be put in perspective to the results presented by Balint *et al.* (2001), who determined significant calcium uptake (about 4 mg/dl) in very sparse nodule-forming cultures of MC3T3-E1 cells. According to them, calcium uptake is however not directly proportional to number and size of forming nodules, but rather depends on the stage of differentiation.

Therefore, to perfectly determine to what extent the measured calcium uptake corresponds to nodule-forming mineralisation, it will be required to use a cell culture model, e.g. MC3T3-E1, and an appropriate concentration of β-GP to only produce nodules, and not any ectopic mineralisation. This has been beyond the work presented in this chapter.

3.6 Conclusions

This chapter, in which the ionic extracellular environment of osteoblast cultures have been monitored over time, provides one clear example of how sensors applied to the tissue engineering environment can be beneficial for characterisation of specific cellular activity. If properly done, such measurements can provide real-time data that can be used as indirect indications of bone tissue growth and development, and contribute to understand how osteoblast-like cells interact with certain biomaterials.

In particular, it has been demonstrated how the ionic extracellular environment may be significantly influenced by osteoblast-like cellular activity with respect to calcium, phosphorus, and pH. Regarding pH, and independent of the specific ionic composition of the cell culture medium used, all cellular cultures induced acidification of their extracellular environment. This effect was apparent also when the ratio of cells to extracellular volume was decreased, and thus, extracellular pH of osteoblast cultures is a highly relevant parameter to monitor to assess metabolic activity.

It was further shown that both SAOS-2 and rMSC activity induced elevated levels of extracellular inorganic phosphorus when provided osteogenic cell culture media containing 10 mM β-glycerophosphate (β-GP). This was

however not the case in MG63 cell cultures. Absence of cell-induced hydrolysis of β-glycerophosphate coincided with low alkaline phosphatase activity. Thus, considerable increase of extracellular phosphorus in cell culture medium containing β-glycerophosphate may be used as indicator of cellular alkaline phosphatase activity. Moreover, efficient cell-induced hydrolysis of β-GP was associated with gradual deposition of calcium into mature extracellular matrix of SAOS-2 and rMSC cultures. Decrease of extracellular calcium in osteoblast-like cultures may therefore be interpreted as presence of a well-developed collagenous extracellular matrix, and as a step towards bone mineralisation.

Bibliography

Abed, E. & Moreau, R. (2007). *Cell Proliferation,* **40**, 849–865.

Addison, W. N., Azari, F., Sorensen, E. S., Kaartinen, M. T., & McKee, M. D. (2007). *The Journal of Biological Chemistry,* **282** (21), 15872–83.

Allori, A. C., Sailon, A. M., & Warren, S. M. (2008a). *Tissue Engineering Part B,* **14** (3), 259–273.

Allori, A. C., Sailon, A. M., & Warren, S. M. (2008b). *Tissue Engineering Part B,* **14** (3), 275–283.

Anderson, H., Hsu, H., Raval, P., Reynold, P., Gurley, D., Aguilera, M., Davis, L., & Moylan, P. (1998). *Cells and Materials,* **8**, 89–98.

Arnett, T. R. (2008). *The Journal of Nutrion,* **138**, 415S–418S.

Arnett, T. R. & Henderson, B. (1998). *Methods in Bone Biology.* London: Chapman & Hall.

Asagiri, M. & Takayanagi, H. (2007). *Bone,* **40**, 251–264.

Aubin, J. & Triffitt, J. (2002). *Principles of Bone Biology,* , 59–81.

Ayers, R., Nielsen-Preiss, S., Ferguson, V., Gotolli, G., Moore, J. J., & Kleebe, H.-J. (2006). *Materials Science and Engineering C,* **26**, 1333–1337.

Baht, G. S., Hunter, G. K., & Goldberg, H. A. (2008). *Matrix Biology,* **27**, 600–608.

Balint, E., Szabo, P., Marshall, F., & Sprague, S. (2001). *Bone,* **28** (1), 21–28.

Beck, G. R. (2003). *Journal of Cellular Biochemistry,* **90**, 234–243.

Behari, J. (2009). *Biophysical Bone Behaviour. Principles and Applications.* Singapore: John Wiley & Sons.

Beloti, M. M. & Rosa, A. L. (2005). *Brazilian Dental Journal,* **16** (2), 156–161.

Beresford, J., Graves, S., & Smoothy, C. (1993). *American Journal of Medical Genetics,* **45**, 163–178.

Bilezikian, J. P., Raisz, L. G., & Martin, T. J., eds (2008). *Principles of Bone Biology*, volume 1. London: Academic Press, 3rd edition.

Boskey, A., Maresca, M., Ullrich, W., Doty, S., Butler, W., & Prince, C. (1993). *Bone and Mineral,* **22**, 147–.159.

Boskey, A. L. (1996). *Connective Tissue Research,* **35** (1-4), 357–363.

Burger, E. H., Klein-Nulend, J., & Smit, T. H. (2008). In: *Encyclopedia of Biomaterials and Biomedical Engineering*, (Wnek, G. E. & Bowlin, G. L., eds) pp. 439–447. Informa Healthcare.

Chang, Y.-L., Stanford, C. M., & Keller, J. C. (2000). *Journal of Biomedical Materials Research,* **52**, 270–278.

Chen, P., Toribara, T., & Warner, H. (1956). *Analytical Chemistry,* **28** (11), 1756–1758.

Chenu, C., Colucci, S., Grano, M., Zigrino, P., Barattolo, R., Zambonin, G., Baldini, N., Vergnaud, P., Demas, P., & Zallone, A. (1994). *The Journal of Cell Biology,* **127**, 1149–1158.

Choi, K.-M., Seo, Y.-K., Yoon, H.-H., Song, K.-Y., Kwon, S.-Y., Luee, H.-S., & Park, J.-K. (2008). *Journal of Bioscience and Bioengineering,* **105** (6), 586–594.

Chung, C., Golub, E., Forbes, E., Tokuoka, T., & Shapiro, I. (1992). *Calcified Tissue International,* **51**, 305–311.

Clover, J. & Gowen, M. (1994). *Bone,* **6**, 585–591.

Dvorak, M. M., Siddiqua, A., Ward, D. T., Carter, D. H., Dallas, S. L., Nemeth, E. F., & Riccardi, D. (2004). *PNAS,* **101** (14), 5140–5145.

Eklou-Kalonji, E., Denis, I., Lieberherr, M., & Pointillart, A. (1998). *Cell and Tissue Research,* **292**, 163–171.

Fassina, L., Visai, L., L.Asti, Benazzo, F., Speziale, P., Tanzi, M., & Magenes, G. (2005). *Tissue Engineering,* **11** (5/6), 685–699.

Fedarko, N., Bianco, P., Vetter, U., & Robey, P. G. (1990). *Journal of Cellular Physiology,* **144** (1), 115–121.

Fournier, B. & Price, P. (1991). *The Joumal of Cell Biology,* **114**, 577–583.

Fratzl-Zelman, N., Fratzl, P., Hrandner, H., Grabner, B., Varga, F., Ellinger, A., & Klaushofer, K. (1998). *Bone,* **23** (6), 511–520.

Fujita, T., Izumo, N., Fukuyama, R., Meguro, T., Nakamuta, H., Kohno, T., & Koida, M. (2001). *Biochemical and Biophysical Research Communications,* **280**, 348–352.

Gentleman, E., Swain, R. J., Evans, N. D., Boonrungsiman, S., Jell, G., Ball, M. D., Shean, T. A. V., Oyen, M. L., Porter, A., & Stevens, M. M. (2009). *Nature Materials,* **8**, 763–770.

Gregory, C. A., Gunn, W. G., Preister, A., & Prockop, D. J. (2004). *Analytical Biochemistry,* **329**, 77–84.

Guyton, A. C. & Hall, J. E. (2005). *Textbook of Medical Physiology.* Philadelphia: Elsevier Saunders.

Habel, B. & Glaser, R. (1998). *European Biophysical Journal,* **27**, 411–416.

Hale, J. & Wuthier, R. (1987). *Journal of Biological Chemistry,* **262**, 1916–1925.

Hale, L., Ma, Y., & Santerre, R. (2000). *Calcified Tissue International,* **67**, 80–84.

Hamlin, N. & Price, P. (2004). *Calcified Tissue International,* **75**, 231–242.

Hausser, H.-J. & Brenner, R. E. (2005). *Biochemical and Biophysical Research Communications,* **333**, 216–222.

Hempel, U., Reinstorf, A., Poppe, M., Fischer, U., Gelinsky, M., Pompe, W., & Wenzel, K. W. (2004). *Journal of Biomedical Materials Research Part B: Applied Biomaterials,* **71** (1), 130–143.

Herzog, E. L., Chai, L., & Krause, D. S. (2003). *Blood,* **102** (10), 3483–3493.

Hoemann, C., El-Gabalawy, H., & McKee, M. (2009). *Pathologie Biologie,* **57**, 318–323.

Hunter, G. K. & Goldberg, H. A. (1993). *PNAS,* **90** (18), 8562–8565.

Jiang, Y., Jahagirdar, B. N., Reinhardt, R. L., Schwartz, R. E., Keene, C. D., Ortiz-Gonzalez, X. R., Reyes, M., Lenvik, T., Lund, T., Blackstad, M., Du, J., Aldrich, S., Lisberg, A., Low, W. C., Largaespada, D. A., & Verfaillie, C. M. (2002). *Nature,* **418**, 41–49.

Jones, J. R., Tsigkou, O., Coates, E. E., Stevens, M. M., Polak, J. M., & Hench, L. L. (2007). *Biomaterials,* **28**, 1653–1663.

Jukkola, A., Risteli, L., Melkko, J., & Risteli, J. (1993). *Journal of Bone and Mineral Research,* **8**, 651–657.

Kelm, R. J., Swords, N. A., Orfeo, T., & Mann, K. G. (1994). *The Journal of Biological Chemistry,* **269**, 30147–30153.

Khouja, H., Bevington, A., Kemp, G., & Russell, R. (1990). *Bone,* **11**, 385–391.

Kim, M. M., Mendis, E., Rajakapse, N., & Kim, S.-K. (2007). *Bioorganic & Medicinal Chemistry Letters,* **17**, 1938–1942.

Leinonen, H. K. V. A. L. (2008). *Archives of Biochemistry and Biophysics,* **473**, 132–138.

Maeda, M., Hirose, M., Ohgushi, H., & Kirita, T. (2007). *Journal of Biochemistry,* **141**, 729–736.

Mahamid, J., Sharir, A., Gur, D., Zelzer, E., Addadi, L., & Weiner, S. (2011). *Journal of Structural Biology,* **174**, 527–535.

Manolagas, S. C. (1999). *Endocrinology,* **130**, 4377–4381.

Marks, S. & Popoff, S. (1988). *American Journal of Anatomy,* **183**, 1–44.

McQuillan, D., Richardson, M., & Bateman, J. (1995). *Bone,* **16**, 415–426.

Mikami, Y., Omoteyama, K., Kata, S., & Takagi, M. (2007). *Biochemical and Biophysical Research Communications,* **362**, 368–373.

Morris, D. C., Masuhara, K., Takaoka, K., Ono, K., & Anderson, H. C. (1992). *Bone and Mineral,* **19** (3), 287–298.

Mundy, G. R. & Poser, J. W. (1983). *Calcified Tissue International,* **35**, 164–168.

Murshed, M., Harmey, D., Millan, J. L., McKee, M. D., & Karsenty, G. (2005). *Genes & Development,* **19**, 1093–1104.

Nakano, Y., Addison, W. N., & Kaartinen, M. T. (2007). *Bone,* **41**, 549–561.

Nauman, E., Sakata, T., Keaveny, T., Halloran, B., & Bikle, D. (2003). *Calcified Tissue International,* **73**, 147–152.

Neuman, W. F. & Neuman, M. W. (1958). *The Chemical Dynamics of Bone Mineral*. : The University Of Chicago Press.

Ohgushi, H., Dohi, Y., Katuda, T., Tamai, S., Tabata, S., & Suwa, Y. (1996). *Journal of Biomedical Materials Research,* **32**, 333–340.

ONeill, C. A. & Galasko, C. S. B. (2000). *Calcified Tissue International,* **67**, 53–59.

Orimo, H. & Shimada, T. (2008). *Molecular and Cellular Biochemistry,* **315**, 51–60.

Porter, A. E., Patel, N., & Best, S. (2008). In: *Encyclopedia of Biomaterials and Biomedical Engineering*, (Wnek, G. E. & Bowlin, G. L., eds) pp. 1451–1463. Informa Healthcare.

Reid, I. R. (1997). *European Journal of Endocrinology,* **137**, 209–217.

Rodan, S. B., Imai, Y., Thiede, M. A., Wesolowski, G., Thompson, D., Bar-Shavit, Z., Shull, S., Mann, K., & Rodan, G. A. (1987). *Cancer Research,* **47**, 4961–4966.

Romberg, R. W., Werness, P. G., Riggs, B. L., & Mann, K. G. (1986). *Biochemistry,* **25**, 1176–1180.

Salgado, A. J., Coutinho, O. P., & Reis, R. L. (2004). *Macromolecular Bioscience,* **4**, 743–765.

Shimko, D. A., Burks, C. A., Dee, K. C., & Neauman, E. A. (2004). *Tissue Engineering,* **10** (9/10), 1386–1398.

Stanford, C. M., Jacobson, P. A., Eanes, E. D., Lembke, L. A., & Midura, R. J. (1995). *The Journal of Biological Chemistry,* **270** (16), 9420–9428.

Stinson, R., Thacker, J., & Lin, C. (1993). *Clinica Chimica Acta,* **221**, 105–114.

Sun, J., Wei, L., Liu, X., Li, J., Li, B., Wang, G., & Meng, F. (2009). *Acta Biomaterialia,* **5**, 1284–1293.

Takagishi, Y., Kawakami, T., Hara, Y., Shinkai, M., Takezawa, T., & Nakamune, T. (2006). *Tissue Engineering,* **12** (4), 927–937.

Takamizawa, S., Maehata, Y., Imai, K., Senoo, K., Sato, S., & Hata, R.-I. (2004). *Cell Biology International,* **28**, 255–265.

Terkeltaub, R. A. (2001). *American Journal of Physiology and Cellular Physiology,* **281**, C1–C11.

Thouverey, C., Strzelecka-Kiliszek, A., Balcerzak, M., Buchet, R., & Pikula, S. (2009). *Journal of Cellular Biochemistry,* **106**, 127–138.

Triffitt, J. (2002). *Journal of Biomedical Materials Research,* **4**, 384–389.

Tuan, R. S., Boland, G., & Tuli, R. (2002). *Arthritis Research and Therapy,* **5** (1), 32–45.

Uccelli, A., Moretta, L., & Pistoia, V. (2008). *Nature Reviews Immunology,* **8**, 726–736.

Valerioa, P., Pereirab, M. M., Goesc, A. M., & Leite, M. F. (2004). *Biomaterials,* **25**, 2941–2948.

Wu, L. N., Genge, B. R., Dunkelberger, D. G., LeGeros, R. Z., Concannon, B., & Wuthier, R. E. (1997). *The Journal of Biological Chemistry,* **272** (7), 4404–4411.

Xiao, Z., Camalier, C. E., Nagashima, K., Chan, K. C., Lucas, D. A., de la Cruz, M. J., Gignac, M., Lockett, S., Issaq, H. J., Veenstra, T. D., Conrads, T. P., & Beck, G. R. (2007). *Journal of Cellular Physiology,* **210**, 325–335.

Yamanouchi, K., Gotoh, Y., & Nagayama, M. (1997). *Journal of Bone and Mineral Metabolism,* **15**, 23–29.

This page is intentionally left blank

Chapter 4

Ion Reactivity of Calcium-deficient Hydroxyapatite

4.1 Introduction

Sensors for characterisation of biochemical activity of biomaterials may be useful to determine how, and to what extent, a given material interacts with its surrounding environment. Historically, biomaterials have been of inert character, but with the birth of tissue engineering, scaffolds are nowadays rather designed to be multi-functional with respect to both its physical and chemical properties. For example, at some occasions biomaterials interact directly with the environment by sending favourable signals to cells residing within, or in close proximity to it, e.g. through drug-release. At other occasions, the interaction is an indirect consequence, e.g. through biodegradation. No matter the reason for the interaction, it is of greatest importance to understand how the presence of a biomaterial influences the instantaenous composition of the tissue engineering environment. Basically, such knowledge contributes to improved designs of biomaterials able to induce or suppress specific cellular activity.

Following this reasoning, in this chapter it is demonstrated how a biomaterial developed for bone tissue engineering, namely calcium-deficient hydroxyapatite (CDHA), interacts ionically on different time-scales, and with two different cell culture media commonly used for *in vitro* osteoblast cell cultures.

4.1.1 In Search for the Ideal Bone Graft Material

Although bone has regenerative capacity, its repair process is impaired in many clinical and pathological situations, something which is emphasised

by the fact that bone is the second most common tissue to be transplanted (blood being by far the most common one). According to Giannoudis *et al.* (2005) more than 2.2 million bone graft procedures in orthopaedics, neurosurgery and dentistry are done annualy all over the world, making it into a highly important socialeconomical event. More important is that behind this number hide the pain and decreased functionality experienced by patients suffering bone loss casued by for example trauma or tumours.

Among the bone grafting methods, three different categories can be distinguished:

1. **Autografts**, i.e. the transplation of tissue from one part of the body to another, is the most successful grafting method. Harvesting bone from the same patient (e.g. from the *iliac crest*) generally provides excellent conditions for a successful bone repair process, but obviously complicates the operation for both the surgeon and the patient.

2. **Allografts**, i.e. the transplantion of tissue from a donor different than the patient, is the most common grafting method. Due to differences between donors this method yields variable results. Also one has to consider the immunological issue. To minimize the latter effect, the graft is commonly decellularised, something which severely decreases its mechanical properties.

3. **Bone-graft substitutes**, i.e. materials of biological or synthetic origin that can provide the necessary mechanical properties of bone, and the fundamental conditions for bone regeneration.

Given the clinical and economical complications related to the two former methods, development of appropriate bone-graft substitutes is since the early 1980s a highly active field of research. The common strategy on which such research relies, is to enhance any or several of the material's *osteoinductive*, *osteoconductive*, and *osseointegrative* properties. This means that primitive, undifferentiated, and pluripotent cells should be stimulated to develop into a bone-forming cell lineage (osteoinduction), and further allowed to grow on its surface and/or towards its interior through pores and channels (osteoconduction), and that finally the construct becomes well anchoraged to the existing bone tissue (osseointegration) (Albrektsson & Johansson, 2001). In addition to these specific requirements, as well as more general issues, such as biocompatibility, minimal fibrotic reaction, sterility and long-term storage, the ideal bone-graft materials should also provide similar mechanical strength and elasticity as healthy bone.

The inherent regenerative capacity of bone has definitely contributed to make bone-graft substitutes one of the areas of biomaterials and tissue engineering research with the highest commerial product activity. As a matter of fact, the amount of bone substitutes for cavity filling is large, and there exist an extensive number of products with a wide variation in both origin, composition and mechanism of action (Hing, 2004; Place *et al.*, 2009). The most simple classification of these materials would be based on their origin; *naturally derived materials* and *ceramic composite* materials (Table 4.1). Although all these materials demonstrate certain desirable properties for bone regeneration, all of them fall well behind when compared to autologous grafts, and at most they match the results that can be obtained with allogenic bone. Therefore, continued research and development of bone-grafting substitutes is well motivated.

Naturally derived materials		
Demineralised bone matrix		
Polymers	Collagen, fibrin, chitosan, starch	
Coralline hydroxyapatite		
Ceramic composites		
Calcium phosphate ceramics		
Hydroxyapatite	HA	$Ca_{10}(PO_4)_6(OH)_2$
β-tricalcium phosphate	β-TCP	$Ca_3(PO_4)_2$
Biphasic calcium phosphate	BCP	HA + TCP
Calcium-deficient hydroxyapatite	CDHA	$Ca_{10-x}(HPO_4)_x(PO_4)_{6-x}(OH)_{2-x}$
Amorphous calcium phosphate	ACP	$Ca_x(PO_4)_y$
Carbonated apatite	CA	
Calcium phosphate cements		
Apatite cements	End product: HA, CA, or CDHA	
Brushite cements		
Bioactive glasses		
Bioglass	SiO_2-CaO-Na_2-P_2O_5	
Bioactive ceramics		
Glass ceramics		

Table 4.1: Common materials used for bone grafts or bone tissue engineering applications.

Among the bone-grafting strategies is also included *bone tissue engineering* (Figure 4.1), where bone-forming cells, e.g. mesenchymal or embryonic stem cells are combined with a scaffold to produce a viable tissue (Jukes *et al.*, 2008; Di-Silvio *et al.*, 2008). The scaffold is typically made from porous ceramics or polymers (Salgado *et al.*, 2004) which should degrade *in vivo* and be replaced by newly formed bone. Although some progress has been made in this field, better understanding of the spatial and temporal distribution of cells and growth factors necessary for osteogenesis remains to be developed. One approach to improve clinical results include the incorporation of bone morphogenic proteins into the scaffold (Haidar *et al.*, 2009).

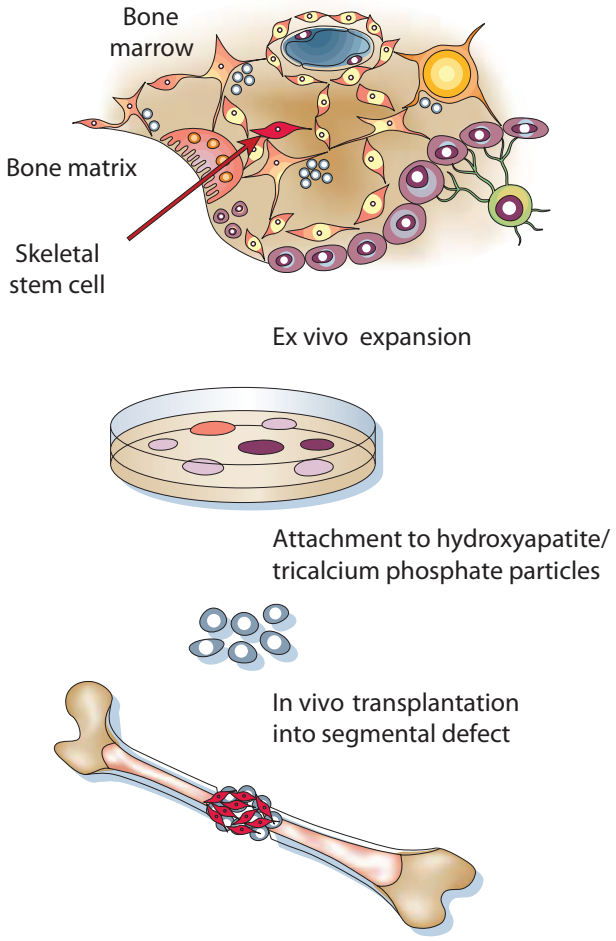

Figure 4.1: A typical bone tissue engineering concept. Image adapted from Bianco & Robey (2001).

4.1.2 Calcium Phosphate Based Bone-graft Substitutes

Calcium minerals based around orthophosphates constitute a particularly interesting candidate group as bone-graft and scaffold material for bone tissue engineering. According to LeGeros (2002), attempts to use calcium phosphates in clincal application dates back to as early as 1920, and the primary interest in these materials obviously stem from its chemical and morphological similarity to the mineral phase of biological apatites of bone, dentin, and enamel.

Calcium phosphate compounds differ in chemical composition (it is convenient to classify them according to their Ca/P molar ration, which can vary between 0.5 and 2.0), as well as in their physiological form, being possible to obtain both as ceramics and cements.

4.1.2.1 Calcium phosphate ceramics

Among the ceramics, hydroxyapatite ($Ca_{10}(PO_4)_6(OH)_2$, HA, with Ca/P = 1.67) was early distinguished as a promising bone-graft substitute due to its very high similarity with the inorganic component of bone and tooth mineral. Indeed, HA has been demonstrated to possess very good osteoconductive properties (Chang *et al.*, 2000a), but still has to be considered a too simple model for human bone mineral since biological apatites usually present impurities in their crystal composition, which in turn lower the Ca/P molar ratio to less than 1.67, and therefore is preferably referred to as calcium-deficient hydroxyapatite (Ben-Nissan & LeGeros, 2008). The impurities mainly derive from carbonate substitution with either hydroxyl or phosphate groups of HA. A more accurate representation of biological bone mineral would be as follows (4.1), with $0 < x < 1$: (Porter *et al.*, 2008)

$$Ca_{10-x}(PO_4)_{6-x}(CO_3)_x(OH)_{2-x}(CO_3)_x \tag{4.1}$$

Impurities in the mineral crystal may induce changes in the material properties, that influences mechanical strength, thermal stability, or solubility of the material. Pure HA does not only have somewhat week mechanical properties (Chen & Boccaccini, 2008; Liu *et al.*, 2008), like poor tensile strength and toughness, but it also has very low resorbability, which means that it will remain in the body for a long time (years) after implantation. The combination of slow degradation and week mechanical properties makes the implant site a serious focus of mechanical stress.

Lowering the Ca/P molar ratio usually enhances the degradation rate, as is the case with tri-calcium phosphate (TCP). TCP exists in two main forms;

α-TCP and β-TCP. While β-TCP can be sintered into a solid ceramic body when heated in the range of 700-1125°C, α-TCP can hardly be sintered, but is used as a cement powder (Ito & Ohgushi, 2008). Both α- and β-TCP have been demonstrated to support osteoblast adhesion, growth, and differentiation, and can therefore be considered osteoconductive (Yuan *et al.*, 2001; Ogose *et al.*, 2005; Seebach *et al.*, 2010). They can be used as bone-graft materials either as individual materials (Kamitakahara *et al.*, 2008), or in combination with other materials, then referred to as biphasic calcium phosphates (BCP) (Daculsi & LeGeros, 2008). The relative dissolution rates of these materials can be ordered like below (Daculsi *et al.*, 2005):

$$\alpha\text{-TCP} >> \beta\text{-TCP} >> \text{BCP} >> \text{HA} \tag{4.2}$$

An increased degradability obviously allows for successive substitution of the bone-graft material with newly formed bone. In addition, it also makes it possible to incorporate into the material certain bone growth factors that are released in a controllable manner via the degradation of the CaP compound.

4.1.2.2 Calcium phosphate cements

While HA and β-TCP have demonstrated reasonable biological properties, their fabrication method, usually sintering at high temperature, poses restriction on the shape and size of the device, which in turn may cause problems of adaptation and fixation of it to the bone cavity. To circumvent this problem, calcium phosphate cements (CPC), being a phase mixture of aqueous liquid and finely pulverised calcium phosphate powders that forms hydroxyapatite at room or body temperature, have been developed. The formability of the material introduces major advantages from a surgical point of view as the material is easily shaped and can be injected with low operative invasion. Besides, as it hardens in the body, the good osteoconductive properties of CaP ceramics can be maintained (Habraken *et al.*, 2007).

When mixing the cement powder with an aqueous solution, it converts into calcium phosphate ceramic by hydrolysis reaction. Ginebra *et al.* (1999) demonstrated that α-TCP hydrolysis into CDHA is a two-step process. First the cement powder particles are dissolved by the liquid water, a process which depends on the surface area of the powder particles. The dissolution creates a local saturation of ions that are reprecipitated on the surface of the cement powder particles. Thus, in the second phase the reaction becomes diffusion controlled, and the CDHA become tangled and join together, which leads to hardening of the cement (Figure 4.3). The result is a low crystalline CDHA

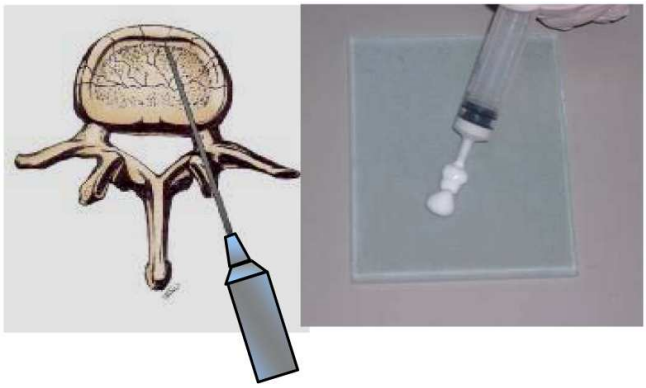

Figure 4.2: Calcium phosphate cements are injectable, and therefore allow for efficient bone cavity filling. Image adapted from SmartCaP project proposal, p.5.

structure, with extremely small particle size, and thus a large surface area, high reactivity, and high adsorption property. In addition, the material is mouldable *in situ* which allows for perfect adaptation to bone cavities, and it further has self-setting ability at *in vivo* conditions.

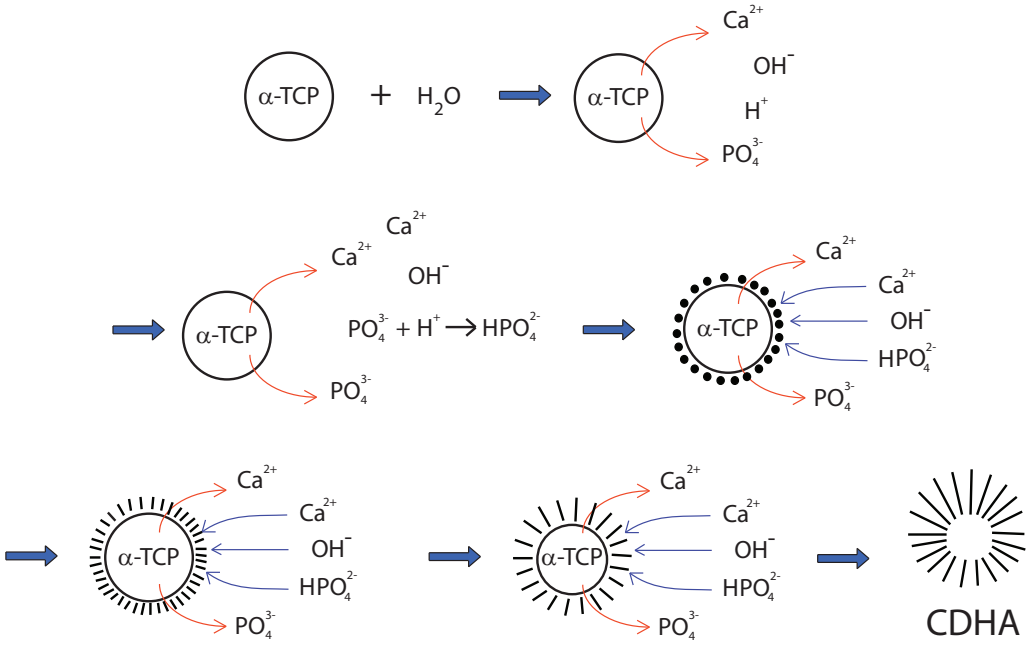

Figure 4.3: The formation of CDHA from α-TCP is a hydrolysis reaction that involves progressive dissolution of the α-TCP particles and precipitation of CDHA. Image adapted from PhD dissertation by Edgar Montufar.

4.1.3 Bioactivity and Ionic Interactions

In addition to a biomaterial's osteoinductive, osteoconductive, and osseointegrative properites, it is also common to discuss its *bioactivity*. As clarified by Bohner & Lemaitre (2009), the concept of bioactivity was initially associated only to materials designed to induce specific biological activity, but nowadays it also includes materials that allow bone-like hydroxyapatite to form selectively onto their surfaces when they are immersed in a solution of ionic concentration and pH value similar to that of human blood plasma. The main attractive feature of bioactive bone-graft materials is their ability to form a direct bond with the host bone, resulting in a strong interface compared to bioinert or biotolerant materials that form fibrous interfaces (Daculsi & LeGeros, 2008).

The bioactive property of CaP compounds is a consequence of dissolution/precipitation processes (Bagambisa *et al.*, 1993) caused by the material's capacity to add and remove ions from its crystal strucutre. If the rate of removal exceeds the rate of addition, the material is dissolved, and calcium and phosphate ions may then reprecipitate as calcium phosphate species, contributing to the formation of an adequate material-tissue interface. In addition to any dissolution process, immmersion of a CaP compound in an aqueous solution will always establish a progressive transistion between the solid and the liquid state. To this *hydration layer*, ions can be both added and removed reversibly (Neuman & Neuman, 1958; Misra, 1999; Eichert *et al.*, 2002; Cazalbou *et al.*, 2005; Boanini *et al.*, 2010).

In summary, both these ionic reaction processes, i.e. dissolution and ionic exchange, may induce significant chemical transformations of the material itself. In addition, and most importantly from a therapeutic point of view, they will also induce changes in the extracellular environment, something which may have consequences for cellular behaviour. Therefore, evaluation of CaP compounds and its reaction products should include both cellular and acellular assays. The latter is traditionally done using simulated body fluid (SBF) which allows bioactive materials to form bone-like hydroxyapatite on its surface (Kokubo & Takadama, 2006). Necessary to mention though is that slight differences in experimental conditions and preparation of the SBF may cause false interpreation of results, and lead to wrong conclusions (Bohner & Lemaitre, 2009).

Regarding cellular *in vitro* evaluations, the biological multitude does not permit any golden-standard assay comparable to the acellular SBF-method. Rather, a variety of cell types of different origins and phenotypes, as well as of different age and malignancy state are used. In addition, each cell type (and even cells of the same phenotype) usually requires its specific cell culture

medium which composition has been derived to provide optimal conditions for growth and function of that specific cell type. Therefore, and with respect to apatitic materials which are known to mirror the composition of the fluid they are immersed in (Neuman & Neuman, 1958), one can expect a great diversity in how such materials interact with the extracellular environment during cellular *in vitro* assays.

Following from above discussion, the importance of characterising the ionic interactions of a biomaterial with its *in vitro* environment, is at least threefold;

1. ions (especially calcium and phosphate) can directly influence numerous essential bone cellular functions (Beck, 2003; Dvorak *et al.*, 2004). Therefore it is desirable to be able to correlate cell behaviour with solution-mediated penomena occuring in the cell culture medium;

2. to avoid generalisation or wrong extrapolation of solution-mediated events from *in vitro* to *in vivo* performace;

3. ionic exchange between material and extracellular fluid can induce significant changes of both chemical and physical charcter of the material surface, with possible subsequent consequences for cellular behaviour (Ducheyne & Qiu, 1999).

4.2 Objective and Strategy

The objective of the work presented in this chapter was to analyse the main ionic interactions induced by calcium-deficient hydroxyapatite (CDHA) when immersed in different standard cell culture media.

The steps taken were the following:

1. CDHA was exposed to different chemical compositions of cell culture medium: DMEM and McCoy, with or without osteogenic factors.

2. Concentrations of ions (Na^+, K^+, Ca^{2+}, and P_i) as well as pH of culture medium were measured at constant intervals during 48 hours of exposure to CDHA. Kinetics of ionic interactions were compared to theoretical sorption models.

3. As CDHA was repeatedly exposed to fresh culture medium, the evolution of ionic interactions between CDHA and culture medium was monitored during three weeks.

4.3 Materials and Methods

4.3.1 Fabrication of α-TCP powder

Powder of α-tricalcium phosphate (α-TCP, $Ca_3(PO_4)_2$) was obtained using previously established protocols (Engel *et al.*, 2008; Espanyol *et al.*, 2009). Briefly, 48.399 g of calcium phosphate dibasic ($CaHPO_4$, Sigma C7263) was mixed with 131.589 g of calcium carbonate ($CaCO_3$, Sigma C4830). The mixture was then heated up step-wise (Table 4.2) to reach 1400°C, which allows for formation of α-TCP according to reaction (4.3):

$$CaCO_3 + 2CaHPO_4 \rightarrow Ca_3(PO_4)_2 + CO_2 + H_2O. \tag{4.3}$$

Stage	$\mathbf{T}_i$	$\mathbf{T}_f$	**Time**
1	25	300	145 min
2	300	300	120 min
3	300	1100	330 min
4	1100	1100	120 min
5	1100	1400	120 min
6	1400	1400	120 min
7	1400	25	1 min

Table 4.2: Heating protocol to obtain α-TCP.

As evident from Table 4.2, the heated mixture was rapidly cooled down to room temperature (to avoid contamination of β-TCP) by crushing the solid body immediately after being removed from the furnace (Figure 4.4a-b). The obtained α-TCP particles were then mechanically milled during 15 minutes at 450 rpm using ten agate balls (Figure 4.4c). Finally, the α-TCP powder was mixed with 2 weight percent precipitated hydroxyapatite (pHA; Alco, ref. 1.02143.1000) that was supposed to work as a seed for apatite formation.

4.3.2 Hydrolysis of α-TCP

Samples of calcium-deficient hydroxyapatite (CDHA) were produced through hydrolysis reaction of α-TCP (4.4),

$$3Ca_3(PO_4)_{2\ (s)} + H_2O_{(aq)} \rightarrow Ca_9(HPO_4)(PO_4)_5OH_{(s)}. \tag{4.4}$$

For each gram of powder, 0.35 mL of distilled water was used (i.e. L/P ratio = 0.35 mL g^{-1}). Water and powder were manually mixed in a mortar for

about one minute, before the obtained paste was spread out in cylindrical holes (diameter of 15 mm and a height of 2 mm) in a Teflon mould (Figure 4.4d). After about five minutes, the moulded samples were immersed in excessive amounts of 0.9% NaCl solution where they remained during seven days at a temperature of 37°C. After this period the samples were removed from the mould, and left to dry at 37° for another two days before placed in tissue culture plates. After vacuum packaged in sealed bags, samples were sterilised with γ-irradiation (25 kGy, AragonGamma).

According to previous characterisations (Engel *et al.*, 2008; Espanyol *et al.*, 2009), these samples possess a specific surface area of about 17-18 $m^2\ g^{-1}$. The initial mass of the CDHA samples was determined to 0.615 $\pm$ 0.159 g (n=16).

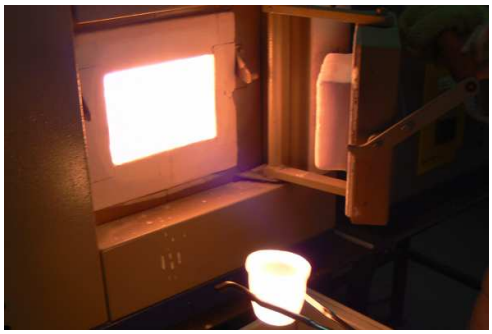

(a) Heating

(b) Cooling

(c) Milling

(d) Molding

Figure 4.4: (a-c) Fabrication steps of α-TCP, and (d) CDHA samples.

4.3.3 Cell culture media preparations

Two different commerical cell culture medium formulations, **Dulbecco's Modified Eagle Medium (DMEM)** and **McCoy's Modified 5A medium (McCoy)** respectively, were used to study how CDHA interacted with inorganic ions present in these media. For the study presented in this chapter, the following three preparations of each medium type were made:

1. **Normal medium**; DMEM or McCoy base medium supplemented with l-glutamine, pen/strep, sodium pyruvate, and FBS.
2. **Serum-free medium (-FBS)**; as (1), but without FBS.
3. **Osteogenic media (og)**; as (1), but with β-glycerophosphate, ascorbic acid, and dexamethasone added.

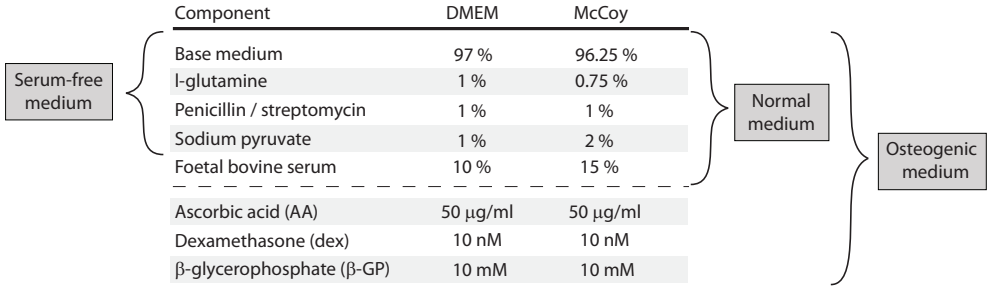

Figure 4.5: The preparation of the different cell culture media.

Preparation and maintenance of cell culture media were done as previously described in Sections 3.3.1 and 3.3.7, and is briefly summarised in Figure 4.5.

4.3.4 Ion Exchange Processes between CDHA and Cell Culture Media

To obtain experimental data on ionic interactions between CDHA samples and cell culture media, sterile CDHA samples were placed in 24-well tissue culture plates (Nunc). Before initiating any measurement, samples were preincubated overnight in 1.0 mL serum-free media at 37° and 5.0% CO_2. After this step, which was done to simulate conditions generally applied in cell culture experiments, the CDHA samples were exposed to 1.25 mL of cell culture media, and incubated in a humidified incubator at 37° with 5.0% CO_2.

To analyse the ionic reactivity of CDHA when exposed to cell culture medium, two different experiments were performed:

1. **Short-term kinetics**: the ionic profile of normal DMEM and McCoy cell culture medium, with and without osteogenic factors, and in contact with CDHA was measured every six hours (if not otherwise indicated) during a period of 48 hours. At each time point, medium from previously unassayed samples was analysed.

2. **Long-term kinetics**: the ionic profile of serum-containing DMEM and McCoy cell culture medium, with and without osteogenic factors, as well as serum-free DMEM and McCoy medium, and in contact with CDHA, was measured every second day ($\approx$ 48 hours) during a period of 21 days. The first measurement was however obtained after only one day. To simulate cell culture conditions, culture medium in contact with CDHA was exchanged on a regular basis so that fresh medium was provided immediately after each ion measurement. After five days, osteogenic medium was applied to one set of samples until the end of the experiment.

Upon ion analyses, 0.50 mL of medium was withdrawn from the different samples and analysed for Na^+, K^+, Ca^{2+}, pH, and inorganic phosphorus (P_i). The former compounds were measured using ion-selective electrodes (ILyte) immediately after harvest of the medium samples. P_i was quantified through reduction of phosphomolybdic acid with ascorbic acid (Chen *et al.*, 1956). For details on both these methods, the reader is referred to Chapter 3 and Sections 3.3.2 and 3.3.3.

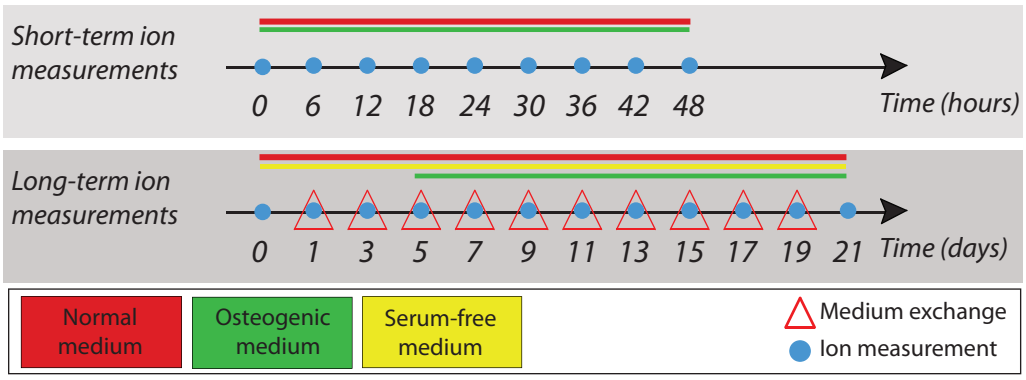

Figure 4.6: Experimental layout to study ionic interactions between CDHA and culture media.

If not otherwise indicated, the amount of sorbed ion x on CDHA, q_x, was calculated as follows (4.5):

$$q_x = \left([x]_i - \frac{[x]_t [x]_i}{[x]_{ctrl}} \right) V_{\text{sample}}, \tag{4.5}$$

where $[x]_i$ is the initial concentration of ion x (mol dm^{-3}), $[x]_t$ is the concentration of ion x (mol dm^{-3}) at time t, $[x]_{ctrl}$ is the concentration of ion x under identical conditions but in absence of CDHA (mol dm^{-3}), and V_{sample} is the volume of culture medium (dm^{-3}). A negative value of q_x indicates desorption, i.e. release of ion from CDHA.

In a similar way, the effect of CDHA on the pH of the cell culture medium was calculated as follows (4.6):

$$\text{pH} = \text{pH}_\text{t} \frac{\text{pH}_\text{i}}{\text{pH}_\text{ctrl}}, \tag{4.6}$$

where pH_t is the pH of the media in contact with CDHA at time t, pH_i is the initial pH of the media, and pH_{ctrl} is the pH of medium incubated under identical conditions but in absence of CDHA.

4.3.5 Scanning Electron Microscopy

CDHA samples exposed to serum-containing cell culture medium according to the conditions for long-term kinetic measurements were coupiuosly rinsed in distilled H_2O, and finally dried at room temperature during several days. The dried samples were sputter-coated with a thin layer of Au before images of their microstructure were taken with a scanning electron microscope (JEOL Model 6400, 15kV).

4.3.6 Spectroscopic Analysis

FTIR spectra of CDHA samples exposed to cell culture medium during a period of 21 days were obtained using a Nicolet 6700 spectrophotometer (Thermo Fisher Scientific Inc.). Dry CDHA samples were prepared as in Section 4.3.5 and after successive bathing in absolute ethanol (3 x 10 minutes). These samples were then gently scratched using a clean scalpel, and the obtained powder was compressed into a thin sample with potassium bromide (Panreac, 331489.1608). IR transmission spectra were obtained at 2 cm^{-1} resolution, and averaging 32 scans.

4.3.7 Statistics

Reported sorption values are mean ± standard deviation ($n = 3$). Statistical difference was determined with Student's t-test ($P < 0.05$). Non-linear curve fitting were done with Microsoft Excel 2007, using its built-in Solver-function with 100 iterations. The corresponding regression coefficients (R^2) were calculated as below (4.7),

$$R^2 = 1 - \frac{\sum (q_i - q_{predicted})^2}{\sum (q_i - q_{average})^2} \tag{4.7}$$

where q_i is obtained from experimental data, $q_{predicted}$ is the sorption that corresponds to the best-fit, and $q_{average}$ is the mean of all sorption data (see Figure 4.7).

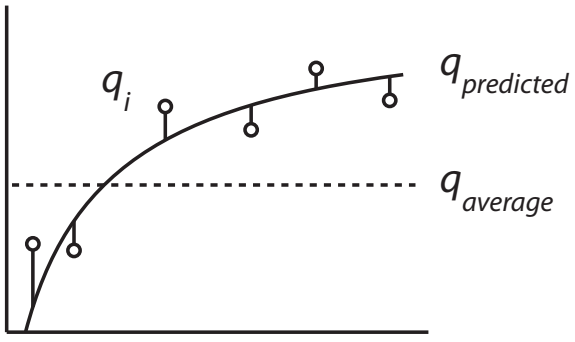

Figure 4.7: Illustration of the parameters for calculation of the regression coefficient.

4.4 Results

4.4.1 Cell Culture Medium Characterisation

The ionic profile of cell culture media was kept stable with respect to investigated ions throughout the full experiment (Table 4.3). This was achieved by preparing aliquots of serum-free media on a weekly basis, and by storing aliquots at 37°C with 5% CO_2.

As was pointed out in Chapter 3 (Section 3.4.1), significant differences in ionic composition exist between DMEM and McCoy preparations. In summary, when compared to DMEM media, McCoy media were low on calcium but high on phosphorus. For example, when supplemented with FBS the amount of Ca^{2+} in McCoy was only 56.1 ± 2.8% of that in DMEM, while $[P_i]$ was 7.97 ± 0.65 times higher in McCoy than in DMEM.

Medium	**Na^+**	**K^+**	**Ca^{2+}**	**pH**	**P_i**
DMEM					
-FBS	148.1 ± 0.6	4.89 ± 0.05	1.35 ± 0.05	7.48 ± 0.07	0.86 ± 0.02
+FBS	146.8 ± 0.6 ^{a}	5.35 ± 0.03 ^{a}	1.37 ± 0.05 ^{a}	7.42 ± 0.06 ^{a}	0.34 ± 0.01 ^{a}
Osteogenic	154.3 ± 1.0 ^{b}	5.19 ± 0.03 ^{b}	1.13 ± 0.05 ^{b}	7.52 ± 0.04 ^{b}	0.40 ± 0.02 ^{b}
McCoy					
-FBS	133.5 ± 0.8 ^{a}	4.92 ± 0.02	0.61 ± 0.02 ^{a}	7.42 ± 0.01 ^{a}	3.88 ± 0.09 ^{a}
+FBS	133.5 ± 0.6 ^{b,c}	5.54 ± 0.07 ^{b,c}	0.77 ± 0.02 ^{b,c}	7.35 ± 0.01 ^{b,c}	2.72 ± 0.18 ^{b,c}
Osteogenic	143.1 ± 0.4 ^{d,e}	5.37 ± 0.04 ^{d,e}	0.61 ± 0.02 ^{d,e}	7.44 ± 0.02 ^{d,e}	2.67 ± 0.05 ^{e}

Table 4.3: Ion levels of cell culture medium (mM). Data was obtained by measuring ion concentrations of fresh medium, and before exposure to CDHA (n = 5 for osteogenic media, otherwise n = 11). Data is mean ± standard deviation. Footnotes indicate statistical difference compared to DMEM -FBS (a), DMEM +FBS (b), McCoy -FBS(c), McCoy +FBS(d), and DMEM osteogenic (e).

4.4.2 Short-term Ion Exchange Processes

To investigate the mechanisms of ion interactions between CDHA and the different cell culture media, a kinetic study of sorption of principal extracellular ions to CDHA during 48 hours was performed. The obtained data proposed that the general ion sorption process was of non-linear character, only exception being sorption of phosphorus from osteogenic media, which was of linear character. To analyse the non-linear sorption, two empirical kinetic rate equations were applied: (1) the pseudo-first-order rate equation,

and (2) the pseudo-second-order rate equation, respectively[1].

4.4.2.1 Pseudo-first-order kinetics

The pseudo-first-order rate equation, more commonly known as the Lagergren rate equation, has been widely used for over a century (Lagergren, 1898), and is given by:

$$\frac{dq_t}{dt} = k_1(q_e - q_t), \tag{4.8}$$

where q_t is the amount of solute sorbed at any time t (moles), q_e is the amount of solute sorbed at equilibrium (moles), and k_1 is the apparent reaction rate constant (mol h^{-1}).

Separation of variables in Equation 4.8, and using boundary conditions $t = 0$ to $t = t$, and $q = 0$ to $q = q_t$, gives:

$$\int_0^{q_t} \frac{dq_t}{(q_e - q_t)} = \int_0^t k_1 dt, \tag{4.9}$$

which is easily solved to obtain:

$$\ln(\frac{q_e}{q_e - q_t}) = k_1 t, \tag{4.10}$$

so that finally:

$$q_t = q_e(1 - e^{-k_1 t}). \tag{4.11}$$

4.4.2.2 Pseudo-second-order kinetics

The pseudo-second-order model is an empirical modification of the Lagergren rate equation, and is based on the kinetic rate equation

$$\frac{dq_t}{dt} = k_2(q_e - q_t)^2, \tag{4.12}$$

where k_2 is the apparent second-order rate constant of sorption (mol^{-1} hour^{-1}), and q_e and q_t as in Section 4.4.2.1.

[1]The reactions are termed *psuedo* in order to differentiate these expressions based on the sorbent concentration from the models based on solute concentration

Proceeding in an identical manner as in previous section, one obtains:

$$\int_0^{q_t} \frac{dq_t}{(q_e - q_t)^2} = \int_0^t k_2 dt. \tag{4.13}$$

The solution to Equation 4.13 can be written on a linear form (see Ho & McKay (1999); Azizian (2004)):

$$\frac{t}{q} = \frac{1}{k_2 q_e^2} + \frac{1}{q_e} t, \tag{4.14}$$

which also can be expressed as:

$$q_t = \frac{k_2 q_e^2 t}{1 + k_2 q_e t} = \frac{ht}{1 + k_2 q_e t}, \tag{4.15}$$

in which the parameter $h = k_2 q_e^2$ is the initial sorption rate for q/t when $t \to 0$, and is in this study expressed in units of (mol h^{-1}).

The application of these two models to the experimental data on short-term ion exchange processes between CDHA and cell culture medium is presented in Figure 4.8a-c, and is also summarised in Table 4.4.

4.4.2.3 pH

During the 48 hours of contact, CDHA provoked acidification of both DMEM and McCoy cell culture medium, and in both normal and osteogenic conditions (Figure 4.8a). For convenience, the acidifying effect of CDHA was not reported as sorption, but directly analysed as pH of cell culture medium in an analogue way as described in Sections 4.4.2.1 and 4.4.2.2:

$$\mathrm{pH}_{\text{1st order}} = \mathrm{pH_i} - \Delta\mathrm{pH_e}(1 - e^{-k_3 t}), \tag{4.16}$$

and

$$\mathrm{pH}_{\text{2nd order}} = \mathrm{pH_i} - \frac{k_4 (\Delta\mathrm{pH_e})^2 t}{1 + k_4 \Delta\mathrm{pH_e} t}, \tag{4.17}$$

in which pH_i is the initial pH of the cell culture medium, pH_e is the pH at equilibrium, so that $\Delta\mathrm{pH}_e = \mathrm{pH}_i$ - pH_e.

In all four cases experimental data was perfectly fitted to any of the two non-linear models presented above. It was observed that CDHA provoked stronger acidification of McCoy media than of DMEM media (i.e., $\Delta\mathrm{pH}_{e,\mathrm{McCoy}} > \Delta\mathrm{pH}_{e,\mathrm{DMEM}}$).

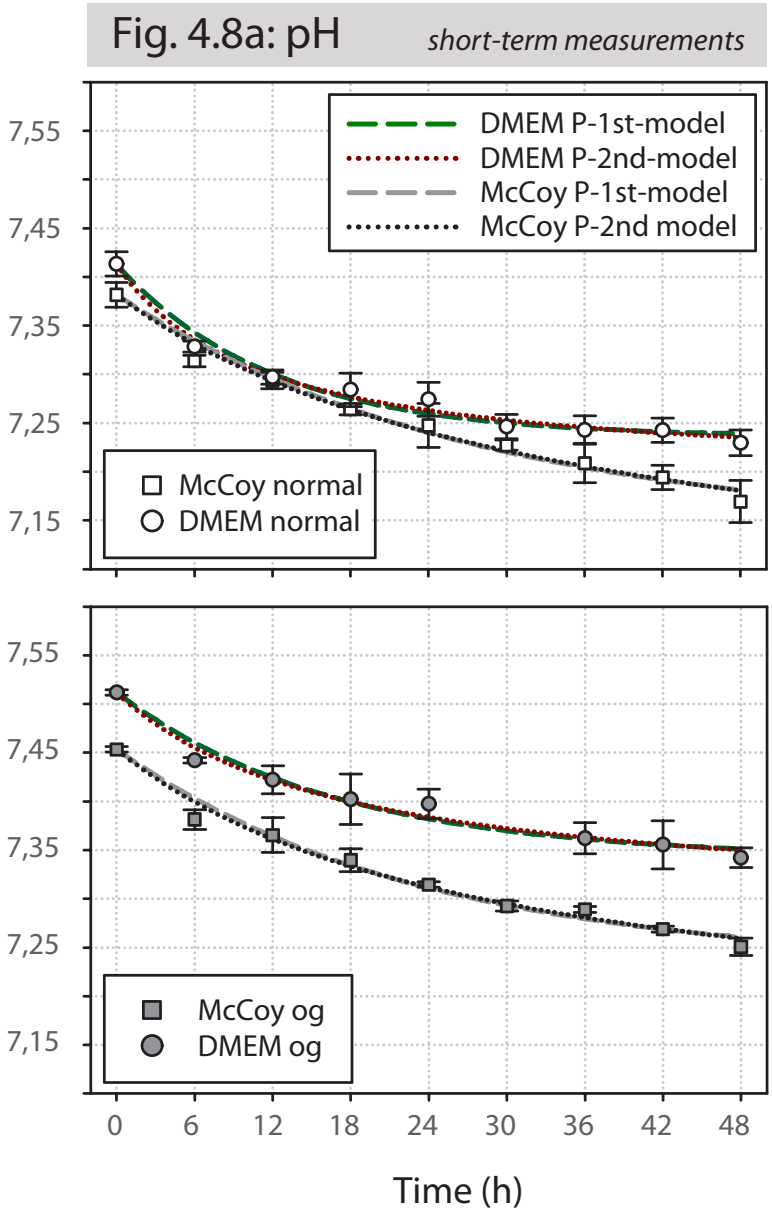

Figure 4.8: (a) pH of DMEM (○) and McCoy (□) medium in contact with CDHA. Data represents mean ± standard deviation (n=3). Modelled data is represented by dashed (first-order model) and dotted (second-order model) lines, respectively. Data obtained with osteogenic medium (bottom graph) is represented according to the same principle, but with filled symbols.

4.4.2.4 Sodium and potassium

Initial sorption of sodium onto CDHA, $q(Na^+)$, attained negative values in both normal DMEM and McCoy medium, indicating a release of sodium from the solid to the liquid phase (Figure 4.8b, left column). However, from $t > 24$ hours and on, this behaviour was reversed. By the of the contact period, more sodium had been sorbed onto CDHA from DMEM compared to McCoy medium. Using osteogenic medium the initial desorption was less pronounced, and further sorption was increased compared to using normal media.

Sorption kinetics of potassium onto CDHA, $q(K^+)$, was successfully represented by any of the non-linear models, in all four medium conditions.

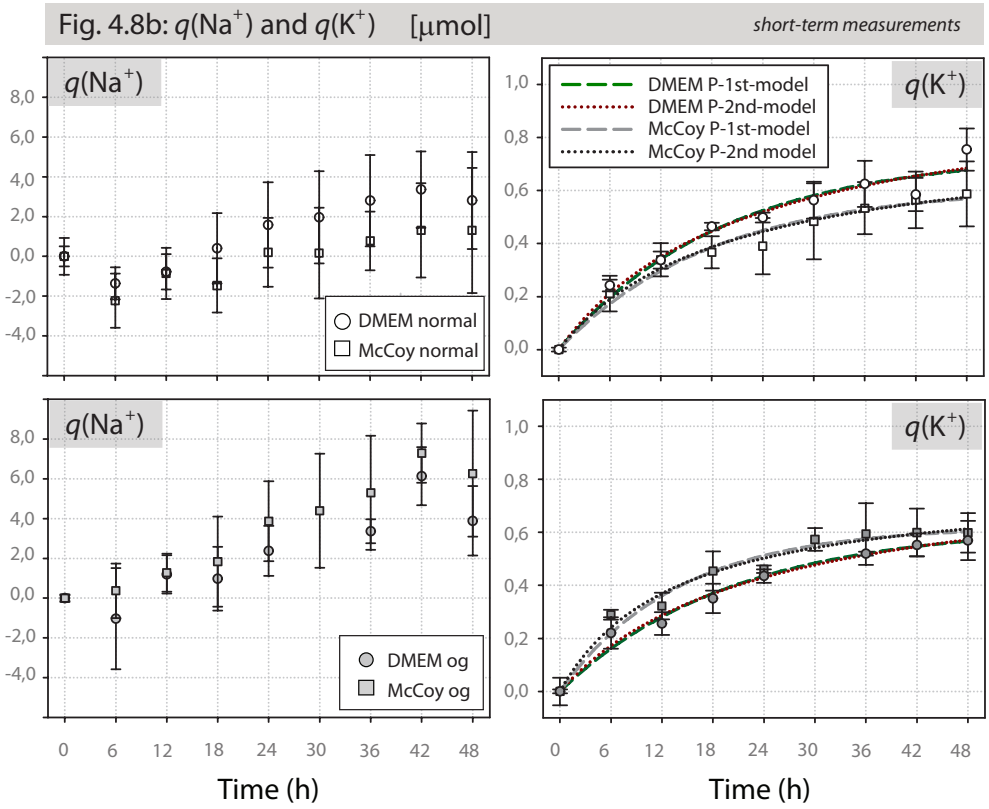

Figure 4.8: (b) Sorption (μmol) of sodium (left column) and potassium (right column), provoked by CDHA maintained in normal and osteogenic DMEM ($\circ$) and McCoy ($\square$) cell culture medium. Data represents mean $\pm$ standard deviation (n=3). Modelled data is represented by dashed (first-order model) and dotted (second-order model) lines, respectively.

4.4.2.5 Calcium and phosphorus

In both normal and osteogenic media, sorption of calcium, $q(Ca^{2+})$, followed non-linear rate mechanisms (Figure 4.8c, left column). The absolute sorption of calcium at equilibrium (q_e) was about two times higher in DMEM than in McCoy media, and a consequence of the higher calcium concentration of DMEMs ($[Ca^{2+}]_{DMEM} \approx 1.8\times [Ca^{2+}]_{McCoy}$). This also meant that q_e was reached earlier in McCoy media than in DMEM media.

An alternative view of calcium removal from cell culture medium exposed to CDHA is presented in Figure 4.9, where sorption kinetics of Ca^{2+} in osteogenic McCoy is drawn on a logarithmic-linear scale. In that case, three separate sections with distinct slopes indicate a stepwise disappearance of Ca^{2+} ions from solution ($0 \leq t_1 \leq 4$, $6 \leq t_2 \leq 12$, and $24 \leq t_3 \leq 48$).

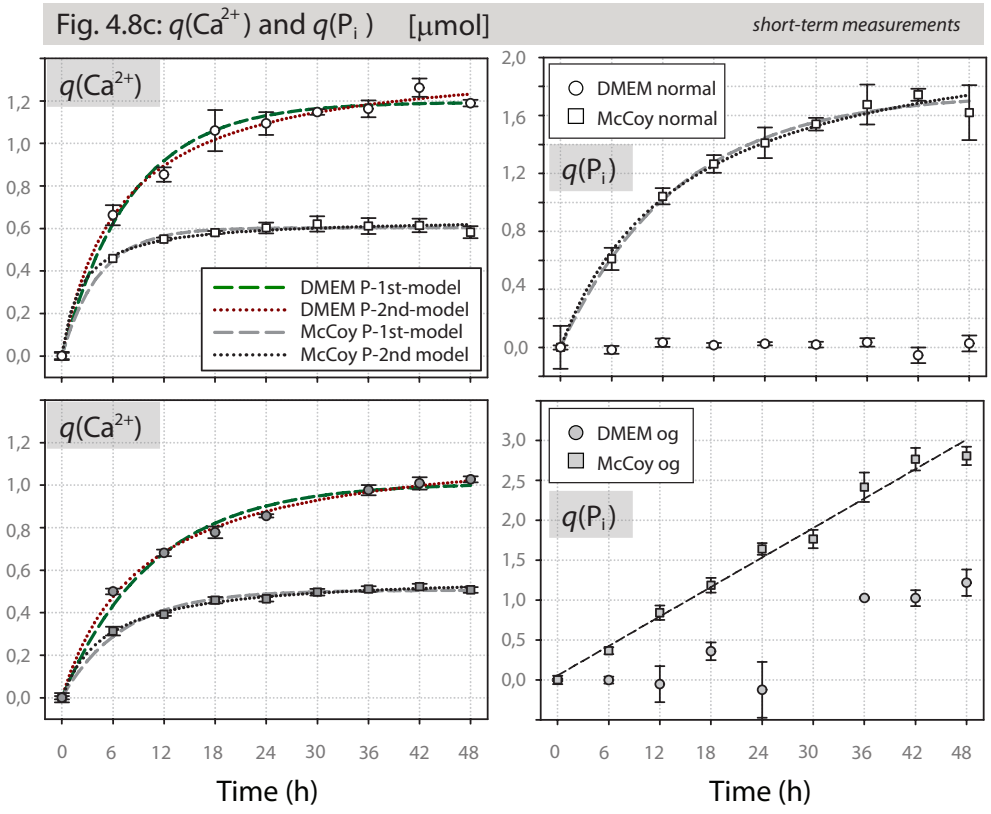

Figure 4.8: (c) Sorption (μmol) of calcium (left column) and phosphorus (right column), provoked by CDHA maintained in cell culture media. Symbols as described in Figure 4.8b.

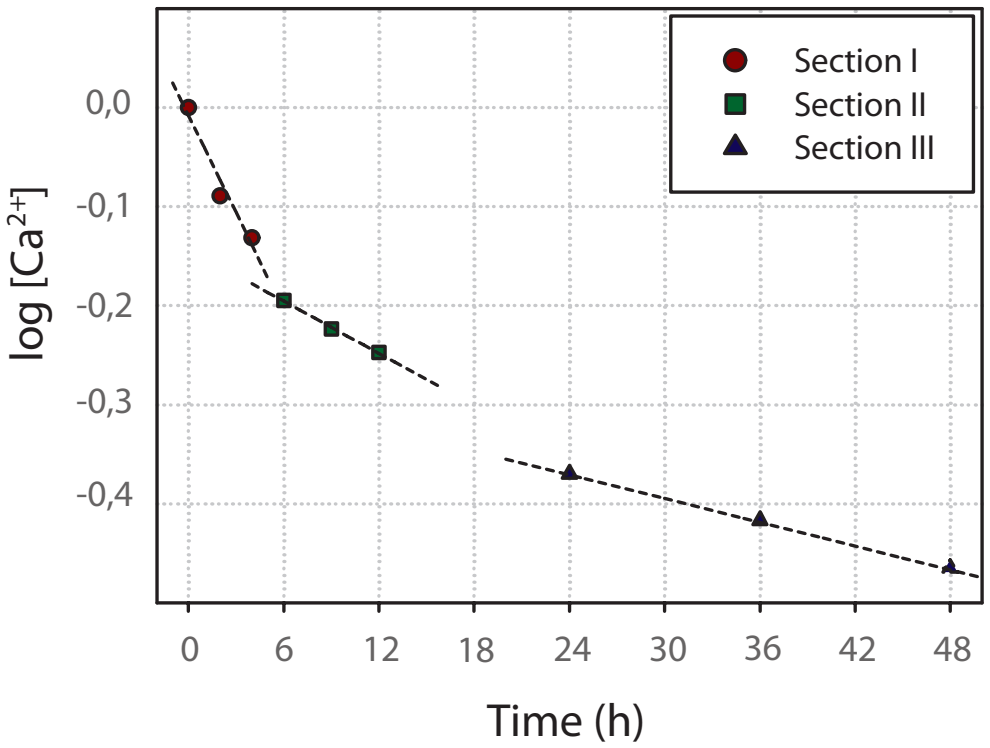

Figure 4.9: Stepwise disappearance of Ca^{2+} from osteogenic McCoy medium visualised on a *log-lin* format. Each separate section exhibited a linear format (R^2 = 0.9587, 0.9967, and 0.9999, respectively).

In contrast to the calcium reaction mechanism, sorption of total inorganic phosphorus, $q(P_i)$, did not demonstrate similar behaviour in McCoy and DMEM media (Figure 4.8c, right column). When CDHA was immersed in normal McCoy medium, P_i was sorbed according to the non-linear rate mechanisms, but when immersed in DMEM, no sorption of P_i was detected. In osteogenic media, where one of the osteogenic factors was β-glycerophosphate (β-GP), a spontaneous, linear increase of P_i occured in both McCoy and DMEM media in absence of CDHA (Fig 4.10). A slightly higher increase-rate was observed in McCoy medium (0.0637 mM h^{-1} with r^2 = 0.9903), than in DMEM medium (0.0519 mM h^{-1}, with r^2 = 0.9954).

To take into account the spontaneous release of P_i from osteogenic medium, the sorption of P_i from osteogenic medium to CDHA, $q(P_i)$, was calculated as follows (4.18):

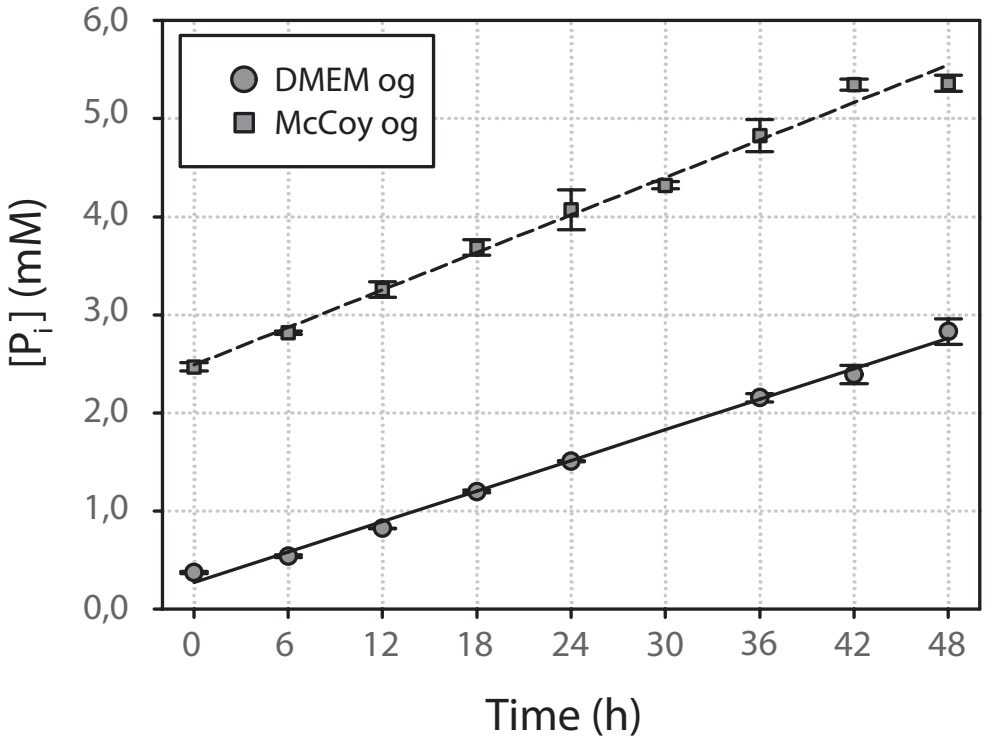

Figure 4.10: In absence of CDHA, the concentration of total inorganic phosphorus increased linearly and spontaneously in both osteogenic media.

$$q(\mathrm{P_i}) = ([\mathrm{P_i}]_{\mathrm{medium}} - [\mathrm{P_i}]_{\mathrm{sample}})V_{\mathrm{sample}}, \tag{4.18}$$

where V_{sample} is the volume of cell culture medium, $[\mathrm{P}_i]_{\mathrm{medium}}$ is the concentration of inorganic phosphorus at time t in osteogenic medium without CDHA, and $[\mathrm{P}_i]_{\mathrm{sample}}$ is the concentration of inorganic phosphorus at time t in osteogenic medium in presence of CDHA.

Using Equation 4.18, it was seen that sorption of P_i onto CDHA when immersed in osteogenic McCoy could be approximated with a linear model (Figure 4.8c, right column). Applying the same model to the experimental data on P_i-sorption from osteogenic DMEM was however not as successful ($r^2 = 0.7837$), since sorption during the first 24 hours was irregular. However, by the end of the contact period, significant sorption of P_i was observed also from osteogenic DMEM.

		Pseudo-first-order model $q = q_e(1 - e^{-k_1 t})$			**Pseudo-second-order model** $q = \frac{ht}{1+k_2 q_e t}$				**Linear model** $q = k^* t + C$		
Ion	Medium	q_e (mol)	k_1 (mol h^{-1})	R^2	h (mol h^{-1})	q_e (mol)	k_2 (mol^{-1}h^{-1})	R^2	k^* (mol h^{-1})	C (mol)	r^2
K$^+$	DMEM	0.740	0.0515	0.989	0.0447	1.005	0.0442	0.991			
	DMEM og	0.624	0.0499	0.996	0.0360	0.854	0.0494	0.997			
	McCoy	0.612	0.0552	0.992	0.0409	0.812	0.0621	0.995			
	McCoy og	0.622	0.0722	0.990	0.0579	0.786	0.0937	0.992			
Ca^{2+}	DMEM	1.194	0.122	0.996	0.204	1.409	0.103	0.998			
	DMEM og	1.010	0.0933	0.998	0.129	1.221	0.0867	1.000			
	McCoy	0.603	0.228	0.999	0.286	0.647	0.684	0.998			
	McCoy og	0.506	0.140	0.997	0.112	0.577	0.335	0.999			
P$_i$	DMEM										
	DMEM og								0.0288	-0.2398	0.784
	McCoy	1.754	0.0724	0.998	0.157	2.262	0.0306	0.997			
	McCoy og								0.0616	0.0658	0.986
		pH$_i$	k_3	ΔpH$_e$	R^2	pH$_i$	h	k_4	ΔpH$_e$	R^2	
pH	DMEM	7.41	-0.0841	0.178	0.992	7.41	0.0201	0.420	0.219	0.996	
	DMEM og	7.51	-0.0602	0.170	0.990	7.51	0.0127	0.262	0.220	0.994	
	McCoy	7.38	-0.0365	0.243	0.994	7.38	0.00991	0.082	0.348	0.995	
	McCoy og	7.45	-0.0433	0.220	1.000	7.45	0.0109	0.116	0.308	1.000	

Table 4.4: Sorbate model data.

From the non-linear models developed concerning sorption kinetics of calcium and phosphorus in normal McCoy media, it was also calculated the molar Ca/P sorption ratio (Figure 4.11). Except for the very begin of the contact period, the Ca/P ratio was far below the values anticipated for precipitation of calcium phosphate, in both normal and osteogenic media.

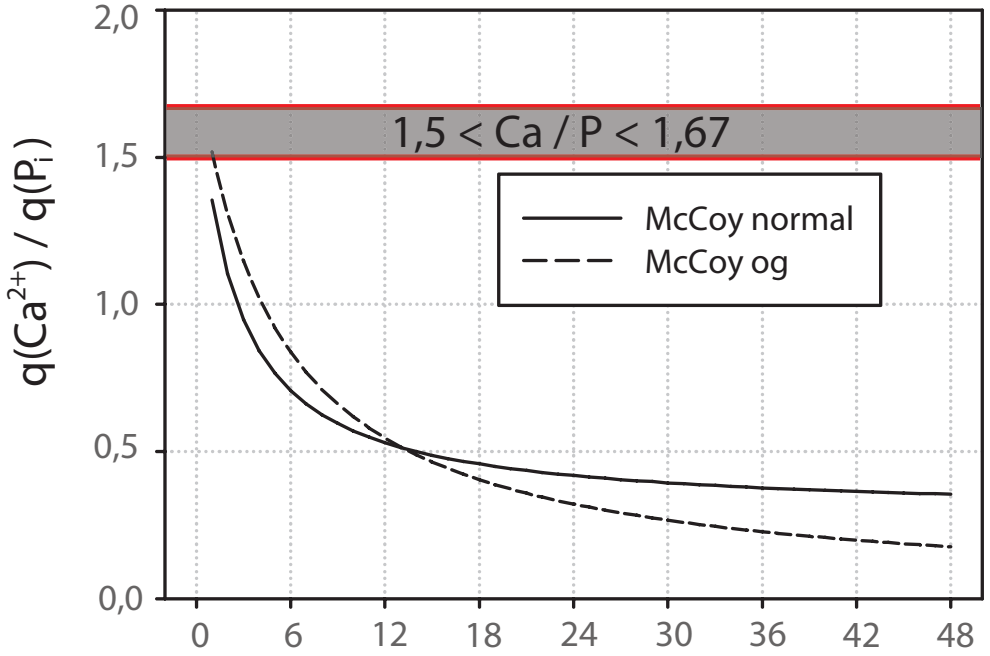

Figure 4.11: Dynamics of Calcium/Phosphorus sorption ratio in McCoy medium exposed to CDHA, calculated using the second-order sorption models.

4.4.3 Long-term Ion Exchange Processes

In addition to the short-term measurements (i.e., 48-hours kinetics), evolution of ionic interactions between CDHA and cell culture media was monitored during a period of three weeks. As opposed to short-term experiments, the cell culture medium was renewed on a regular basis in long-term experiments. Also, these experiments included serum-free cell culture medium (-FBS).

4.4.3.1 pH

Figure 4.12a shows how the acidification of cell culture media provoked by CDHA gradually decreased with time, and that towards the end of the 21 days-long contact period it was clearly decreased.

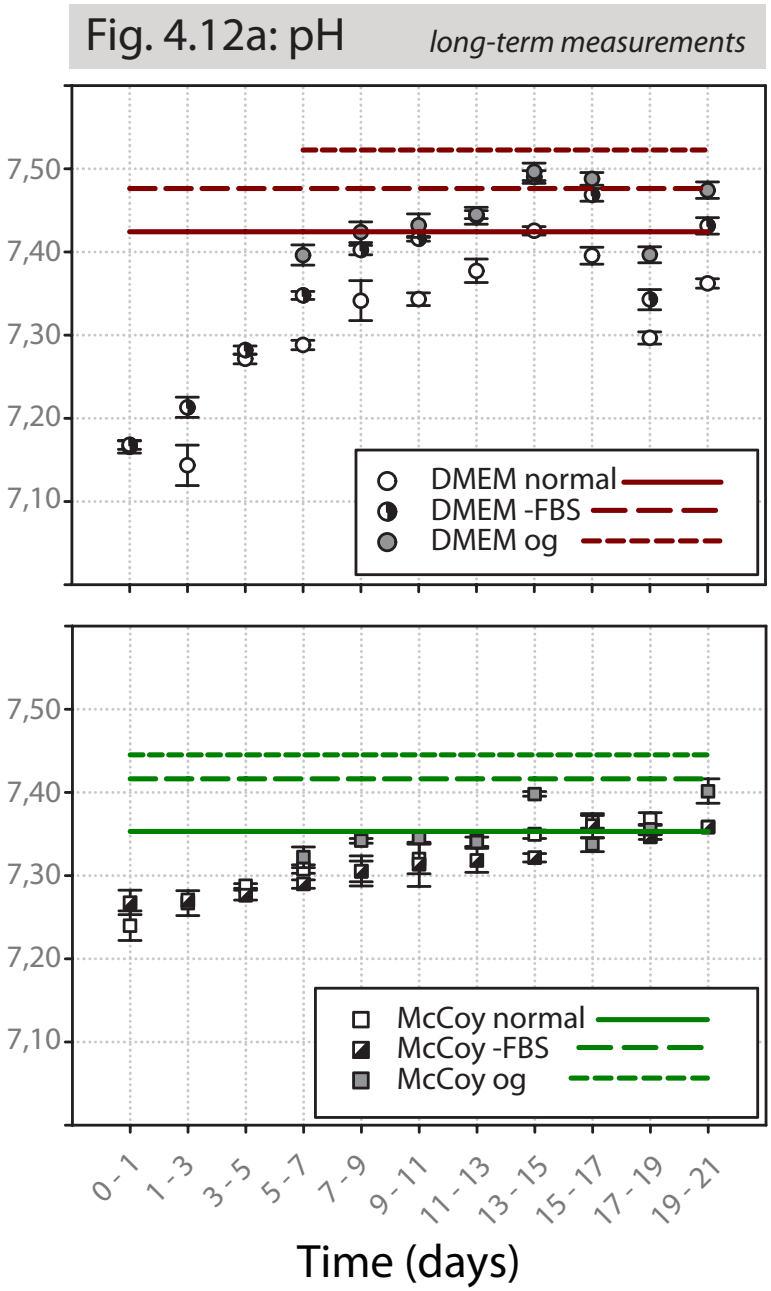

Figure 4.12: (a) pH of DMEM (○) and McCoy (□) medium after contact with CDHA and during different stages of the long-term experiments. Data represents mean ± standard deviation (n=3). Horizontal lines indicate the mean initial pH values of each medium type before exposure to CDHA (see Table 4.3).

4.4.3.2 Sodium and potassium

As already indicated by the short-term kinetic measurements (Figure 4.8b), CDHA provoked a release of sodium into the cell culture medium during the first 24 hours of contact (i.e. $q(Na^+) < 0$). In long-term experiments, where cell culture medium was repeatedly renewed with fresh medium, it was observed that beyond the first day, $q(Na^+)$ attained positive values, indicating sorption onto the material (Figure 4.12b, left column). With time, $q(Na^+)$ gradually decreased to approach zero by the end of the experiment.

Sorption of potassium, $q(K^+)$, was also observed to gradually decrease with time (Figure 4.12b, right column), and the sorption was clearly ceased by the end of the experiment. These observations were valid for all formulations of cell culture medium that were tested.

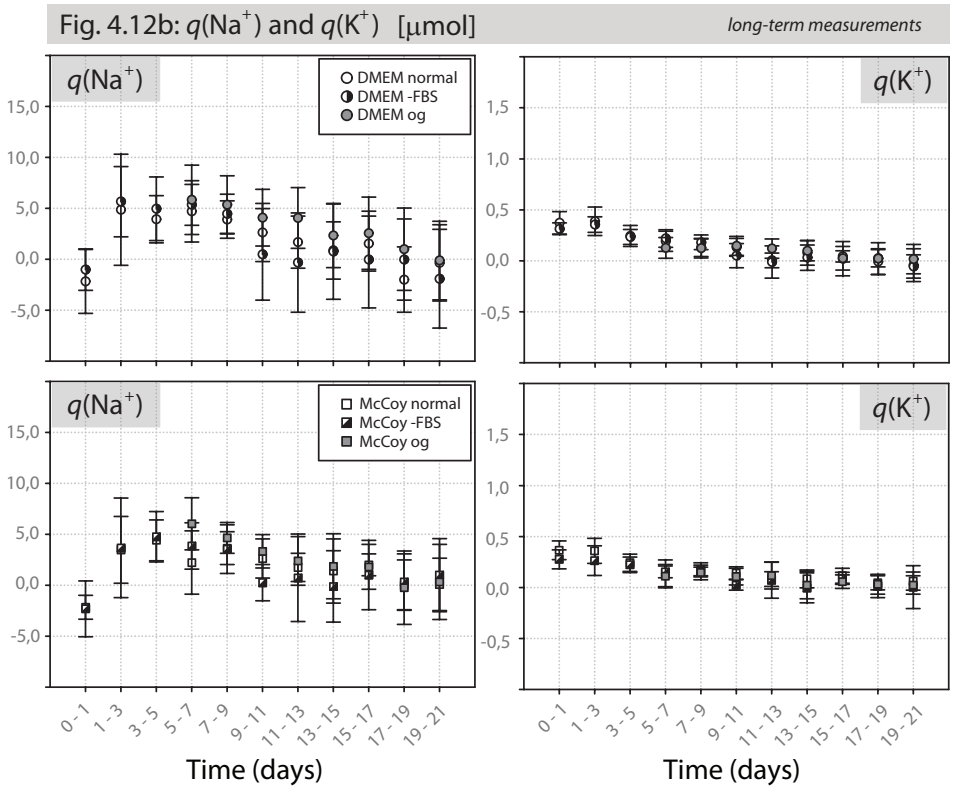

Figure 4.12: (b) Long-term CDHA/culture medium interactions. The experimental data (mean ± standard deviation, n=3) represents accumulated sorption during indicated time period, and is expressed in units of μmol. Left and right columns show sorption of Na^+ and K^+, respectively, from DMEMs (top row) and McCoys (bottom row).

4.4.3.3 Calcium and phosphorus

Sorption of calcium, $q(Ca^{2+})$, onto CDHA from cell culture medium was observed to continue throughout the full length of the experiment (Figure 4.12c, left column). While the absolute values of $q(Ca^{2+})$ gradually increased during the first week in McCoy medium (not taking into account the first value which represents the accumulation during only 24 hours), sorption of calcium from DMEM media was relatively stable from the very beginning. It was also observed that all different culture medium formulations provoked the same sorption behaviour, only difference being the absolute values.

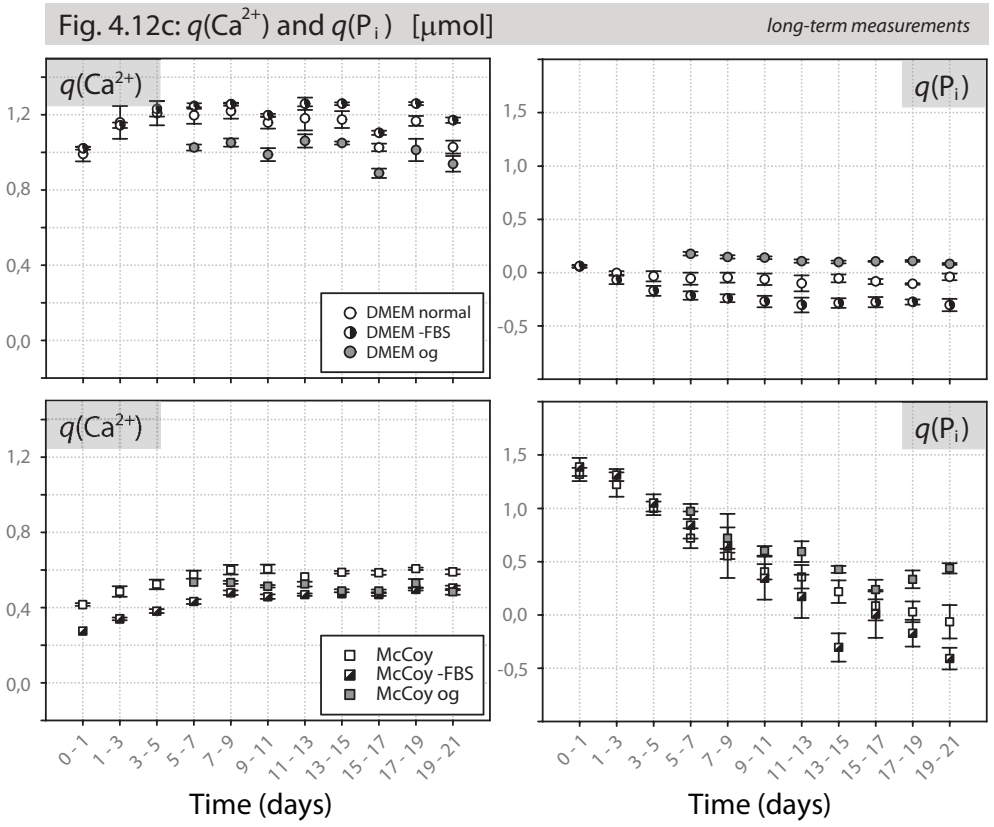

Figure 4.12: (c) Long-term CDHA/culture medium interactions. The experimental data (mean ± standard deviation, n=3) represents accumulated sorption during indicated time period, and is expressed in units of μmol. Left and right columns show sorption of Ca^{2+} and P_i, respectively, from DMEMs (top row) and McCoys (bottom row).

With respect to inorganic phosphorus, short-term experiments had revealed that CDHA provoked different interaction with normal DMEM compared to normal McCoy medium (recall Figure 4.8c). During long-term experiments (Figure 4.12c, right column), and in normal DMEM, it was observed that $q(\mathrm{P}_i)$ attained negative values with time (i.e. release of P_i from CDHA into the cell culture medium). The amount of P_i released into DMEM reached a stable level after about one week. The same effect, but even more pronounced, was observed using serum-free DMEM (-FBS). However, when CDHA was immersed in osteogenic DMEM, sorption of P_i was observed, and its absolute value was repeated until the end of the experiment.

To investigate the P_i-release mechanism observed using DMEM medium, a short-term kinetic study was performed with CDHA that had already been exposed to normal DMEM during eleven days according to the protocol of the long-term sorption experiments. It was observed that P_i initially was sorbed onto the CDHA, but between 12 h $< t <$ 24 h the sorption behaviour was reversed, resulting in an accumulated release of P_i by the end of the contact period (Figure 4.13).

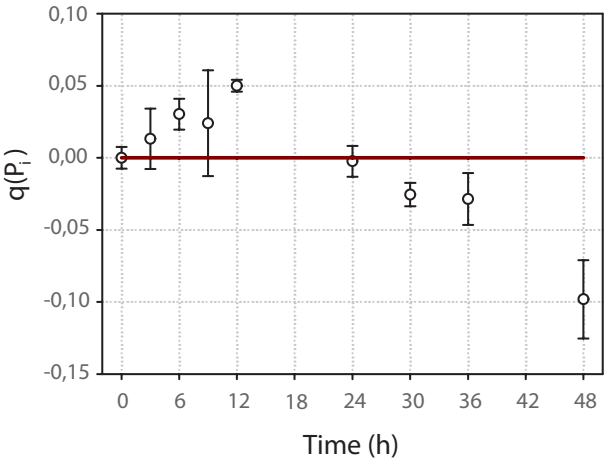

Figure 4.13: Short-term sorption kinetics of P_i provoked by CDHA immersed in normal DMEM. Data was obtained between day 11-13, and represents mean $\pm$ standard deviation (n=3), and is expressed in units of μmol.

CDHA in McCoy medium (both with and without FBS) induced sorption of P_i onto material. However, the effect was gradually decreased with time, and by the end of the experiment, $q(\mathrm{P}_i)$ approached values close to, or below, zero. When exposing CDHA to osteogenic McCoy, the sorption was also decreased with time, but beyond day 13, $q(\mathrm{P}_i)$ seemed to stabilise at positive value.

4.4.4 Surface Analysis

Long-term exposure of CDHA to cell culture media did not induce any drastic morphological changes of its surface (Figure 4.14). However, qualitative FTIR analyses revealed certain transformations of its chemical composition (Figure 4.15). Samples obtained from the interior core of the CDHA substrate (i.e. samples not directly exposed to cell culture medium) presented in both media peaks at 3569 cm^{-1} (hydroxyl stretch, ν_s), 1190-970 cm^{-1} (phosphate stretch, ν_3), 962 cm^{-1} (phosphate stretch, ν_1), 660-520 cm^{-1} (phosphate bend, ν_4), and 472 cm^{-1} (phosphate bend, ν_2). As there was little or no evidence of the most intesne CO_3^{2-} peaks (ν_3, around 1465 and 1410 cm^{-1}) in the core of CDHA, especially when exposed to McCoy medium, the peak observed around 870 cm^{-1} could be assigned to P-O(H) stretch of HPO_4^{2-} rather than to the carbonate ν_2 vibration mode, which also absorbs near this frequency (Wilson *et al.*, 2005). On the contrary, the surface of samples exposed to either of the serum-free cell culture media presenter clear peaks in the carbonate ν_3 region (Figure 4.15b). When cell culture media contained serum, the presence of proteins contributed with additional peaks, mainly in the region 1600-1700 cm^{-1}, and which were due to vibration of amide groups (Steiner *et al.*, 2007). Still one could clearly distinguish carbonate ν_3 peaks in the samples exposed to FBS-containing media, as well as osteogenic media. Additional peaks at 1595-1710 cm^{-1} (O-H bending) and 3000-3700 cm^{-1} (O-H stretching) were present in all media, and were associated to vibration of water (Baudot *et al.*, 2010).

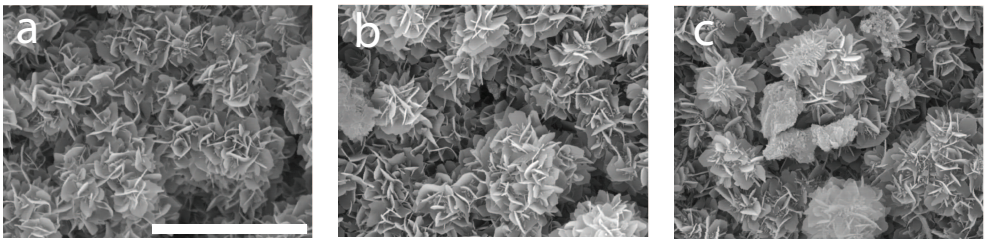

Figure 4.14: Micrographs of CDHA (a) before exposure to cell culture medium, (b) after exposure to DMEM, and (c) after expsoure to McCoy medium. Images were taken after 15 days in contact with culture medium. Scale bar represents 10 μm and applies to all three images.

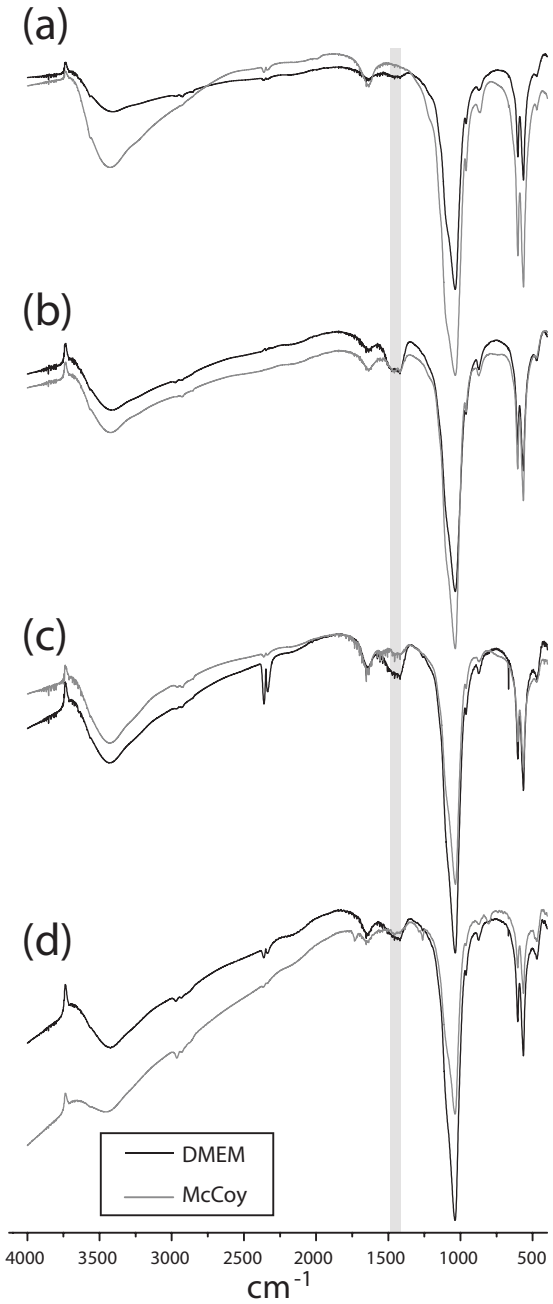

Figure 4.15: Transmission FTIR spectra of aged CDHA exposed to DMEM and McCoy, respectively. The spectra correspond to samples obtained from the interior of CDHA (a), or from the surface of CDHA exposed to media without FBS (b), media with FBS (c), and osteogenic media (d). Shaded zone indicate carbonate ν_3 vibrational mode.

4.5 Discussion

Development of new and improved medically useful biomaterials always requires specific attention to its surface properties (Kasemo, 2002). In the case of bone-substituting materials, the surface chemistry is particularly important for successful *in vivo* osteoconduction and osseointegration (LeGeros, 2002). To evaluate the clinical potential of these materials *in vitro*, the model system is reduced to a complex, but equilibrated, aqueous solution (e.g. simulated body fluid or cell culture medium), possibly in combination with biological material (e.g. cells and proteins). Although being extremely simplified, such model systems allow for a first screening of possible reactions induced by the material, and which may be of further importance for successful *in vivo* applications.

In this chapter it has been investigated how calcium-deficient hydroxyapatite, formed by hydrolysis of α-TCP, interacts with such simplified *in vitro* system when formed by cell culture medium, but in absence of cells. To emphasise the importance of the chemical composition of the aqueous phase, two different cell culture media have been used. Also, effort has been made to produce test conditions as authentic as possible, including working in sterile, protein-containing medium, at physiological temperature, and at CO_2 partial pressure of 0.05 atm. In these conditions, it was demonstrated that CDHA provoked ionic interactions with both cell culture media. However, the interactions varied both with time, and chemical composition of the cell culture medium, as illustrated schematically in Figure 4.16.

4.5.1 Ionic Interaction Mechanisms

Calcium phosphate-based biomaterials may interact with its aqueous environment through degradation (Lu *et al.*, 2002), as well as through ion-exchange processes (Boanini *et al.*, 2010). With respect to the latter reactions, if they only involve surface ion-exchange they are considered adsorptive and nonreactive, but if they result in precipitation or complexation of solute with the lattice ions, they should be considered as reactive processes. In aqueous solutions, where the CaP surface is electrically charged, potential-determining ions (among them Na^+, K^+, Ca^{2+}, P_i, and pH) can affect both degradation and ion-exchange processes, just as well as the ions themselves can be affected by the chemical composition of the CaP compound. And since the chemical composition of both the aqueous and solid phase is of greatest importance for the developing tissue, it is desirable to understand the mechanisms underlying the ionic interaction between them.

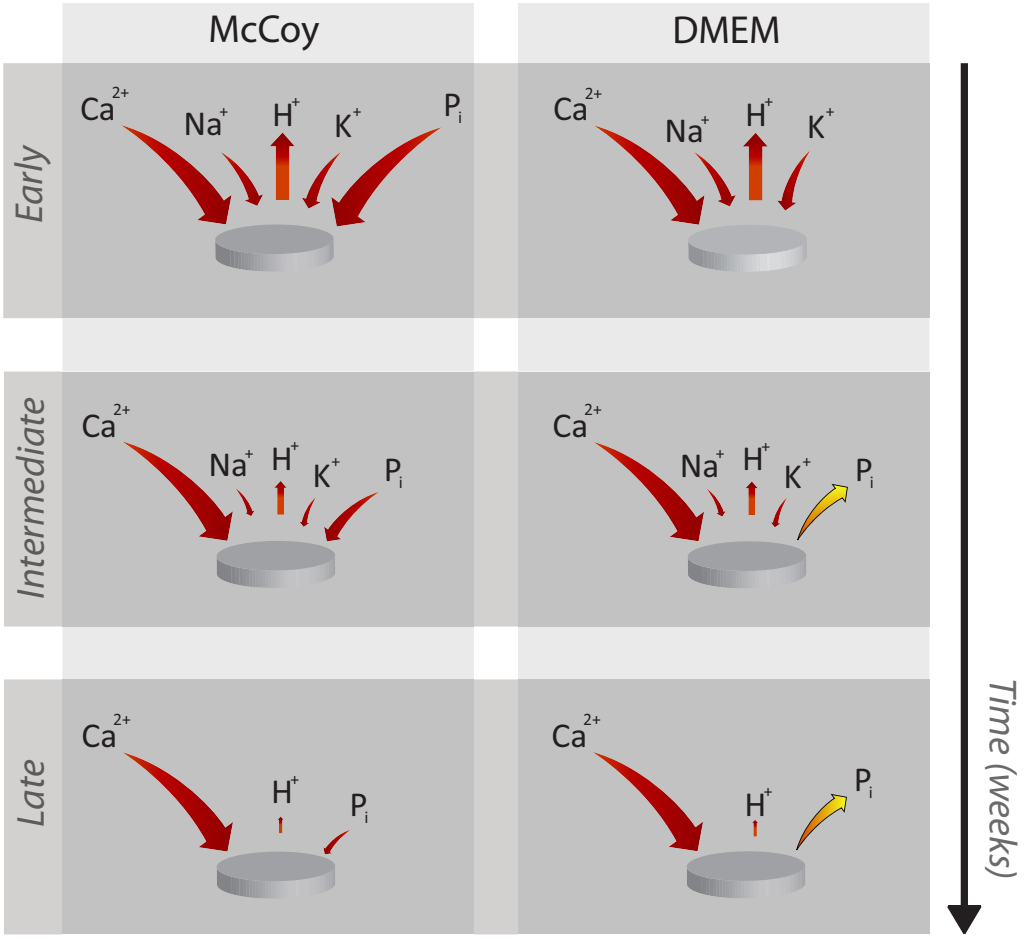

Figure 4.16: Schematic summary of ionic interactions provoked by CDHA, at different time intervals, when immersed in cell culture medium.

4.5.1.1 Short-term kinetics

In the present research, analyses of ionic interactions between CDHA and cell culture medium were carried out to correlate experimental kinetic data with theoretical sorption models which have been extensively used to study sorption and desorption processes related to solid/liquid phases (see Ho & McKay (1999) for a review), including cation removal from hydroxyapatite (Smiciklas *et al.*, 2008). However, little has been known about the theoretical origins of these non-linear models, and when they are suitable to apply. To clarify that issue, Azizian (2004) applied classical theory of Langmuirian kinetics to show that both models rely on the same fundamental equilibrium reaction:

$$\mathrm{A} + * \underset{k_d}{\overset{k_a}{\longleftrightarrow}} \mathrm{A_{(a)}}, \tag{4.19}$$

where A is the solute, $*$ is a vacant site, $\mathrm{A_{(a)}}$ is the solute sorbed onto the sorbent, and where k_a and k_d are the intrinsic adsorption and desorption rate constants. The common origin of these two models has also been demonstrated by Rudzinski & Plazinski (2006, 2009) by applying the concepts of Statistical Rate Theory. Thus, it follows that experimental data that was successfully represented by any of the non-linear models has to be considered subject to the sorption/desorption equilibrium reaction 4.19. Azizian (2004) further proposed that the pseudo-first-order model is appropriate to use when the sorption affects only little the initial concentration of solute. In this study, sorption was most pronounced for Ca^{2+}, which concentration typically decreased around 50% during the full contact period in all media, compared to concentrations of sodium and potassium which decreased only about 1-3% and about 8%, respectively. Although the interaction with phosphours depended on the type of medium, strong interaction was detected upon initial contact with McCoy medium ($\approx 50\%$). Despite the significant interaction with Ca^{2+} and P_i, absolute sorption of these ions onto CDHA was apparently not sufficient to disqualify the use of the pseudo-first-order model. Therefore, in the described experimental conditions, both models are equally useful to describe kinetic and equilibrium data related to ionic sorption provoked by CDHA.

The cases where the ionic interaction could not be represented by any of the non-linear models included P_i-interactions in normal DMEM and in both osteogenic media, as well as sorption of Na^+ from any of the different media. To begin with, osteogenic media contained β-GP which is known to be enzymatically hydrolysed by alkaline phosphatase present in the serum (Khouja *et al.*, 1990). The higher concentration of FBS in normal McCoy medium compared to normal DMEM medium resulted in a slightly higher β-GP-hydrolysis rate in osteogenic McCoy medium compared to osteogenic DMEM medium. It is important to realise that in presence of alkaline phosphatase-active cells (e.g. osteoblasts) the hydrolysation rate is likely to further increase (Chung *et al.*, 1992), and in that way β-GP is commonly employed as the external source of phosphate required to induce bone mineralisation *in vitro*. Here, simple FBS-induced hydrolysis of β-GP increased concentration of P_i sufficiently to affect the rate equation of equilibrium reaction (4.19). Since hydrolysis of β-GP lasted throughout the full time of contact, and

as the hydrolysis rates in both media were faster than sorption of P_i onto CDHA, $[P_i]_{\text{media}}$ and $q(P_i)$ both increased with time without acquiring equilibrium. Interestingly, hydrolysis of β-GP gradually created conditions for sorption of P_i from osteogenic DMEM, which indicates that absent sorption of phosphorus from normal DMEM could be due to its low initial concentration of P_i. Here it is however important to also consider that other ions more present in DMEM than in McCoy (e.g. carbonate: $[NaHCO_3]_{\text{DMEM}} \approx 1.68 \times [NaHCO_3]_{\text{McCoy}}$, see Table 3.4) might have played a role in the different P_i-interactions observed in the both media, and as will be further discussed in Section 4.5.1.2.

Regarding Na^+, it has to be taken into account that during hydrolysis of α-TCP, the calcium phosphate cement was maintained in NaCl-solution for one week, and it can be speculated that Na^+ ions sorbed during setting of the cement interfered at an initial stage in the kinetic measurements. This idea is supported by the desorption of Na^+ during the early stage of the contact period.

Given the basic assumption that ions in culture medium are sorbed into vacant sites on CDHA, the non-linear sorption models provide information on for example sorption rate and equilibrium state. However, the exact location of these vacant sites are not explicitly specified. Yet, kinetic sorption data can to some extent indicate the site of ionic exchange, or rather, that these are located in principally different compartments of the solid/liquid interface. As demonstrated in Figure 4.9, removal of calcium from cell culture medium could be reasonably well represented as a three-step, logarithmic function, i.e. $\log([Ca^{2+}]) \propto t$, although kinetic data is sparse. As proposed by Neuman & Neuman (1958), these steps correspond, in turn, to an exchange of ions between (1) bulk solution and the hydrated layer of the solid, (2) the hydrated layer and the non-hydrated surface of the solid, and finally (3) between the crystal surface and successive layers of the internal lattice. Moreover, when studying phosphate exchange with L-apatite, it was demonstrated that the rate of step 2, but not step 3, was influenced by the ionic strength of the aqueous phase (Neuman & Neuman, 1958, p.69). The latter observation indicated that, in the third phase the reactants were out of solution and within the crystal. Whether the same principle applies to the model system studied in this chapter has to be further investigated.

In summary, the absolute levels of short-term ionic interactions provoked by CDHA, mainly with respect to Ca^{2+}, but also P_i in McCoy medium, are of such magnitude that their biological influence should be carefully considered. It is well-known that both extracellular calcium and phosphate regulate essential osteoblastic functions (Beck, 2003; Dvorak *et al.*, 2004; Liu

et al., 2009), and previous works with calcium phosphate based materials have demonstrated that solution-mediated surface reactions by themselves potentially can influence bone tissue development both positively and negatively (Knabe *et al.*, 2000; Hempel *et al.*, 2004; Radin *et al.*, 2005; Engel *et al.*, 2008). In such context it is important to also mention the acidifying effect provoked by CDHA. Although the acidification was relatively low (about 3%), the absolute change (up to 0.3 pH units) is more than sufficient to influence cellular behaviour (Brandao-Burch *et al.*, 2005). The mechanism of acidification is complex, as it may be a consequence not only of expulsion of "H^+" or uptake of OH^- ions by the material, but also an indirect effect of phosphorus and carbonate interactions which both can influence the pH of the aqueous phase (see Section 2.1.1.3, and Section 3.1.4).

4.5.1.2 Long-term kinetics

Presence of proteins in the extracellular environment is not only a requisite for cell growth and viability, but is also a consequence of cellular activity. With respect to bone tissue, several proteins in the extracellular environment may act either as inhibitor or promotor of mineralisation (Boskey, 1996), and adsorption of proteins to the bone biomaterial surface may also influence the material's nucleation rate (Combes & Rey, 2002), as well as its dissolution and ion-exchange processes (Kandori *et al.*, 2005).

Absence of FBS in the cell culture medium influenced the absolute sorption levels. It has previously been reported that FBS can provoke significant shifts in surface zeta potential of hydroxyapatite materials (Suzuki *et al.*, 1998). Still, the physical character of ion reactivity of CDHA with respect to any of investigated ions was not influenced by FBS. In strong contrast to the relatively small effect of serum proteins, the parameter of time had great influence on CDHA reactivity. When repeatedly exposed to fresh cell culture medium, CDHA underwent a maturation, or ageing, process, as judged by its changed ion reactivity. In this study, ionic reactivity of CDHA was observed to go in all directions: decrease, increase, or remain stable, depending mainly on the specific ion investigated.

First, gradual decrease until no more sorption occurred was observed for both sodium and potassium ions, and in both media. That observation indicates that CDHA has low acceptance for these ions in a longer perspective, and suggests that there is limited, or no space for these ions to incorporate into the crystal structure.

Decreased activity was also observed for P_i when CDHA was immersed in normal and serum-free McCoy medium. However, in that case, the sorption did not slowly cease like with Na^+ and K^+, but rather followed a close to

linear decrease, and actually seemed to be driven towards a change of character, i.e. release of P_i, by the end of the experiment. To understand this behaviour, it is advantageous to first consider how CDHA interacted with P_i when immersed in normal and serum-free DMEM medium. In both those cases, the ionic reactivity was increased with time, in the sense that release of P_i gradually increased from being almost undetectable, until reaching a significant and stable level. As was shown in Figure 4.13, the kinetics of such release did not follow any of the previously adopted models, but rather seemed to involve two distinct mechanisms: first sorption (0 h $\leq t <$ 12 h), and then release of P_i (12 h $\leq t <$ 48 h). The progressive release of P_i ions is likely due to ion replacement with ions available in the culture medium, typically carbonate. FTIR analyses support the idea of ion replacement processes in aged CDHA samples, as they showed that carbonate ions were incorporated into the CDHA. Specifically, occupancy of carbonate ν_3 sites are reported to depend on competition between the phosphate and carbonate ions (Rehman & Bonfield, 1997), and were detected in all samples directly exposed to culture media. Their presence suggests that decreased P_i reactivity in McCoy partly could be due to release of P_i when replaced by carbonate. Whether this P_i/CO_3^{2-}-replacement process accounts for all the decreased sorption of P_i from McCoy medium, or if sorption also was decreased due to reduction of the hydrated layer cannot be determined from the data presented here.

As carbonate may incorporate into the crystal structure on the account of phosphate ions, it may also replace for OH^-. Since one of the long-term effects of CDHA reactivity is a decreased acidification of the cell culture medium, one can speculate that incorporation of carbonate lead to expulsion of OH^-. While P_i/CO_3^{2-}-replacement is represented by carbonate ν_3 peaks, OH^-/CO_3^{2-} replacement rather influence the ν_2 peak (Rehman & Bonfield, 1997). However, in our qualitative FTIR study it is difficult to judge the efficiency of such replacement since this peak coincide with the P-(OH)-stretch.

Finally, ionic reactivity of CDHA with respect to Ca^{2+} was the only observed to maintain stable throughout the full experiment. This proposes that Ca^{2+} interactions are independent of CDHA ageing, and that the sorption capacity of CDHA with respect to Ca^{2+} was far from reached during the course of three weeks. As a consequence of above observations, and in combination with its relatively fast sorption kinetics, it is tempting to believe that CDHA must have presented excessive vacant sites for incorporation of calcium into its crystal structure. Additional studies are however required to fully confirm this theory.

Taken altogether, the obtained results clearly demonstrate that ion reactivity of CDHA is highly dependent on the chemical composition of its aqueous environment. Since it is well known that changes of the ionic culture environment, especially with respect to calcium and phosphate, can have significant effects on the activity of bone cells and mesenchymal stem cells (Beck, 2003; Dvorak *et al.*, 2004; Liu *et al.*, 2009), this observation becomes important in order to correctly interpret cellular response to CDHA and many other calcium phosphate based biomaterials that undergo solution-mediated surface reactions. As in all aspects of biomaterials and tissue engineering research, the possibility to correlate test results obtained *in vitro* with clinical performance is very attractive, but our data demonstrates that direct translation of any proof of concepts obtained *in vitro* has to be very carefully done. Possible consequences of the presented data in this chapters may be that different cellular response to the tested material is observed only because cells are provided a different culture medium. Moreover, it is known solution-mediated surface reactions are known to play a key role for the *in vivo* behaviour of bioactive ceramics Knabe & Ducheyne (2008). Specifically, release of calcium and phosphate ions are claimed to induce bioactivity of calcium phosphate biomaterials (LeGeros, 2002; Chang *et al.*, 2000b; Boyde *et al.*, 1999), and it is also speculated that such processes can contribute to the osteoinductive capacity of the biomaterial (de Bruijn *et al.*, 2008; Yuan *et al.*, 2010). The data presented in this chapter could therefore in the worst case mean that slight physiological differences between patients could provoke different response of the material upon implantation. One should therefore be extremely cautious when extrapolating results obtained with surface-reactive materials *in vitro* to its possible *in vivo* performance.

Finally, given the perfect accordance between experimental data and theoretical sorption models it is encouraged continued exploration and use of models for precise description of biomaterial activity in complex physiological environments. Such approach could contribute positively to the process of developing biomaterials with capacity to biochemically guide tissue growth and function.

4.6 Conclusions

This chapter, in which it has been detailed how the ionic reactivity of calcium-deficient hydroxyapatite may influence the *in vitro* ionic extracellular environment, has given one example of how sensors applied to the *in vitro* tissue engineering environment can be beneficial for characterisation of the activity of certain biomaterials.

In particular, fresh CDHA exposed to cell culture medium was shown to be subject to ion sorption/desorption equilibrium processes which could be mathematically described with high coefficients of determination using the pseudo-first and pseudo-second-order sorption models. The provoked interactions were most pronounced with respect to calcium and phoshporus, and of such magnitude that they potentially could influence cellular behaviour. Important to notice however is that slight variations in the chemical composition of the cell culture media did provoke different ion reactivity with respect to total inorganic phosphorus. It was further shown that ion reactivity of CDHA was a function of material maturity as sorption kinetics changed greatly over time. Long-term kinetic sorption data and FTIR surface analyses provided indications on that specific ion replacement processes had occurred.

This work specifically demonstrates that the ion reactivity of CDHA (and many other CaP compounds) is dependent on two main external parameters; the chemical composition of the aqueous environment, and time of exposure. It is therefore emphasised that classification of the ionic reactivity of a biomaterial always should to be presented in relation to these two parameters.

Bibliography

Albrektsson, T. & Johansson, C. (2001). *European Spine Journal,* **10**, S96–S101.

Azizian, S. (2004). *Journal of Colloid and Interface Science,* **276**, 47–52.

Bagambisa, F., Joos, U., & Schilli, W. (1993). *Journal of Biomedical Materials Research,* **27** (8), 1047–1055.

Baudot, C., Tan, C. M., & Kong, J. C. (2010). *Infrared Physics & Technology,* **53** (6), 434–438.

Beck, G. R. (2003). *Journal of Cellular Biochemistry,* **90**, 234–243.

Ben-Nissan, B. & LeGeros, R. (2008). In: *Encyclopedia of Biomaterials and Biomedical Engineering*, (Wnek, G. E. & Bowlin, G. L., eds) pp. 225–235. Informa Healthcare.

Bianco, P. & Robey, P. G. (2001). *Nature,* **414**, 118–121.

Boanini, E., Gazzano, M., & Bigi, A. (2010). *Acta Biomaterialia,* **6**, 1882–1894.

Bohner, M. & Lemaitre, J. (2009). *Biomaterials,* **30**, 2175–2179.

Boskey, A. L. (1996). *Connective Tissue Research,* **35** (1-4), 357–363.

Boyde, A., Corsi, A., Quatro, R., Cancedda, R., & Bianco, P. (1999). *Bone,* **24**, 579–589.

Brandao-Burch, A., Utting, J. C., Orriss, I. R., & Arnett, T. R. (2005). *Calcified Tissue International,* **77**, 167–174.

Cazalbou, S., Eichert, D., Ranz, X., Drouet, C., Combes, C., Harmand, M., & Rey, C. (2005). *Journal of Materials Science: Materials in Medicine,* **16**, 405–409.

Chang, B.-S., Lee, C.-K., Hong, K.-S., Youn, H.-J., Ryu, H.-S., Chung, S.-S., & Park, K.-W. (2000a). *Biomaterials,* **21**, 1291–1298.

Chang, Y.-L., Stanford, C. M., & Keller, J. C. (2000b). *Journal of Biomedical Materials Research,* **52**, 270–278.

Chen, P., Toribara, T., & Warner, H. (1956). *Analytical Chemistry,* **28** (11), 1756–1758.

Chen, Q.-Z. & Boccaccini, A. R. (2008). In: *Encyclopedia of Biomaterials and Biomedical engineering*, (Wnek, G. E. & l. Bowlin, G., eds) pp. 142–151. Informa Healthcare.

Chung, C., Golub, E., Forbes, E., Tokuoka, T., & Shapiro, I. (1992). *Calcified Tissue International,* **51**, 305–311.

Combes, C. & Rey, C. (2002). *Biomaterials,* **23**, 2817–2823.

Daculsi, G., Laboux, O., & Weiss, P. (2005). In: *Engineered Bone*, (Petite, H. & Quarto, R., eds) chapter 6, pp. 60–71. Eurekah.com / Landes Bioscience.

Daculsi, G. & LeGeros, R. (2008). In: *Encyclopedia of Biomaterials and Biomedical Engineering*, (Wnek, G. E. & Bowlin, G. L., eds) pp. 359–366. Informa Healthcare.

de Bruijn, J., Shankar, K., Huan, Y., & Habibovic, P. (2008). *Bioceramics and their clinical applicaitons* chapter Osteoinduction and its evaluation, pp. 199–219. Cambridge: Woodhead publishing Ltd.

Di-Silvio, L., Gurav, N., & Tsiridis, E. (2008). In: *Encyclopedia of Biomaterials and Biomedical Engineering*, (Wnek, G. E. & Bowlin, G. L., eds), pp. 2652–2659. Informa Healthcare.

Ducheyne, P. & Qiu, Q. (1999). *Biomaterials,* , **20**, 2287–2303.

Dvorak, M. M., Siddiqua, A., Ward, D. T., Carter, D. H., Dallas, S. L., Nemeth, E. F., & Riccardi, D. (2004). *PNAS,* , **101** (14), 5140–5145.

Eichert, D., Sfihi, H., Banu, M., Cazalbou, S., Combes, C., & Rey, C. (2002). In: *CIMTEC 2002 Proceedings*, ,, 10th International Ceramics Congress & 3rd Forum of New Materials Florence, Italy: CIMTEC.

Engel, E., del Valle, S., Aparicio, C., Altankov, G., Asin, L., Planell, J. A., & Ginebra, M. P. (2008). *Tissue Engineering,* **14**, 1341–1351.

Espanyol, M., Perez, R., Montufar, E., Marichal, C., Sacco, A., & Ginebra, M. (2009). *Acta Biomateriala,* **5** (7), 2752–2762.

Giannoudis, P. V., Dinopoulos, H., & Tsiridis, E. (2005). *Injury. International Journal of the Care of the Injured,* **36S**, S20–S27.

Ginebra, M.-P., Fernandez, E., Driessens, F. C. M., & Planell, J. A. (1999). *Journal of the American Ceramic Society,* **82** (10), 2808–2812.

Habraken, W., Wolke, J., & Jansen, J. (2007). *Advanced Drug Delivery Reviews,* **59**, 234–248.

Haidar, Z. S., Hamdy, R. C., & Tabrizian, M. (2009). *Biotechnology Letters,* **31**, 1817–1824.

Hempel, U., Reinstorf, A., Poppe, M., Fischer, U., Gelinsky, M., Pompe, W., & Wenzel, K. W. (2004). *Journal of Biomedical Materials Research Part B: Applied Biomaterials,* **71** (1), 130–143.

Hing, K. A. (2004). *Philosophical Transactions of the Royal Society A: Mathematical, Physical & Engineering Sciences,* **362**, 2821–2850.

Ho, Y. & McKay, G. (1999). *Process Biochemistry,* **34**, 451–465.

Ito, A. & Ohgushi, H. (2008). In: *Encyclopedia of Biomaterials and Biomedical Engineering*, (Wnek, G. E. & Bowlin, G. L., eds) pp. 461–469. Informa Healthcare.

Jukes, J. M., Both, S. K., van Blitterswijk, C. A., & de Boer, J. (2008). *Regenerative Medicine,* **3** (6), 783–785.

Kamitakahara, M., Ohtsuki, C., & Miyazaki, T. (2008). *Journal of Biomaterials Applications,* **23**, 197–212.

Kandori, K., Masunari, A., & Ishikawa, T. (2005). *Calcified Tissue International,* **76**, 194–206.

Kasemo, B. (2002). *Surface Science,* **500**, 656–677.

Khouja, H., Bevington, A., Kemp, G., & Russell, R. (1990). *Bone,* **11**, 385–391.

Knabe, C. & Ducheyne, P. (2008). *Bioceramics and their clinical applications* chapter 6 Cellular response to bioactive ceramics, pp. 133–164. Cambridge: Woodhead publishing Ltd.

Knabe, C., Planell, F. C. M. D. A. J. A., Gildenhaar, R., Berger, G., Reif, D., Fitzner, R., Radlanski, R. J., & Gross, U. (2000). *Journal of Biomedical Materials Research,* , **52**, 498–508.

Kokubo, T. & Takadama, H. (2006). *Biomaterials,* , **27**, 2907–2915.

Lagergren, S. (1898). *Kungliga Svenska Vetenskapsakademiens Handlingar,* , **24** (4), 1.

LeGeros, R. Z. (2002). *Clinical Orthopaedics and Related Research,* , **395**, 81–98.

Liu, H., Park, G. E., & Webster, T. J. (2008). In: *Encyclopedia of Biomaterials and Biomedical Engineering*, (Wnek, G. E. & Bowlin, G. L., eds), pp. 179–194. Informa Healthcare.

Liu, Y. K., Lu, Q. Z., Pei, R., Ji, H. J., Zhou, G. S., Zhao, X. L., Tang, R. K., & Zhang, M. (2009). *Biomedical Materials,* , **4**, 1–8.

Lu, J., Descamps, M., Dejou, J., Koubi, G., Hardouin, P., Lemaitre, J., & Proust, J.-P. (2002). *Journal of Biomedical Materials Research,* , **63** (4), 408–412.

Misra, D. (1999). *Journal of Biomedical Materials Research,* , **48** (6), 848–855.

Neuman, W. F. & Neuman, M. W. (1958). *The Chemical Dynamics of Bone Mineral*. : The University Of Chicago Press.

Ogose, A., Hotta, T., Kawashima, H., Kondo, N., Gu, W., Kamura, T., & Endo, N. (2005). *Journal of biomedical materials research. Part B, Applied biomaterials,* **72B** (1), 94–101.

Place, E. S., Evans, N. D., & Stevens, M. M. (2009). *Nature Materials,* **8**, 457–470.

Porter, A. E., Patel, N., & Best, S. (2008). In: *Encyclopedia of Biomaterials and Biomedical Engineering*, (Wnek, G. E. & Bowlin, G. L., eds) pp. 1451–1463. Informa Healthcare.

Radin, S., Reilly, G., Bhargave, G., Leboy, P., & Ducheyne, P. (2005). *Journal of Biomedical Materials Research,* **73A**, 21–29.

Rehman, I. & Bonfield, W. (1997). *Journal of Materials Science: Materials in Medicine,* **8**, 1–4.

Rudzinski, W. & Plazinski, W. (2006). *The Journal of Physical Chemistry B,* **110**, 16514–pp.

Rudzinski, W. & Plazinski, W. (2009). *Adsorption,* **15**, 181–192.

Salgado, A. J., Coutinho, O. P., & Reis, R. L. (2004). *Macromolecular Bioscience,* **4**, 743–765.

Seebach, C., Schultheiss, J., Wilhelm, K., Frank, J., & Henrich, D. (2010). *Injury - International Journal of the care of the injured,* **41** (7), 914–921.

Smiciklas, I., Onjia, A., Raicevic, S., Janackovic, D., & Mitric, M. (2008). *Journal of Hazardous Materials,* **152**, 876–884.

Steiner, G., Tunc, S., Maitz, M., & Salzer, R. (2007). *Analytical Chemistry,* **79**, 1311–1316.

Suzuki, T., Yamamoto, T., Toriyama, M., Nishizawa, K., Yokogawa, Y., Mucalo, M. R., Kawamoto, Y., Nagata, F., & Kameyama, T. (1998). *Journal of Biomedical Materials Research,* **34**, 507–517.

Wilson, R. M., Elliott, J. C., Dowker, S. E., & Rodriguez-Lorenzo, L. M. (2005). *Biomaterials,* **26**, 1317–1327.

Yuan, H., Fernandes, H., Habibovic, P., de Boer, J., Barradas, A. M. C., de Ruiter, A., Walsh, W. R., van Blitterswijk, C., & de Bruijn, J. D. (2010). *PNAS,* **107**, 13614–13619.

Yuan, H., Yang, Z., de Bruijn, J. D., de Groot, K., & Zhang, X. (2001). *Biomaterials,* **22**, 2617–2623.

Chapter 5

Cellular Response to the Dynamic Ionic Environment Induced by Calcium-deficient Hydroxyapatite

5.1 Introduction

Results presented in Chapter 3 and Chapter 4 clearly demonstrate that osteoblast-like cellular activity and biochemical activity of calcium-deficient hydroxyapatite (CDHA) both may influence the ionic environment with respect to major extracellular ions. When combining those two components in the same environment it is therefore reasonable to believe that they may influence each other. Therefore, in this chapter it has been studied to what extent osteoblast-like cells are affected by the dynamic ionic environment induced by CDHA when immersed in protein-containing cell culture medium.

5.1.1 Ionically Reactive CaP Compounds and its Possible Influnce on Osteoblast Behaviour

CDHA, like many other calcium phosphate based compounds (including bioglass), is a chemically active material that when immersed in aqueous solutions, can induce both non-reactive ion-exchange and reactive complexation of solute with the lattice ions (Cazalbou *et al.*, 2005; Boanini *et al.*, 2010). The consequences of such ionic reactivity may on one hand be that proteins and cells are influenced by changes in the ionic extracellular environment, and on the other hand that dissolution and precipitation of ions physically

change the surface chemistry and topography of the reacting material. With other words, calcium phosphate (CaP) compounds may transmit to cells both chemical and physical signals which can act both synergistically or agonistically to influence cellular growth and function.

Regarding the chemical influence, most of it is directly attributed to its influence on the extracellular ionic concentrations of calcium and phosphate (and silica in the case of bioglass), which act as important regulators of different osteoblast functions. It is well known that many cell types present calcium cell-surface receptors, indicating that this intracellular messenger ion also may be a potent extracellular signaling molecule (Hofer, 2005). In osteoblasts, this receptor is expressed at relatively low levels, but has been detected in a variety of osteoblast-like cell lines, including SAOS-2 (Yamaguchi, 2008). It has further been demonstrated that the calcium-receptor plays a vital role in osteoblast fate (Dvorak *et al.*, 2004), and the observed effects of variations in the concentration of extracellular calcium on osteoblast function include influence on chemotaxis, proliferation, differentiation, and gene expression (Dvorak *et al.* (2004), and references within).

The consequences of lowering the concentration of calcium, as CDHA tends to do when exposed to cell culture medium (see Chapter 4), comes with much discrepancy. While for example Eklou-Kalonji *et al.* (1998) did not observe any influence on neither cell proliferation nor differentiation when lowering $[Ca^{2+}]$ from 2.2 mM to 0.5 mM, Dvorak *et al.* (2004) observed both decreased proliferation and ALP activity when $[Ca^{2+}]$ was lowered from 1.2 mM to 0.5 mM. In strong contrast to above studies stand the works by Matsumoto *et al.* (1991) and Farley *et al.* (1994) that both have documented increased osteoblast proliferation (e.g by SAOS-2 cells) as a response to low concentrations of calcium (0.29 mM and 0.2 mM, respectively). In addition, Matsumoto *et al.* (1991), just like Yoshimura *et al.* (1996), detected increased ALP activity at low calcium concentrations. Above studies indicate that the effect of lowering extracellular calcium may differ with the choice of osteoblast model, and is also most probably related to the stage of cell maturation.

In parallel to the importance of calcium interactions between material and the extracellular environment, also the concentration of extracellular phosphate should be considered as a potential influence on the osteoblast fate. Presence of inorganic phosphate is not only a requirement for osteoblast-induced mineralisation (Allori *et al.*, 2008a,b), but has also been demonstrated to influence events preceding mineralisation through modulation of osteoblast gene expression (Beck *et al.*, 2000; Fujita *et al.*, 2001). Especially, elevation of intracellular inorganic phosphate may trigger a series of cellular and molecular changes that influence the transition of cells, matrix vesicles, and the extracellular matrix into a mineralisation competent state (Beck,

2003). Explicit data on lowering the concentration of phosphate is however less abundant, but has been mentioned to decrease proliferation and differentiation of mesenchymal stem cells (Liu *et al.*, 2009).

The spontaneous ionic reactivity of most CaP compounds, in combination with the important role of calcium and phosphate for osteoblast behaviour, have brought about several studies related to the ionic effects induced by CaP compounds on cellular fate, and vice versa. El-Ghannam & Ning (2006) illustrated how bone marrow stem cells grown on a silicia-calcium phosphate compound influenced its chemical activity by preventing back-precipitation of dissolved ions onto the material. In the reverse direction, Hempel *et al.* (2004) demonstrated how carbonated calcium-deficient hydroxyapatite influenced the ionic extracellular environment through dissolution in such a way that osteoblast growth and differentiation was reduced. Those studies exemplify the two-way cell-material interactions that arise when osteoblasts are in direct contact with CaP compounds. Although efforts have been made to distinguish between these two effects (Engel *et al.*, 2008), interpretation of cellular response to ionically active biomaterials remains a complex task. Isolation of the chemical effect has been done at several occasions, e.g. to determine the effect of extracellular calcium and inorganic phosphate on the growth and osteogenic differentiation of mesenchymal stem cells (Liu *et al.*, 2009), but this is a strong simplification. First, one has to remember that the chemical effect is a function of reacting surface area. Second, most studies concerning the influence of extracellular ions on osteoblast function are performed in static conditions, i.e. with fixed ion concentration throughout the full length of the experiment. This is not only a simplification of the dynamic ionic extracellular environment that CaP compounds usually creates when immersed in cell culture medium, and it neglects the capacity of cells to detect the time derivative of ionic activity (Habel & Glaser, 1998).

5.2 Objectives

The objective of the work presented in this chapter was to study how:

1. **cells and CDHA, respectively as well as when combined, influenced the extracellular ionic concentrations of Ca^{2+}, P_i, and pH, at different stages of long-term culture**;
2. **the dynamic ionic extracellular environment induced by CDHA influenced osteoblast behaviour with respect to cellular proliferation, alkaline phosphatase activity, and calcium deposition in the extracellular matrix**.

5.3 Materials and Methods

5.3.1 Calcium-deficient hydroxyapatite

Samples of calcium-deficient hydroxyapatite (CDHA) obtained through hydrolysis of α-TCP, were produced and further processed as has been previously described in Chapter 4.

5.3.2 Cell Culture

The chemical influence of CDHA on cellular response was evaluated by growing cells on specific membrane inserts (Nunc, 137052) that on one hand prohibited cells to pass through the membrane, but on the other hand allowed for ions and proteins to diffuse through it (Figure 5.1). In that way, cells were continuously exposed to any changes in the extracellular environment provoked by the material.

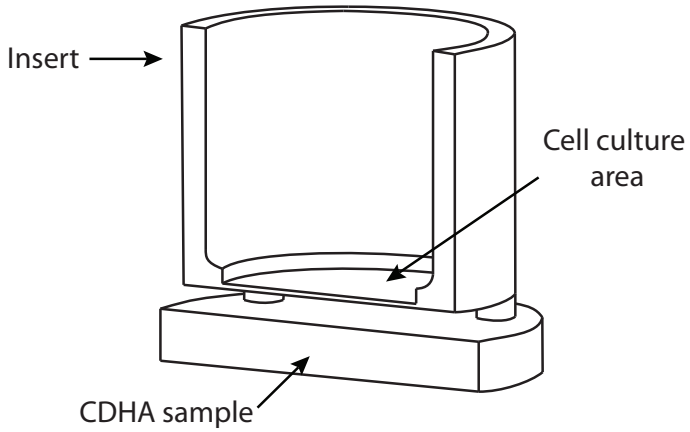

Figure 5.1: Cross-sectional view of the experimental setup used to study the chemical influence of CDHA on cellular response. The cell culture insert had a diameter of 10 mm, and the polycarbonate membrane had a pore size of 0.4 μm.

5.3.2.1 Cell culture media

Four different cell culture media were prepared and used for growing cells (Figure 5.2). All of them were based on McCoy's Modified 5A medium, and were further supplemented with l-glutamine, penicillin / streptomycin, sodium pyruvate, and 15% foetal bovine serum as in Chapter 3 (Table 3.5). From this basic formulation, referred to as *normal medium*, *osteogenic medium* was obtained by adding to it ascorbic acid (AA), dexamethasone (dex), and

β-glycerophosphate (β-GP). The final concentration of each of the osteogenic factors was 50 μg/mL AA, 10^{-8} M dex, and 10 mM β-GP. Moreover, *calcium-deficient medium* was prepared by adding 1 mM EGTA (Sigma E3889) to the normal medium, and *osteogenic calcium-deficient medium* was in turn prepared by providing abovementioned osteogenic factors to the calcium-deficient medium.

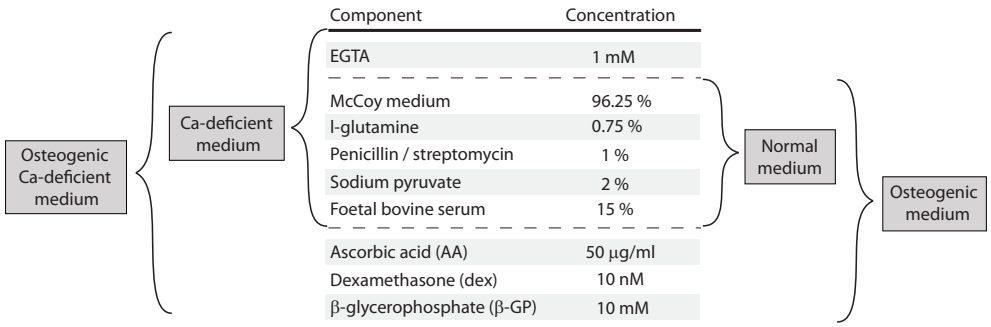

Figure 5.2: The preparation of the different cell culture media.

In practise, normal medium without FBS was prepared and aliquoted in 50 ml Falcon tubes and were then stored in the cell culture incubator. Fresh aliquots were prepared a couple of times during long-term experiments. Upon changes of the cell culture medium during the experiments, one new aliquot was opened, and from it was prepared the different medium variations by addition of FBS and other factors. All media were filtered before used.

5.3.2.2 Cell seeding and handling

Before cell seeding, CDHA samples were preincubated overnight in McCoy's modified medium (without any further supplements) at 37°C and 5% CO_2. SAOS-2 cells (passage 16-17) were then seeded at a density of 25 000 cells/inserts using normal medium. The interior of the insert held a volume of 0.50 mL, while the exterior part contained 0.75 mL. Before incubation it was controlled that no air was trapped between the insert and the CDHA sample.

The cell culture medium was exchanged after 24 hours, and from then renewed every second day of incubation. During the first five days of culture (i.e, more or less until reaching confluence), all samples were maintained in normal medium. Thereafter, the four different media preparations described in section 5.3.2.1 were applied to separate sets of samples.

5.3.3 Ion Measurements of Cell Culture Media

Concentration of calcium and pH of cell culture media and supernatants was evaluated using commercial ion selective electrodes (ILyte). The ionic concentrations were measured directly after preparation of the media, as well as immediately after each medium exchange during cell culture. Supernatants were composed of equal parts of medium obtained from the interior and exterior parts of the culture inserts.

After analysis of the media and supernatants for Ca^{2+} and pH, samples were frozen. Upon thawing, samples were diluted 15-30 times, and then assayed for inorganic phosphorus using the ascorbic acid-molybden blue method. For details on these methods, see Sections 3.3.2 and 3.3.3 (Chapter 3).

5.3.3.1 Long-term measurements

In long-term experiments, cell culture media were exposed to cells or CDHA, respectively, as well as to both of them at the same time, and during a period of 21 days. Medium not exposed to any of above components was used as a control. For all experiments, medium was exchanged for the first time after 24 hours, and from then on every two days ($\approx$ 48h). Osteogenic medium was used between day 5 and day 21. See Figure 5.3 for a scheme of the experiment layout

5.3.3.2 Short-term measurements

In short-term experiments, osteogenic cell culture medium was exposed to cells, CDHA, or both of them at the same time, during a period of 48 hours. Those conditions were repeated at three different stages of the long-term experiments. First between day seven and nine (7-9), then between day 13 and 15, and finally between day 19 and 21. During these periods, ion concentrations of the culture medium was evaluated in general every sixth hour. As a control, measurements of the ionic concentrations were made of culture medium not exposed to CDHA or cells.

5.3.4 Cell Proliferation

Cell proliferation was monitored using the alamarBlue Cell Viability Reagent (Invitrogen, DAL1025). The assay contains an oxidation-reduction growth indicator (resazurin-resorufin) that changes colour (and fluorescence) in response to reduction reactions of metabolically active cells. The indicator is minimally toxic, which makes it possible to monitor metabolic activity from

the same cell population but at different stages of the culture. In the present study, absorbance of alamarBlue was measured at 570 nm, using 600 nm as reference wavelength, and the percentage of alamarBlue reduction was calculated as below (Eq. 5.1),

$$\% \text{ alamarBlue reduction} = \frac{(E(ox)_{600} \times A_{570}) - (E(ox)_{570} \times A_{600})}{(E(red)_{570} \times A'_{600}) - (E(red)_{600} \times A'_{570})} \times 100 \qquad (5.1)$$

where A_λ and A'_λ represent the absorbance of cell culture medium measured in presence and absence of cells, respectively, and at wavelength λ (nm). $E(ox)_\lambda$ and $E(red)_\lambda$ are the molar extinction coefficients of oxidised and reduced alamarBlue at wavelength λ (nm), and as given in Table 5.1.

λ	E(Oxidised)	E(Reduced)
570	80586	155677
600	117216	14652

Table 5.1: The molar extinction coefficients of alamarBlue at the relevant wavelengths. Data obtained from AbD Serotec.

For detection of cell-induced reduction of alamarBlue, cell culture inserts were moved from its culture plate, and then exposed to fresh normal medium containing 1:10 to 1:20 of alamarBlue during 1 to 2 hours, with the lower concentration and shorter incubation time used for the later stages of the culture. After this period, inserts were returned to its original culture plate (that contained the CDHA samples), and where they remained until the next measurement. Absorbance measurements of media containing alamarBlue were done immediately after harvest and using a microplate spectrophotometer reader (BioTek PowerWave XS).

5.3.5 Alkaline Phosphatase Activity and Total Protein

Alkaline phosphatase (ALP) activity and total protein content of cultured cells were assayed after 3,5,9,15, and 21 days of culture, following the procedure that has been previously described in Section 3.3.9 (Chapter 3). This data was used to calculate the ALP activity, expressed in units of μmol min^{-1} (mg protein)$^{-1}$.

5.3.6 Extracellular Calcium Deposition

Deposition of calcium in the extracellular matrix was evaluated in cell cultures after 9, 15, and 21 days respectively, using Alizarin red-S. For staining, inserts were moved to an empty 24-well plate, and the samples were

rinsed, fixed, and stained according to the procedure explained in Section 3.3.8 (Chapter 3). While one set of stained samples were frozen, another set was used to visualise the calcium deposition with a vertical microscope (Nikon Eclipse E-600 A). The supporting membrane of the insert, holding the fixed cells and matrix, was carefully removed from the insert using a scalpel and then fixed on a microscope slide.

Quantitave evaluation of calcium deposition was obtained from the frozen stained samples. After thawing, a 10% solution of CPC diluted in 10mM sodium phosphate was added to each sample to extract the stain.

5.3.7 Statistics

Data are expressed as means standard deviations. Statistical analysis was performed using unpaired, two-tailed student t-test. Non-linear curve fitting was done as explained in Section 4.3.7.

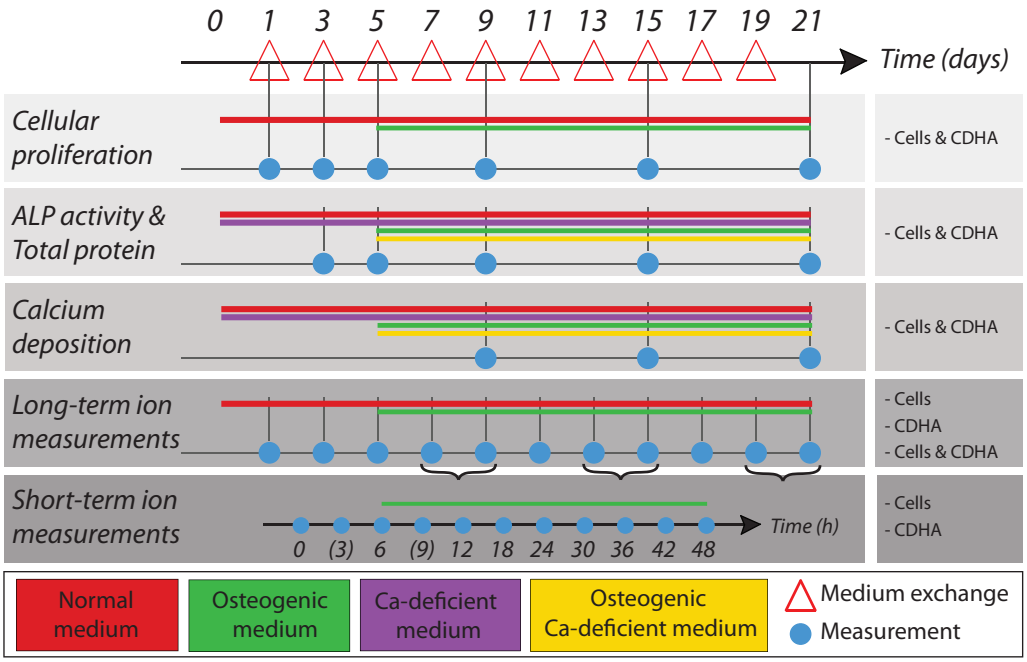

Figure 5.3: A schematic summary of the experiment layout showing which were media used and at which time points different measurements were done.

5.4 Results

5.4.1 Cell Culture Media

The ionic concentrations of Na^+, K^+, Ca^{2+}, pH, and total inorganic phosphorus (P_i) of the four different culture media were continuously evaluated prior to changing the culture medium for cells throughout the 21-days long experiment. The ionic profile is presented in Table 5.2, revealing that EGTA chelated calcium, while leaving unaffected the concentration of sodium, potassium, and phosphorus. Important to notice though was that EGTA lowered the pH significantly.

	Standard media		**Calcium-deficient media**	
	Normal	Osteogenic	EGTA	EGTA Osteogenic
Na^+	133.1 ± 0.9	143.4 ± 1.3	133.6 ± 0.6	142.9 ± 2.3
K^+	5.55 ± 0.07	5.33 ± 0.06	5.56 ± 0.04	5.37 ± 0.05
Ca^{2+}	0.78 ± 0.028	0.63 ± 0.022	0.19 ± 0.03	0.15 ± 0.02
pH	7.37 ± 0.02	7.46 ± 0.03	7.08 ± 0.02	7.20 ± 0.04
P_i	2.66 ± 0.163	2.67 ± 0.069	2.66 ± 0.19	2.66 ± 0.20

Table 5.2: Ionic levels of cell culture media. The values (expressed in units of mM, except for pH) are given as mean ± standard deviation. For normal media $n = 33$, otherwise $n = 24$.

5.4.2 The Extracellular Ionic Environment

The ionic concentration of calcium and phosphorus of supernatants in contact with cells and / or CDHA, as well as its pH value, was regularly evaluated during periods of either 48 hours (short-term) or 21 days (long-term). While in the long-term experiments the ion measurements were of end-point character (i.e. measurements were done before and after exposure), in short-term experiments they were of continuous character (i.e. the evolution of ionic interaction was monitored during exposure).

5.4.2.1 Long-term experiments

The long-term ionic interactions with respect to calcium, phosphorus, and pH for normal and osteogenic medium are presented in Figure 5.4a-c, where the initial concentration is drawn as a dashed (normal medium) or a dotted (osteogenic medium) line, while the end-point ion concentrations of supernatants and controls are represented by symbols.

Regarding the extracellular concentration of calcium in normal medium, it was observed to be highly influenced by the presence of CDHA (Figure 5.4a, top), which repeatedly between days 1 to 21 during the around 48 hours of contact decreased the levels of calcium to in average 36.4 ± 5.9% of the initial concentration. A similar trend was observed when CDHA and cells were combined, while cells on their own did not remarkably influence the levels of extracellular calcium, and especially not during the first week of growth.

Also when using osteogenic medium (Figure 5.4a, bottom), CDHA was observed to decrease the concentration of extracellular calcium (in average to 33.1 ± 2.5% of the initial concentration for each period of 48 hours between days 5 and 21). As opposed to using normal medium, in osteogenic medium cells were observed to significantly influence the concentration of calcium. During the first two days of growth in osteogenic medium (i.e. between day 5-7), the extracellular concentration of calcium was however very little affected, but between days seven to nine it began to drop significantly. Then beyond day nine a clear decrease of calcium was provoked by cells until the end of the experiment. During all these measurements, medium without cells or CDHA maintained its concentration of calcium stable, and close to the initial concentration.

The extracellular concentration of total inorganic phosphorus was decreased in presence of CDHA when using normal medium, although the decrease gradually became less pronounced with time (Figure 5.4b, top). During the first 24 hours of contact (i.e. between day 0 and day 1), the concentration of P_i decreased 37.9 ± 3.1%, while at the end of the experiment, the decrease was much less significant (4.8 ± 0.8%). Meanwhile, cells alone did not influence [P_i] when using normal medium.

Above observations with respect to P_i were drastically changed when using osteogenic medium. First, medium in absence of cells as well as CDHA, increased spontaneously the concentration of P_i, in average to 5.1 ± 0.1 mM (i.e. almost twice its initial value). Second, presence of cells promoted additional increase of the concentration of P_i, in average to 8.1 ± 0.7 mM. Third,

in presence of CDHA the concentration of P_i increased from its initial value, but did not approach the levels of P_i in control medium until the very end of the experiment. Finally, when cells and CDHA were combined, the concentration of P_i increased above the concentration of control medium, but below the concentration of P_i when only cells are present.

Also the pH of the cell culture medium was influenced by CDHA as well as by cells (Figure 5.4c). Using normal medium, CDHA had an acidifying effect on the medium, provoking the pH to decrease. That effect gradually decreased with time, making it more pronounced during the first half of the experiment. On the contrary, presence of cells did not influence the pH significantly during that initial period. However, beyond 11 days of culture heavy acidification due to cellular activity was observed. As a consequence, the pH of normal culture medium holding both CDHA and cells was acidified throughout the full experiment.

Above observations related to the pH of normal culture medium were in principle valid also when using osteogenic medium. The major difference was that cells in osteogenic medium had a less acidifying effect than cells grown in normal medium. However, when cells and CDHA was combined, the acidifying effect once again resembled that one of normal medium.

5.4.2.2 Short-term experiments

The short-term experiments were performed with osteogenic medium that was in contact with either CDHA or cells. The ionic concentrations of calcium, phosphorus, and pH are illustrated in Figure 5.5a-c.

As shown in Figure 5.5a (top), the kinetics of the decrease in concentration of calcium induced by CDHA was reproduced at all three measurements, i.e. the calcium uptake by CDHA was identical between day 7-9, day 13-15, and day 19-21. Moreover, the concentration of calcium in culture medium exposed to CDHA was successfully modelled ($R^2 = 0.998$) using Equation (5.2):

$$[Ca^{2+}] = [Ca^{2+}]_i - \frac{k_1(\Delta[Ca^{2+}])^2 t}{1 + k_1(\Delta[Ca^{2+}])t}, \tag{5.2}$$

where $[Ca^{2+}]_i$ is the initial concentration of calcium (mM), k_1 the apparent sorption constant ($mM^{-1}\ h^{-1}$), and $\Delta[Ca^{2+}]$ is the calcium uptake at steady-state (mM). Specifically, with $[Ca^{2+}]_i = 0.651 \pm 0.05$ mM, then $\Delta[Ca^{2+}]$ was determined to 0.482 mM, and k_1 to 0.293 $mM^{-1}\ h^{-1}$.

As opposed to the case of CDHA, kinetics of the concentration of extracellular calcium influenced by cellular activity, was different between the three measurement stages. As demonstrated in Figure 5.5a (bottom), early cultures (day 7-9) influenced the calcium concentration both to lesser degree and in a slower way compared to more mature cultures.

With respect to phosphorus, it was observed that the spontaneous increase of P_i in osteogenic medium without CDHA nor cells, was of linear character ($R^2 = 0.994$), so that:

$$[\mathrm{P_i}] = k_2 t + C, \tag{5.3}$$

where k_2 was determined to 0.0504 ± 0.01 mM h^{-1}, and C to 2.715 ± 0.05 mM ($n = 6$).

When examining the kinetics of $[P_i]$ in presence of CDHA, it was not only observed that its effect (i.e. sorption of P_i) was less pronounced the longer the material had been incubated with medium, and as had been previously shown in the long-term experiments, but also that CDHA influenced the concentration of P_i mainly towards the second half of the 48-hour long contact period.

In presence of cells, the concentration of P_i increased rapidly, and the steady-state concentration was in principle reached within the first 24 hours. Yet, slight differences could be observed depending on the maturity of the cell culture. Mainly, the conversion of organic phosphorus to inorganic phosphorus was slowed down during the end of the culture (day 19-21), while being fastest in the middle of the culture (day 13-15). Both between day 7-9 and day 13-15 the turnover of cellular-induced conversion of phosphorus was similar.

Finally, pH of the cell culture medium was gradually decreased by CDHA as well as by cells (Figure 5.5c). In the first case, not only the steady-state pH value after 48 hours of contact was less accentuated with time, but also the initial acidification rate seemed to decrease. Compared to CDHA, acidification provoked by cells increased with maturity of cells, both with respect to steady state value and initial acidification rate.

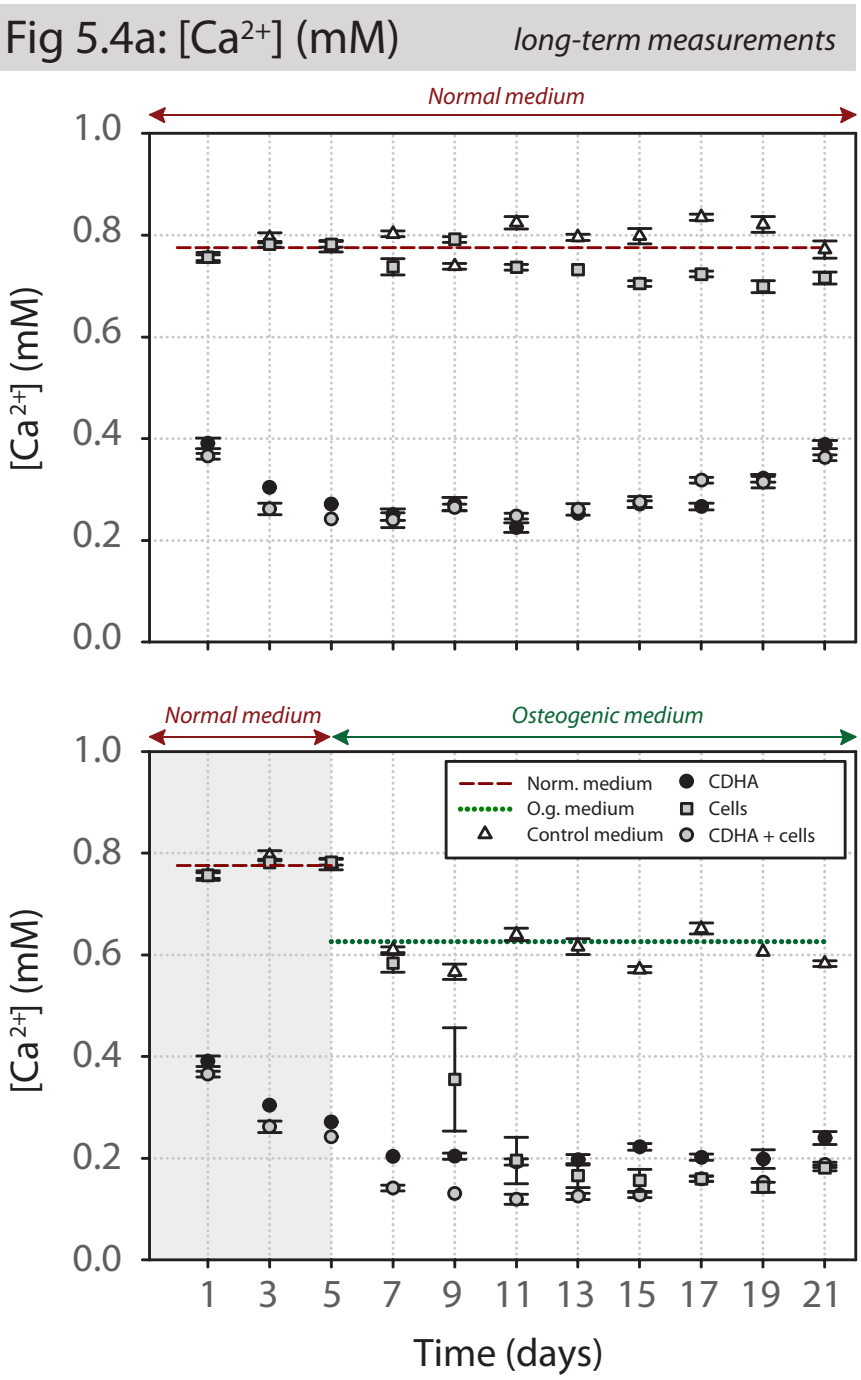

Figure 5.4: (a) Calcium concentration of osteoblastic cell culture media in contact with CDHA and cells during long-term cultures. Top: normal medium. Bottom: normal and osteogenic medium.

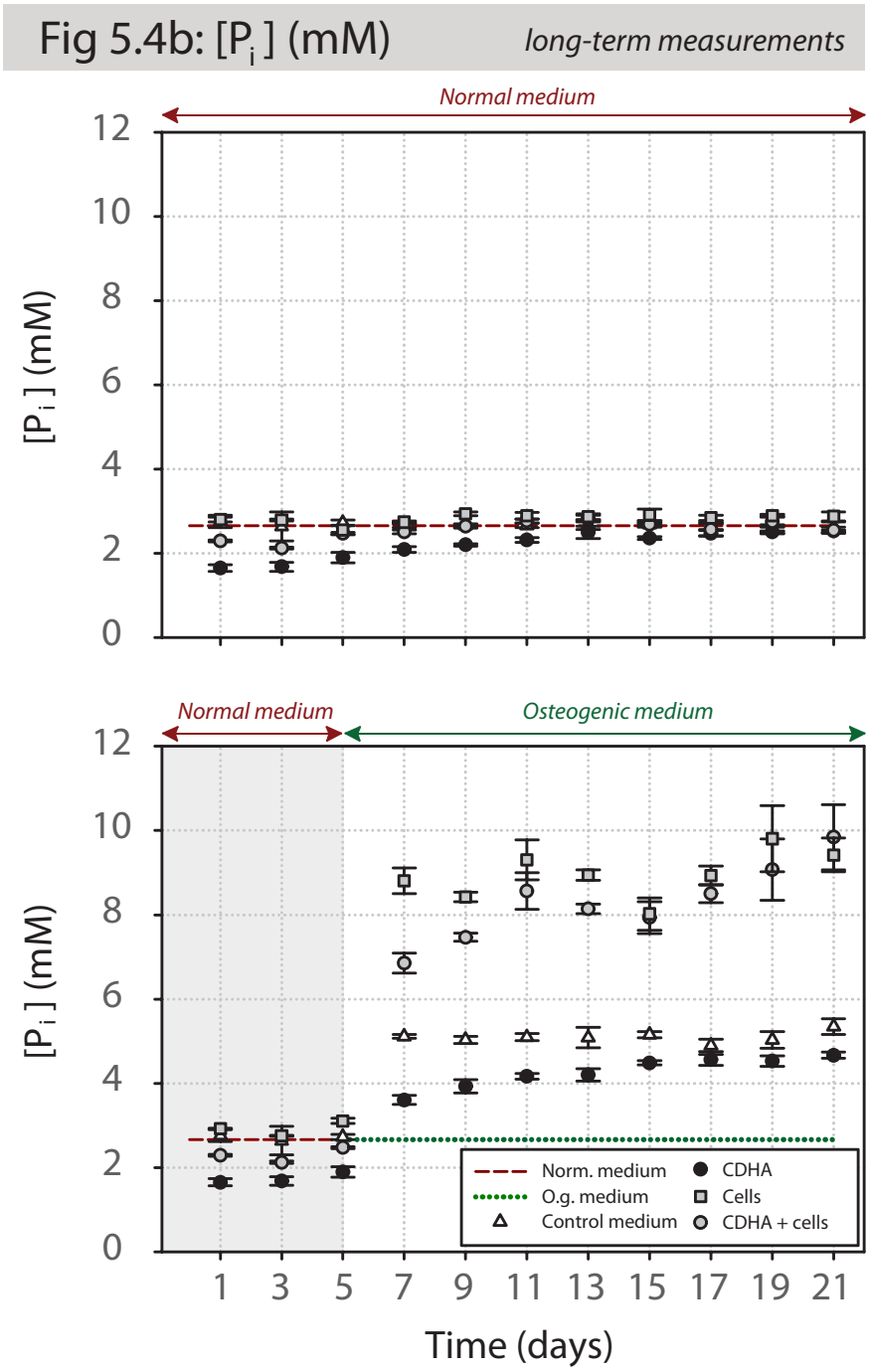

Figure 5.4: (b) Phosphorus concentration of osteoblastic cell culture media in contact with CDHA and cells during long-term cultures. Top: normal medium. Bottom: normal and osteogenic medium.

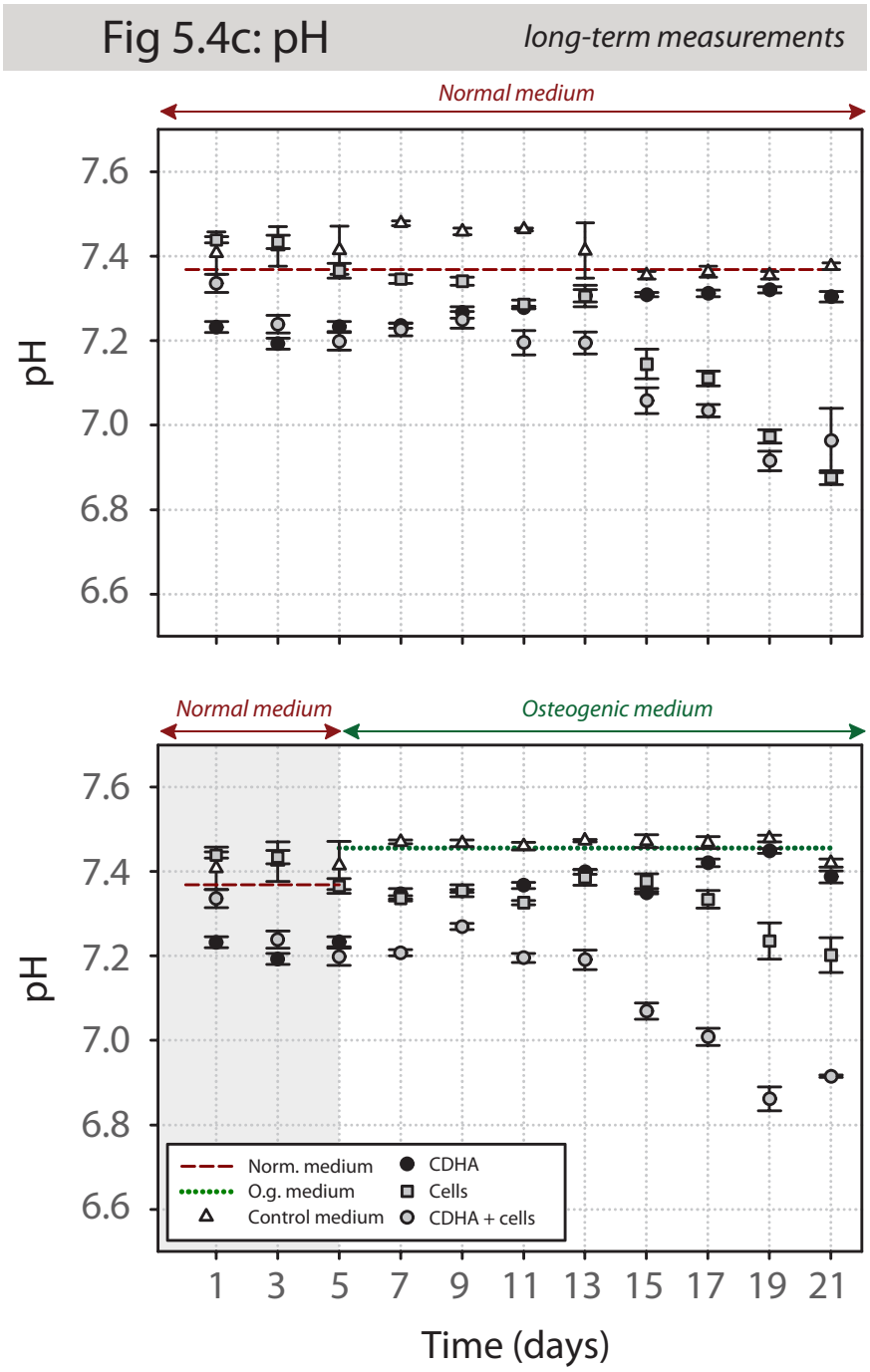

Figure 5.4: (c) pH of osteoblastic cell culture media in contact with CDHA and cells during long-term cultures. Top: normal medium. Bottom: normal and osteogenic medium.

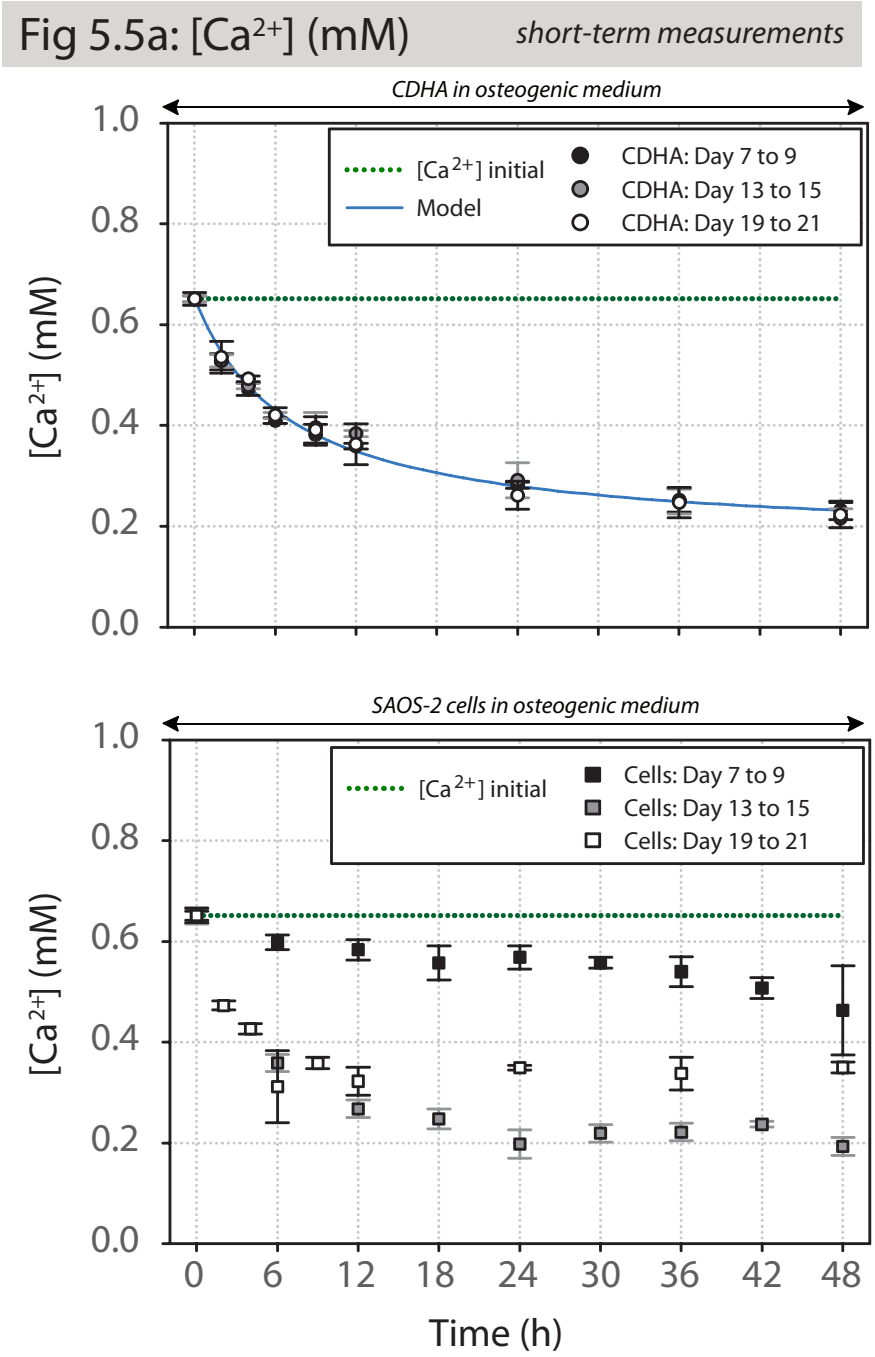

Figure 5.5: (a) Calcium concentration of osteoblastic cell culture media during short-term experiments. Top: CDHA in osteogenic medium. Bottom: SAOS-2 cells in osteogenic medium. Top: CDHA in osteogenic medium. Bottom: SAOS-2 cells in osteogenic medium.

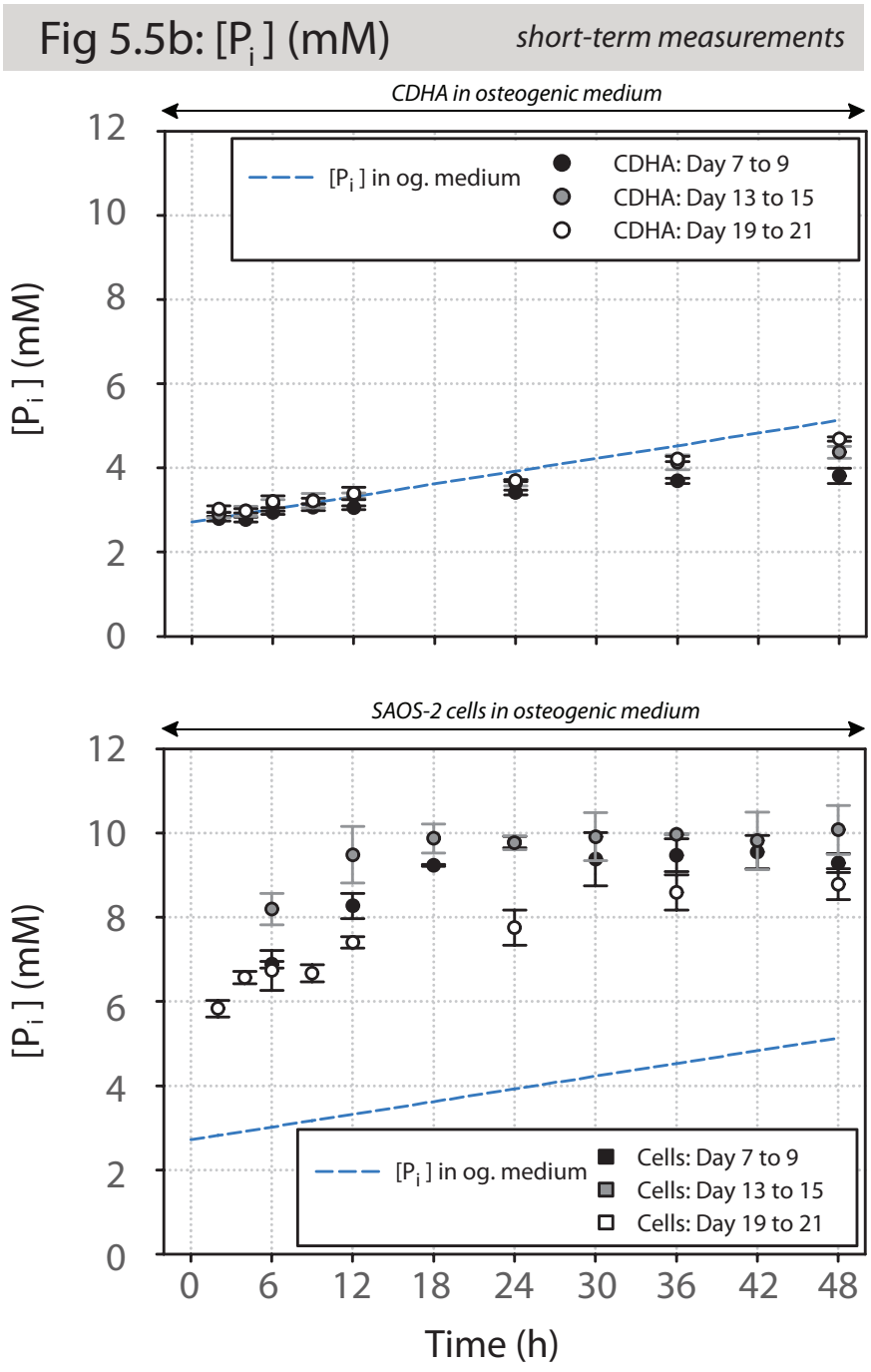

Figure 5.5: (b) Phosphorus concentration of osteoblastic cell culture media during short-term experiments. Top: CDHA in osteogenic medium. Bottom: SAOS-2 cells in osteogenic medium.

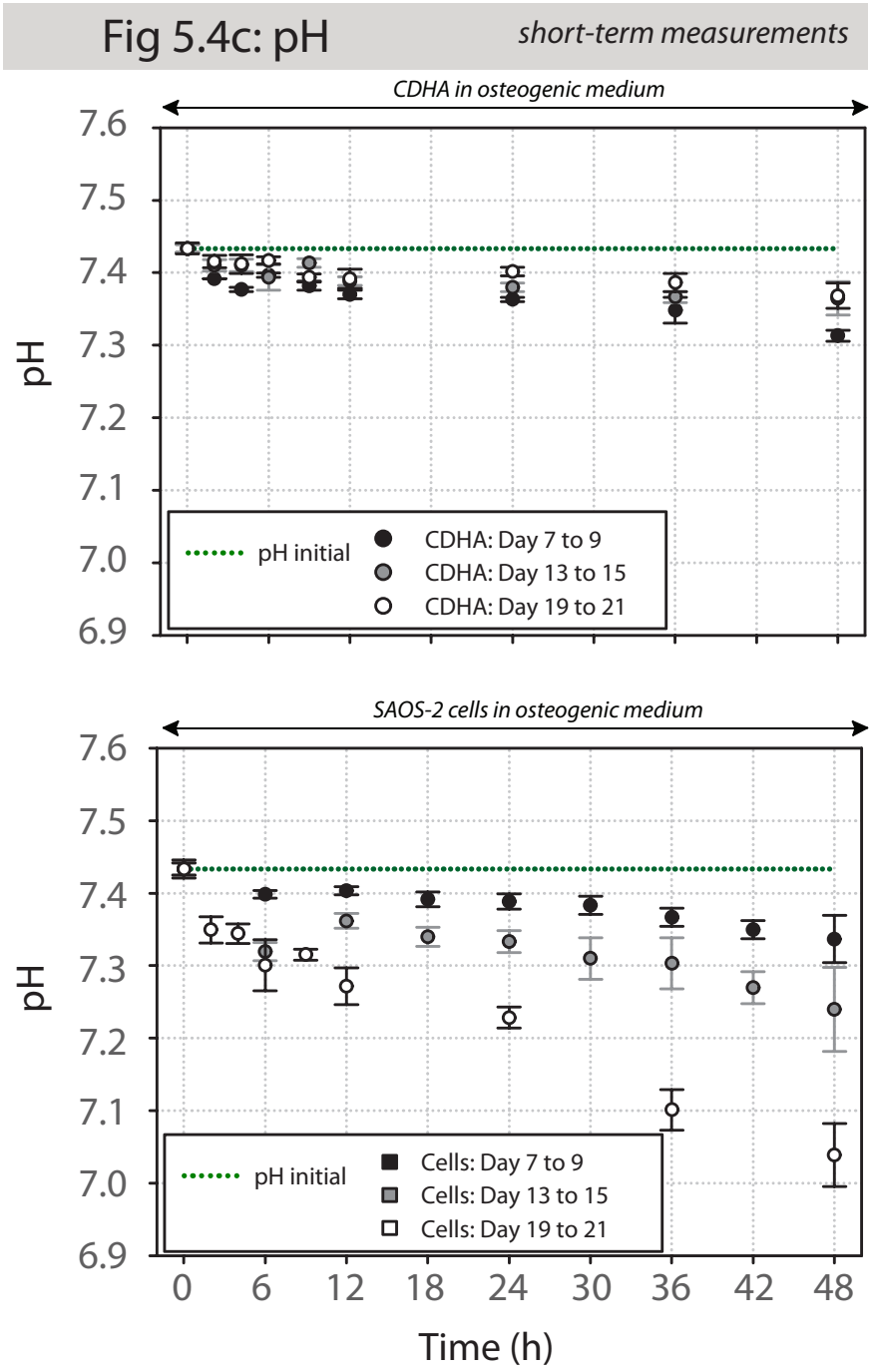

Figure 5.5: (c) pH of osteoblastic cell culture media during short-term experiments. Top: CDHA in osteogenic medium. Bottom: SAOS-2 cells in osteogenic medium.

5.4.3 Cell Proliferation

Cell proliferation was quantified as reduction of alamarBlue, and measured at different time points during cell culture. As shown in Figure 5.6, cells exposed to CDHA proliferated with a comparable rate as cells grown in absence of CDHA when using normal medium. Slight differences were detected at day 5 ($P = 0.041$) and at day 21 ($P = 0.017$).

The use of osteogenic medium had no effect on cell proliferation at day 9. However, after fifteen days in culture, cells grown in osteogenic control conditions were significantly less than cells grown in normal control conditions. This was not observed with cells exposed to CDHA. At the end of the experiment (i.e. day 21), growth of cells in osteogenic control conditions continued to be significantly suppressed if compared to normal control conditions, as well as to cells exposed to CDHA in osteogenic conditions. Moreover, at day 21 it was also observed that proliferation of cells exposed to CDHA was slowed down when using osteogenic medium ($P = 0.0044$).

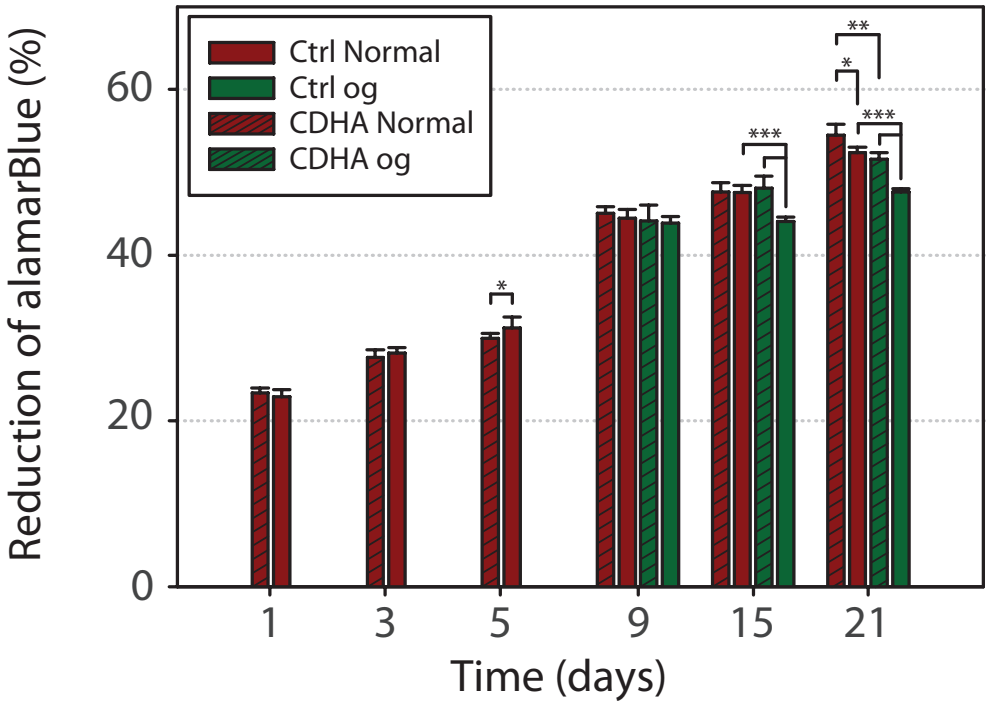

Figure 5.6: Cell proliferation was quantified as reduction of alamarBlue (%). Data is presented as mean ± standard deviation ($n = 6$ to 12).

5.4.4 Alkaline Phosphatase Activity and Total Protein

The alkaline phosphatase activity of cells grown in standard and calcium-deficient medium (EGTA), with and without osteogenic factors and in presence and absence of CDHA, was normalised to the amount of total protein in the sample (i.e. intra- and extracellular protein). The latter data is presented in Figure 5.7 while the statistical analysis of that data is given in Table 5.3.

At the first two measurement points (day 3 and 5), no difference in amount of total protein was detected between cells grown in presence and absence of CDHA. However, when using EGTA medium the amount of total protein was severely lowered at this stage of culture, and continued to be so until the end of the experiment if compared to cells grown in control conditions using normal medium. Yet, if comparing the use of EGTA medium with the use of normal medium, then the difference in total protein decreased with time, and by day 21 it was comparable to the amount of total protein in cell cultures exposed to CDHA.

The influence of using osteogenic medium was most accentuated for cells grown in absence of CDHA, but opposed when comparing standard osteogenic medium and calcium-deficient osteogenic medium. While in standard osteogenic medium the amount of total protein was suppressed beyond day 9, in calcium-deficient osteogenic medium it was increased throughout the experiment.

The alkaline phosphatase activity varied both with time and the type of medium used. Presence of CDHA suppressed ALP activity using normal medium at day 3 and 9 (-11.8 ± 6.8 % and -19.4 ± 5.2 %, respectively), while no influence was seen at day 5, 15, and 21. During the first half of the cell culture, also EGTA medium was observed to suppress the ALP activity (-52.9 ± 2.9 % at day 3, -27.3 ± 3.6 % at day 5, and -64.7 ± 3.6 % at day 9).

Osteogenic media increased ALP activity of cells independent of the medium used, and no matter if exposed to CDHA or not. The relative influence of osteogenic media compared to non-osteogenic media was however not synchronised in time. In absence of CDHA, the major relative effect of osteogenic factors was observed at day 21 for control medium (+60.4 ± 16.6 %), while for EGTA medium it was observed already at day 9 (+75.2 ± 17.7 %). In presence of CDHA, at day 15 the major effect of osteogenic factors (+108.8 ± 19.8 %) coincided with the highest ALP activity of that particular condition.

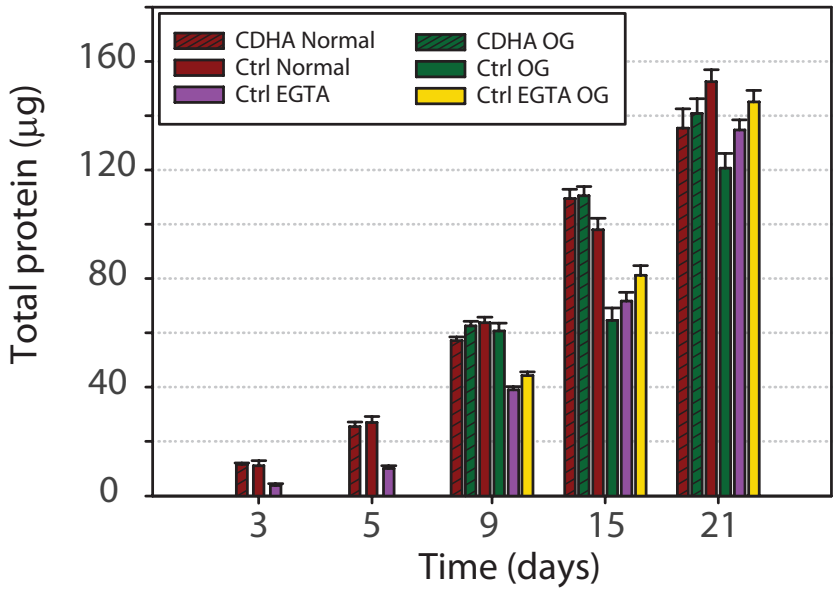

Figure 5.7: The amount of total protein in cell cultures grown in presence of CDHA was compared to cells grown in absence of CDHA, using either normal or calcium-deficient medium. Data is presented as mean ± standard deviation ($n = 4$).

		Normal			Osteogenic	
Sample	**Day**	CDHA	Control	EGTA	CDHA	Control
Control	3	ns				
	5	ns				
	9	**				
	15	**				
	21	**				
EGTA	3	***	***			
	5	***	***			
	9	***	***			
	15	***	***			
	21	ns	***			
CDHA OG	9	**				
	15	ns				
	21	ns				
Control OG	9		ns		ns	
	15		***		***	
	21		***		**	
EGTA OG	9			**	***	***
	15			**	***	**
	21			*	ns	***

Table 5.3: Statistical analysis of data preseted in Figure 5.7. Symbols correspond to the P-value: ns = not significant ($P \geq 0.05$), * ($0.01 \leq P < 0.05$), ** ($0.001 \leq P < 0.01$), and *** ($P < 0.001$).

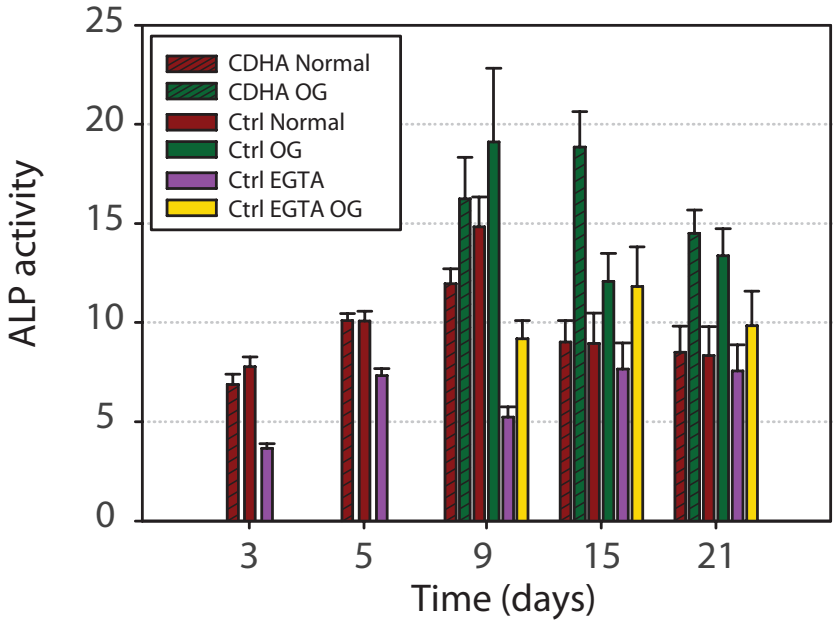

Figure 5.8: The alkaline phosphatase activity of cells grown in presence of CDHA was compared to that one of cells grown in absence of CDHA, and in both normal and calcium-deficient medium. Data is presented as mean ± standard deviation ($n = 4$).

		Normal			Osteogenic	
Sample	**Day**	CDHA	Control	EGTA	CDHA	Control
Control	3	*				
	5	ns				
	9	*				
	15	ns				
	21	ns				
EGTA	3	***	***			
	5	***	***			
	9	***	***			
	15	ns	ns			
	21	ns	ns			
CDHA OG	9	**				
	15	***				
	21	***				
Control OG	9		ns		ns	
	15		*		**	
	21		**		ns	
EGTA OG	9			***	***	**
	15			*	**	ns
	21			ns	**	*

Table 5.4: Statistical analysis of the alkaline phosphatase activity data preseted in Figure 5.8. Symbols as in Table 5.3.

5.4.5 Extracellular Calcium Deposition

The deposition of calcium in the extracellular matrix was evaluated through Alizarin red staining. Images of the stained cell layers were obtained after 9, 15, and 21 days in culture, and are shown in Figure 5.9a-d. Incorporated dye of the stained cell layers was then extracted and colourimetrically quantified (Figure 5.10).

After nine days in culture (Figure 5.9a), only cells grown in control conditions stained positive for calcium in their extracellular matrix. Use of osteogenic medium clearly enhanced the amount of calcium in the cell layer, where the staining appeared as small areas (typically <50 μm) that were distributed randomly throughout the sample. After an additional six days in culture, control cultures maintained in osteogenic medium had its matrix loaded with calcium. It was also possible to observe a few areas of calcium in cultures grown in control conditions using normal medium. However, if using osteogenic medium containing EGTA, or if cells were cultured in presence of CDHA, no or very little (see Figure 5.9d) positive staining was detected after 15 days in culture. However, reaching the end of the experiment, it was indeed possible to observe calcium deposition in cell cultures exposed to CDHA if the medium contained osteogenic factors (Figure 5.9c-d). Still, no calcium deposition was observed in cultures provided medium containing EGTA.

The qualitative evaluation of the stained cell layers was confirmed by the quantitative evaluation (Figure 5.10a) where the extracted stain was normalised to the amount of incorporated dye in cell layers grown in normal medium and in absence of CDHA at each specific time point. As shown, incorporation of calcium in the cell layers exposed to CDHA could be detected already at day 15, and even more at day 21, but never in cultures maintained in EGTA containing media. Yet, compared to osteogenic control conditions, presence of CDHA severely decreased the amount of incorporated dye.

Taking advantage of that control cultures stained positive for calcium already at day 9 when using osteogenic medium, it was tested if presence of CDHA during the initial culture period (days 1-5) influenced the capacity of cells to deposit calcium in the matrix if thereafter grown in absence of CDHA between days 5-9 (i.e. Ctrl conditions). In Figure 5.10b-c it is shown how cells exposed to CDHA between day 1-5 (i.e. period 1 = CDHA), and then grown in osteogenic medium in absence of CDHA (i.e. period 2 = Ctrl), stained equally positive for calcium as cells grown in absence of CDHA during both periods (i.e. Period 1 = 2 = Ctrl). It is also shown that cells grown in absence of CDHA during the first five days, but then in presence of CDHA during the last four days, did not incorporate calcium in their matrix.

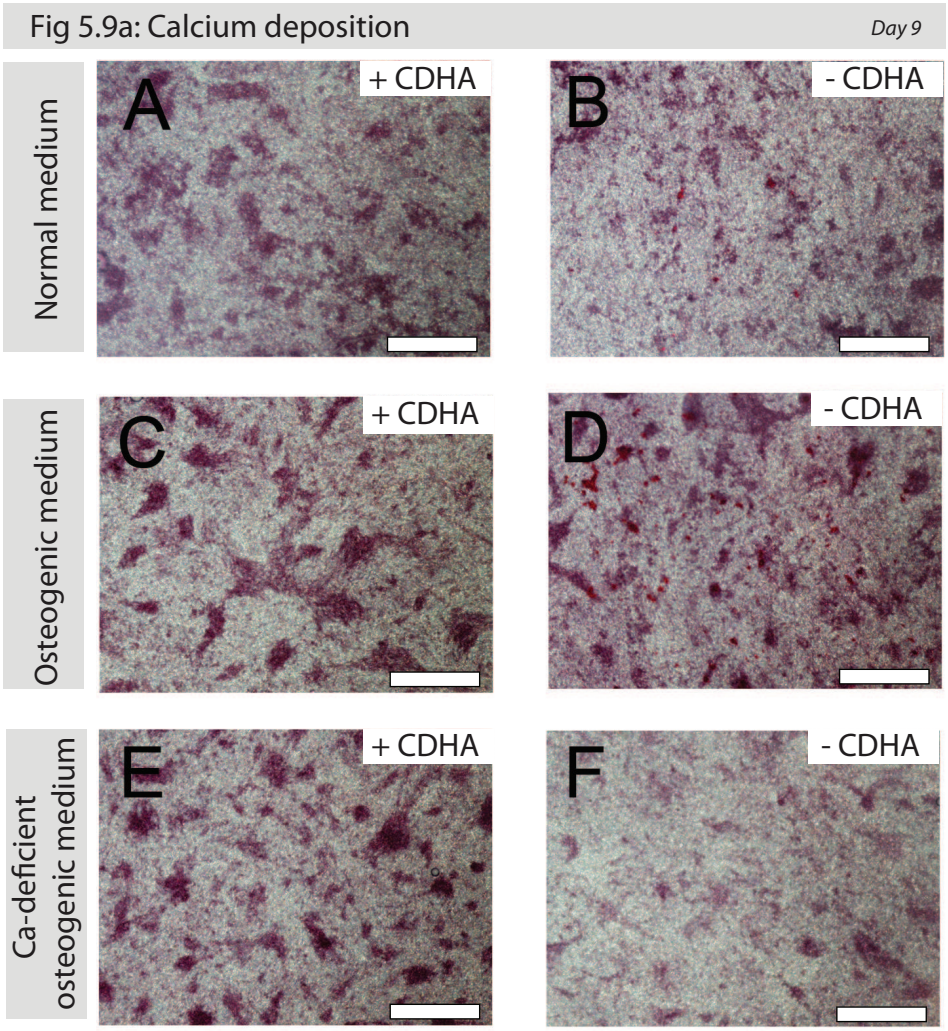

Figure 5.9: (a) Calcium deposition in extracellular after 9 days in culture. (A) Normal media, +CDHA; (B) Normal media, -CDHA; (C) Osteogenic media, +CDHA; (D) Osteogenic media, -CDHA; (E) Osteogenic media with EGTA, +CDHA; (F) Osteogenic media with EGTA, -CDHA. Scale bars indicate 500 μm.

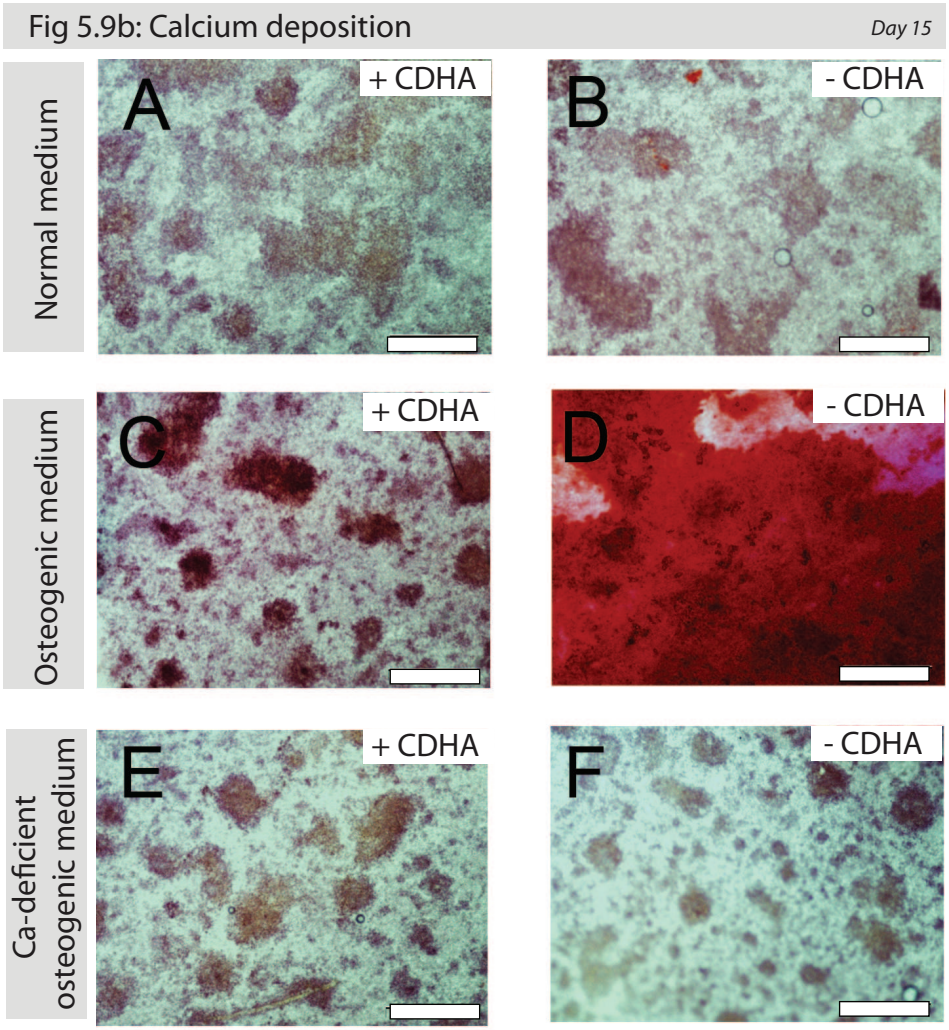

Figure 5.9: (b) Calcium deposition in extracellular matrix after 15 days in culture. Symbols as in Figure 5.9a.

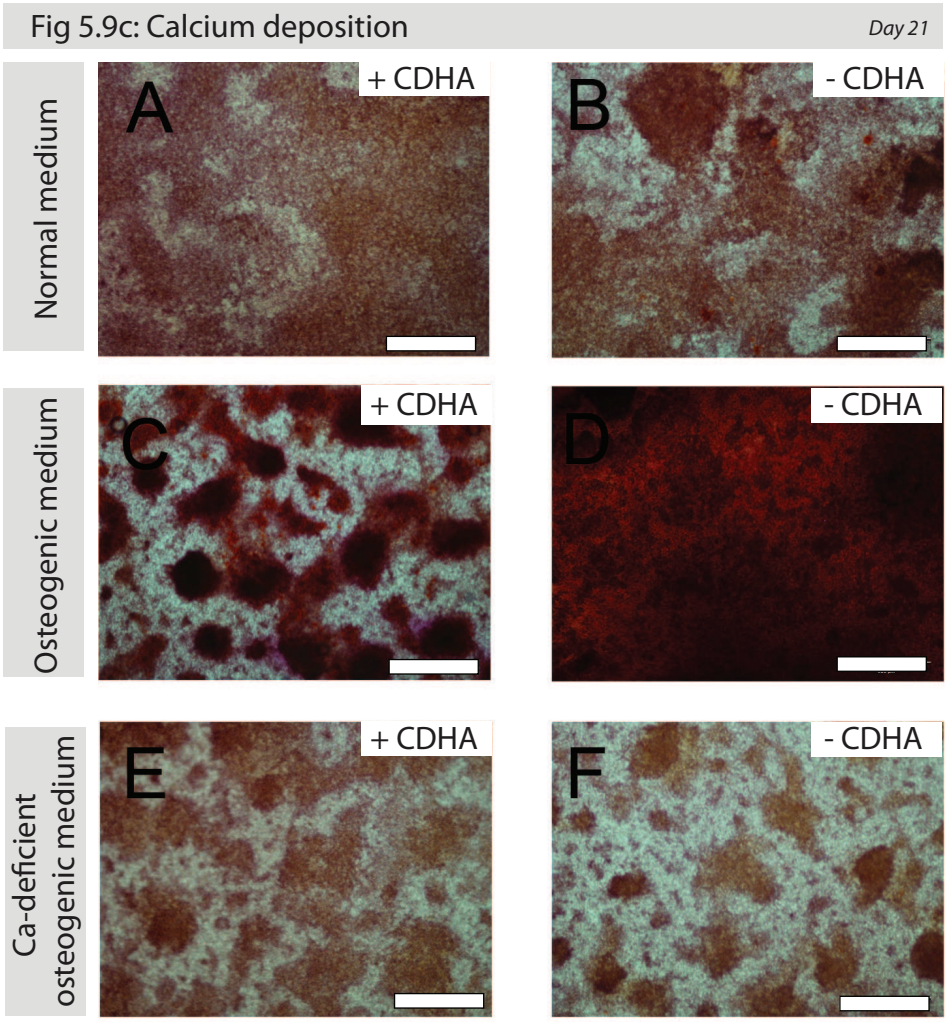

Figure 5.9: (c) Calcium deposition in extracellular matrix after 21 days in culture. Symbols as in Figure 5.9a.

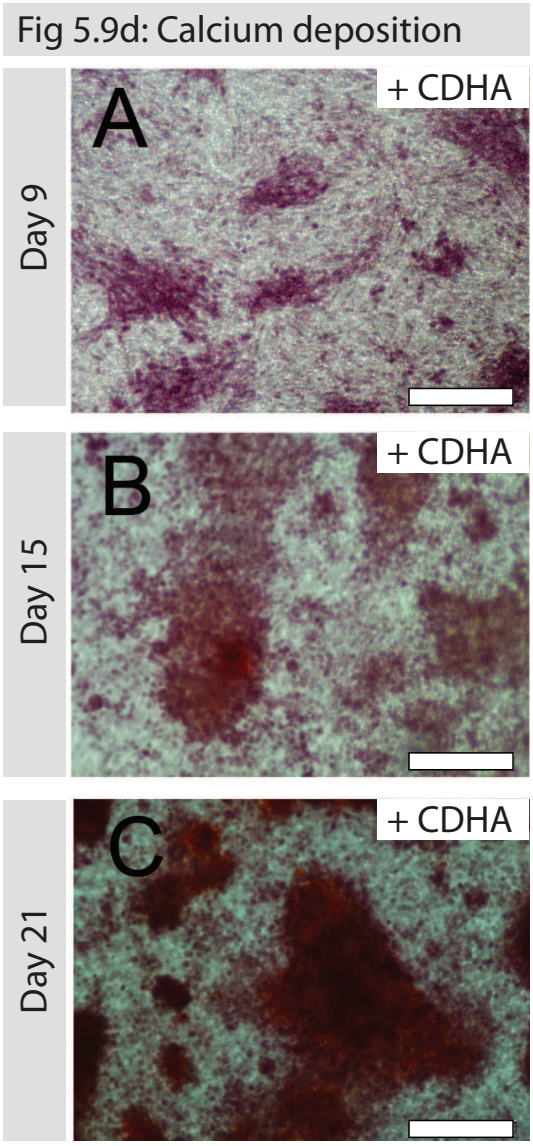

Figure 5.9: Alizarin red staining of cells grown in presence of CDHA, and provided osteogenic medium. (A) 9 days, (B) 15 days, and (C) 21 days. Scale bar = 200 μm.

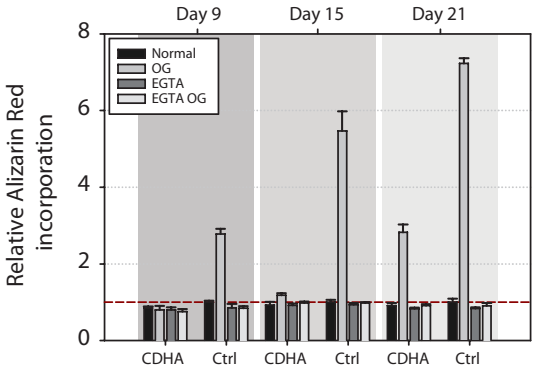

(a) Alizarin extraction

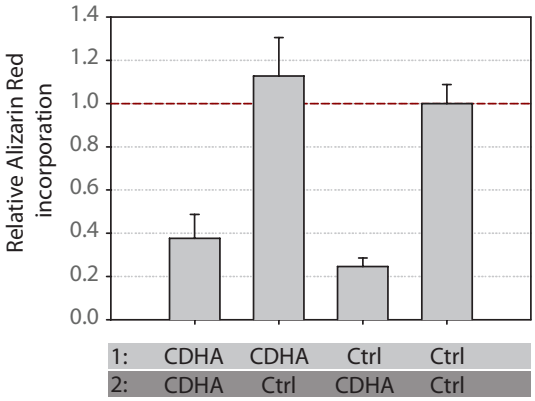

(b) Alizarin extraction

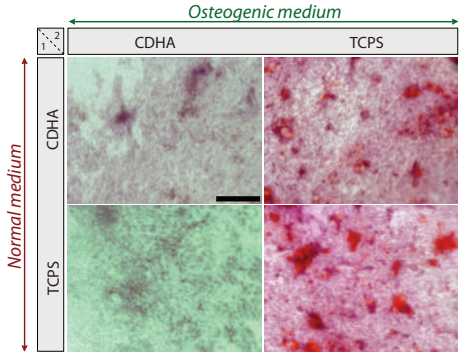

(c) Alizarin staining

Figure 5.10: (a) Evaluation of extracted Alizarin red dye from stained cell cultures maintained during 9, 15, and 21 days. (b,c) Alizarin incorporation in cell layers maintained during 9 days. The first five days (=period 1) without osteogenic medium, and the last four days (=period 2) with osteogenic medium in presence or absence of CDHA. Scale bar = 500 μm.

5.5 Discussion

The chemical influence of CDHA on cellular response was evaluated by cultivating cells on permeable membranes so that cells could be separated from the material but still would directly experience the ionic interactions induced by it. In particular, it was studied how both the material and cells influenced the ionic extracellular environment, and then when combined, how presence of CDHA influenced cellular proliferation, alkaline phosphatase activity, and calcium deposition in the extracellular matrix.

It should be emphasised that from an *in vitro* study of this kind, it is not possible to directly extrapolate the results to the *in vivo* situation. The reasons for this are many. For example, in Chapter 4, it was clearly demonstrated that the CDHA behaves slightly different depending on the chemical composition of the culture medium. Therefore, if the ionic interaction is supposed to influence the cellular behaviour, one would expect high variability in the *in vivo* performance if the ionic concentrations of the extracellular fluid would differ between the hosts of the implanted material. While concentration of calcium is normally strictly regulated in blood, the concentration of phosphorus can differ significantly between individuals, especially if they are of different age (Neuman & Neuman, 1958; Guyton & Hall, 2005). Moreover, in Chapter 3 it was demonstrated that cells, although of similar origin, may behave very differently when exposed to similar conditions.

Taking above considerations into account, but still trying to learn something about the material's possible osteogenic properties, it was decided to work with the culture medium that had been found to be most influenced by the material with respect to calcium and phosphorus (i.e. McCoy), and with cells that used both ions to reinforce its extracellular matrix with calcium (e.g. SAOS-2 cells). In that way, it was created a competitive situation between cells and material with respect to certain ions, and which outcome could not be predicted without performing the experiments. At the same time such experiment could be considered as a 'worst-case' scenario, and thus be used as a preliminary measure of the materials minimally osteoinductive and osteogenic chemical properties.

5.5.1 The Ionic Extracellular Environment

It has in previous chapter been demonstrated that CDHA induces changes with respect mainly to calcium, phosphorus, and pH when immersed in cell culture medium. Important to mention is that probably also the concentration of carbonate ions was influenced by the presence of CDHA, but this has been neglected in this study. However, in future studies on CDHA, it

is highly recommended that protocols for assaying carbonate concentrations are developed and used.

However, through monitoring of the pH of cell culture medium which held cells and CDHA either separetely or in combination (Figure 5.4c), it was clearly shown the chemical composition of the medium was influenced by the temporal chemical activity of each of these two components. Initially the pH value of the medium was mainly determined by the chemical activity of CDHA, but as the material decreased its interaction with respect to pH, and as cells grew in number, metabolic activity became the most important influence on extracellular pH. In that sense, pH measurements were not only informative on tissue development, but also clearly demonstrated that the effect of both components seemed to be superimposed.

Also the concentration of calcium was considerably influenced throughout the experiment when cells and material were combined in the same environment. With respect to the concentration of calcium in normal and osteogenic medium, it was significantly decreased until the end of the experiment. Since cells themselves, at least when maintained in normal medium, did not induce any drastic change of the calcium concentration, the decreased concentration of calcium in normal medium could be almost entirely ascribed to the presence of CDHA. The same conclusion could however not be made when osteogenic medium was used. In that case both cells and CDHA affected the concentration of calcium, and it could not be determined from the ion measurements solely which of the two components that was mainly responsible for the observed decrease, nor to what extent. Yet it was observed that while CDHA took up calcium of osteogenic medium in a very reproducible manner throughout the full experiment (Figure 5.5a), cellular influence on the concentration of calcium in osteogenic medium was a process which depended on the maturation of the cell layer, and which required between four to six days from the first addition of osteogenic factors to reach the maximum uptake rate of calcium. With other words, cells required more time than CDHA to begin to influence the calcium concentration. Yet, the cell-induced calcium uptake rate was at occasions comparable, or even faster, than the Ca^{2+}-uptake induced by the material. That indicates that mature cells and material would compete for the same calcium under seemingly similar ("fair") conditions.

CDHA and cells also influenced significantly the concentration of total phosphorus of both normal and osteogenic medium. On one hand, and similar to its influence on pH but opposed to its interaction with calcium, sorption of phosphorus decreased with time. On the other hand, cells maintained in osteogenic medium efficiently hydrolysed organic phosphorus into inorganic phosphorus already at day 7 and day 9 (Figure 5.4b and 5.5b). The efficiency

of hydrolysis of β-GP maintained relatively stable until the very end of the experiment as in principle all organic phosphorus was hydrolysed within 48 hours also at day 21. Therefore, when cells and CDHA were combined in the same environment and when using osteogenic medium, it could be clearly seen that the concentration of extracellular phosphorus was a superposition of cellular activity (i.e. hydrolysis of β-GP) and CDHA activity (i.e. sorption of P_i). As CDHA decreased its chemical activity with respect to P_i over time, this implied that cells became the most important influence on the extracellular concentration of P_i as the culture progressed.

5.5.2 Cellular Response

In summary, CDHA was observed to influence the ionic extracellular environment of cell cultures by (1) constantly reducing the calcium, (2) decreasing the total phosphorus, and (3) acidifying the environment. The last two observations were however gradually diminished with time. The chemical activity was significant, and introduced changes of the ionic extracellular environment that normally would be considered to have potential to influence cellular behaviour (Beck, 2003; Dvorak *et al.*, 2004; Engel *et al.*, 2008; Liu *et al.*, 2009). However, in this experiment cells did not experience constant low or high concentrations of ions, but instead they experienced gradual changes. Since the kinetics of the CDHA sorption processes were relatively slow, the changes were also less drastic.

Considering that the material was most reactive in the first days of the experiment, it is intuitive to think that its possible chemical influence on cellular response ought to be most obvious at early stages of the cell culture. However, neither cell proliferation, nor total protein, nor alkaline phosphatase activity were highly influenced during the first five days of culture. As a matter of fact, it was not until the very last day of the three-week long experiment that cell proliferation was influenced by presence of CDHA, and then in the sense that it promoted cell growth. The latter observation was a first indication that presence of CDHA might have influenced the cellular capacity of differentiation, as decreased rate of cell proliferation is a common consequence of active differentiation. Further indications in the same direction, i.e. that presence of CDHA influenced the differentiative capacity of cells (at least through a temporal point of view), were given by the alkaline phosphatase activity which was slightly decreased in presence of CDHA in the early phase of the experiment. The dynamics of SAOS-2 alkaline activity has previously been characterised by Rodan *et al.* (1987), revealing that during the first days of culture ALP activity is gradually decreased until reaching a minimum activity, then increases continuously until reaching its

maximum after about 10 days, and then slowly begins to decline once again. Such dynamics is in accordance with the observed ALP activity of cells grown in control conditions. The experimental data suggests that ALP activity is negatively influenced by the presenece of CDHA during the first nine days if normal medium is used, with the only exception being the measurement after five days in culture which coincides with the time point when ALP activity typically begins to rise from its minimal value (Rodan *et al.*, 1987). When using osteogenic medium, experimental data indicated that ALP activity was decreased in presence of CDHA at day nine, but then increased at both day 15 and 21. This indicates that in absence of CDHA the maximum ALP activity was reached earlier, and that the subsequent decreased ALP activity therefore also was turned on faster. With other words, presence of CDHA in general seemed to somewhat delay ALP activity.

The most obvious influence of CDHA on cellular response was however cells capacity to deposit calcium in its matrix. SAOS-2 is an osteoblast-like model that has been extensively used to study mineralisation *in vitro*, relying on the use of osteogenic medium containing β-glycerophosphate (Fassina *et al.*, 2005; Hausser & Brenner, 2005; Schroder *et al.*, 2005; Orimo & Shimada, 2008; Thouverey *et al.*, 2009). Although it has been debated both the relevance of such artificial system, as well as the appropriate concentration of β-GP (Chung *et al.*, 1992), we applied the traditional protocol using 10 mM (e.g. Arnett & Henderson (1998); Gentleman *et al.* (2009); Thouverey *et al.* (2009)), and in such way trying to better understand the importance and relationship of extracellular concentrations of calcium and phosphorus for SAOS-2 cells to induce mineralisation of their extracellular matrix. The results of combining cells and CDHA in osteogenic medium was that calcium deposition was severely decreased compared to the control, but still detectable towards the end of the culture period. It was further shown that calcium-deficient medium (i.e. calcium concentration similar to the steady-state concentration of culture medium in contact with CDHA) completely incapacitated cells to mineralise its matrix, although they expressed proper ALP activity. Thus, it could be concluded that when cells which are grown in presence of CDHA begin to deposit calcium in its matrix, it is because it successfully competes with the material with respect to the extracellular calcium. Until that happens however, cell-induced calcium deposit is suppressed either because (1) cells have not developed an appropriate collagenous matrix, (2) alkaline phosphatase activity is suppressed, or (3) because the ionic concentrations of calcium and phosphorus are inappropriate (Allori *et al.*, 2008a,b). While the first condition remains to be carefully checked (e.g. through immunostaining), it was indirectly shown that cells grown in presence of CDHA in principle already at day 7 to 9 had developed a matrix that

allowed for calcium deposition if the ionic concentrations were not influenced by CDHA (Figure 5.10b-c). Regarding the second condition, ALP activity of cells grown in osteogenic medium and in presence of CDHA was not observed to be greatly influenced neither at day 9 nor at day 21 if compared to cells grown in osteogenic control conditions. Moreover, at day 15 ALP activity of cells grown in presence of CDHA was perfectly comparable to the maximum ALP activity detected from cells grown in absence of CDHA (day 9), but still very little calcium deposition was produced in presence of CDHA at that time point. Therefore, absent calcium deposition in the extracellular matrix ought not to be entirely ascribed to defect ALP activity of cells. It follows that the chemical influence of CDHA on the ionic extracellular environment contribute to the suppressed cell-induced calcium deposition in the extracellular matrix. Following this reasoning, and knowing that CDHA interacts with calcium in a completely predictable and reproducible way throughout the full experiment (as shown in Figure 5.5a), and that therefore it is mainly the concentration of phosphorus that differs between day 9, day 15, and day 21, it is suggested that the extracellular concentration of phosphorus rather than calcium is the requirement for proper calcium deposition in presence of CDHA. The importance of phosphorus for proper mineralisation of the extracellular matrix is in agreement with the experiments made *in vivo* by Murshed *et al.* (2005), and is a message that has been stressed by Allori *et al.* (2008a,b).

Trying to conclude anything about the osteoinductive and osteogenic properties of CDHA based on above *in vitro* study is, as mentioned in the beginning of the discussion, not appropriate. Yet, creating a worst-case scenario where the cell culture medium is depleted on ions important for proper cellular function, it has been revealed that the chemical environment induced by the material may delay certain cellular functions, but in principle it made minimal damage to the cells. Taking into account that a different cell culture medium may create a completely opposite effect on the concentration of phosphorus (e.g. DMEM, see Chapter 4), it can be speculated if instead of delaying ALP activity and cellular mineralisation, rather it could promote it. Therefore, the study presented in this chapter should be considered a careful demonstration of how solution-mediated surface reactions of CDHA (but also other calcium phosphate compounds) can influence cellular response towards the material. This knowledge is necessary to correctly interpret results obtained *in vitro*, and it may in future be used to improve or develop new biomaterials with tuned biochemical activity that promotes specific cellular activity.

5.6 Conclusions

The experiments presented in this chapter have permitted to study the biochemical influence of CDHA on osteoblast behaviour. Solution-mediated reactions occuring when CDHA was immersed in culture media created a dynamic ionic extracellular environment with respect to calcium, phosphorus, and pH. Calcium and total inorganic phosphorus were sorbed from the culture medium onto CDHA, and culture medium was acidified by CDHA. Sorption kinetics of calcium was repeated at every exchange of culture medium, and throughout the full length of experiment. On the contrary, sorption of phosphorus and acidification of culture medium became gradualy less significant with time.

It was revealed that SAOS-2 cells exposed to the dynamic ionic extracellular environment induced by CDHA proliferated well and only had its alkaline phosphatase activity modified in time rather than in absolute levels. While ALP activity of SAOS-2 cells grown in absence of CDHA created conditions for cell-induced calcium deposition in the extracellular matrix, presence of CDHA provoked competition between cells and material with respect to calcium and phosphorus. However, as sorption of phosphorus onto CDHA gradually decreased with time, conditions for mineralisation were slowly created for SAOS-2 cells also in presence of CDHA. Obtained results indicate that sorption of phosphorus rather than sorption of calcium was the main limiter for bone mineralisation around CDHA.

Bibliography

Allori, A. C., Sailon, A. M., & Warren, S. M. (2008a). *Tissue Engineering Part B,* **14** (3), 259–273.

Allori, A. C., Sailon, A. M., & Warren, S. M. (2008b). *Tissue Engineering Part B,* **14** (3), 275–283.

Arnett, T. R. & Henderson, B. (1998). *Methods in Bone Biology.* London: Chapman & Hall.

Beck, G. R. (2003). *Journal of Cellular Biochemistry,* **90**, 234–243.

Beck, G. R., Zerler, B., & Moran, E. (2000). *PNAS,* **97** (15), 8352–8357.

Boanini, E., Gazzano, M., & Bigi, A. (2010). *Acta Biomaterialia,* **6**, 1882–1894.

Cazalbou, S., Eichert, D., Ranz, X., Drouet, C., Combes, C., Harmand, M., & Rey, C. (2005). *Journal of Materials Science: Materials in Medicine,* **16**, 405–409.

Chung, C., Golub, E., Forbes, E., Tokuoka, T., & Shapiro, I. (1992). *Calcified Tissue International,* **51**, 305–311.

Dvorak, M. M., Siddiqua, A., Ward, D. T., Carter, D. H., Dallas, S. L., Nemeth, E. F., & Riccardi, D. (2004). *PNAS,* **101** (14), 5140–5145.

Eklou-Kalonji, E., Denis, I., Lieberherr, M., & Pointillart, A. (1998). *Cell and Tissue Research,* **292**, 163–171.

El-Ghannam, A. & Ning, C. Q. (2006). *Journal of Biomedical Materials Research. Part A,* **76** (2), 386–397.

Engel, E., del Valle, S., Aparicio, C., Altankov, G., Asin, L., Planell, J. A., & Ginebra, M. P. (2008). *Tissue Engineering,* **14**, 1341–1351.

Farley, J., Hall, S., Tanner, M., & Wergedal, J. (1994). *Journal of Bone and Mineral Research,* **9**, 497–508.

Fassina, L., Visai, L., L.Asti, Benazzo, F., Speziale, P., Tanzi, M., & Magenes, G. (2005). *Tissue Engineering,* **11** (5/6), 685–699.

Fujita, T., Izumo, N., Fukuyama, R., Meguro, T., Nakamuta, H., Kohno, T., & Koida, M. (2001). *Biochemical and Biophysical Research Communications,* **280**, 348–352.

Gentleman, E., Swain, R. J., Evans, N. D., Boonrungsiman, S., Jell, G., Ball, M. D., Shean, T. A. V., Oyen, M. L., Porter, A., & Stevens, M. M. (2009). *Nature Materials,* **8**, 763–770.

Guyton, A. C. & Hall, J. E. (2005). *Textbook of Medical Physiology.* Philadelphia: Elsevier Saunders.

Habel, B. & Glaser, R. (1998). *European Biophysical Journal,* **27**, 411–416.

Hausser, H.-J. & Brenner, R. E. (2005). *Biochemical and Biophysical Research Communications,* **333**, 216–222.

Hempel, U., Reinstorf, A., Poppe, M., Fischer, U., Gelinsky, M., Pompe, W., & Wenzel, K. W. (2004). *Journal of Biomedical Materials Research Part B: Applied Biomaterials,* **71** (1), 130–143.

Hofer, A. M. (2005). *Journal of Cell Science,* **118** (5), 855–862.

Liu, Y. K., Lu, Q. Z., Pei, R., Ji, H. J., Zhou, G. S., Zhao, X. L., Tang, R. K., & Zhang, M. (2009). *Biomedical Materials,* **4**, 1–8.

Matsumoto, A., Tagushi, H., & Hisada, Y. (1991). *Toxic In Vitro,* **5**, 51–62.

Murshed, M., Harmey, D., Millan, J. L., McKee, M. D., & Karsenty, G. (2005). *Genes & Development,* **19**, 1093–1104.

Neuman, W. F. & Neuman, M. W. (1958). *The Chemical Dynamics of Bone Mineral.* : The University Of Chicago Press.

Orimo, H. & Shimada, T. (2008). *Molecular and Cellular Biochemistry,* **315**, 51–60.

Rodan, S. B., Imai, Y., Thiede, M. A., Wesolowski, G., Thompson, D., Bar-Shavit, Z., Shull, S., Mann, K., & Rodan, G. A. (1987). *Cancer Research,* **47**, 4961–4966.

Schroder, H. C., Boreiko, O., Krasko, A., Reiber, A., Schwertner, H., & Mller, W. E. G. (2005). *Journal of Biomedical Materials Research. Part B,* **75B** (2), 387–392.

Thouverey, C., Strzelecka-Kiliszek, A., Balcerzak, M., Buchet, R., & Pikula, S. (2009). *Journal of Cellular Biochemistry,* **106**, 127–138.

Yamaguchi, T. (2008). *Journal of Bone and Mineral Metabolism,* **26**, 301–311.

Yoshimura, Y., Hisada, Y., Suzuki, K., Deyama, Y., & Matsumoto, A. (1996). *Archives of Oral Biology,* **41**, 41–45.

This page is intentionally left blank

Chapter 6

Fabrication, Characterisation, and Application of Ion Sensors in Bone Tissue Engineering

6.1 Introduction

In previous chapters it has been demonstrated that, on one hand osteoblast-like cells, and on another hand certain biomaterials used in bone tissue engineering, both may interact with extracellular ions present in the tissue engineering environment. Understanding the art of such interactions on both a global and local level is helpful in order to develop optimised protocols for bone tissue engineering. For that reason there was a desire to develop a generic platform that could allow for real-time monitoring of ions in complex solutions and at physiological *in vitro* conditions. In this chapter, special focus is paid to the development, characterisation, and application of miniaturised potentiometric calcium selective ion sensors.

6.1.1 Potentiometric Ion Sensors

Potentiometry is a versatile analytical method that can be used to obtain the concentration of a species in solution from measurements of the electromotive force (EMF), or the voltage difference, between an *indicator electode* and a *reference elctrode* immersed in the test solution (Fig 6.1). If the electric current between both electrodes is maintained under a nearly zero-current condition, and if the potential arising from the reference electrode is kept constant, then the potential difference between the two electrodes depends only on the indicator electrode. To ensure that the indicator electrode re-

sponds to the analyte in a predictable way, it should not repsond to, nor react chemically with any other species present in the analyte (i.e., it should be as specific and inert as possible). Also, the surface of the indicator electrode should remain uncharged, even when small currents pass through the cell.

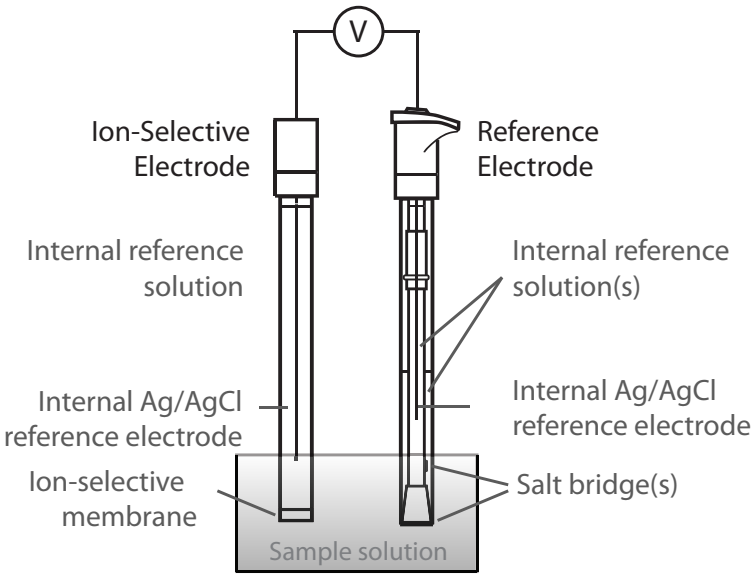

Figure 6.1: Representation of a typical cell used for potentiometric measurements.

When above criteria are met with, the potential difference (EMF) between indicator and reference electrodes obeys the *Nernst equation* (Eq. 6.1):

$$EMF = \text{constant} - 2.303\frac{RT}{nF}\log a \tag{6.1}$$

where R is the gas constant (8.313 J K^{-1} mol^{-1}), T is the absolute temperature (K), n is the charge number of the analyte ion, F is the Faraday constant (96487 C mol^{-1}), and a is the activity of the analyte of interest. The proportionality constant between measured potential and logarithm of the activity of the ion is (0.0591/n) at $T = 25°C$, which means that the electrode potential changes $59.1/n$ mV for each ten-fold change of activity of an n-charged ion. It also means that a change of 1.0 mV corresponds to a change of 4.0% in activity for a monovalent ions, and 8.1% for divalent ions.

The Nernst equation thus allows to correlate the electrode potential to the activity of analyte in the test solution. The activity is however a complex function of the concentration of the analyte, as well as any possible interference from other ions present in the sample, and will be further discussed in section 6.1.1.1.

Figure 6.2: Walther Hermann Nernst was a German physicist that made fundamental contribution in physical chemistry and thermodynamics. Here he is portraied on a Swedish stamp in honour of his Nobel prize in Chemistry 1920.

6.1.1.1 Ions in solution

Obviously, any complex test solution will inevitably contain other ions than the ion of interest. Even an ionic test solution of the simplest formulation will be subject to certain interference from surrounding counterions, as any ionic solid dissociated in a polar solvent always give rise to both positive and negative ions (6.2).

$$AB + H_2O(l) \rightarrow A^+(aq) + B^-(aq) \tag{6.2}$$

When AB is dissolved, A^+ ions and B^- ions arrange themselves in a regular pattern where each cation is surrounded by a fixed number of anions, and vice versa. Also, due to the polar nature of the water molecules they will shield both positive and negative ions, creating an insulation layer around any ion. In very dilute solutions there will be sufficient water molecules to fully surround each ion, and as long as the analyte concentration is low, the distance between a given ion and its nearest neighbour will be relatively large. Therefore, in dilute solutions each ion can be considered as a separate entity which will behave independently of all other ions present. However, when the concentration increases, there may be insufficient water molecules to completely solvate each ion, and then the ions may not be fully insulated from its neighbours. In higher concentrated solutions the ions will also be arranged closer together and forces of attraction and repulsion between opposite and like charged ions will occur. Thus, in concentrated solutions each individual ion will be influenced by the presence of other ions. An ion of one charge will be surrounded by an ion atmosphere of oppositely charged ions. While this gives rise to some short-term order within the solution, it is not a permanent arrangement. Random motions of solvated ions occur and the composition of the ion atmosphere changes. Therefore, as the concentration increases, the

degree of non-ideality also increases. Due to this arrangement and shielding, measurements of non-ideal solutions result in concentrations that seem lower than they really are.

In order to compensate for the effect of shielding in non-ideal solutions, the concept of *ion activity* has been introduced, and which takes into account the influence of other ions surrounding the ion of interest. The activity of a solution is defined as

$$a_A = \gamma_A c_A \tag{6.3}$$

where a_A is the activity of ion A, γ_A is the activity coefficient ($0 \leq \gamma_A \leq 1$), and c_A is the concentration of ion A. As defined, the activity is measured in units of moles dm^{-3}.

The activity coefficient, γ_A, depends on the concentration of the ions in the sample solution. For ideal solutions (i.e., for very low concentrations), then $\gamma_A \approx 1$. With increased concentrations, non-ideality increases and the activity coefficient becomes smaller as the forces of attraction between oppositely charged particles becomes stronger. Debye and Hückel defined a solution property known as the *ionic strength* (I) which increses with concentration and charge:

$$I = 0.5 \sum_i c_i z_i^2 \tag{6.4}$$

where c_i and z_i are the stoichiometric concentration and charge of an ion i. Provided the total ionic strength of a solution, Debye and Hückel went further on to show that the activity coefficient of a given ion is related to the total ionic strength by the empirical expression:

$$\log \gamma = \frac{-Az^2\sqrt{I}}{1 + Bd\sqrt{I}} \tag{6.5}$$

where A and B are constants (0.5108 and 0.328 respectively), z is the charge number of the ion under consideration, I is the total ionic strength as defined in equation 6.4, and d is the effective diameter of the hydrated ion (Ammann, 1986).

The Debye-Hückel theory makes it possible to estimate the activity of a certain ion knowing its concentration.

6.1.1.2 Electrodes of first and second kind

The simplest ion sensors are the metal electrodes, which can be of either *first* or *second* kind category. Ion electrodes of first kind develop an electric potential in direct relationship to changes in activity of an ion, while ion electrodes of second kind develop such dependence towards ion activity through the formation of a complex. In both cases, the electrical potential that develops in response to ion activity is derived from the redox reactions that these electrodes undergo in contact with the analyte (6.6):

$$\mathrm{M^{n+}(aq) + ne^{-}(s) \rightleftharpoons M(s)} \tag{6.6}$$

where M^{n+}(aq) is the oxidised state, and M(s) the reduced state of the electrode metal.

Therefore, when a first- or second-order electrode is immersed in a test solution, charge transfer between the liquid and solid phases may occur. The electrode itself does not necessarily have to be directly involved in this charge transfer, but it can act as a source or sink of a tiny amount of electrons. As the energy levels are equalled out and the system reaches equilibrium, the charge transfer rapidly ceases. Important though is that when electrons can move from one phase to another, the phases can become electrically charged with respect to each other, and so they give rise to a potential difference, also known as the *electrode potential*.

To calculate the electrode potential, one has to take into account both the *electrical* energy required to move a charged particle over two different phases, and the *chemical* energy of reactants and products of the reaction. The electrical energy, expressed on per mole basis, can be expressed as (6.7):

$$\left(\text{Electrical energy}\right)_A = z_A F \Phi \tag{6.7}$$

where z_A is the charge of molecule A, F is the Faraday constant which represents the electrical charge in one mole of electrons, and Φ is the electrical potential of the particular phase in which molecule A resides. Next, the chemical energy (μ_A) of species A in solution can be expressed as (6.8):

$$\mu_A = \mu_A^{\theta} + RT \ln a_A \tag{6.8}$$

where μ_A^{θ} is the standard chemical potential that depends on the temperature, R is the gas constant, T is the temperature, and a_A is the activity of

species A.

For the general redox reaction (6.6), the total electrochemical energy of reactants and products are equal. While the reduced form of the metal is uncharged and only contributes with chemical energy, the oxidised metal ion and the electron contribute with both electrical and chemical energy to the system:

$$(\mu_{\mathrm{M^{n+}}} + nF\Phi_{\mathrm{solution}}) + (\mu_{\mathrm{e^-}} - nF\Phi_{metal}) = \mu_{\mathrm{M}} \tag{6.9}$$

From above equation it can be easily calculated the potential difference between the two phases (i.e., EMF $= \Delta\Phi = \Phi_{\mathrm{metal}} - \Phi_{\mathrm{solution}}$),

$$\Delta\Phi = \Delta\Phi^{\theta} + \frac{RT}{nF} \ln \frac{a_{\mathrm{M}^{n+}}}{a_{\mathrm{M}}} \tag{6.10}$$

where $\Delta\Phi^{\theta} = (\mu^{\theta}_{M^+} + \mu^{\theta}_{e} - \mu^{\theta}_{M})/nF$ is a constant at fixed temperature and pressure. Equation 6.10 is the *Nernst equation*, which was previously mentioned (see Eq. 6.1) and that correlates the electrode potential with the activity of the reduced and oxidised species in the redox reaction.

Electrodes of first and second kind may be simple and easy to use, but they are only available for a limited amount of analytes (Table 6.1). Moreover, they are little selective, and they may not withstand extreme alkaline or acidic conditions. Yet, these electrodes can find important applications. For example, the Ag/AgCl electrode is one of the most used electrodes in electrochemistry, due to its great stability which allows the use of it as a variant of reference electrode. The Ag/AgCl electrode is subject to the following redox reaction:

$$\mathrm{AgCl(s) + e^- \rightleftharpoons Ag(s) + Cl^-(aq)} \tag{6.11}$$

If one applies the Nernst equation (Eq. 6.10) to above reaction, then one obtains that

$$\Delta\Phi = \Delta\Phi^{\theta} + \frac{RT}{nF} \ln \frac{a_{\mathrm{AgCl}}}{a_{\mathrm{Ag}} a_{\mathrm{Cl^-}}} = \Delta\Phi^{\theta} - \frac{RT}{nF} \ln a_{\mathrm{Cl^-}} \tag{6.12}$$

Thus, submerging a Ag/AgCl electrode in a solution of chloride ions establishes an electrode potential that directly depends on the activity of chloride ions in the solution, and that changes 59.1 mV for each ten-fold change in activity.

Electrode Category	Electrode material	Electrode reaction
1st kind	Zn	$Zn^{2+} + 2e^- \rightleftharpoons Zn(s)$
	Cu	$Cu^{2+} + 2e^- \rightleftharpoons Cu(s)$
	Ag	$Ag^+ + e^- \rightleftharpoons Ag(s)$
2nd kind	Ag/AgCl	$AgCl(s) + e^- \rightleftharpoons Ag(s) + Cl^-(aq)$

Table 6.1: Examples of ion electrodes of first and second kind.

6.1.2 Ion Selective Electrodes

To be able to asses a greater variety of ions than what is possible with the metal electrodes of first and second kind, potentiometric chemical sensors referred to as ion selective electrodes (ISEs) were invented in the 1960s. Until today, ISEs for more than 60 different analytes have been reported (Bakker *et al.*, 1999). Moreover, ISEs can easily be miniaturised, consume low amounts of energy, and are relatively cheap to produce.

The ISE arrangement includes two fundamental components: (1) the *ion selective membrane* which composition decides the electrode properties, and (2) the physical *electrode body* onto which the ion selective membrane is attached. In sections 6.1.2.1 - 6.1.2.4 it is discussed the construction, working principle, and characterisation of ISEs.

6.1.2.1 Electrode bodies

While the composition of the ion selective membrane strictly depends on the ion to be detected, the design of the electrode body is independent of the analyte, but is rather choosen given the specific environment that the application presents. Therefore, a multitude of ISE designs exist (Arnold & Solsky, 1986), among which four main categories can be distinguished: conventional ISEs, solid-state ISEs, coated-wire ISEs, and ion-selective field effect transistors (ISFETs) (Figure 6.3).

The conventional ion selective electrode is constructed from an internal reference electrode bathing in a solution which is separated from the test solution via a polymeric membrane. Conventional ISEs can be produced with active sensor diameters between *mm* all way down to *nm*. In the lower range, the electrode body is typically a glass pipette which has had its tip narrowed. Although such electrodes allow for ion measurements in usually inaccesible microenvironments (e.g. detection of nerve cell action potentials and cell membrane ion channel activity), decreased sensor size is commonly

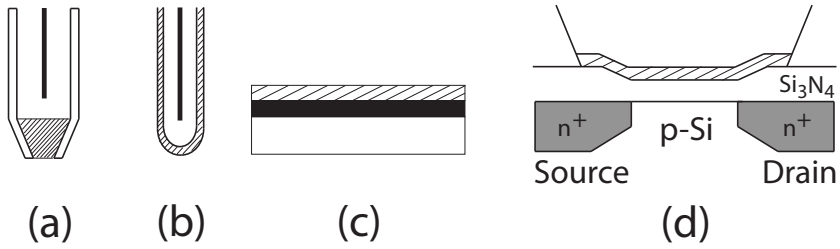

Figure 6.3: The most common ISE designs all involve the attachment of the ion-selective membrane onto a solid electrode body. The latter one can take different shapes: (a) conventional ISE, (b) solid-state electrode, (c) coated-wire electrode, and (d) ISFET.

linked to fragile and less durable electrode bodies.

To achieve miniaturised electrodes with reasonable mechanical properties, coated-wire and solid-state ISEs can be used. The drawback of such designs is that when removing the internal filling solution, the interface between the electrode and the ion selective membrane becomes ill-defined due to osmotic transport of water. To avoid such parasitic side-reactions, the membrane can be contacted to the electrode through an intermediate redox-active polymer layer. Such layer, typically made from electroactive polymers (see Table 6.2), improves the attachment of the membrane, and allows for fast and reversible ion-to-electron transduction in the solid state (Bobacka, 1999; Suzuki, 2000; Sutter *et al.*, 2004; Bobacka *et al.*, 2008). It has also been proposed to incorporate the conducting polymer directly in the ion-selective membrane (Maminska & Wroblewski, 2006).

Polymer	**Electrode body**	**IS membrane**	**Reference**
Polypyrrole	SiO2	K^+	Zine *et al.* (2006)
PEDOT	carbon disk	K^+	Bobacka (1999)
	carbon disk	Ca^{2+}	Kikas & Ivaska (2007)
polyHEMA	Au & Ag	K^+	Toczylowska *et al.* (2005)

Table 6.2: Polymers commonly used to improve the electrical properties of the membrane-electrode interface of solid state electrodes.

6.1.2.2 Ion selective membranes

To generate a stable electrode potential which relates to the analyte concentration, the ion selective membrane obviously has to contain some kind of ligand to the analyte. Depending on the nature of that ligand, one traditionally distinguishes between *solid* and *liquid* ion selective membranes. Solid

membranes (e.g. glass or ceramics) have fixed sites for exchange of ions, while liquid membranes rely on specific complexing agents with high selectivity towards the ion of interest, and that further are mobile within the membrane. The complexing agents, known as *ionophores*, can be of either synthetic or natural origin. To develop synthetic ionophores that complex with a specific ion in a fast and reversible way, it has to be taken into account many parameters, among them the structural flexibility of the molecule, its binding site geometry and molecular topology, its lipophilicity, as well as binding and stabilising interactions (e.g. through hydrogen bonding, charge, π-electron interactions, Lewis acid-base chemistry) (Johnson & Bachas, 2003). Controlled influence on all these parameters has brought about more than 100 different ionophores, most of them being selective to cations, even though ionophores for certain anions have been reported (Antonisse & Reinhoudt, 1999)).

In addition to high selectivity towards the analyte, the function of the ion-selective membrane also is to separate the aqueous sample solution from the electrode, as well as provide appropriate mechanical properties. This is achieved by incorporating the ionophore into a *polymeric matrix*. Among the various matrices that have been tested, poly(vinyl chloride) (PVC) has shown the far best performance. Usually PVC is a tough glassy polymer, but adding to it an appropriate *plasticizer* its glass transistion temperature is decreased, and so it can be transformed into a mechanically strong and flexible membrane. The plasticizer, which is a lipophilic liquid, further dictates the dielectric constant, lipophilicity, and viscosity of the membrane, and its polarity may influence the selectivity of the membrane. The major problems using PVC as membrane matrix are (1) possible leakage of the plasticizer and/or ionophore from the polymer bulk, which in turn could reduce the lifetime of the sensor, and (2) that it might be considered as less biocompatible (Yajima *et al.*, 2006). Still, no other polymers have been able to provide as good mechanical and chemical stability as PVC, and its biocompatibility may be improved by chemical modification of its surface chemistry (Radomska *et al.*, 2008).

Additional components that may be added to further enhance the membrane properties include certain membrane *additives*. These molecules, typically lipophilic salts (e.g. potassium tetrakis(*p*-chloro-phenyl)borate), are used to reduce interference caused by anions present in the test solution, and so they contribute to improve the membrane selectivity.

After mixing all membrane components, they are dissolved in an appropriate solvent which is then allowed to evaporate to form a solid, but flexible, polyermic membrane. Each component of the ion-selective membrane has significant influence on the establishment of the membrane potential, and

even tiny changes in composition can influence the final electrode properties such as its selectivity, membrane resistance, and lifetime. Table 6.3 reports on the traditional composition of liquid ion-selective membranes.

Component	**Function & Example**	**Amount**
Ionophore	Ion complexing agent; $>$ 100 different ones	1-2 wt.-%
Matrix	Provides mechanical and chemical stability; Poly(vinyl chloride) Polyurethane	30-50 wt.-%
Plasticizer	Solvent of all membrane components; bis(2-ethylhexyl)sebacate Dioctyl phenylphosphonate o-nitrophenyloctylether Dioctyl phthalate Phthalic acid esters	60-90 wt.-%
Additive	Reduces anionic interference KTpClPB	0-1 wt.-%
Solvent	Disolve the matrix components tetrahydrofuran	

Table 6.3: Typical composition of ion selective membranes.

6.1.2.3 Response mechanism

The electrochemical cell for the conventional ion-selective electrode (Fig 6.1), with corresponding interfacial potentials (E_i), can be written as:

$$\underset{E_1}{\text{Ag}} \mid \underset{E_2}{\text{AgCl}} \mid \underset{E_3}{\text{KCl}} \mid \underset{E_J}{\text{salt bridge}} \mid \underset{}{\text{sample}} \mid \underbrace{\underset{E_M}{\text{IS-membrane}}}_{} \mid \underset{E_4}{\text{internal solution}} \mid \underset{E_5}{\text{AgCl}} \mid \text{Ag}$$

The potential difference measured between the indicator electrode and the reference electrode is the sum of all interfacial potentials (6.13):

$$EMF = (E_1 + E_2 + E_3 + E_4 + E_5) + E_J + E_M \tag{6.13}$$

At constant temperature, E_1 to E_5 are all constant, and if the internal reference electrolyte closely resembles the sample solution, then $E_J \approx 0$, which reduces Equation 6.13 to

$$EMF = \text{constant} + E_M \tag{6.14}$$

Although at least three different, and to some extent contradictory(!), theoretical models are available to describe the dependence of E_M on the ion activity of the sample (Bakker *et al.*, 1999), the phase boundary potential model predicts very well experimental data obtained with convential ISEs, where at the junction between the membrane and the solution, an equilibrium between the ion of interest (X) will be formed with the ionophore (I) according to reaction (6.15) and Figure 6.4:

$$\mathrm{X(aq) + I(membrane) \leftrightarrows XI(membrane\ surface)} \tag{6.15}$$

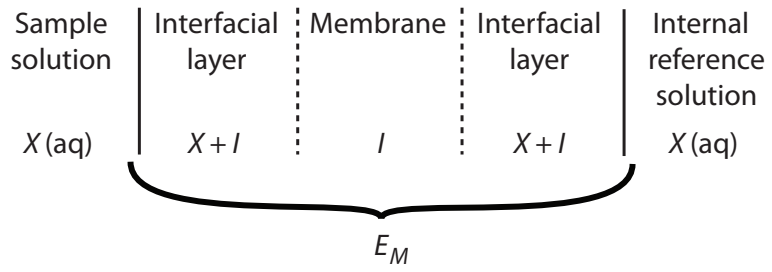

Figure 6.4: Representation of the half cell of a conventional ion-selective electrode.

The phase boundary potential model is dervied from thermodynamic equilibria much in accordance with the previous derivation of the Nernst equation (Section 6.1.1.2), and gives that:

$$E_M = \text{constant} + \frac{RT}{zF} \ln \frac{a_i(\text{sample})}{a_i(\text{internal})} \tag{6.16}$$

where a_i(sample) and a_i(internal) are the ion activities of the sample solution and the internal filling solution, respectively. The latter parameter is constant, which reduces Eq.(6.16) to Eq.(6.1).

6.1.2.4 Sensor characterisation

The practical usefulness of any ISE depends to a great extent on the three 'Ss': ***s**electivity*, ***s**ensitivity*, and ***s**tability*. In addition, it is required that the electrode possesses a low detection limit and often also a fast response in time. To determine these properties, the EMF between ISE and a reference electrode is measured in a range of known concentrations (activities) of analyte solutions. The obtained data is used to produce a calibration curve from which can be obtained important characterisation data such as working region, detection limit, and sensitivity (Figure 6.5).

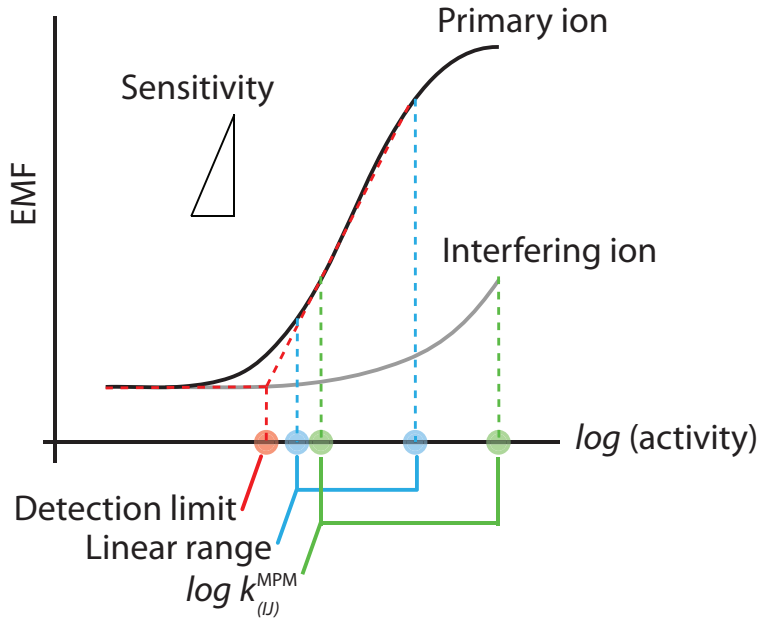

Figure 6.5: A typical calibration curve for potentiometric measurements.

With respect to the sensitivity of the electrode, the slope of the calibration curve in its linear region is determined by the proportionality constant of the Nernst equation (Eq 6.1). As previously mentioned, an ideal ISE detecting monovalent ion at 25°C should provide a slope of 59.1 mV for every ten-fold activity change, and if the ion is divalent this value is halfed. In practice, slope values between 55-59.1/n mV decade^{-1} are referred to as Nernstian, and are acceptable for analysis. Values below 55/n mV decade^{-1} are sub-Nernstian and generally indicate a badly prepared electrode (Evans, 1987). At very low and very high activities, the calibration curve typically deviates from linearity and the electrode cannot be used to predict analyte activity. The detection limit of the electrode has been defined as the deviation of experimental data from the extrapolated Nernstian response by s log 2 mV.

Presence of other ions than the analyte ion i may interfere with the ISE potential response, and the experimental data then deviates from the theoretical response. To evaluate such interference, various methods have been developed. Traditionally the semiempirical Nikolskii-Eisenman (NE) equation has been used to assess the selectivity of ISEs. The NE equation predicts the potential response in presence of interfering ions (j), by assigning each ion a specific selectivity coefficient (K_{ij}).

$$E = constant + \frac{RT}{z_i F} \ln \left(a_i^{sample} + \sum K_{ij}^{pot} a_j^{z_i/z_j} \right) \tag{6.17}$$

The selectivity coefficient is often expressed as $\log K_{ij}$, and negative values indicate a preference for the analyte ion, while positive values indicate preference for the interfering ion. It is important to emphasize that K_{ij} are experimental values, and they depend both on activity and method of determination, but can be regarded as a true membrane parameter. In such way the NE equation deals correctly with interference from ions of the same charge as the primary ion, but when the ions present opposite charge or if any of primary or interfering ion do not show Nernstian response which often is the case in many practical situations, the equation fails to predict the electrode response (Bakker, 1997).

An alternative, and more generally applicable, method to determine selectivity coefficients is the *mathed potential method* (Bakker, 1997; Horvai, 1997; Umezawa *et al.*, 2000). In practice, a specified activity of primary ions is added to a reference solution and the membrane potential is measured. In a separate experiment, interfering ions are successively added to an identical reference solution until the membrane potential matches the one obtained before by adding primary ions. The matched potential method selectivity coefficient is then calculated as the ratio of the primary ion to interfering ion activity:

$$k_{ij}^{MPM} = \frac{a_i}{a_j} \tag{6.18}$$

6.2 Objectives

The primary objective of the work presented in this chapter was to develop a platform for ion selective electrode measurements. That task included:

1a. the construction of an electronic device for potentiometric measurements of several ion selective electrodes simultaneously,

1b. the implementation of a software program to handle and anlyse data obtained from potentiometric measurements using above device.

Once achieved, a secondary objective was established: **the elaboration and characterisation of a calcium selective electrode for *in vitro* tissue engineering applications**. This task included:

2a. fabrication and characterisation of an internal Ag/AgCl reference electrode,

2b. fabrication of a conventional Ca^{2+}-selective electrode,

2c. traditional ISE characterisation of Ca^{2+}-selective electrode,

2d. evaluation of calcium selective electrode biocompatibility and performance in complex biological solutions (cell culture medium containing protein).

Finally, both the Ag/AgCl and the Ca^{2+}-electrode were applied in environments related to bone tissue engineering processes. The Ag/AgCl electrode was used to measure Cl^{-}-activity in NaCl during hydrolysis of α-tricalcium phosphate. The Ca^{2+}-electrode was used to first measure Ca^{2+}-interactions between cell culture medium and calcium-deficient hydroxyapatite (CDHA), and then to measure Ca^{2+}-activity in highly mature osteoblast-like cell cultures.

6.3 Materials and Methods

6.3.1 Potentiometric Instrumentation

The instrumentation for potentiometric measurements consisted of two parts; hardware and software. The hardware was built to convert the potential difference between the working electrodes and the reference electrode into digital data, while the software was designed to record the digital signal, and to facilitate data analysis.

6.3.1.1 Hardware

Chemical sensors may present high output impedance, something which can cause current leakage problems when connected to a data-aquistion (DAQ) board. This problem can be overcome by reading the sensor signal via a voltage-follower circuit, which significantly reduces the output impedance of its input signal. In this work, an instrumentation amplifier (Ultra Low Input Bias Current INA116, Burr-Brown) with a gain set to 1.5 (R_G=100kΩ) was feeded with the signals from the indicator and reference electrodes. The output signal, i.e. the voltage difference between indicator and reference electrode, was then read with a DAQ-board that was connected via USB to a PC to log the acquired data (Figure 6.6).

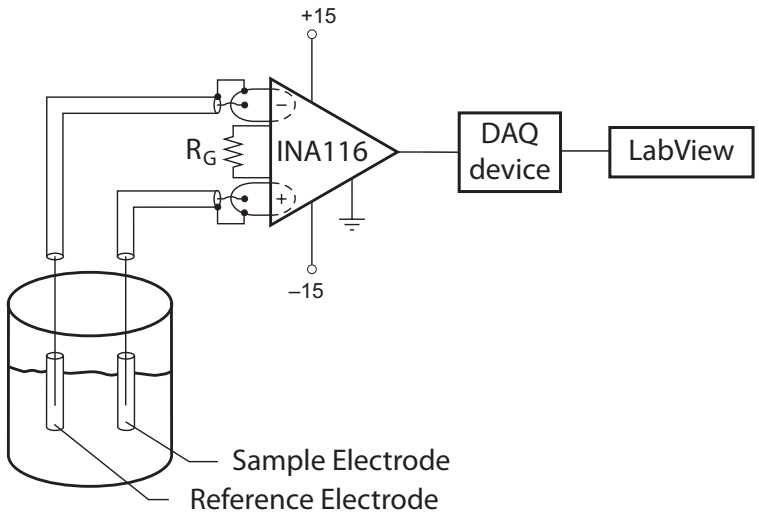

Figure 6.6: Simplified model of potentiometric measurement setup.

The hardware was further designed to provide data from four separate sensors simultaneously. Therefore, four separate voltage-follower circuits were housed within a metallic box together with a ±15V power supply (CE-BEK FE73) that fed each operational amplifier. The exterior part of the box had input connections for each of the four sensor (I1-I4) as well as for one reference electrode. There were also four output connections (O1-O4), one for each sensor, as well as one connection for ground, which was used for the DAQ-device.

The DAQ device was of simplest model (National Instruments, USB 6009). It had eight analog input channels, a resolution of 13 bits in RSE mode (Reference Single Ended), a sample rate of 48000 samples s^{-1}, and it could be adjusted to read voltages between ±1 V and up to ±20 V. The smaller the input range is, the higher is the resulting accuracy, and as for our purpose an input range of ±1V would be more than sufficient, the accuracy or smallest signal that could be detected by the DAQ device in such configuration would be $2/2^{13} = 0.24$ mV.

6.3.1.2 Software

As stated above, the main function of the software was to record the signal provided by the hardware, and to facilitate data analysis. Specifically, the requirements on the software were the following:

1. acquire the open-circuit potential of the ion-selective electrode against the reference electrode,
2. visualise the open-circuit potential in real time,
3. continuously write data to file to reproduce the EMF-t-graph,
4. for calibration purposes, and upon request from user, write data to file during a specific (user defined) time period,
5. visualise the calibration curve in real time,
6. acquire above information from four sensors at the same time.

To implement above requirements, the LabView 8.2 software (National Instruments) was used, as it allows for easy aquisition and analysis of digital data, and which previously has been successfully used to handle similar multi-channel electrochemical measurements (Li *et al.*, 2004; Stevic *et al.*, 2008). The structure of the LabView program was divided in two independent platforms; the first part reads, write, and visualise the data provided by

the DAQ device (Figure 6.7a), and the second part calculates and plot the mean value of a signal that has been recorded during a certain time period that was specified by the user of the software (Figure 6.7b).

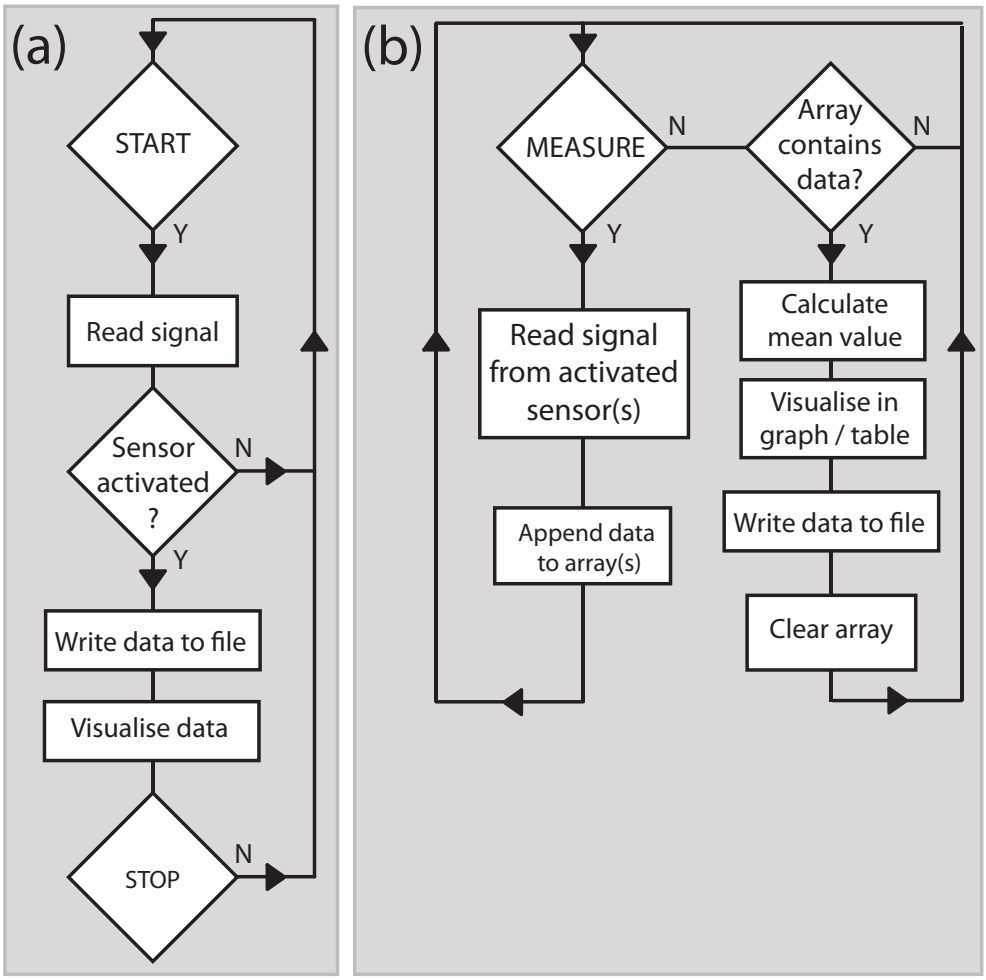

Figure 6.7: Flow charts on the signal processing for the two different parts of the LabView implementation.

In the first part the electrode signals coming from the DAQ device were digitally processed, at a frequency defined by the user, using the LabView `DAQ Assistant function` in which it was specified the nature of the signal (i.e. voltage), input range, and time setting (± 1V and 100 Hz sampling rate, respectively). Signals from different channels were easily handled simultaneously since each channel was represented as a separate column of the input signal. The program was written to automatically check if the user had activated any of the sensor channels, and if so, corresponding data was extracted

from the output of the DAQ Assistant by first changing the data type from `Dynamic data` to `Array type`, and then by using the `Index array` function to specify the channel(s) of interest. Data from all input channels was then converted to `String` format, and written to file along with the running time of the experiment. At the same time, data from the activated channels was visualised on the screen using a `Waveform chart` with multiplot function.

The second part of the software was implemented to facilitate calibration of any ion-selective electrode with the idea to provide the user with an instant view of how the electrodes responded to various known concentrations/activities of a given solute. The principle behind the measurement was that the user recorded the electrode signal during a certain time period. The software read the data, allocated it in an array that was updated typically every half a second. By the end of the recording, the mean value of the recorded data was calculated, printed on the screen in a table format together with the concentration of solute which had been specified by the user. The data was also plotted in a graph to make it easy to quickly evaluate the quality of the electrode (such as sensitivity, detection limit, and linear range).

The potentiometric instrumentation (hardware + software) was initially tested against a commercial setup (VoltaLab PGZ301) in its open-circuit potentiometric mode. After confirmation that the instrumentation reproduced well the data, it was used throughout all experiments presented in this chapter.

6.3.2 Ag/AgCl Reference Electrode

Two different designs of silver/silver chloride (Ag/AgCl) reference electrodes, referred to as **Ag/AgCl wire** and **Ag/AgCl disk**, respectively, have been used throughout this work. Both designs are based on a 0.2 mm diameter silver wire of 99.99% purity which was insulated by a thin layer of teflon (Advent Research Materials Ltd, AG549511). In both designs, the wire was cut in lengths of about 4-6 cm and the teflon insulation was carefully removed at both ends of the wire using a surgical blade. One end of the stripped wire was soldered onto an electrical wire (diameter 1 mm), and the soldering point was protected with a heat shrink tubing. The silver wire was then threaded through a syringe needle (BD Microlance 3, 0.9 mm x 25 mm) so that the bare end of the Ag wire slightly protruded the needle.

For the Ag/AgCl disk electrode, the needle was then backfilled with epoxy resin (Robnor, PX771C), and left to cure during 48 hours. The sharp end of the needle with the protruding Ag wire was then cut with a rotating diamond saw, polished, and finally cleaned with ethanol and distilled water. At this

stage, the needle presented a flat cross section of epoxy that embedded the teflon insulated Ag wire. The active electrode area, A_{disk}, was approximately 0.03 mm^2.

In the other design, i.e. the Ag/AgCl wire electrode, the needle was cut flat as above, but before it was backfilled with epoxy resin. The Ag wire was then inserted into the needle, and left to protrude it about 1-2 cm from its flat end. The interior of the needle was then solidified with epoxy resin, but it still had the Ag wire protruding from its end. The exposed Ag electrode area, A_{wire}, was approximately 3 mm^2. The both designs are schematically shown in Figure 6.8.

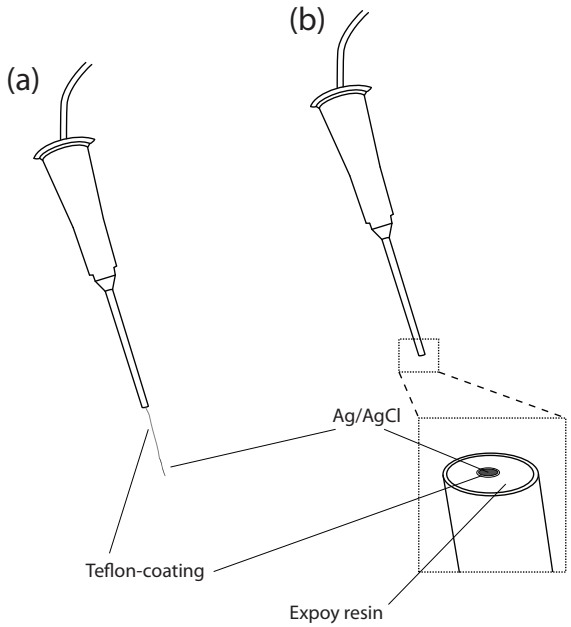

Figure 6.8: Ag/AgCl electrodes were prepared in shape of (a) wire and (b) disk, respectively.

In both designs, the active Ag electrode area was cleaned by dipping the electrode into concentrated ammonia (NH_3), followed by rinsing it in distilled water. To coat the Ag electrode with AgCl, the electrode was connected to the positive pole of a battery (4.5V), and immersed in a solution of 0.1M hydrogen chloride (HCl). To the negative pole of the battery was connected a 0.2 mm thin platinum (Pt) wire (Advent Research Materials Ltd, PT541507) in series with a resistor appropriate to obtain a current density of ≈ 0.4 mA cm^{-2} ($R_{disk} = 4$ kΩ, and $R_{wire} = 400$ kΩ respectively), as suggested by Ives & Janz (1961). The circuit was connected for 40 minutes, allowing the chloride ions of the solution to deposit a porous layer of AgCl onto the Ag electrode

according to the reaction below (6.19). Before any use of the electrode, it was left in distilled water overnight.

$$\mathrm{Ag(s) + Cl^-(aq) - e^-(metal) \rightarrow AgCl(s)} \tag{6.19}$$

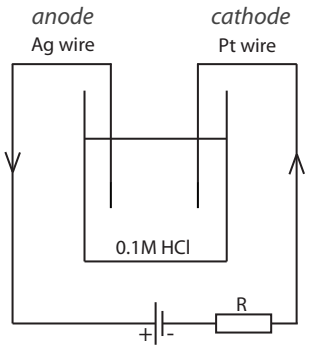

Figure 6.9: The Ag/AgCl reference electrodes were prepared by electro-oxidising the Ag wires in a medium containing chloride ions.

To assess the physical aspect of the AgCl deposition, the wire was subject to scanning electron microscopy (SEM) investigation. The electrochemical characterisation of the Ag/AgCl electrode was divided in several steps. First, it was evaluated how the potential of the electrode, measured against a commercial double junction Ag/AgCl reference electrode (Thermo Scientific, 900200), responded to changing concentrations of three different salt solutions; KCl, $CaCl_2$, and KNO_3. Thereafter it was carefully tested the potential response to chloride ions by incremental increases of the concentration of KCl from 10^{-8} M to 10^{-1} M. The potential response was plotted against the logarithm of the activity of chloride ions in the solution. From that measurement it was obtained the detection limit, linear range, and sensitivity of the Ag/AgCl electrode. The same process was repeated during a period of several weeks in order to see how the sensitivity of the Ag/AgCl electrode was influenced over time. Between measurements the electrodes were stored in a solution containing 150 mM NaCl, 5 mM KCl, 3 mM LiCl, 0.8 mM $MgCl_2$, and 1 mM $CaCl_2$. It was also evaluated the drift of the Ag/AgCl electrode when left in a solution of constant concentration of chloride ions (10^{-3}M KCl) over a longer period of time (4 days). Finally, with the intention to use this electrode in cell culture environments, it was also tested how the potential response was affected by (1) soaking the electrode in 70% ethanol, (2) autoclaving, and (3) storing the electrode in a biological solution (DMEM cell culture medium with 10% serum).

6.3.3 Calcium Selective Electrodes

The polymeric calcium selective membrane consisted of five components (Figure 6.10): *ionophore* (calcium ionophore V; Sigma, 21203), *additive* (potassium tetrakis (*p*-chloro phenyl) borate; Sigma, 60591), *polymer matrix* (poly(vinyl chloride), PVC; Sigma, 81392), *plasticizer* (NPOE; Sigma, 73732), and *solvent* (tetrahydrofuran, THF; Sigma 87369).

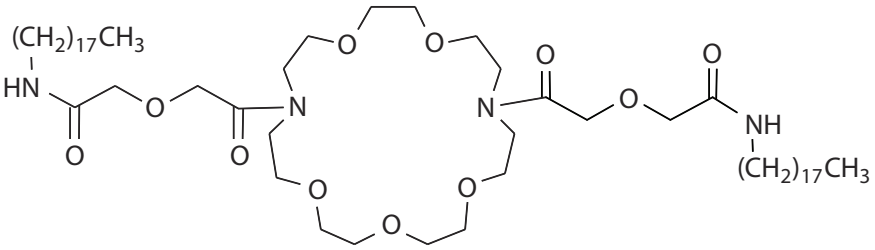

(a) Ionophore

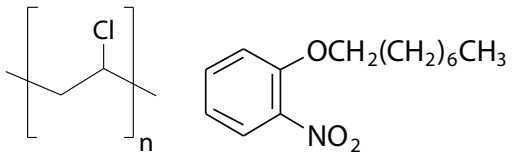

(b) Matrix

(c) Plasticizer

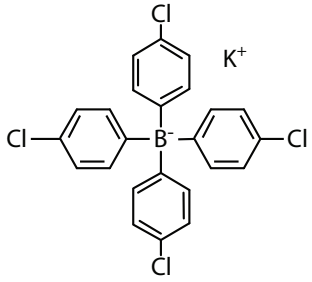

(d) Additive

Figure 6.10: Membrane components.

To prepare the membrane the solid components (i.e., ionophore, additive, and PVC) were weighted individually according to Table 6.4, and put in a glass vial (5 ml). The liquid plasticizer and solvent were subsequently added, and the mix was left in a sonicator for 30 minutes. At this stage, the cocktail was ready to be applied onto the electrodes, but it could also be stored (4°C) during several months, with no influence on the electrode performance.

Component	**Other name**	**Weight percent**	**Amount**
Ionophore	Calcium V	2.0	2.4 mg
Plasticizer	NPOE	66.0	79.2 mg
Matrix	PVC	31.1	37.3 mg
Additive	K-TCPB	0.90	1.1 mg
Solvent	THF	-	0.7 ml

Table 6.4: The precise composition of the calcium selective membrane.

The calcium selective electrodes based on above polymeric membrane were prepared using disposable pipette tips as the electrode body (Brand, 200 μl). The pipette tip was carefully introduced in the well-mixed membrane cocktail, and then slowly withdrawn from it. In this way, the capillary effect filled the tip with membrane solution up to about 1 mm. The coated pipette was then left to dry at room temperature overnight. As the solvent evaporated, a sealing polymeric membrane sensitive to calcium was formed at the distal end of the pipette, and the interior of the electrode could then be filled with 100 μl 0.1M $CaCl_2$. Care was taken that no air was trapped in the electrolyte-membrane interface. The Ag/AgCl reference electrode (wire design) was used as internal reference electrode, and its electrode body adjusted perfectly into the wider end of the pipette body, so the calcium selective electrode was perfectly sealed also at the other end. The complete setup (Figure 6.11) can therefore be drawn as:

Ext. RE | test solution | membrane | 0.1 M $CaCl_2$, AgCl; Ag

Before any calibration measurements, the membrane was conditioned in 0.1M $CaCl_2$ during at least 12 hours. In between measurements, the electrode was stored in 0.1M $CaCl_2$ at 4°C.

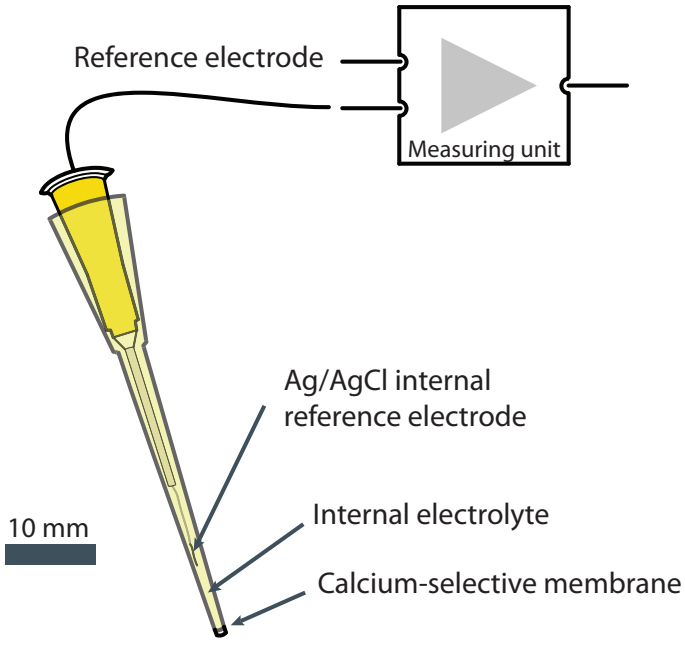

Figure 6.11: Calcium selective electrode design.

6.3.3.1 ISE characterisation

To assess the characteristics and quality of the produced ion selective electrodes their sensitivity, selectivity, and stability was initially evaluated. Standard calibration curves were obtained by continuous measurements of the potential difference between the working electrode against a double junction Ag/AgCl reference electrode (Orion 900200, ThermoScientific) immersed in a test solution (starting with 25 ml dH_2O). Incremental changes of concentration of the test solution were obtained by adding aliquots of salt standard solutions prepared from serial dilutions (concentration range 1M down to 10^{-5}M). All measurements were made at room temperature (25°C). The potential response was plotted versus the logarithm of the activity of the primary ion in the test solution. The activity was calculated using the modified Debye-Hückel model (equation 6.20).

$$\log \gamma = \frac{-0.53 z^2 \sqrt{I}}{1 + \sqrt{I}} \tag{6.20}$$

The sensitivity of the electrodes was obtained by calculating the slope of the linear part of the calibration curve between 10^{-5}M and 10^{-1}M. The stability of the electrodes was estimated by repeated calibrations on a semi-daily basis over a longer time period (4 weeks). The selectivity was evaluated using the matched-potential method by exposing the electrodes to different salt solutions (KCl, $MgCl_2$, NaCl, $Ca(NO_3)_2$) at varying concentrations in a constant background solution of 10^{-3}M $CaCl_2$.

After the standard characterisation explained above, the developed calcium selective electrodes were further tested when being exposed to typical *in vitro* environments. First, sterilisation of the electrodes was achieved by exposing them to UV-irradiation during 10 minutes in dry conditions immediately before use. Thereafter, electrodes were rapidly rinsed in sterile PBS solution and the stability of the potential signal at constant concentration of calcium was measured in protein-containing culture medium at 37°C and 5%CO_2 during a period of 48 hours. Calibraton curves were obtained as above both before and after exposure to UV irradiation and culture medium. Moreover, the possible cytotoxic effects of the calcium selective electrodes was evaluated by growing SAOS-2 cells both in presence and absence of the electrodes during 72 hours. The viability was qualitatively assesed through calcein/propidium iodine staining, while quantitatively determined by direct cell counting using a hemocytometer after trypsinisation of cells from their culture substrate.

6.3.4 Sensor Applications

6.3.4.1 Cl^--activity during α-TCP-hydrolysis

The evolution of chloride activity during setting of α-tri calcium phosphate (α-TCP) in 0.9% NaCl was measured using the Ag/AgCl disk electrodes. The electrodes were incorporated, from below, into a well of a 12-well polystyrene plate. To protrude the electrodes through the plate, the bottom of the well had been drilled on beforehand. When the electrodes were fixed to the plate, the well was filled with a well-mixed paste of fine-milled[1] α-TCP-powder and distilled water (L/P ratio of 0.65 ml/g), so that the active area of the electrodes would be located in the liquid-solid interface. After a few minutes, the well was filled with 2 ml of 0.9% NaCl, and a double junction Ag/AgCl reference electrode was introduced from above. All measurements were done at room temperature.

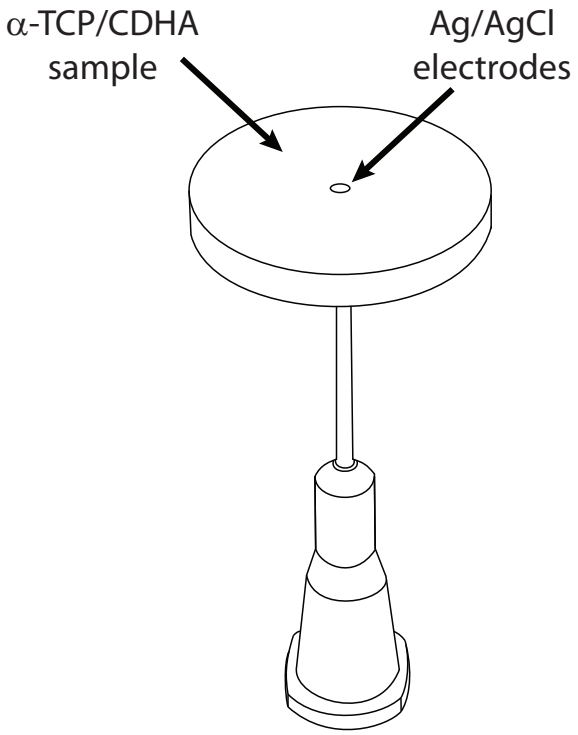

Figure 6.12: Setup for measuring chloride activity during setting of α-TCP in a solution of sodium chloride.

[1]Milling protocol: 3 × 20 min at 450 rpm + 30 min at 500 rpm.

6.3.4.2 Ca^{2+}-activity of CDHA in cell culture medium

The activity of calcium in cell culture medium exposed to calcium-deficient hydroxyapatite (CDHA) was monitored in real-time during a period of 24 hours. For that purpose, CDHA was prepared as described in Chapter 4, and cell culture medium was prepared from Dulbecco's Modified Eagle Medium (DMEM), and supplemented with 1% of l-glutamine, penicillin / streptomycin, and sodium pyruvate, as well as with 10% fetal bovine serum (FBS).

Calcium selective electrodes, assembled as described in Section 6.3.3 and which had been maintained in 0.1M $CaCl_2$, were rinsed in distilled water, and then their tip areas were exposed to UV irradiation in dry conditions during at least 10 minutes in a laminar flow hood aimed for cell culture labour. The electrodes were then briefly moisturised in sterile PBS, before conditioned in sterile DMEM culture medium at 37°C and at 0.05 atm CO_2, during a period of at least 24 hours.

The CDHA sample was placed inside a plastic well which had been isolated from a 24-well cell culture plate. The sample was exposed to 1.25 ml of fresh DMEM medium, and the calcium electrode was inserted into the well from above (Figure 6.13a). The measurement was performed against a mini-Ag/AgCl/3M KCl reference electrode (Flex-Ref, Dri-Ref^{TM} World Precision Instruments) which previously had been immersed in 70% ethanol, and then copiously rinsed in sterile PBS.

The calcium selective electrodes were calibrated before and after the measurement according to Section 6.3.3.1. Reference determination of calcium was performed using the ILyte analyser (Instrumentation Laboratory) as explained in Section 3.3.2.

6.3.4.3 Ca^{2+}-activity during osteoblast mineralisation

Cultures of SAOS-2 osteoblast-like cells were done in 24-well plates, while using culture media of both high and low concentration of total inorganic phosphorus (McCoy and DMEM, respectively). In general, the culture medium was exchanged every three to four days. After five days in culture, the culture medium was in some cases further supplemented with osteogenic factors: ascorbic acid (50 μg/mL), dexamethasone (10^{-8}M), and β-glycerophosphate (3 mM in DMEM medium, and 10 mM in McCoy medium).

To evaluate the effect on calcium deposition in osteoblast cultures of culture medium low on phosphorus (i.e. DMEM with 3 mM β-GP) the concentration of extracellular calcium was measured on a regular basis (after 8, 16, 24, and 32 days in culture) with the ILyte analyser according to Section 3.3.2). Moreover, evaluation of calcium deposition in the extracellular

matrix of above cultures was done with Alizarin Red S staining as described in Section 3.3.8.

The activity of calcium ions in osteogenic media was also mesured in real-time using the developed Ca^{2+}-electrodes. Measurements were made in presence of cells during periods of 24 hours at different stages during the culture period (specifically, after 13, 19, and 35 days in culture). As in previous section, the procedure of measurement went through the following steps: (1) sterilisation of electrodes with UV irradiation, (2) pre-conditioning of sensors in medium at physiological *in vitro* conditions, and (3) measurement against a mini-Ag/AgCl/3M KCl reference electrode. Reference measurements were done with the ILyte analyser. Measurements with the developed Ca^{2+}-electrodes were also made in absence of cells to be able to distinguish cell-induced changes in calcium activity from intrinsic drift of the electrodes. Cell morphology/viability was qualitatively assessed by staining non-fixed cell layers with 0.5% fluorescein diacetate (Sigma, F7378).

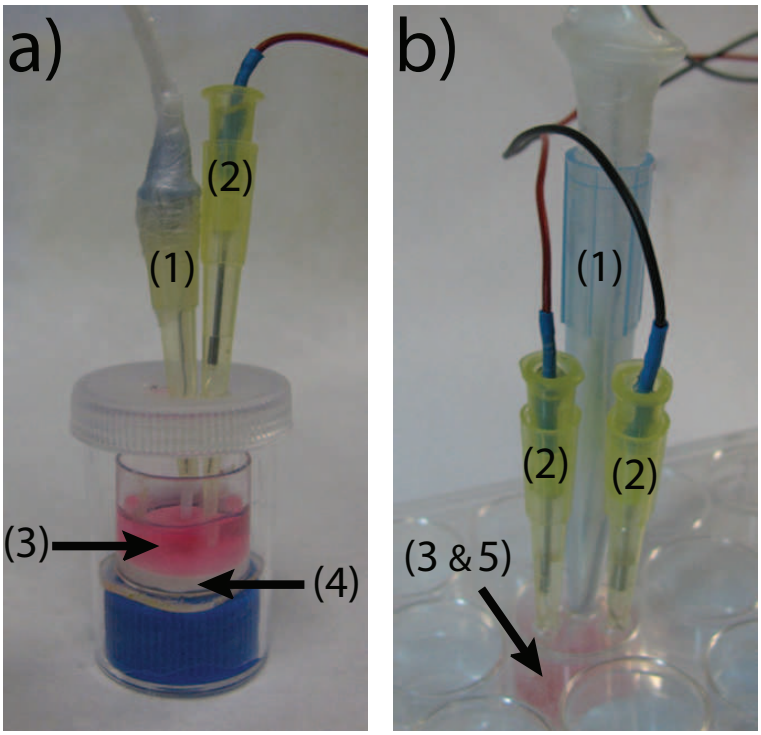

Figure 6.13: Setups for measuring [Ca^{2+}] in bone tissue engineering applications: (a) cell culture medium exposed to CDHA, and (b) osteoblast cultures. The numbers indicate reference electrode (1), Ca^{2+}-selective electrode (2), cell culture medium (3), CDHA sample (4), and osteoblast culture (5).

6.4 Results

6.4.1 Potentiometric Instrumentation

The potentiometric instrumentation has been used to monitor potentials of Ag/AgCl electrodes and calcium selective electrodes of different designs. The software visualises in real-time the potential difference of up to four different electrodes versus a common reference electrode. Also, the software makes it possible to easily obtain calibration data of these electrodes as the user can specify the activity of monovalent or divalent calibration solutions.

The software is divided in three main screens: (1) experiment initiation, (2) signal visualisation, and (3) calibration data analysis. In the first screen the user specifies which of the four sensors that are connected to the instrumentation, and whether the calibration solution is of monovalent or divalent character. Also it is possible to specify any details about the experiment, such as types of indicator and reference electrode. In the second screen the signal of each activated sensor is visualised in real time (Figure 6.14, top). The potentials measured by the device are presented in both numerical and graphical form. Furthermore, and if known, the user can specify the activity of the test sample solution. At any time, the user can also activate a recording of the signal(s) so that the software collects data (time, potential, and activity) of each activated sensor. The latest obtained data is then presented in a box at the bottom of the screen.

In the third screen (Figure 6.14, bottom), potential and activity data obtained from any recordings of the signal(s) are presented in both tabular and graphical form. This allows the user to rapidly decide whether the sensor responds normally or is defect. When the experiment is finished the user has access to two `txt`-files. The first file provides continous potential data obtained throughout the full experiment, and the second file contains average potentials and corresponding activity values obtained from the second screen (i.e. calibration data).

6.4.2 Ag/AgCl Reference Electrode

The Ag/AgCl reference electrodes were produced through electrolytic deposition of Cl^--ions onto a Ag wire. It could be observed by eye how that process left behind a dark layer of AgCl on top of the Ag wire, and through scanning electron micrographs it was revealed that the surface of the Ag wire had turned from a flat layer into a unifrom, porous surface (Figure 6.15).

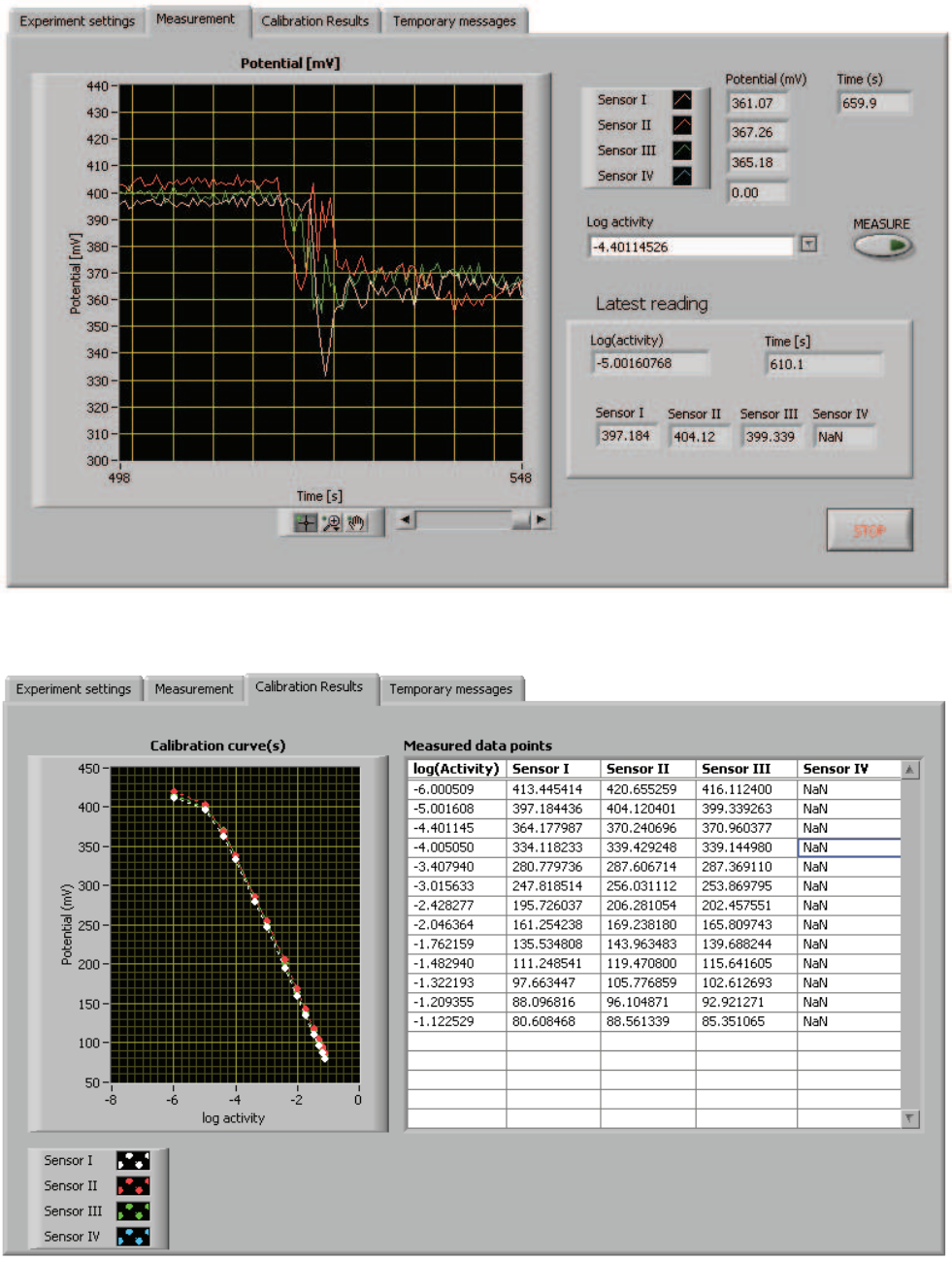

log(Activity)	Sensor I	Sensor II	Sensor III	Sensor IV
-6.000509	413.445414	420.655259	416.112400	NaN
-5.001608	397.184436	404.120401	399.339263	NaN
-4.401145	364.177987	370.240696	370.960377	NaN
-4.005050	334.118233	339.429248	339.144980	NaN
-3.407940	280.779736	287.606714	287.369110	NaN
-3.015633	247.818514	256.031112	253.869795	NaN
-2.428277	195.726037	206.281054	202.457551	NaN
-2.046364	161.254238	169.238180	165.809743	NaN
-1.762159	135.534808	143.963483	139.688244	NaN
-1.482940	111.248541	119.470800	115.641605	NaN
-1.322193	97.663447	105.776859	102.612693	NaN
-1.209355	88.096816	96.104871	92.921271	NaN
-1.122529	80.608468	88.561339	85.351065	NaN

Figure 6.14: The sensor software has three main screens. In the first one (not shown here) the experiment is initiated by activating the sensor channels. In the second screen (top) the sensor signals are visualised in real-time both graphically and numerically. In the third screen (bottom) the measured calibration data is presented for rapid assessment of the sensor response.

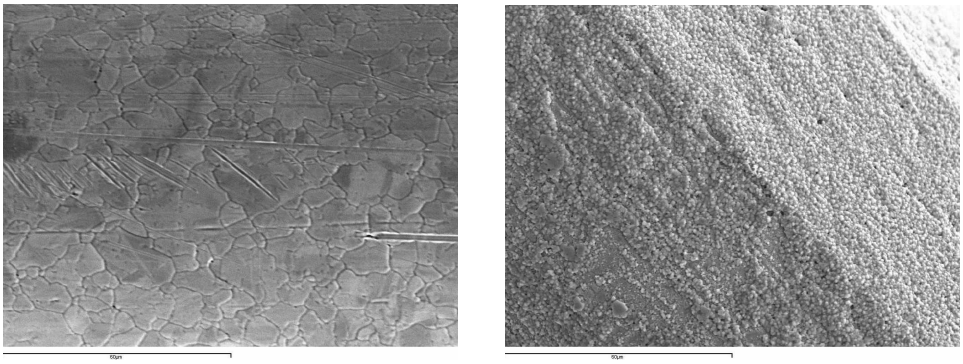

(a) Before depositon. (b) After deposition.

Figure 6.15: Micrographs of Ag-wire before and after electrodeposition of AgCl.

The potential between the Ag/AgCl wire and a double-junction Ag/AgCl reference electrode was monitored upon exposure to different concentrations of potassium chloride, observing that beyond $\approx 10^{-5}$M KCl the potential decreased with increasing concentration of KCl (Figure 6.16). From the same data, when plotting the EMF against the logarithm of the activity of chloride ions, a typical calibration curve for an ion selective electrode was obtained (Figure 6.17). The potential response was further seen to depend mainly on the presence of Cl^- ions, as the electrode responded equally well to calcium chloride ($CaCl_2$) as to KCl, while its response to potassium nitrate (KNO_3) was close to absent.

Furthermore, the durability, or life-time, of the Ag/AgCl electrode was tested by repeated calibrations on a weekly basis. As follows from Table 6.5 both the wire design and the disk design maintained their characteristics for a period of at least three weeks when stored in a solution of ionic strength similar to blood. Also, if exposed to cell culture medium containing proteins, the sensitivity of the Ag/AgCl electrode was maintained. The influence of different sterilisation methods on the electrode response was then tested, and it was observed that both UV irradiation and 70% ethanol can be applied without affecting the electrode sensitivity. However, steam autoclaving caused damage to the electrode body (the epoxy resin), which resulted in unstable signal.

Finally it was examined how the electrode signal maintained over a longer time period (four days) in a solution of constant concentration of KCl. As evident from Figure 6.18, no significant drift was observed.

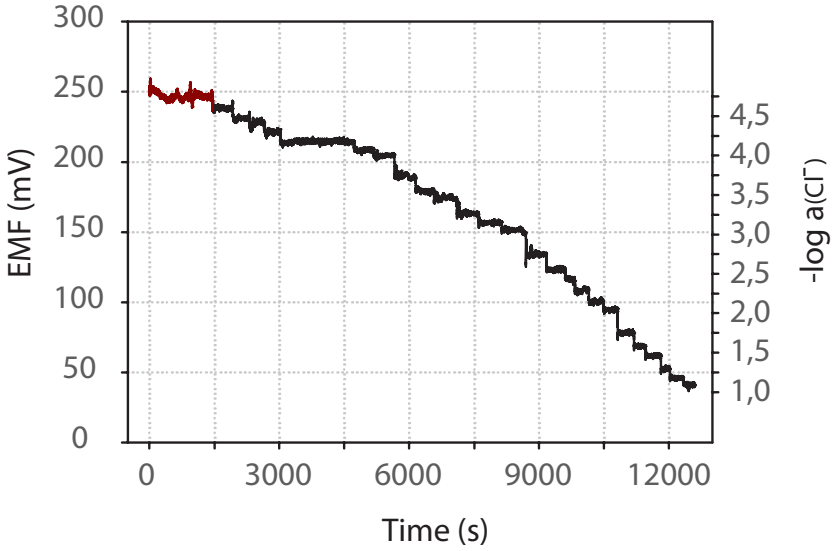

Figure 6.16: Potential response of Ag/AgCl electrode when exposed to incrementing concentrations of KCl. The initial period ($0\text{ s} < t < 1500\text{ s}$) represents potential response to 10^{-7}M and 10^{-6}M KCl, and is out of range of the right Y-axis.

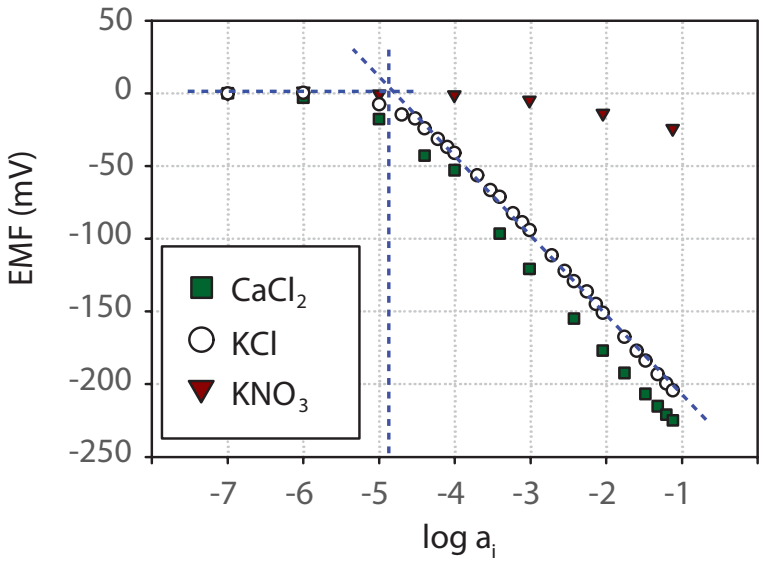

Figure 6.17: Potential response of Ag/AgCl wire when exposed to varying concentrations of KCl, $CaCl_2$, and KNO_3.

	Wire electrode (mV decade^{-1})	**Disk electrode** (mV decade^{-1})
Ionic solution		
Day 1	-58.24 ± 0.43	-57.75 ± 0.57
Day 7	-58.86 ± 0.24	-
Day 14	-60.04 ± 0.17	-57.80 ± 0.56
Day 21	-59.19 ± 0.20	-58.46 ± 0.22
Cell culture media		
24h exposure	-58.21 ± 1.37	-
Sterilisation methods		
UV (15 min)	-60.19 ± 0.89	-
Ethanol (70%)	-58.70 ± 0.21	-
Autoclave (steam)	-	not working

Table 6.5: Sensitivity and stability of Ag/AgCl electrode at different time points and in different conditions ($n = 3$).

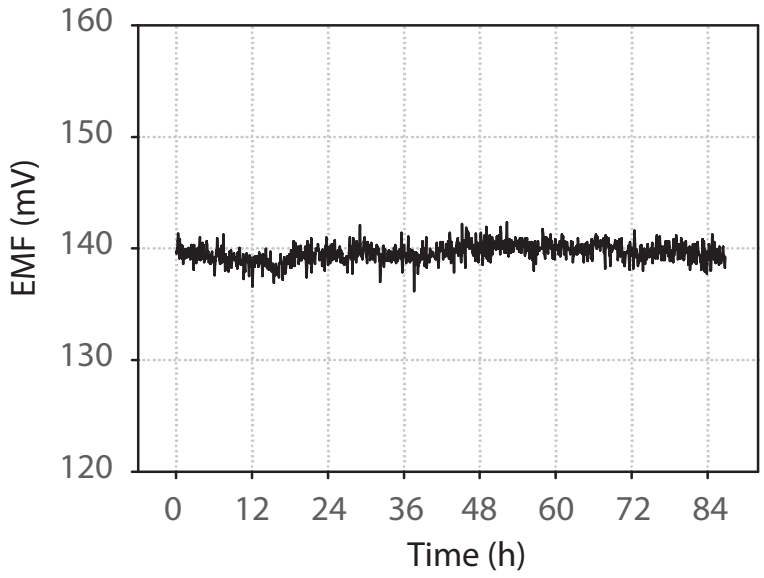

Figure 6.18: Stability of Ag/AgCl wire potential exposed to 10^{-3}M KCl during four days.

6.4.3 Calcium Selective Electrode Characterisation

Calcium selective electrodes were prepared by attaching a Ca^{2+}-selective membrane on the tip of a plastic micropipette. The membrane separated the test solution from an internal reference electrolyte and an internal reference electrode (Ag/AgCl wire electrode). Characterisation of the electrodes was done both with simple ionic solutions (Section 6.4.3.1), and with cell culture medium containing proteins (Section 6.4.3.2).

6.4.3.1 Standard characterisation

When exposed to increasing concentrations of $CaCl_2$ (10^{-7} M to 10^{-1} M), the potential of the electrode versus an external reference electrode increased gradually (Figure 6.19). Decreasing the concentration, resulted in a decrease in potential, indicating reversible complexation of Ca^{2+} ions to the selective membrane. The time required to achieve 90% of steady state potential upon changes in concentration of $CaCl_2$ was 31.4 ± 4.9 s in the range -5.01 ≤ log a(Ca^{2+}) ≤ -3.47 (Figure 6.20).

Plotting the potentials obtained from Figure 6.19 versus the logarithm of the activity (Figure 6.21), it was revealed a typical ISE response with a linear range in the range -5.01 ≤ log a(Ca^{2+}) ≤ -1.722 (which corresponds to a Ca^{2+}-concentration range of 10^{-5}M to 10^{-1} M). The detection limit was around log a(Ca^{2+}) = -6.13 (i.e. [Ca^{2+}] ≈ 10^{-6} M), while the slope of the curve in the linear range was determined to 30.3 ± 2.4 mV decade^{-1} (R^2 = 0.992, n = 45), which is considered a Nernstian behaviour for positively charged divalent ions.

Regarding the selectivity of the Ca^{2+}-selective electrode, it was observed to respond equally well to $Ca(NO_3)_2$ as to $CaCl_2$ (Figure 6.21), and neither did changing the pH of the test solution influence the electrode potential at constant concentration of Ca^{2+}. The selectivity of the electrode was further evaluated by measuring the potential of the electrode as aliquots of different ionic solutions (NaCl, KCl, and $MgCl_2$, respectively and separately) were added to a background reference solution of 10^{-3}M $CaCl_2$. Interference to the electrode potential was detected mainly from potassium with k^{MPM}=1.56, meaning that the electrode was more than 36 times more selective to calcium than to any other of the tested cations.

Finally, the life-time of the electrode was evaluated by repeated calibration on a daily basis, and as indicated in Figure 6.22, the electrode maintained its sensitivity for at least up to one month when stored in 0.1 M $CaCl_2$ between measurements.

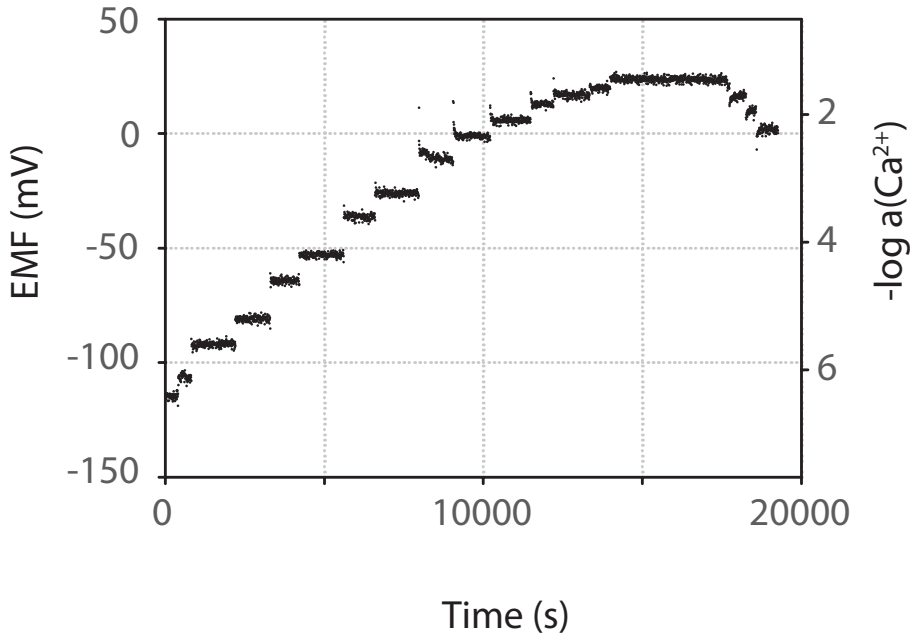

Figure 6.19: Potential response of the calcium selective electrode when exposed to changing concentrations of $CaCl_2$.

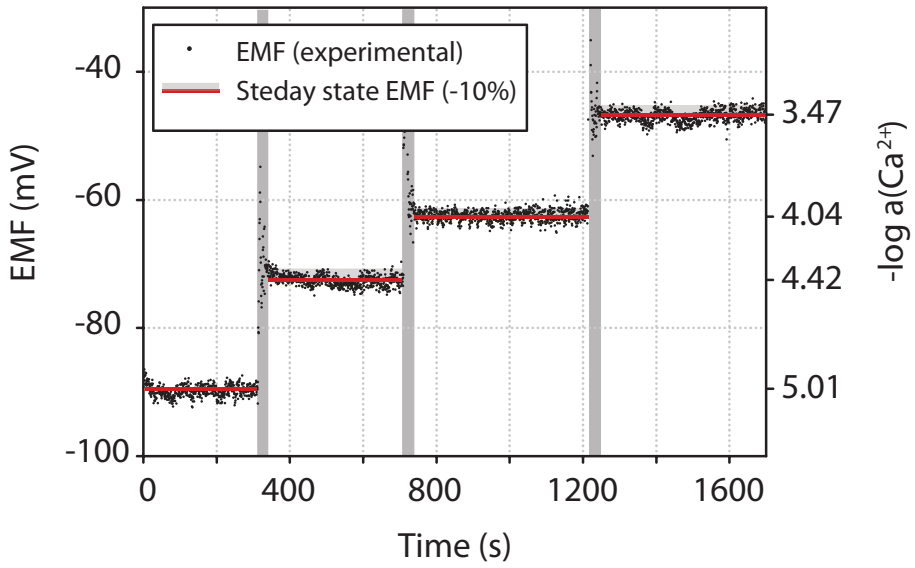

Figure 6.20: Typical potential response of the calcium selective electrode upon changes in concentration under agitation. The potential typically reaches 90% of the steady-state value after about 30 seconds (grey shaded vertical zones).

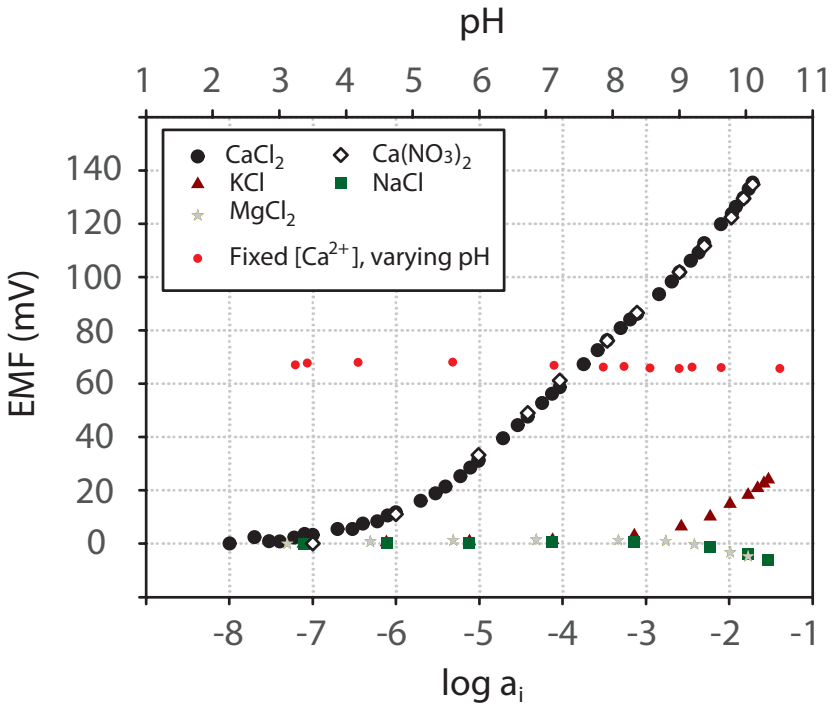

Figure 6.21: Ca^{2+}-electrode potential response to different ions.

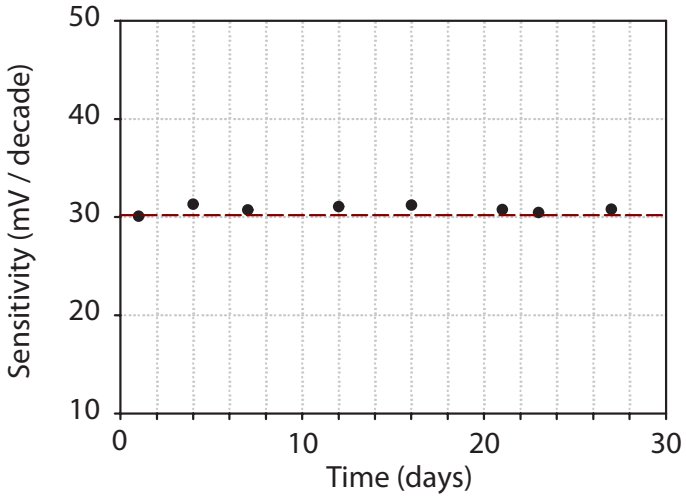

Figure 6.22: Life-time of one specific Ca^{2+}-electrode, evaluated through its sensitivity. Dashed line indicates the mean sensitivity of a larger set of sensors ($n = 45$).

6.4.3.2 ISE characterisation in complex solutions

For *in vitro* applications of the Ca^{2+}-selective electrode related to tissue engineering, it was also required to evaluate the influence of issues such as UV irradiation (for sterilisation), protein biofouling, drift, and biocompatibility / cytotoxicity of the sensor when exposed to cell cultures.

As shown in Figure 6.23, Ca^{2+}-sensors exposed to UV irradiation during 10 minutes did maintain its sensitivity in the activity range -5.01 $\leq$ log a(Ca^{2+}) $\leq$ -1.722. Although it is indicated that the detection limit might have been influenced, more data is required to conclude if this observation is true.

After sterilisation through UV irradiation, the sensors were exposed to cell culture medium containing serum proteins. As shown in Figure 6.24, the electrode responded by a rapid decrease in potential. The potential was stabilised within 6 to 24 hours, and from then on all sensors demonstrated a linear drift towards more negative potentials. This intrinsic drift was calculated to 0.095 $\pm$ 0.02 mV h^{-}1 when sensors were maintained in DMEM with 10% FBS ($n = 6$).

Following UV irradiation and exposure to protein-containing cell culture medium, the sensors were recalibrated according to Section 6.3.3.1, demonstrating not only maintained functionality, but also preserved sensitivity: 29.9 $\pm$ 2.4 mV decade^{-1} with $R^2 = 0.988$, and for $n = 14$ (Figure 6.25).

Finally it was observed that osteoblast-like SAOS-2 cells grown with presence of Ca^{2+}-sensors in their cell culture medium during 72 hours, maintained a healthy aspect (Figure 6.26). It was quantitatively confirmed that cellular proliferation was not influenced by the presence of sensors in the cell culture medium (Figure 6.27).

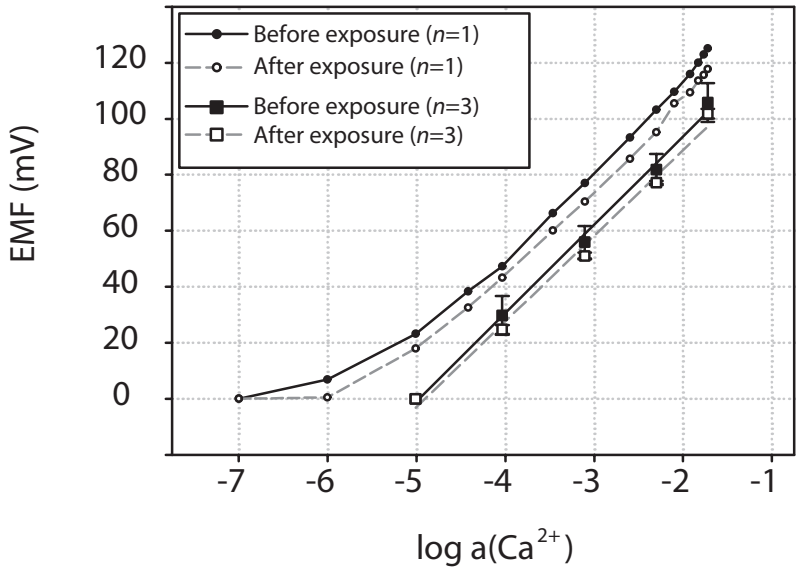

Figure 6.23: The influence of UV irradiation on Ca^{2+}-selective electrode performance. Calibration was done from 10^{-7}M $CaCl_2$ ($n = 1$), or from 10^{-5}M ($n = 3$).

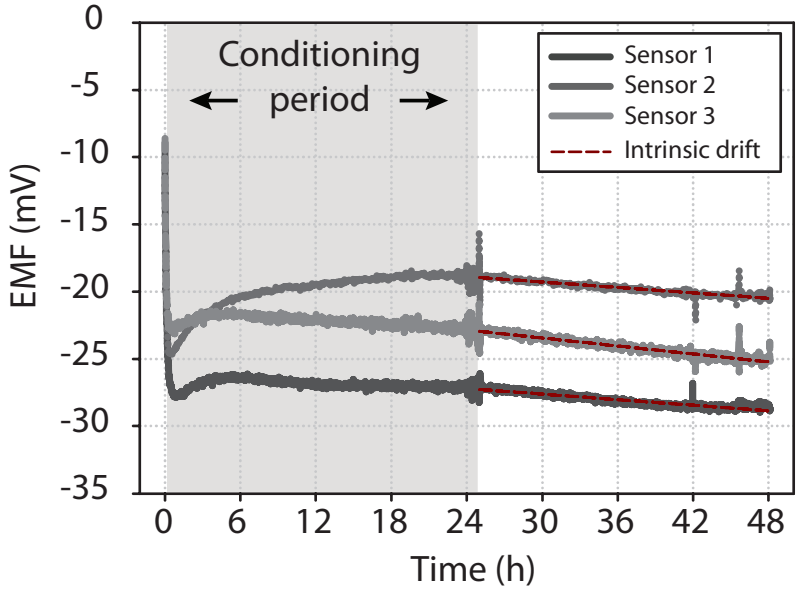

Figure 6.24: Typical potential response upon initial contact with cell culture medium but in absence of cells (here shown for three different sensors). The conditioning period indicates the time required to assure steady state potential.

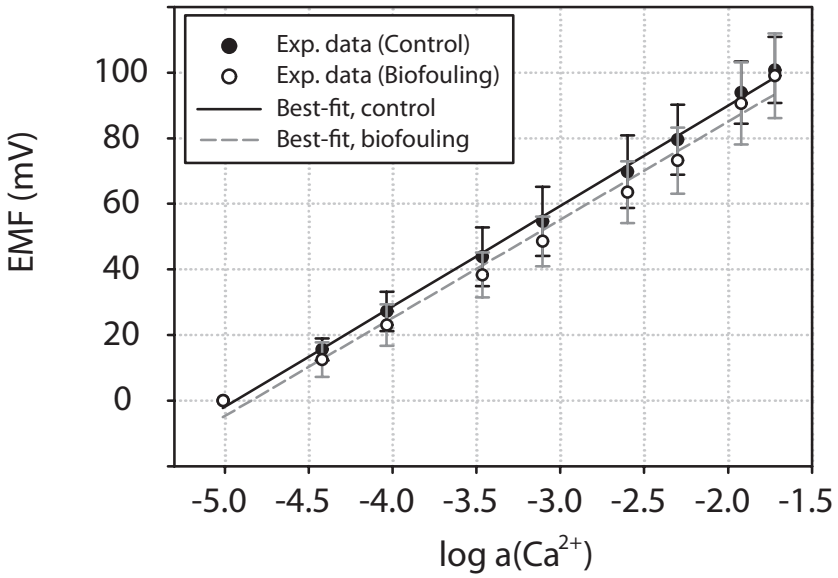

Figure 6.25: Calibration curve, before and after exposure to protein containing cell culture medium during 24-96 hours. Data is expressed as mean ± standard deviation, with $n = 14$.

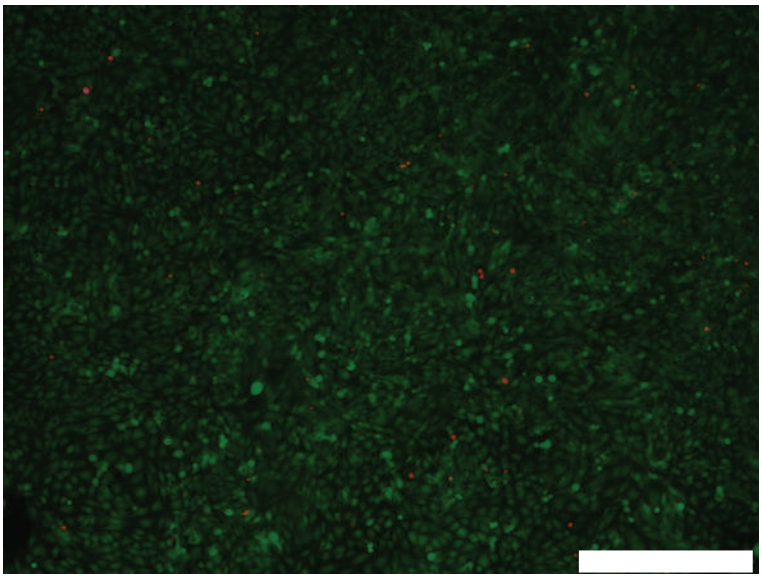

Figure 6.26: Calcein (green) / Propidium Iodine (Red) viability staining of SAOS-2 cells grown in presence of a Ca^{2+}-sensor in its cell culture medium. Scalebar = 500 μm.

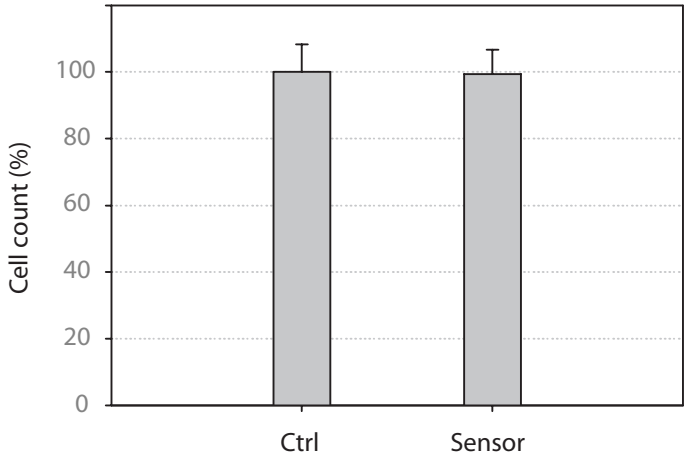

Figure 6.27: Cell proliferation during 72 hours both in presenece and absence (control) of Ca^{2+}-sensors ($n = 6$).

6.4.4 Sensor Applications

6.4.4.1 Cl^--activity during α-TCP-hydrolysis

The Ag/AgCl electrodes, originally aimed as internal reference electrodes of the Ca^{2+}-selective electrodes, were also taken advantage of as individual sensors to measure Cl^--activity in a bone TE related application. Incorported as disk electrodes at the interface between curing α-TCP and Ringer's solution, its potential against an external reference electrode was measured during 25 hours at room temperature. As shown in Figure 6.28, the EMF increased non-lineraly during a period of about six hours, before the potential was completely stabilised. The increase of potential, which corresponds to a decrease in $[Cl^-]$, was 11 mV. The Nernst equation allowed to convert experimental data to a ratio of chloride activity to initial chloride activity, $a(Cl^-)$ / $a_i(Cl^-)$, revealing that the chloride activity of the Ringer's solution decreased to about 65% of its initial value (i.e., $a_{\text{steady state}} = 0.65 \times 0.9\% = 0.585\%$).

The experimental data was further observed to closely follow an analog to the pseudo-second order model[2] (R^2=0.983), indicating an equilibrium reaction (6.21). The initial sorption rate was determined to $h = 55.9$ mol h^{-1}, and the apparent sorption coefficient, k, to 0.046 mol^{-1} h^{-1}.

$$A + * \longleftrightarrow A_{(a)} \tag{6.21}$$

[2]For details on the sorption model see Chapter 4.

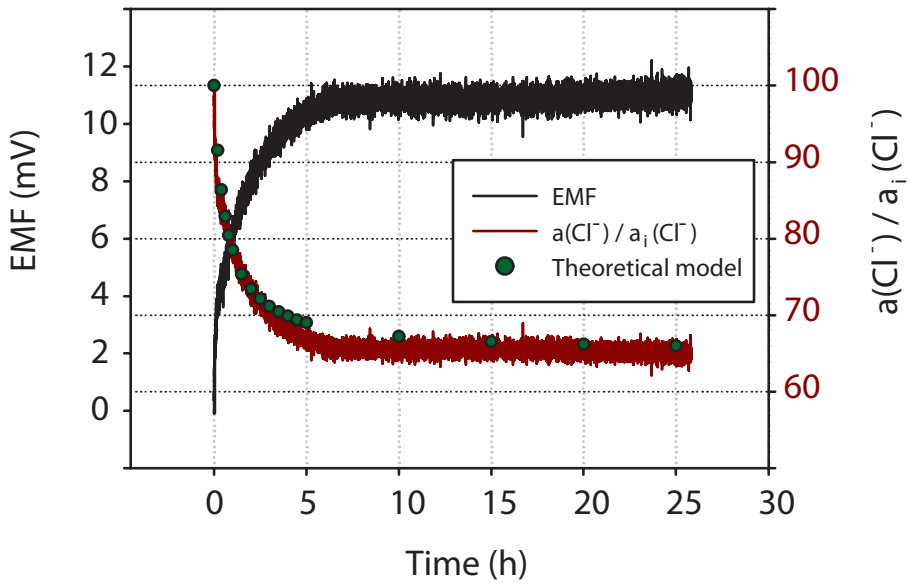

Figure 6.28: Cl^--activity in Ringer's solution (i.e. 0.9% NaCl) during hydrolysis of α-TCP at room temperature.

6.4.4.2 Ca^{2+}-activity of CDHA in cell culture medium

The first application related to bone tissue engineering using the Ca^{2+} sensors was the real-time monitoring of calcium in cell culture medium exposed to calcium-deficient hydroxyapatite. After conditioning the sensors in cell culture medium during 24 hours, they were exposed to CDHA. During a period of 24 hours, the potential decreased constantly, although the Ca^{2+}-uptake rate decreased towards the end of the contact period (Figure 6.29). The experimental EMF data, corrected for intrinsic drift, was converted via the Nernst equation to express the ratio of $Ca^{2+}-$activity to initial $Ca^{2+}-$activity, $a(Ca^{2+})$ / $a_i(Ca^{2+})$, which decreased to 43%, and was in accordance with the reference measurement of initial and final calcium concentration of the culture medium (1.40 mM and 0.60 mM, respectively).

The experimental data was further observed to perfectly obey the kinetics predicted by the concentration analog of the pseudo-second order model, with $R^2 = 0.990$. Calibration of the sensors after the measurement indicated that sensor maintained their sensitivity (Figure 6.25).

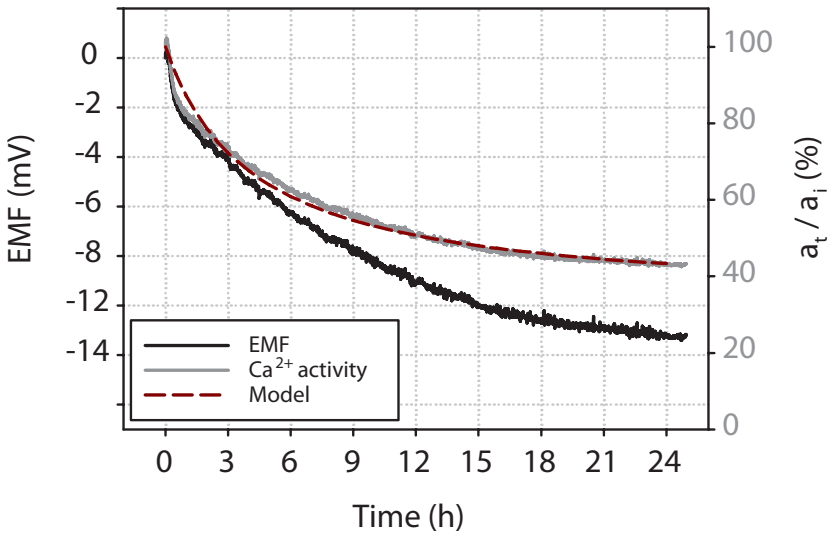

Figure 6.29: Real-time Ca^{2+}-activity of cell culture medium exposed to CDHA. Signal is an average of three different sensors in the same environment.

6.4.4.3 Ca^{2+}-activity during osteoblast mineralisation

The second application of the Ca^{2+} sensors related to bone tissue engineering was the real-time monitoring of calcium in osteoblast *in vitro* cultures. Following the previous results (Chapter 3 and 5), it was desired to evaluate the effect of lowering the β-GP concentration, and extend the culture period with another week, and so provide improved conditions for biologically relevant calcium deposition (see Section 3.5.4). For that reason, the sensor was tested in two different chemical conditions: (1) 10 mM β-GP in McCoy medium, and (2) 3 mM β-GP in DMEM medium which has a much lower initial concentration of phosphate than McCoy medium.

Similar to the observations when using McCoy medium (see Chapter 3) and commercial calcium electrodes, SAOS-2 cultures maintained in normal DMEM had relatively little effect on the concentration of extracellular calcium compared to when grown in osteogenic DMEM medium (Figure 6.30). Yet, between day 30 and 32 (i.e. $\approx$ 48 hours) the concentration of calcium in normal medium decreased 5.8 $\pm$ 2.0% in presence of cells, while in the normal medium itself (i.e. absence of cells) no change in calcium concentration was detected. In parallel, cells provided with osteogenic DMEM decreased the calcium concentration by 29.2 $\pm$ 0.6%, while that of osteogenic medium alone decreased only 1.3 $\pm$ 0.7%. The heavy decrease of calcium in osteogenic medium and presence of cells was related to an increased calcium deposition in the extracellular calcium (Figure 6.31).

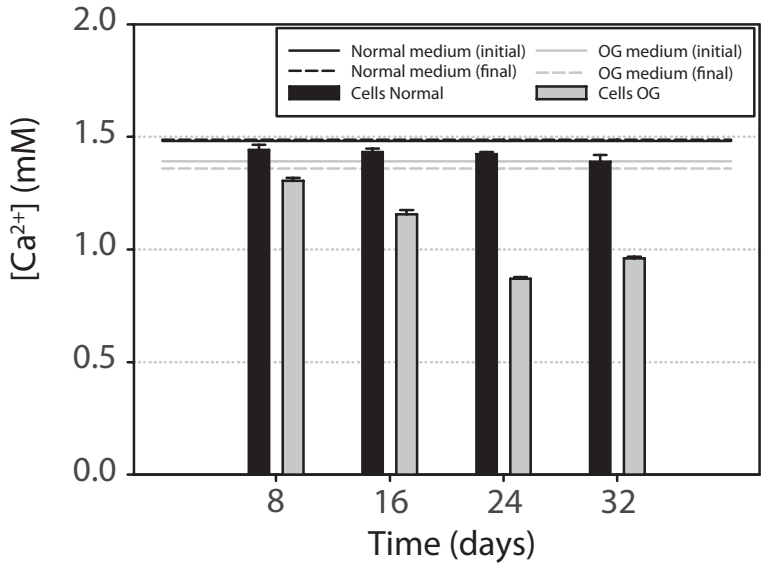

Figure 6.30: Concentration of calcium in DMEM medium in presence of SAOS-2 cells during $\approx$ 48 hours at different stages of the culture ($n = 6$). Osteogenic medium contains 3 mM β-GP.

The real-time evolution of the calcium concentration in osteogenic media exposed to SAOS-2 cells was measured during 24 hours, using either McCoy medium with 10 mM β-GP (Figure 6.32a), or DMEM medium with 3 mM β-GP (Figure 6.32b). In both cases the EMF was also measured in absence of cells, indicating a slight negative drift comparable to previous observations (recall Figure 6.24), i.e. about 2.5 mV per 24 hours.

In McCoy medium, the cellular influence on the calcium activity was compared at two different time points, after 13 and 19 days in culture. After 13 days cellular activity provoked the concentration of calcium to decrease linearly. The drop in EMF was -12 mV, corresponding to a relative activity change close to 2.5 at $T = 37°$ C, and which was confirmed by ILyte reference measurements ($a_i \approx 0.66$ mM, $a_f \approx 0.27$ mM). Six days later, the kinetics was non-linear, and the calcium drop had also increased in size (-20 mV). In DMEM medium, and with lower concentration of β-GP, highly mature cells provoked a non-linear uptake of calcium, that decreased the EMF about -8.6 mV during 24 hours. That change corresponds to a relative decrease in activity about 1.9 times. Control measurements gave $a_i \approx 1.34$ mM, $a_f \approx 0.73$ mM.

Cells exposed to the sensors and reference electrode stained positively with fluorescein diacetate, indicating that they maintained alive by the end of the experiment (Figure 6.33).

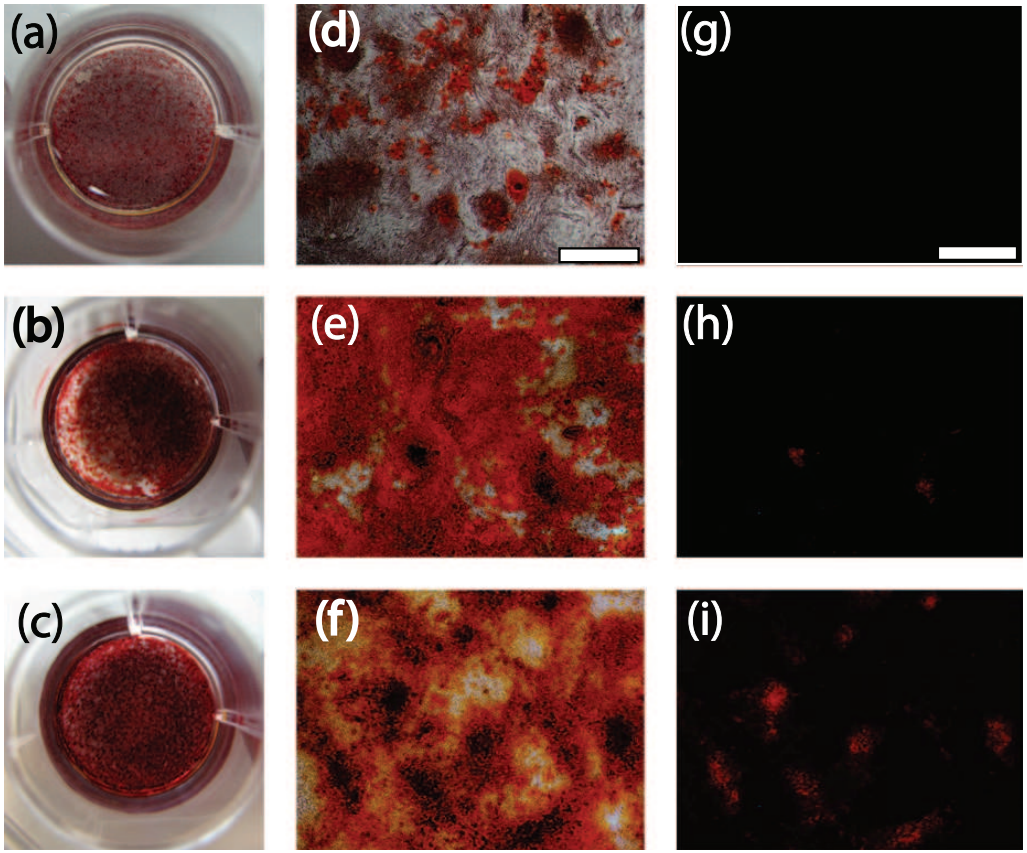

Figure 6.31: Representative images of calcium deposition in SAOS-2 cell layers after 16 (a,d,g), 24 (b,e,h), and 32 days (c,f,i), respectively. Middle and right column represent the same area, viewed either through phase contrast (d-f) or epifluorescence (g-i). Scalebar = 500 μm.

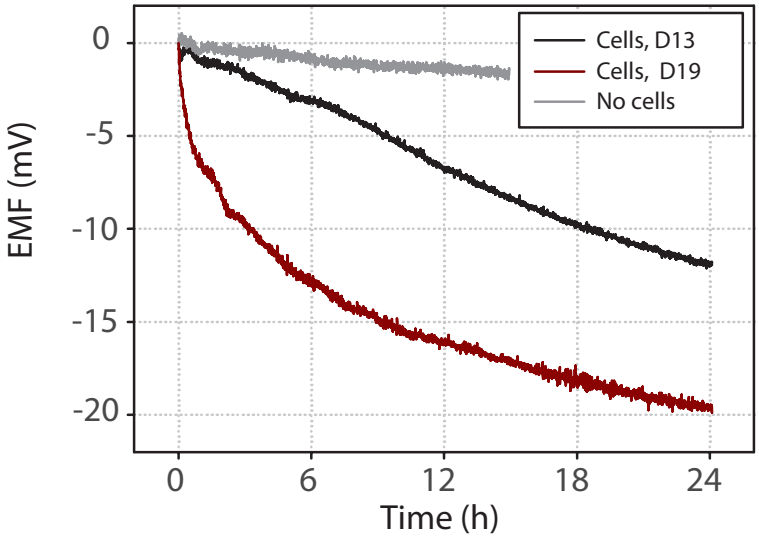

(a) Day 13 and 19, McCoy (10 mM β-GP).

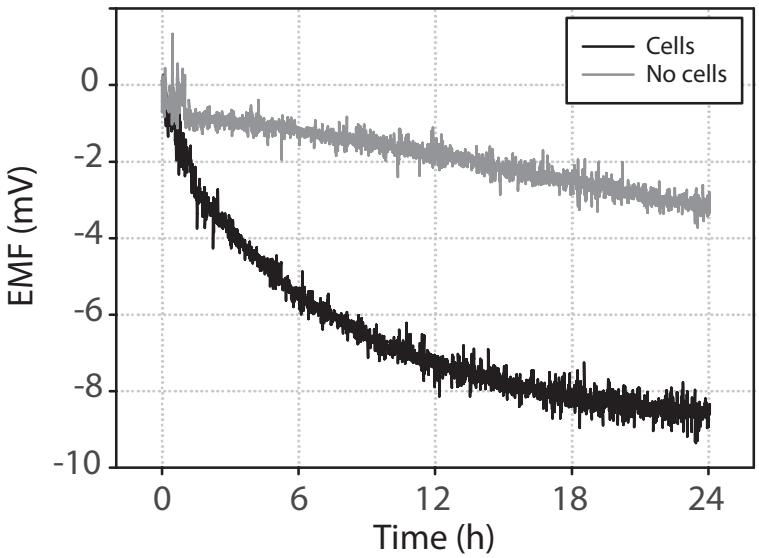

(b) Day 35, DMEM (3 mM β-GP).

Figure 6.32: Real-time monitoring of SAOS-2 cellular influence on Ca^{2+}-activity in osteogenic cell culture medium.

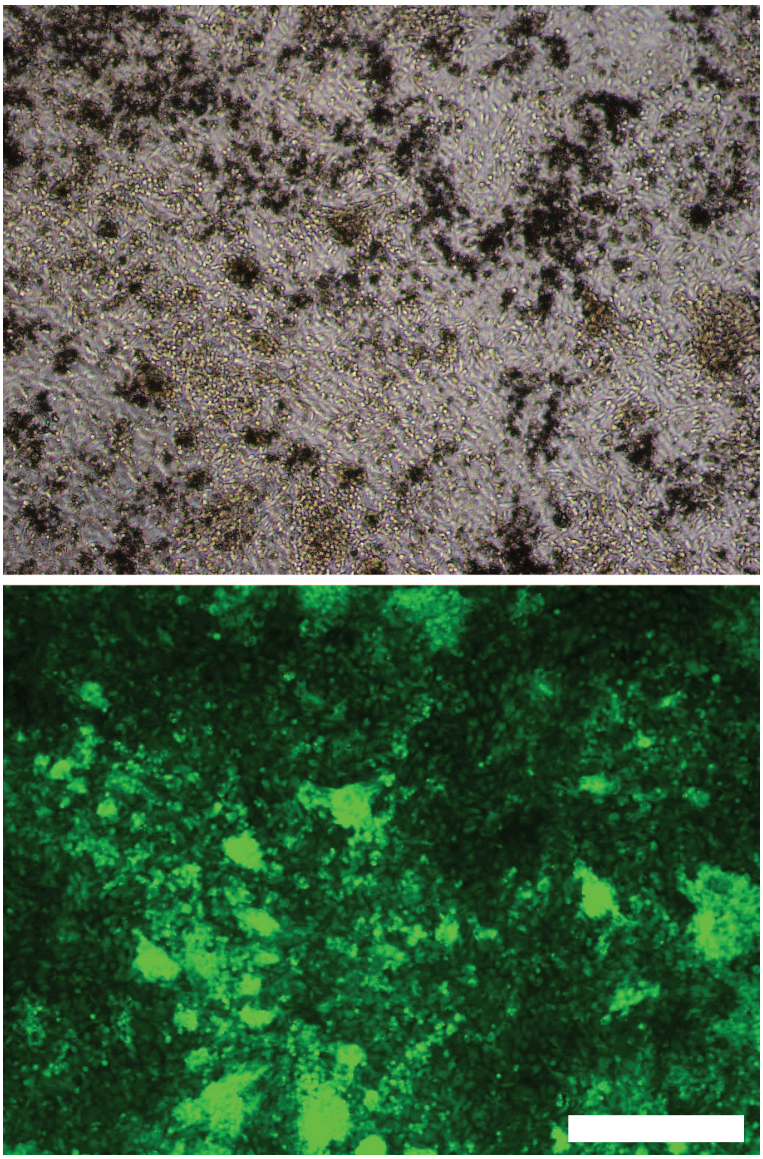

Figure 6.33: Representaqtive images of the aspect and viability of SAOS-2 cells that had been exposed to real-time Ca^{2+}-measurements were observed through phase contrast (top), as well as with epifluorescence (bottom) after staining with fluorescein diacetate (FDA). Both images represent the same field of view. Scalebar = 500 μm.

6.5 Discussion

In previous chapters it has been clearly demonstrated the utility of ion selective electrodes in certain bone tissue engineering applications. In accordance with the conclusions of the second chapter, sensors can be beneficial to the TE process in two ways. They can provide real-time data, for example on vital processes related to growth and state of the developing tissue, as well as information from environments normally inaccessible to standard evaluation technologies. Therefore, the ambition of this chapter has been to develop a general platform for measurements of ions in the TE environment. The platform has in this chapter been evaluated for calcium selective electrodes, and applied in three separate processes related to bone tissue engineering.

6.5.1 On the Design of the Sensor Platform

The sensor platform included instrumentation for real-time potentiometric measurements, as well as chemical sensors selective to chloride and calcium, respectively. Regarding the former platform component, it has been demonstrated in this chapter that it provides acceptable means for real-time monitoring of potential differences between indicator and reference electrode, at time scales relevant to most TE applications. If required, the accuracy of the signal could be further improved by band-pass filters following the output signal of the operational amplifier, by decreasing the maximum voltage range of the DAQ device, and / or by implementation of software filters. Further shielding of the electronic device and cables may be beneficial to reduce externally induced noise. Additional channels are easily incorporated according to the same principle as existing channels. On a more sophisticated level, wireless communication of the sensor signals can be considered as an attractive feature for further miniaturisation of the platform (Johannessen *et al.*, 2004).

Regarding the chemical sensors, the strategy was to develop a generic sensor design which allowed for minimally invasive measurements in different physical environments, e.g. cell culture microplates or different bioreactors, and which in the future could be modified for detection of other ions than the one described in this chapter. In the end, the adopted design fell on the conventional ISE with an internal reference electrode and electrolyte, and which had been previously described by Radomska *et al.* (2008). Besides being the most well-established design, the great benefit was that it allowed for fabrication of a high number of sensors in short time and at low cost, which was considered necessary in order to be able to characterise well their behaviour in complex TE environments, and also for developing new formulations of

the polymeric membranes for future applications. The polymeric membrane was easily attached on the pipette tip and kept the aqueous internal electrolyte separated from the test solution. The membrane could be exchanged for any similar ion selective membrane, thus making the electrode design highly versatile. If desired, the internal electrolyte can be partly solidified by adding agar powder, typically 2-4 weight % (Hassel *et al.*, 1999). Obviously, the use of an internal reference electrolyte puts limits on the final size of the electrode, but it also eliminates the problem of electrode packaging and wire insulation which are two additional requirements for solid-state electrodes. Also, since the main part of the electrode was made from material routinely applied in cell culture handlings, the electrode body was anticipated to not introduce any toxic effects. This was confirmed by the presented results.

In the configuration presented in this chapter, the ion selective electrodes had a chemically active area of < 1 mm^2 (this can be decreased using a smaller electrode body), and which made it perfectly possible to apply it to volumes < 100 μl. This is an acceptable working volume with respect to cell culture applications and bioreactor designs, but still such measurements have to be considered as global measurements of the TE environment, and further minaturisation of the sensor would be required for use in local microenvironments. The first initiatives of such miniaturisation have been taken through the fabrication of prototypic solid-state electrodes, as was the case with the Ag/AgCl disk electrode which could be integrated in the α-TCP material interface. However, to be able to use such electrode design as an ion selective electrode, it is likely that the electrode surface will require chemical modification for an acceptable attachment of the ion selective membrane. Such treatments and tests have been out of scope in this thesis due to time limitations.

In the current design of ion-selective electrodes, inexpensive internal Ag / AgCl reference electrodes were reproducibly prepared from electrolysis of Ag wires in HCl. Other methods to form AgCl on Ag include chemical oxidation, thermal or plasma treatment in chlorine containing atmospheres, or immersion in sodium dichromate dihydrate solution (see references within Polk *et al.* (2006)). The reference electrode could be made from other silver salts, e.g. Ag_3PO_4, and then produced e.g from electrolysis using K_3PO_4 (Ciobanu *et al.*, 2002, 2004). The Ag/Ag_3PO_4 reference electrode is a perfect option when the ion selective polymeric membrane is aimed at phosphate and when the internal electrolyte contains hydrogen phosphate (Kivlehan *et al.*, 2007).

6.5.2 Calcium selective electrodes

Methods for development of liquid membrane ion selective electrodes are well established (Ammann, 1986), and all necessary components are commerically available. Therefore, in this chapter it was used a well-established protocol to produce calcium selective polymeric membranes. The ionophore, a synthetic molecule specifically designed to bind calcium reversibly had been reported to possess sufficient sensitivity and lipophilicity for determination of Ca^{2+} in blood and human serum (Suzuki *et al.*, 1995). Specifically, it was demonstrated that the ionophore, when housed in a polymeric membrane prepared according to Table 6.4, provided a Nernstian ISE response in the range 10^{-5} M to 10^{-1} M Ca^{2+}, both in absence and presence of interfering ions typically present in the extracellular environment (Suzuki *et al.*, 1995). That particular data, in combination with the results on to what extent osteoblasts and CDHA may influence the extracellular calcium in cell culture medium (Chapter 3 and 4 of this thesis), motivated the use of that specific ISE membrane configuration.

The standard characterisation of the calcium selective electrode carried out in this chapter not only confirmed that the selected ionophore was appropriate for detection of calcium (i.e. Nernstian behaviour, low interference with major extracellular cations), but also that the complete sensing platform (including internal reference electrode, electrolyte, and electrode body) was properly prepared, and that it responded relatively quickly to changes in calcium concentration. Although not reported by Suzuki *et al.* (1995), it was further observed that the electrodes maintained their calcium selective property during a period well above four weeks, and that they were completely insensitive to changes in pH. All this data indicated that the calcium selective membrane was a promising candidate for real-time monitoring of calcium in conditions related to *in vitro* TE applications. However, to be really sure about its appropriateness for such applications, it was required a characterisation of the electrode behaviour upon UV irradiation as well as when in contact with proteins present in the test sample. It was also required to determine the intrinsic drift during longer measurements, and to test if the sensor provoked any cytotoxic effects when combined with cellular cultures. As demonstrated in Section 6.4.3.2, neither of above potentially damaging conditions provoked any major deteriorating effects on the sensor functioning. Neither was the intrinsic drift observed to be excessively large, nor did the sensor provoke any cellular damage. Taken altogether, characterisation of the calcium selective electrode indicated that the electrode was possible to use for measurements of calcium in complex ionic solutions containing proteins and cells also during longer time periods.

6.5.3 Sensors Applications

Applications of the developed sensors have been aimed at *in vitro* bone tissue engineering since results obtained in previous chapters have indicated that both materials and cells typically used in bone tissue engineering may interact with its ionic environment. Specifically, the developed sensors were applied to measure (1) Cl^--activity during setting of α-TCP, (2) calcium activity in cell culture medium exposed to CDHA, and (3) osteoblast-induced calcium deposition in the extracellular matrix.

6.5.3.1 Cl^--activity during setting of α-TCP

Hydrolysis of α-TCP leads to the formation of calcium-deficient hydroxyapatite (Ginebra *et al.*, 1997). The transformation process of apatitic calcium phosphate cement typically involves active dissolution and precipitation of calcium and phosphate, and usually extends over a period of several days (Ginebra *et al.*, 1999). Also, the pH of the aqueous phase is typically influenced during this period (see further Chapter 7). As most calcium phosphate cements are being developed with the purpose of being injectable, its chemical transformation is obviously supposed to take place *in vivo*. To somehow mimic biological conditions, setting of α-TCP *in vitro* has traditionally been done using Ringer's solutions (Engel *et al.*, 2008).

So far, the work presented in this thesis has only concerned ionic interactions provoked by the end product obtained after seven days of hydrolysis of α-TCP maintained in Ringer's solution. In addition, that interaction has only been characterised with respect to typically biologically relevant extracellular cations and phosphate. Therefore, the measurement of Cl^--activity during hydrolysis of α-TCP is important in several aspects. First, it serves as a reminder that the ionic activity of the studied material may involve other ions than the one mainly focused on in Chapters 4 and 5. Second, it highlights that the material possesses certain biochemical activity during its transformation phase into CDHA. Third, due to the all-solid-state nature of the Ag/AgCl disk electrode, a technological mean to measure the ionic activity in the direct interface between the biomaterial and its aqueous environment is provided. That is, the measurement was performed in the same region where cells would develop their affinity to the material if implanted *in vivo*.

Specifically, it was shown that the forming material provokes a non-linear, relatively rapid, and highly significant, uptake of chloride from the solution. The induced change of the ionic strength of the material is of biological relevance in bone tissue engineering, as chloride ions on one hand can regulate

protein function (Stasio, 2004), and on the other hand can subsitute for hydroxyl ions in hydroxyapatite mineral (Dykes & Elliott, 1971).

The successful modeling of the chloride uptake does not only contribute to elucidate the nature of ionic interaction provoked by the material, but it also opens up a possibility to apply the Ag/AgCl electrode as a potentiometric pseudo-reference electrode (Matsumoto *et al.*, 2002) in applications related to α-TCP and CDHA. Then, and if combined with other solid-state ion electrodes incorporated in the material, such configuration would make it possible to obtain a large variety of ion measurements in the critical interface between material and extracellular environment.

6.5.3.2 Ca^{2+}-sensor

Initial evaluation of the developed miniaturised calcium-sensors exposed to standard *in vitro* conditions was done by provoking depletion of calcium in protein-containing cell culture medium by presence of CDHA. The nature of the calcium-uptake provoked by this material is well-known (see Chapter 4), and by measuring the relation between intial and final concentrations of calcium using commercial calcium electrodes, it was confirmed that the generated EMF signal represented well the calcium activity in the sample with respect to both kinetics and magnitude. The miniaturised Ca^{2+}-sensor therefore can be considered an enabling tool for characterisation of biomaterial activity related to calcium uptake or release in standard *in vitro* conditions. For such applications, the major benefit of the proposed sensor design is its relatively small size, which easily allows for measurements in volumes down to 0.1 mL. To work with minimal volumes is preferable because it reduces costs, but even more important is that it may improve the representation of the environment that is created upon implantation.

CDHA is just one of many biomaterials that interacts with calcium, and has served as an example. The interest to monitor calcium however goes beyond the pure material induced interactions since calcium is known to be a vital molecule in many cellular function (see Section 2.1.2.1). Therefore, to further test the developed calcium-sensor in a cellular application, osteoblasts were stimulated to develop a mineralised matrix, and the sensors were then used to monitor calcium deposition in the extracellular matrix during a period of 24 hours. Since such cell-induced calcium deposition strictly requires the combination of a properly developed collagenous matrix, biological regulation of possible inhibitors of mineralisation, as well as presence of phosphate (typically through alkaline phosphatase activity), a decreasing EMF signal due to calcium deposition could be considered as an indirect indication of the maturation stage of the osteoblasts (Allori *et al.*, 2008a,b). Moreover,

as the kinetics of calcium deposition was observed to be different in young and more mature cell layers (Figure 6.32a), the continuous EMF signal to some extent may mirror the maturation of the cell layer. The dynamic data provided by the calcium sensors corresponds well with the kinetics of calcium deposition provoked by maturing SAOS-2 cells when obtained using commercial calcium electrodes at discrete time points, and which was earlier presented in Chapter 5 (Figure 5.5).

As cells were little affected by the presence of the miniaturised calcium sensors, these sensors may therefore serve perfectly well as enabling tools of performing character in mineralising osteoblast cultures, and possibly also in other cell cultures where fluctuations in extracellular calcium can be related to cellular activity.

6.6 Conclusions

In this chapter it has been described the development of a generic setup for online potentiometric ion measurements. The indicator electrode, which was based on an internal Ag/AgCl reference electrode and a polymeric ion selective membrane, was designed to physically allow for ion measurements in relatively small volumes (easily down to 0.1 mL). The applicability of the setup in standard *in vitro* tissue engineering conditions, i.e. in protein-containing solutions of physiological ionic strength, was evaluated using a calcium selective polymeric membrane attached to the indicator electrode. The obtained calcium electrode exhibited a Nernstian response to calcium, and was little influenced by other major extracellular ions. Moreover, the electrode resisted sterilisation through UV irradiation, did not induce any cytotoxic effects in contact with osteoblasts, and the signal was subject only to minor drift during longer measurements.

The developed Ag/AgCl and Ca^{2+}-sensors were successfully applied to measure ionic activity of different bone tissue engineering components. The Ag/AgCl electrodes, originally aimed as internal reference electrodes, were used to measure Cl^{-}-activity in the immediate interface between chemically transforming α-TCP and Ringer's solution, revealing a material-induced non-linear uptake of chloride. Ca^{2+}-electrodes were used to successfully monitor sorption of calcium onto calcium-deficient hydroxyapatite immersed in cell culture medium, as well as osteoblast-induced calcium deposition in the extracellular matrix during a time frame of 24 hours.

Bibliography

Allori, A. C., Sailon, A. M., & Warren, S. M. (2008a). *Tissue Engineering Part B,* **14** (3), 259–273.

Allori, A. C., Sailon, A. M., & Warren, S. M. (2008b). *Tissue Engineering Part B,* **14** (3), 275–283.

Ammann, D. (1986). *Ion-Selective Microelectrodes Principles Design and Application.* London: Springer Verlag, first edition.

Antonisse, M. M. & Reinhoudt, D. N. (1999). *Electroanalysis,* **11** (14), 1035–1048.

Arnold, M. A. & Solsky, R. L. (1986). *Analytical Chemistry,* **58**, 84R–101R.

Bakker, E. (1997). *Electroanalysis,* **9** (1), 7–12.

Bakker, E., Bhlmann, P., & Pretsch, E. (1999). *Electroanalysis,* **11** (13), 915–933.

Bobacka, J. (1999). *Analytical Chemistry,* **71**, 4932–4937.

Bobacka, J., Ivaska, A., & Lewenstam, A. (2008). *Chemical Reviews,* **108**, 329–351.

Ciobanu, M., Wilburn, J. P., Buss, N. I., Ditavong, P., & Lowy, D. A. (2002). *Electroanalysis,* **14** (14), 989–997.

Ciobanu, M., Wilburn, J. P., & Lowy, D. A. (2004). *Electroanalysis,* **16** (16), 1351–1358.

Dykes, E. & Elliott, J. (1971). *Calcified Tissue International,* **7**, 241–248.

Engel, E., del Valle, S., Aparicio, C., Altankov, G., Asin, L., Planell, J. A., & Ginebra, M. P. (2008). *Tissue Engineering,* **14**, 1341–1351.

Evans, A. (1987). *Potentiometry and Ion Selective Electrodes.* London: ACOL, Thames Polytechnic.

Ginebra, M., Fernandez, E., Maeyerl, E. D., Verbeeckl, R., Boltong, M., Ginebra, J., Driessens, F., & Planell, J. (1997). *Journal of Dental Research,* **76** (4), 905–912.

Ginebra, M.-P., Fernandez, E., Driessens, F. C. M., & Planell, J. A. (1999). *Journal of the American Ceramic Society,* **82** (10), 2808–2812.

Hassel, A. W., Fushimi, K., & Seo, M. (1999). *Electrochemistry Communications,* **1**, 180–183.

Horvai, G. (1997). *Sensors and Actuators B,* **43**, 94–98.

Ives, D. J. G. & Janz, G. J. (1961). *Reference electrodes : theory and practice.* New York: Academic Press.

Johannessen, E. A., Wang, L., Cui, L., Tang, T. B., Ahmadian, M., Astaras, A., Reid, S. W. J., Yam, P. S., Murray, A. F., Flynn, B. W., Beaumont, S. P., Cumming, D. R. S., & Cooper, J. M. (2004). *IEEE Transactions on Biomedical Engineering,* **51** (3), 525.

Johnson, R. D. & Bachas, L. G. (2003). *Analytical and bioanalytical chemistry,* **376**, 328–341.

Kikas, T. & Ivaska, A. (2007). *Talanta,* **71**, 160–164.

Kivlehan, F., Mace, W. J., Moynihan, H. A., & Arrigan, D. W. (2007). *Analytica Chimica Acta,* **585**, 154–160.

Li, H., Luo, X., Liu, C., Jiang, L., Cui, D., Cai, X., & Yang, Q. (2004). *Proceedings of 2004 International Conference on Information Acquisition,* , 224–227.

Maminska, R. & Wroblewski, W. (2006). *Electroanalysis,* **18** (13-14), 1347–1353.

Matsumoto, T., Ohashi, A., & Ito, N. (2002). *Analytica Chimica Acta,* **462**, 253–259.

Polk, B. J., Stelzenmuller, A., Mijares, G., MacCrehan, W., & Gaitan, M. (2006). *Sensors and Actuators B,* **114**, 239–247.

Radomska, A., Singhal, S., Ye, H., Lim, M., Mantalaris, A., Yue, X., Drakakis, E. M., Toumazou, C., & Cass, A. E. (2008). *Biosensors and Bioelectronics,* **24**, 435–441.

Stasio, E. D. (2004). *Biophysical Chemistry,* **112**, 245–252.

Stevic, Z., Andjelkovic, Z., & Antic, D. (2008). *Sensors,* **8**, 1819–1831.

Sutter, J., Peper, A. R. A. S., Bakker, E., & Pretsch, E. (2004). *Analytica Chimica Acta,* **523**, 53–59.

Suzuki, H. (2000). *Electroanalysis,* **12** (9), 703–715.

Suzuki, K., Watanabe, K., Matsumoto, Y., Kobayashi, M., Sato, S., Siswanta, D., & Hisamoto, H. (1995). *Analytical Chemistry,* **67** (2), 324–334.

Toczylowska, R., Pokrop, R., Dybko, A., & Wroblewski, W. (2005). *Analytica Chimica Acta,* **540**, 167–172.

Umezawa, Y., Buhlmann, P., Umezawa, K., Tohda, K., & Amemiya, S. (2000). *Pure and Applied Chemistry,* **72** (10), 1851–2082.

Yajima, S., Shiraya, M., & Kimura, K. (2006). *Chem. Anal. (Warsaw),* **51**, 939.

Zine, N., Bausells, J., Vocanson, F., Lamartine, R., Asfar, Z., Teixidor, F., Crespo, E., de Oliveira, I. M., & ad A. Errachid, J. S. (2006). *Electrochimica Acta,* **51**, 5075–5079.

This page is intentionally left blank

Chapter 7

pH Microelectrodes Applied in Bone Tissue Engineering

7.1 Introduction

The pH of the tissue engineering environment is important for proper tissue development, and is usually influenced by at least one of the TE components. For example, in previous chapters of this thesis it has been clearly demonstrated that both osteoblasts and calcium-deficient hydroxyapatite (CDHA) induce acidification of their environments. It has also been shown that solid-state microelectrodes can be easily incorporated into the CDHA material, and in such way can permit for potentiometric measurements at the immediate interface between material and surrounding liquid. In this chapter, it is described the initial efforts to develop pH microelectrodes that can be applied in traditionally inaccessible environments created in and around calcium phosphate cements.

7.1.1 pH Detection

The pH of a solution reflects the amount of hydrogen ions contained within it, and is defined as in equation 7.1,

$$pH = -\log a_{H^+} \tag{7.1}$$

where a_{H^+} is the activity of hydrogen ions (mol dm^{-3}). In practice, free hydrogen ions do not exist in aqueous solution, and a_{H^+} is rather the activity of hydronium ions (H_3O^+) and its higher associates (Kurzweil, 2009).

There exist a number of different pH sensors: e.g. glass-membrane electrodes, liquid ion-exchanger electrodes, and solid-state electrodes. The conventional glass electrode has several drawbacks such as being fragile, expensive, complicated to build, and is moreover sensitive to monovalent cation interference (Fog & Buck, 1984). The liquid ion-exchanger electrode is quite analog to the calcium selective electrode presented in Chapter 6, and therefore in principle simple to construct. Yet, these pH electrodes generally have a very short life-span (Bezbaruah & Zhang, 2002). In contrast, solid-state electrodes such as ion selective field effect transistors (ISFETs) or metal-metal oxide (MMO) electrodes may overcome above problems. Mainly, these electrodes are mechanically more rugged and are easily miniaturised for measurements in small sample-volumes.

7.1.2 Metal-Metal Oxide Electrodes

The pH sensing capability of metal-metal oxide electrodes has been well documented, and includes a wide number of metal oxides: TiO_2, RuO_2, RhO_2, SnO_2, Ta_2O_5, PtO_2, and IrO_2. As opposed to the glass and liquid membrane pH electrodes where the signal originates from a membrane potential, the electrode potential of MMO electrodes arises from a redox reaction taking place on the surface of the electrode in contact with the solution (Glab *et al.*, 1989):

$$\mathrm{M_xO_y + 2yH^+ + 2ye^- = xM + yH_2O} \tag{7.2}$$

The potential of such MMO electrode, with respect to a reference, is given by

$$E = E^0 - 2.303\frac{RT}{F}pH \tag{7.3}$$

where R, T, and F have their usual meaning. E^0 incorporates the standard electrode potentials and the solubility product of the metal oxide and the ionization product of water.

Electrodes made of hydrated metal oxides, MO(OH), take part in redox reactions where upon oxidation of the oxide having the lower valence, a proton is ejected into the electrolyte:

$$\mathrm{MO(OH)_{\,(m)} \leftrightarrow MO_{2\,(m)} + H^+_{(es)} + e^-_{(m)}} \tag{7.4}$$

where (m) represents the metal oxide phase and (es) represents the electrolyte solution phase. The two oxide phases are perfectly miscible and thus form a single phase, (m). According to Hendrikse *et al.* (1998), the electrode potential of such system is equal to

$$E = E^0 - \frac{kT}{q} \ln \left(\frac{\gamma_{MO(OH)}[MO(OH)]}{\gamma_{MO_2}[MO_2]} \right) + \frac{kT}{q} \ln a_{\mathrm{H^+}} \tag{7.5}$$

The last term on the right-hand side of equation 7.5 suggests that the use of these electrodes as pH sensors is possible.

7.1.2.1 Iridium oxide pH electrodes

Among the different pH metal oxide electrodes, the group of IrO_x electrodes are especially interesting candidates because they respond quickly over a wide pH range, are stable over long periods (Wang *et al.*, 2002), and possess low sensitivity to the redox interference. Moreover, they are not sensitive to stirring, and can even be applied in non-aqueous solutions (Smiechowski & Lvovich, 2003). Consequently, IrO_2 electrodes have been successfully used in many different environments, covering both *in vitro* and *in vivo* extracellular measurements (Marzouk *et al.*, 1998; Ges *et al.*, 2005; Bitziou *et al.*, 2008).

Preparation of iridium oxide films can be done through various techniques (Glab *et al.*, 1989), as well as on various kind of substrates (e.g. pure iridium, gold, glassy carbon, boron doped diamond, titanium, stainless steel, etc.). In general, one can distinguish between thermally and electrochemically derived iridium oxide films (O'Hare *et al.*, 2006). The latter method produces anodic iridium oxidation films (AIROF) and can be done through potential cycling (typically in H_2SO_4 between the oxygen and hydrogen evolution regimes) or electrodeposition. Electrodeposition of AIROF is preferably done under alkaline conditions since iridium oxide is not soluble in alkaline solutions (Yamanaka, 1989). Interestingly, the AIROF electrodes tend to exhibit super-Nernstian pH response, varying from 59 to ∼80 mV per decade depending on the preparation method. As discussed by Glab *et al.* (1989), the potential determining equilibrium reaction for AIROF is given by (7.6)

$$2\mathrm{IrO_2(OH)_{(2-x)}(H_2O)_{(2+x)}^{(2-x)-}} + (3-2\mathrm{x})\mathrm{H^+} + 2\mathrm{e^-} \leftrightarrow \mathrm{Ir_2O_3(OH)_3(H_2O)_3^{3-}} + 3\mathrm{H_2O} \tag{7.6}$$

and which makes the AIROF electrodes respond to pH with a slope of 59(3-2x)/2 mV/pH at $T = 25°\mathrm{C}$, where x depends on the precise composition of the AIROF.

7.1.2.2 Microelectrodes

Microelectrodes are defined as electrodes whose critical geometric dimensions are in the micrometre range (Stulik *et al.*, 2000). Reducing the electrode size obviously is required to measure in spatially restricted environments, but it also makes diffusional mass transport extremely efficient. The latter effect has several important consequences such as a decreased ohmic drop of potential, fast establishment of a steady-state signal, a current increase due to enhanced mass transport at the electrode boundary, and increased signal-to-noise ratio (Forster, 1994).

Iridium oxide pH electrodes can be perfectly miniaturised, and the many different preparation methods allow for different approaches to obtain micro- and even nano-electrodes (Wipf *et al.*, 2000; Ndobo-Epoy *et al.*, 2007; Li *et al.*, 2007). The ease of fabrication make these electrodes a powerful tool for microscale measurements in variuos scientific fields.

7.2 Objectives

The overall objective of the work presented in this chapter was to develop potentiometric pH microelectrodes for application in processes related to bone tissue engineering, where traditional pH sensors cannot be applied. For that purpose, this chapter includes

1. the description of the fabrication steps required to obtain pH microelectrodes based on electrodeposited anodic iridium oxide films,

2. the characterisation of the obtained iridium oxide microelectrodes as pH sensors,

3. application of the iridium oxide microelectrodes to measure pH both inside and outside α-tri calcium phosphate cement during its setting reaction,

4. application of the iridium oxide microelectrodes to measure pH at the material/liquid interface of set α-TCP in contact with protein-containing cell culture medium in standard *in vitro* conditions.

7.3 Materials and Methods

7.3.1 Solid-state Microelectrode Body

The microelectrode body used to construct miniaturised solid-state pH sensors were produced in a similar way as the Ag/AgCl disk electrodes (see Section 6.3.2), but with the silver wire replaced by insulated gold wires of 99.99% purity and a diameter of 75 μm (Advent RM, AU518710). The design of the electrode body, which is drawn schematically in Figure 7.1, was to a large extent adopted from the work by Bitziou *et al.* (2008).

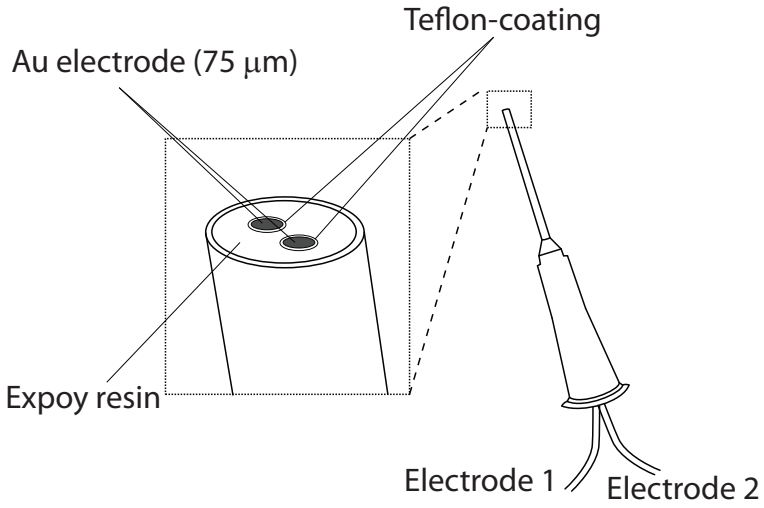

Figure 7.1: Schematic view of the microelectrode body (not drawn to scale). In this case, the electrode tip holds two separate Au electrodes.

To briefly describe the microelectrode fabrication, insulated gold wires (total diameter 0.112 mm) were cut in lengths of about 6-7 cm, and their Teflon-insulation was carefully removed at both ends. Each Au-wire was then soldered onto a cable, and the soldering point was covered with a polymer shrink tube. The wires were then inserted into a surgical needle (BD Microlance^{TM}, 0.9 mm diameter, 25 mm long) which was later backfilled with epoxy resin (Robnor Quality Systems, PX771C). After curing the resin (48 hours), the sharp end of the sensor needle was cut flat using a rotating diamond saw blade, and then polished in four subsequent steps: (1) with silicon carbide grinding paper (Buehler, Grit P400/800), and (2-4) with a slurry of aluminum microparticles (Buehler; 1.0, 0.3, and 0.05 μm, respectively). Between each polishing step, the electrode body was cleaned with distilled water in a sonicating bath. As a final cleaning step, the sensor tip was immersed in 0.5M H_2SO_4 and potential cycling was applied between the oxygen

and hydrogen evolution regimes (0-1.4 V, scan rate 50 mV second^{-1}) using a platina counter electrode (BASi, MW-1032) and a Ag/AgCl double junction electrode as a reference electrode (Orion 900200). The Au electrode served as the working electrode in this conventional three-electrode electrochemical cell. The Au electrodes were considered clean when the voltammograms were reproducible.

The quality of the active surface of the microelectrodes was assessed by potential cycling in an identical setup as above, but now between 0.5 and -0.2 V, and with 10 mM potassium ferricyanide(III) (Sigma, 244023) in supporting electrolyte (0.5 M KCl). The scan rate was 5 mV second^{-1}.

7.3.2 Iridium Oxide Deposition

Iridium oxide films were formed on the Au microelectrodes through anodic electrodeposition using an alkaline iridium tetrachloride solution. The solution was prepared following the steps given by Yamanaka (1989) and Bitziou *et al.* (2008):

1. 0.15 g of iridium(IV) chloride hydrate ($IrCl_4 \cdot H_2O$, Sigma 516996) was dissolved in 100 ml of milliQ water under magnetic stirring during 30 minutes.

2. 1 ml of aqueous hydrogen peroxide (H_2O_2 33% w/v, Panreac 211077 1214) was added to above solution to facilitate the use of low current density upon electrodeposition. The obtained solution was stirred for another 30 minutes.

3. 0.5 g of oxalic acid ($(COOH)_2 \cdot 2H_2O$, Sigma 247537) was then added to the solution to avoid spontaneous precipitation of IrO_2. Once again, the solution was left under stirring during 30 minutes.

4. Finally, about 5 g of anhydrous potassium carbonate (Sigma, 590681) was required to gradually adjust the pH of the solution to 10.5.

The resulting solution, having a pale green-yellowish colour, was left standing for two days at room temperature until a colour change towards blue was achieved. From that on, the solution was stored cold (4° C), and could be used during several months to successfully produce AIROFs through anodic electrodeposition. For that process, the cleaned Au-electrodes were inserted into an electrochemical cell containing the degassed iridium oxalate solution, together with a double junction Ag/AgCl reference electrode (Thermo, Orion 900200), and a Pt counter electrode (BASi MW-1032). A potentiostat (CH

Instruments CHI1232) was used to apply a constant potential (0.65 V) during three minutes while reading the current running in the circuit during deposition. After deposition, the coated microelectrodes were washed and left in water for at least two days prior to use as pH sensors.

7.3.3 pH Electrode Characterisation

Calibration of the pH electrodes was performed in 0.1 M TRIS (Sigma, 15456-3)[1], to which different volumes of 0.1M or 1M hydrochloric acid (HCl) or sodium hydroxide (NaOH) were added. The voltage between the pH electrode and a reference electrode (Ag/AgCl) was recorded using either the potentiometric instrumentation developed and described in Chapter 6, or a commercial potentiostat (CH Instruments, CHI1232). At the same time, the pH of the analyte solution was measured with a commercial pH meter (Crison GLP 21). All chemical response experiments were performed at room temperature (25°C) using chemicals of analytical reagent grade.

With above procedure the relationship between pH and electrode potential could be characterised. To determine the long-term stability of the sensors, the measurements were repeated during several weeks. Analogously, it was also determined the time required for the sensor to stabilise after a change in pH. Between measurements the sensors were stored in distilled H_2O, in dark and at room temperature.

7.3.4 Sensor Applications

The developed pH sensors were used to measure pH in solutions containing α-tricalcium phosphate cement of different maturity (see Chapter 4).

First, the evolution of pH during setting of α-TCP was measured with the pH sensors mounted directly inside the cement paste which was obtained upon mixing α-TCP with dH_2O (liquid to powder ratio = 0.65 ml/g). For that measurement (Figure 7.2a), a miniaturised Ag/AgCl electrode housed within a Teflon body was used as reference electrode (Flex-Ref, Dri-Ref^{TM} World Precision Instruments).

Second, the evolution of pH was then measured in 0.5 mL simulated body fluid (SBF), which was in direct contact with hydrolysing α-TCP (liquid to powder ration = 0.65 ml/g). For this measurement the sensors were mounted in the immediate interface between cement paste and SBF (Figure 7.2b-c), and potentiometric reading against a Ag/AgCl reference electrode was done during a period of four days, and at room temperature. The complete setup

[1] tris(hydroxymethyl)aminomethane buffer solution

was placed in a surrounding water bath to provide a humid atmosphere and avoid evaporation of the sample volume. The setup was sealed from below using a RTV silicone adhesive of implant grade (Applied Silicon, PN40064).

Finally, the pH of protein-containing (15%) McCoy cell culture medium (Sigma, M4892) in contact with mature/set α-TCP (i.e. CDHA) was measured at standard cell culture conditions (i.e. 37°C, 5% CO_2) during 24 hours, using the same setup as described above (Figure 7.2b-c). To obtain CDHA samples with integrated pH sensors, α-TCP was hydrolysed (L/P = 0.35 ml/g) and then set at 37°C during seven days in 0.9% NaCl with an electrode dummy placed inside the curing cement. When finally set, the dummy electrode was removed, and the obtained CDHA samples were rinsed and dried before fresh pH microelectrodes were introduced in the sample. The electrode body was first sterilised by immersion in 70% ethanol, and then after mounting and rinsing in dH_2O, also through UV irradiation. Before and after treatment, electrodes were subject to calibration in 0.1M TRIS as described in Section 7.3.3.

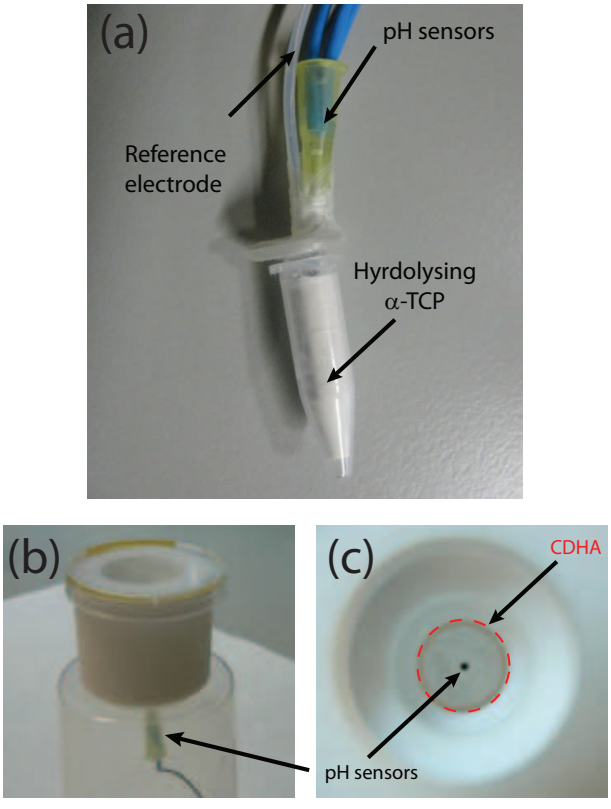

Figure 7.2: Setups for pH measurement of curing α-TCP (a), and of curing as well as cured α-TCP (=CDHA) at the material/liquid interface (b,c).

7.4 Results

7.4.1 Microelectrode Characterisation

Contaminants such as hydrocarbons may arise from the environment and adsorb non-specifically to Au surfaces (Amrein & Muller, 1999), making cleaning a necessary step prior to further chemical modifications. For that purpose, electrodes were electrochemically cleaned through repetitive potential cycling in H_2SO_4, so that contaminants were oxidised at potentials where the metal oxide layer forms or where water discharge commences (Zoski, 2007). The voltammograms did stabilise with increased number of repetitions (Figure 7.3a), indicating a clean Au electrode. The observed peaks correspond to (incipient) formation of oxide at 1.0-1.4 V vs. Ag/AgCl during the positive exploration, and reduction of oxygen (around 0.94 V vs. Ag/AgCl) during the negative exploration (Tian *et al.*, 2003; Vertova *et al.*, 2008).

The conductive properties of Au, and the ability of Fe^{2+}/Fe^{3+} ions to exchange electrons with the bare Au substrate, result in a characteristic current as the potential is varied, and which directly depends on the electrode area (Forster, 1994). As shown in Figure 7.3b, the CV response at slow scan rates for the oxidation of 10 mM potassium ferricyanide(III) in supporting electrolyte (0.5 M KCl) at the Au electrode reproduced a sigmoidal-shaped curve which is typical for microelectrodes (Forster, 1994).

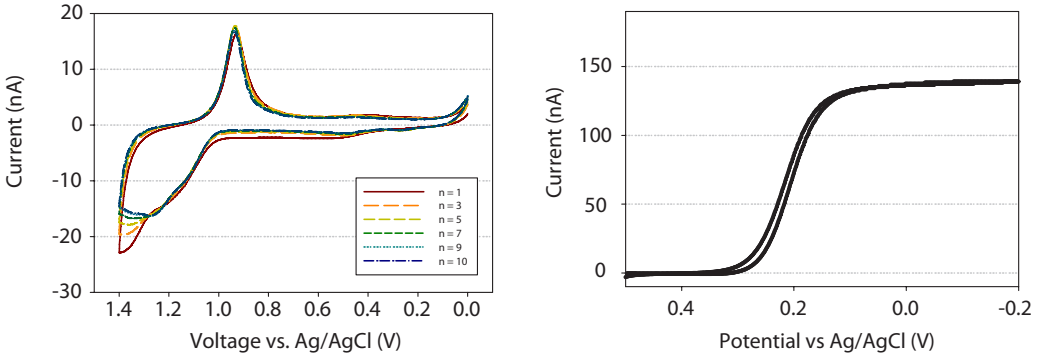

(a) 0.5 M H_2SO_4, scan rate 50 mV sec^{-1}.

(b) 10 mM $K_3Fe(CN)_6$, scan rate 5 mV sec^{-1}.

Figure 7.3: Characterisation of Au microelectrodes by cyclic voltammetry.

Given the observed steady-state current for the disk electrode ($i_{ss} = 139.3 \pm 25.6$ nA), it could be calculated the effictive electrode radius (r) from equation 7.7,

$$i_{ss} = 4nFDCr \tag{7.7}$$

where n is the number of electrons transferred (= 1), F is the Faraday's Constant (96487 C mol^{-1}), C is concentration (10 mM), and D the diffusion coefficient of $K_3Fe(CN)_6$. As the typical value of D for an aqueous solution is in the range 10^5 cm^2 s^{-1}, the average effective radii of the electrodes was calculated to $r = 36.1$ μm, indicating a well prepared microelectrode.

7.4.2 Iridium Oxide Deposition

The deposition of iridium dioxide films onto the clean Au microelectrodes was achieved amperometrically using a constant-potential method. During this process (Figure 7.4a), the oxalate ligand becomes oxidised and forms CO_2 leading to the deposition of a hydrated form of iridium oxide according to reaction (7.8):

$$[Ir(COO)_2(OH)_4]^{2-}(aq) + 2OH^- \rightarrow [IrO_2(OH)_2 \cdot 2H_2O](s) + 2CO_2 + 2e^- \qquad (7.8)$$

The cyclic voltammogram of IrO_2-modified microelectrode was recorded immediately after deposition (Figure 7.4b), and did show the characteristic reversible redox behaviour Ir(III)/Ir(IV) which have been previously reported in literature (e.g. by Marzouk *et al.* (1998); Juodkazyte *et al.* (2005); O'Hare *et al.* (2006); Bitziou *et al.* (2008)), indicating a proper formation of an iridium oxide layer. The deposition was also clearly apparent upon investigation with scanning electron microscope (Fig 7.5d).

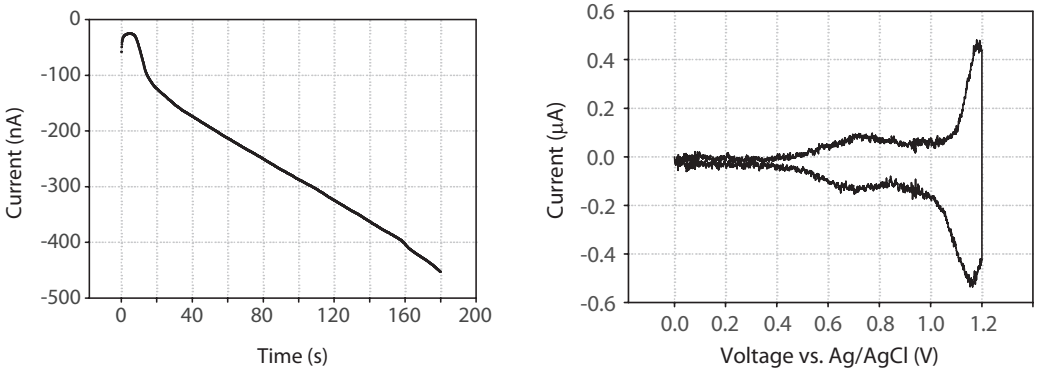

(a) Electrodeposition of IrO_2.

(b) CV after IrO_2-deposition.

Figure 7.4: IrO_2 deposition. (a) Anodic IrO_2-deposition on Au microelectrode at constant potential (0.65 V). (b) CV of the IrO_2-modified microelectrode in 0.5 H_2SO_4 vs Ag/AgCl reference electrode. Scan rate 50 mV second^{-1}.

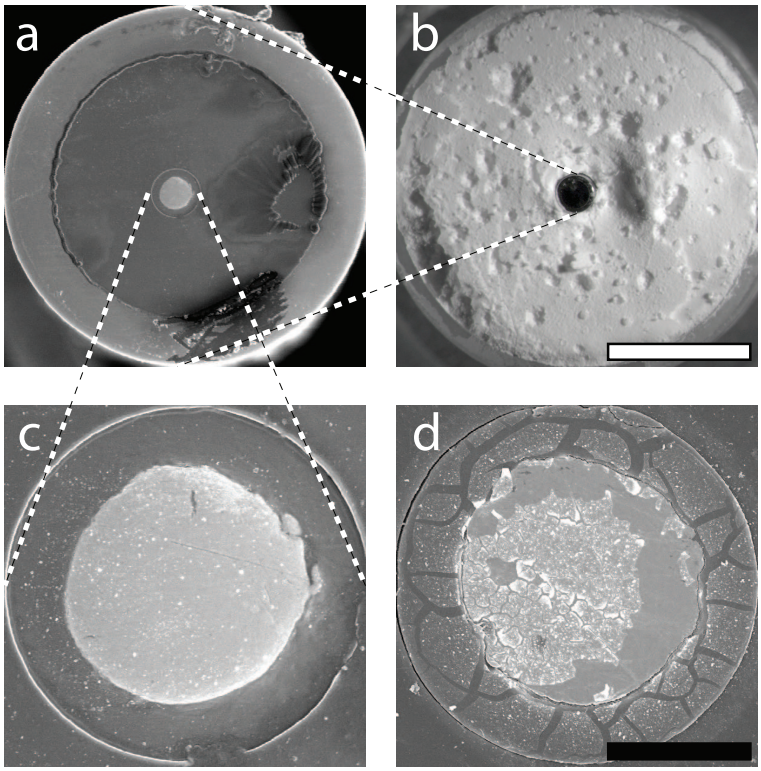

Figure 7.5: (a,c) SEM images of bare Au microelectrode; (b) Incorporation of the microelectrode in CDHA for pH measurements in the material interface; (d) SEM image of IrO_2 modified microelectrode. Scalebars: white = 3.6 mm, black = 50 μm.

7.4.3 pH Electrode Characterisation

After the electrodeposition procedure, the electrodes were left for at least two days to allow for hydration of the IrO_2 film, before they were subject to characterisation as pH electrodes. As shown in Figure 7.6a, while the pH of TRIS buffer was decreased by addition of HCl, the electrode potential against the reference electrode increased stepwisely. The time required for the sensor to acquire a stable potential upon changes in pH was approximately 10 seconds (Figure 7.6c).

From data as the one presented in Figure 7.6a, the calibration curve of pH microelectrodes could be obtained (Figure 7.6b), revealing a perfectly linear relationship between pH and electrode potential. Calibration from pH 3 to 10.5 resulted in a super-Nernstian response (-64.9 $\pm$ 2.4) mV per decade (n = 51, r^2 = 0.997) at T = 25°C. The sensitivity decreased gradually with time, but still after 24 days their behaviour was super-Nernstian (Figure 7.6d).

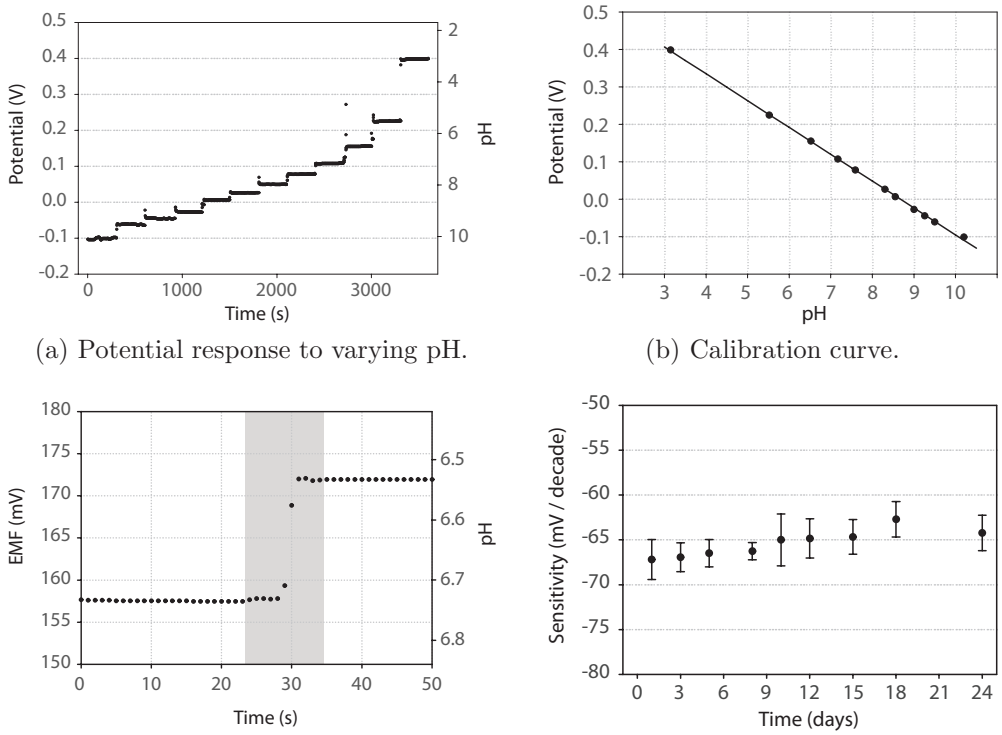

(a) Potential response to varying pH.

(b) Calibration curve.

(c) Time reponse.

(d) Stability.

Figure 7.6: Calibration of IrO_2 pH microelectrodes. (a) Typical open-circuit potential response of IrO_2 electrodes to varying pH. (b) Calibration curve. (c) Time response upon changing pH. (d) pH sensitivity over time.

7.4.4 Sensor Applications

The IrO_2 microelectrodes were applied to measure pH evolution of hydrolysing α-TCP (both inside and outside the cement paste), as well as of cured cement (CDHA) in protein-containing cell culture medium.

The mixing of α-TCP powder with water provoked the potential of the IrO_2 microelectrodes to rapidly decrease until reaching a minima around pH 10 after about 40 minutes (Figure 7.7). Thereafter, the potential increased linearly during the following 2 hours, and from then on increased non-linearly until the end of the experiment. During 24 hours, the material caused pH to change almost 2.5 units.

The same trend was observed when measuring the pH of simulated body fluid in contact with hydrolysing α-TCP (Figure 7.8). In that case, the pH sensors were incorporated in the interface between material and the aqueous phase. First, the pH of SBF increased, and reaching a maximum after about 13 hours, it began to decrease in a non-linear way, but did not reach its

steady-state value during the 92 hour-long measurement.

Finally it was investigated how set α-TCP (CDHA) influenced the pH of cell culture medium (Figure 7.9). Initially it was observed that in absence of any other component, culture medium by itself became more alkaline when incubated in standard *in vitro* conditions. However, in presence of CDHA, the pH of cell culture medium was decreased. After normalising (i.e., subtracting the alkaline medium effect), the acidification induced by CDHA was revealed to be a non-linear process which could be successfully modelled (R^2 = 0.995) using equation 7.9,

$$EMF = \frac{at}{1+bt} \tag{7.9}$$

where a = 3.38 mV h^{-1} and b = 2.36×10^{-2} h^{-1}. Equation 7.9 is analog to the second-order sorption model applied in Chapter 4.

After measurements, the sensors were calibrated once again to confirm their proper functioning (Figure 7.10).

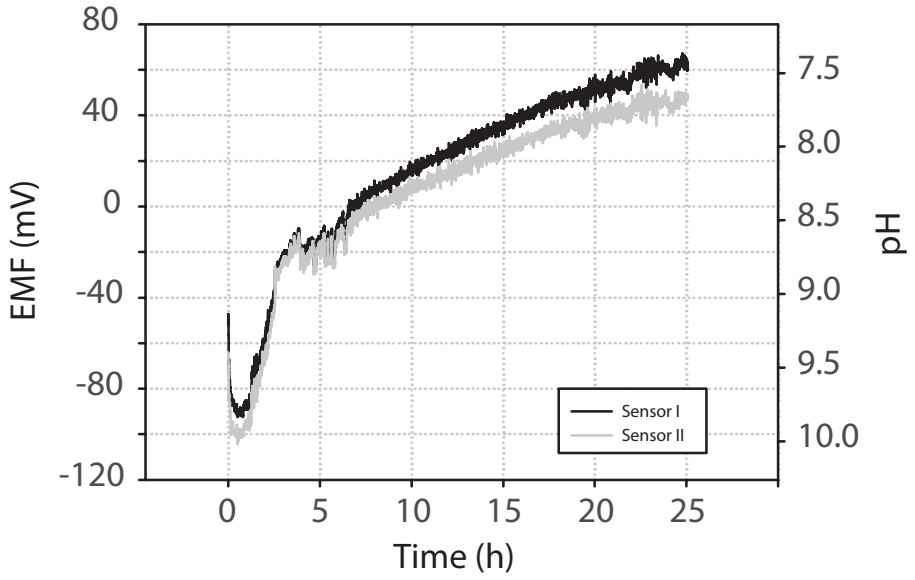

Figure 7.7: pH measurement performed with two independent IrO_2 microelectrodes placed inside curing α-TCP cement prepared with a liquid to powder ratio of 0.65 ml/g.

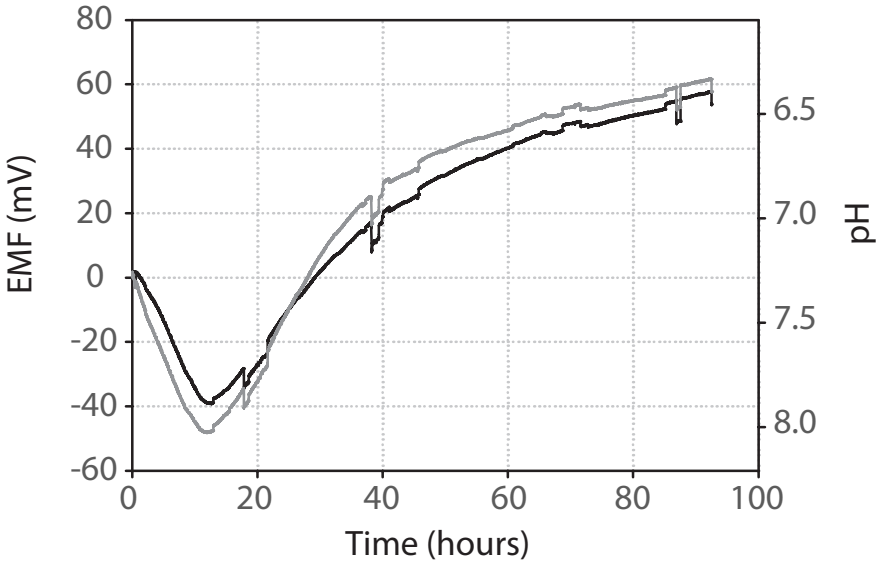

Figure 7.8: pH measurement performed with two independent IrO_2 microelectrodes placed at the interface between curing α-TCP (L/P = 0.65 ml/g) and simulated body fluid.

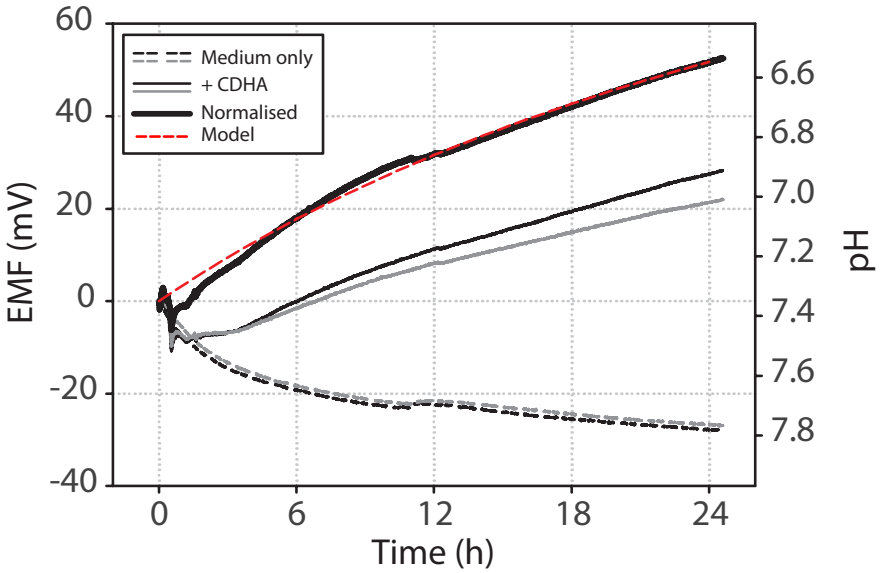

Figure 7.9: pH measurement performed with two independent IrO_2 microelectrodes placed at the interface between CDHA and McCoy cell culture medium with 15% FBS (solid thin lines). Measurements in absence of CDHA are indicated with dashed lines.

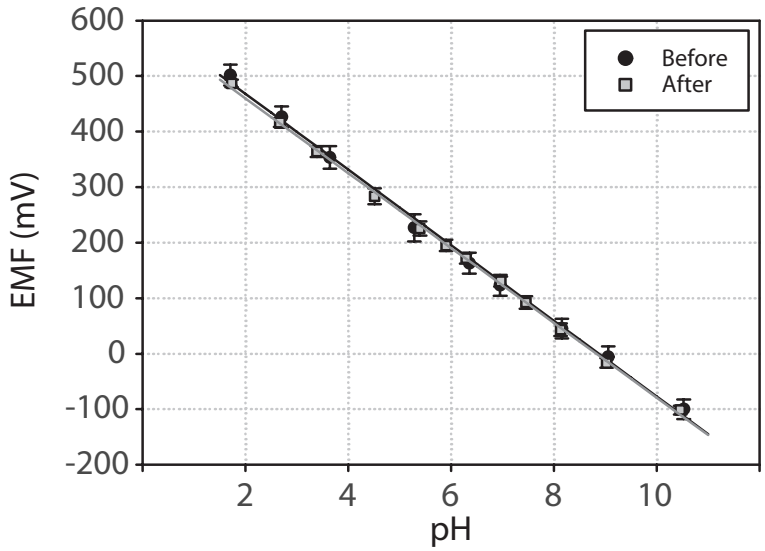

Figure 7.10: Calibration curve of IrO_2 microelectrodes before and after exposure to cell culture medium.

7.5 Discussion

Application of sensors in tissue engineering environments can be useful to determine the instantaneous activity of components held in the environment. Just like cellular metabolic activity tends to acidify the extracellular environment, certain scaffold materials may interact chemically with its environment, and induce ionic interchanges between the solid and aqueous phases. One such group of materials is the apatitic calcium phosphate cements, including α-TCP which undergoes hydrolysis reaction in contact with water. The hydrolysis reaction is accompanied by changes in the pH as ions are released and precipitated back onto the material (see Figure 4.3). To appropriately evaluate the effect of the chemical activity of such materials on tissue development, it is necessary to characterise its behaviour in biologically and volumetrically relevant environments. Therefore, sensors applied to such environments should be made small, preferably be applied in the solid/liquid interface, and obviously perform correctly in solutions of ionic strength and protein content similar to that human blood. In this chapter effort has been made to fulfill above requirements when evaluating the chemical influence of α-TCP on the pH of its aqueous environment.

Among the different approaches to produce pH and ion sensors, solid-state electrodes are especially interesting as they can be easily miniaturised

and produced in a wide variety of shapes, and so be adapted to different measurement environments. In this work, the desire was to incorporate sensors in specific microenvironments created around calcium phosphate cements, and this required collocation of sensors in the solid/liquid interface as well as directly inside the curing cement. For that purpose, the electrode body was constructed in a needle-like shape that could easily penetrate through the cement material. However, the active sensing electrodes, located at the tip of the needle, were made perfectly flat, and can be subject for further chemical modifications to develop sensors for a variety of analytes. In the proposed design, which was greatly inspired by the work of Bitziou *et al.* (2008), the electrode body is able to house several microelectrodes, and can in principle be made much smaller if desired.

The well-documented advantages of anodically grown iridium oxide films as pH sensor (Yamanaka, 1992; Bezbaruah & Zhang, 2002), including low interference from cations (Fog & Buck, 1984; Bezbaruah & Zhang, 2002) and fast response, as well as the fact that the production does not require any sophisticated instrumentation, made this method highly suitable for fabrication of pH microelectrodes. Among the advantages should also be emphasised the super-Nernstian behaviour of the anodically electrodeposited iridium oxide film electrodes, i.e. their sensitivity was greater than 59 mV decade^{-1} at 25°C. Such behaviour has been previously reported (e.g. Glab *et al.* (1989)), and it favours the sensor accuracy. Due to changes with time in the oxide hydration, the sensitivity gradually drops but the changes were slow compared to the time frames of the specific applications reported in this chapter.

After essential characterisation of the pH microelectrodes they were applied in bone tissue engineering environments that involved α-TCP of different maturity. This material, either by itself or in combination with other calcium phosphate cements, has been or is explored both as a scaffold material (Engel *et al.*, 2008) and as drug delivery vehicle e.g. for growth factors and antibiotics (Ginebra *et al.*, 2006). The most attractive feature of α-TCP is its capacity for self-setting at physiological conditions and which allows for using the material in an injectable form. The latter feature of α-TCP provides improved adaptation to the site of implant, but it also means that the material will undergo its chemical setting reactions with the environment of the local site of implant. Since the chemical composition of that environment is crucial, not only for correct development of the material but also for the biological response to the material, a careful investigation of the chemical reactivity of α-TCP is highly motivated. Preferably, such characeterisation should be made in real-time and in conditions as similar as possible to the *in vivo* environment. This chapter takes the first step towards such characterisation by providing pH measurements in biologically relevant volumes

and chemical composition. Despite that many biomaterials are biochemically reactive, the application of miniaturised sensors for real-time measurements of relevant biomaterial environments has until now been inexistent.

First, pH was measured during hydrolysis of α-TCP, which is given by the following reaction (7.10),

$$3(\alpha Ca_3(PO_4)_2) + H_2O \rightarrow 2Ca_9(HPO_4)(PO_4)_5OH \tag{7.10}$$

and which is known to be a dynamic process where the α-TCP particles progressively become surrounded by layers of CDHA (see Figure 4.3). Application of pH microelectrodes both inside and outside the curing cement demonstrated that pH varied greatly during the first 24 hours of hydrolysis, which according to Ginebra *et al.* (1999) is a period long enough to allow for about 80% of α-TCP to react. Both the interior and the exterior pH measurements of hydrolysing α-TCP indicated an initial release of OH^- ions, which was followed by a continuous acidification. The calibration of sensors before and after each measurement indicated proper sensor function. Moreover, the obtained data is in good agreement with measurements realised with commercial pH electrodes, but then using completely non-relevant liquid to powder ratio (typically L = 200 mL / g, see Ginebra (1996)). With the IrO_2 pH microelectrodes, the liquid to powder ratio could be decreased several orders of magnitude, and thus allow for a much more exact control of the pH environment provoked by hydrolysing α-TCP.

The significant pH changes of the reacting cement paste should be carefully considered when selecting biomolecule candidates for incorporation into the cement paste to enhance its biological properties. In a similar way, hydrolysing α-TCP also caused the pH of any surrounding liquid to change when the material was maintained in static conditions. That measurement provides an indication of what influence the cement paste will have on its environment when injected *in vivo*.

It was finally demonstrated that also after a week-long period of hardening, the material continued to provoke pH changes. As at this stage of material maturity, several *in vitro* studies with the material have been performed (e.g. Chapter 5 of this thesis, and Engel *et al.* (2008)), it was of special interest to measure pH evolution right in the interface between CDHA material and protein-containing cell culture medium, as this is the local environment where cell-material interaction is directly determined. As demonstrated, the possible effects of biofouling did not influence the IrO_2 microelectrode performance, and pH of the cell culture medium could be perfectly monitored

revealing acidification of the culture medium in presence of CDHA, in perfect agreement with previous presented data (see Chapter 4).

As a final remark on the work presented in this chapter, the proposed application of solid-state microelectrodes incorporated into biomaterials is meant to be an alternative mean to study interactions induced by components of the tissue engineering environment. The proposed setups allow for modifications both with respect to the analyte, as well as to size and number of sensors. If properly designed, it may even introduce the possibility to approach the interface between cells and material. In that sense, this study is an initial step to begin to explore the local microenvironments created around scaffold materials, and bring the traditionally biomaterial characteristion to a new and much more precise level.

7.6 Conclusions

In this chapter it has been explained the details of fabrication and characterisation of iridium oxide microelectrodes, with the aim to apply them as potentiometric sensors for real-time monitoring of pH in tissue engineering environments.

Even though the fabrication process is easy and does not require sophisticated instrumentation, the obtained pH electrodes are of very high quality. They are both fast-responding and demonstrated a super-Nernstian behaviour (-64.9 $\pm$ 2.4) mV/pH in a wide pH range (1.5-10.5). Moreover, they could be applied in complex ionic solutions such as simulated body fluid and protein-containing cell culture medium during prolonged times.

The small size and robustness of the pH electrodes further allowed for simultaneous measurements from more than one sensor in environments which traditionally are considered inaccessible. In particularly it has been demonstrated the usefulness of these sensor to measure pH in the interior of hydrolysing α-tri calcium phosphate, as well as its immediate interface with extracellular fluid. In both these cases the pH sensors clearly indicated how the material initially provoked a very alkaline environment, which with time became more and more acidic. As the absolute pH variation provoked by the material was detected to be of such magnitude that it may influence both its own and adjacent biological environment, the developed sensor setup provides key information for future tuning of the material properties towards its improved biological functionality.

Bibliography

Amrein, M. & Muller, D. (1999). *Nanobiology,* **4**, 229–256.

Bezbaruah, A. N. & Zhang, T. C. (2002). *Analytical Chemistry,* **74**, 5726–5733.

Bitziou, E., OHare, D., & Patel, B. A. (2008). *Analytical Chemistry,* **80** (22), 8733–8740.

Engel, E., del Valle, S., Aparicio, C., Altankov, G., Asin, L., Planell, J. A., & Ginebra, M. P. (2008). *Tissue Engineering,* **14**, 1341–1351.

Fog, A. & Buck, R. (1984). *Sensors and Actuators,* **5** (2), 137–146.

Forster, R. J. (1994). *Chemical Society Reviews,* **23**, 289–297.

Ges, I. A., Ivanov, B. L., Schaffer, D. K., Lima, E. A., Werdich, A. A., & Baudenbacher, F. J. (2005). *Biosensors and Bioelectronics,* **21**, 248–256.

Ginebra, M., Traykova, T., & Planell, J. (2006). *Journal of Controlled Release,* **113**, 102–110.

Ginebra, M. P. (1996). *Desarrollo y caracteririzacin de un cemento seo basado en fosfato triclcico-α para aplicaciones quirrgicas.* PhD thesis Universitat Politcnica de Catalunya.

Ginebra, M.-P., Fernandez, E., Driessens, F. C. M., & Planell, J. A. (1999). *Journal of the American Ceramic Society,* **82** (10), 2808–2812.

Glab, S., Hulanicki, A., Edwall, G., & Ingman, F. (1989). *Critical Review in Analytical Chemistry,* **21** (1), 29–47.

Hendrikse, J., Olthuis, W., & Bergveld, P. (1998). *Sensors and Actuators B,* **53**, 97–103.

Juodkazyte, J., Sebeka, B., Valsiunas, I., & Juodkazis, K. (2005). *Electroanalysis,* **17**, 947–952.

Kurzweil, P. (2009). *Sensors,* **9**, 4955–4985.

Li, J., Du, Y., & Fang, C. (2007). *Electroanalysis,* **19** (5), 608–611.

Marzouk, S. A., Ufer, S., Buck, R. P., Johnson, T. A., Dunlap, L. A., & Cascio, W. E. (1998). *Analytical Chemistry,* **70** (23), 5054–5061.

Ndobo-Epoy, J.-P., Lesniewska, E., & Guicquero, J.-P. (2007). *Analytical Chemistry,* **79**, 7560–7564.

O'Hare, D., Parker, K. H., & Winlove, C. P. (2006). *Medical Engineering & Physics,* **28**, 982–988.

Smiechowski, M. & Lvovich, V. (2003). *Sensors and Actuators B - Chemical,* **96** (1-2), 261–267.

Stulik, K., Amatore, C., Holub, K., Marecek, V., & Kutner, W. (2000). *Pure and Applied Chemistry,* **72** (8), 1483–1492.

Tian, M., Pell, W. G., & Conway, B. E. (2003). *Electrochimica Acta,* **48**, 2675–2689.

Vertova, A., Borgese, L., Cappelletti, G., Locatelli, C., Minguzzi, A., Pezzoni, C., & Rondinini, S. (2008). *Journal of Applied Electrochemistry,* **38**, 973–978.

Wang, M., Yao, S., & Madou, M. (2002). *Sensors and Actuators B,* **81**, 313–315.

Wipf, D. O., Ge, F., Spaine, T. W., & Baur, J. E. (2000). *Analytical Chemistry,* **72**, 4921–4927.

Yamanaka, K. (1989). *Japanese Journal of Applied Physics,* **28** (4), 632–637.

Yamanaka, K. (1992). *Japanese Journal of Applied Physics,* **30** (6), 1285–1289.

Zoski, C. G., ed (2007). *Handbook of electrochemistry.* Unknown: Elsevier Science.

Chapter 8

Conclusions and Future Work

8.1 Conclusions

Below are summarised the main conclusions from each chapter of experimental character (i.e. Chapters 3-7).

8.1.1 The Cells (Chapter 3)

1. Standard cell culture media for osteoblast-like *in vitro* cultures, specifically Dulbecco's Modified Eagle Medium (DMEM) and McCoy's 5A Modified medium (McCoy), were of different chemical composition. As a consequence, the concentrations of major physiological ions differed significantly between both media. For example, concentration of calcium was less than half in McCoy medium compared to DMEM medium and concentration of total phosphorus (P_i) was more than four times higher in McCoy medium than in DMEM medium.

2. The ionic concentration of culture medium typically changed upon addition of essential cell culture supplements. In both DMEM and McCoy media [K^+] increased while [P_i] decreased upon addition of serum proteins (FBS). Addition of FBS also increased [Ca^{2+}] and [Na^+] in McCoy medium (but not in DMEM). Addition of osteogenic factors (i.e. ascorbic acid, dexamethasone, and β-glycerophosphate) to culture medium increased [Na^+] and [P_i], but decreased [Ca^{2+}] and [K^+] in all media. The pH of culture medium increased upon addition of osteogenic factors.

3. Three different osteoblast-like cell models (MG63, SAOS-2, and rMSC) were used to investigate cellular influence on the ionic extracellular con-

centrations. Cell-induced changes on the extracellular ionic concentrations were detected for calcium and phosphorus. Also, pH of culture medium was influenced by cellular activity. Presence of cells had no detectable influence on extracellular $[Na^+]$ or $[K^+]$.

a) SAOS-2 cells maintained in normal McCoy medium had no effect on the ionic extracellular environment with respect to investigated ions. However, using osteogenic medium then extracellular $[Ca^{2+}]$ decreased significantly during a time period of $\approx$ 48 hours in presence of mature SAOS-2 cells (around 60%). At the same time, $[P_i]$ in osteogenic McCoy medium was significantly increased in presence of SAOS-2 cells.

b) Beyond five days in culture, rMSCs maintained in aDMEM were observed to slightly decrease $[Ca^{2+}]$ during a time period of $\approx$ 48 hours (3-7%). The decrease in $[Ca^{2+}]$ was greatly enhanced using osteogenic aDMEM (up to about 60%). As with SAOS-2 cells, rMSCs significantly increased $[P_i]$ of osteogenic medium.

c) Mature MG63 cells maintained in DMEM medium were observed to decreased $[Ca^{2+}]$ slightly during the time period of $\approx$ 48 hours (7-9%). In contrast to SAOS-2 and rMSCs, no or little influence on $[Ca^{2+}]$ and $[P_i]$ was observed when MG63 cells were maintained with osteogenic medium.

4. Cell-induced influence on the extracellular concentrations of calcium and total inorganic phosphorus was associated with deposition of calcium in the extracellular matrix.

5. SAOS-2 cells induced deposition of calcium in their extracellular matrix using either osteogenic McCoy or osteogenic DMEM. In contrast, MG63 cells did not induce calcium deposition in its extracellular matrix using any of the two media.

6. SAOS-2 and rMSCs expressed significantly higher alkaline phosphatase activity than MG63 cells. Thus, the increase of extracellular P_i in osteogenic medium can potentially be used as an indicator of cellular alkaline phosphatase activity.

7. The decrease of extracellular ionised calcium could serve as an indirect indication of the combined presence of a collagenous extracellular matrix and alkaline phosphatase active cells. In that way, decrease of extracellular calcium can potentially serve as an indicator of a first step towards mineralisation of the osteoid.

8.1.2 The Scaffold Material (Chapter 4)

1. Calcium-deficient hydroxyapatite (CDHA) induced changes in the chemical composition of both DMEM and McCoy culture media. The size and nature of the changes were dependent on initial chemical composition of the aqueous phase as well accumulated time of exposure to medium.

2. During the initial 48 hours of contact, CDHA induced sorption of sodium, potassium, and calcium from all investigated media (i.e. normal and osteogenic DMEM and McCoy, respectively). CDHA also caused acidification of all media. Moreover, sorption of total inorganic phosphorus was observed using normal and osteogenic McCoy media and osteogenic DMEM medium, but not using normal DMEM medium.

3. Most sorption processes were successfully described using pseudo-first or pseudo-second-order sorption models. Exceptions were sorption of sodium (all media), and sorption of phosphorus (osteogenic media). In the latter case, serum-induced hydrolysis of β-glycerophosphate increased the concentration of P_i linearly during the contact period. As a consequence, sorption of P_i onto CDHA from osteogenic media was better described with a linear model.

4. Upon repeated exposure to fresh culture medium during 21 days, material-induced acidification of culture medium gradually decreased with time in all media formulation.

5. Sorption of sodium and potassium gradually decreased with time during long-time experiments and was completely undetectable towards the end of the experiment. That observation proposes that CDHA has limited space for incorporation of those ions into the crystal structure.

6. Sorption of calcium onto CDHA from all culture media persisted throughout the full length of the experiment. It follows that the material must have possessed a high number of vacant sites for calcium.

7. While sorption of P_i decreased with time using McCoy medium, CDHA was observed to release P_i when repeatedly exposed to fresh normal and serum-free DMEM media. The release mechanism involved both sorption and desportion of P_i, but with a net desorption effect during 48 hours. FTIR analyses indicated that phosphate/carbonate replacement processes had occured in all samples. Therefore, such ion-exchange must be taken into account when explaining CDHA reactivity with respect to phosphorus in both DMEM and McCoy media.

8.1.3 Cells and Scaffold Combined (Chapter 5)

1. It was observed that CDHA decreased the extracellular concentration of calcium in osteogenic McCoy medium in a reproducible manner during the three-week long experiments. Moreover, the decrease could be perfectly described by a second-order sorption model. In contrast, the influence of CDHA on extracellular total phosphorus (i.e. sorption) and pH of culture medium (i.e. acidification) was not constant over time, but was observed to gradually decrease for each time the culture medium was exchanged.

2. SAOS-2 cells maintained in osteogenic medium influenced the extracellular concentration of total inorganic phosphorus by hydrolysis of β-glycerophosphate through its alkaline phosphatase (ALP) activity. In absence of CDHA, cell-induced hydrolysis of β-GP was highly efficient throughout the full length of experiment as $[P_i]$ always increased rapidly in presence of cells.

3. Moreover, SAOS-2 cells grown in absence of CDHA caused calcium in culture medium to be gradually deposited into the extracellular matrix already at an early stage (nine days in culture).

4. Using semi-permeable culture inserts, SAOS-2 cells could be directly exposed to the dynamic changes of the ionic extracellular environment induced by CDHA. Therefore, when using osteogenic medium it was created a situation where CDHA and cells would compete for the same calcium and where CDHA would sorb P_i which had been liberated by cellular activity.

5. In normal McCoy culture medium that contained cells separated from CDHA, the concentrations of calcium and total inorganic phosphorus were observed to be mainly determined by CDHA. In contrast, when using osteogenic McCoy culture medium the concentration of total inorganic phosphorus was clearly subject to both ion reactivity of CDHA and cellular ALP activity. It was however not possible to determine from the ion measurements if the observed decrease in $[Ca^{2+}]$ of osteogenic medium was due mainly to material-induced sorption or cell-induced calcium-deposition.

6. The dynamic ionic environment induced by CDHA did not influence greatly cellular proliferation using normal McCoy medium. Yet, by the end of the experiment (i.e. after three weeks), higher cell proliferation was observed for cells grown in presence than in absence of CDHA. It

was also observed that osteogenic medium slowed down cellular proliferation earlier in absence than in presence of CDHA. Both observations could be due to that cells grown in presence of CDHA were delayed in their cellular differentiation compared to cells grown in absence of CDHA.

7. In absence of CDHA, cell-induced deposition of calcium in the extracellular matrix was observed already after nine days in culture using osteogenic medium. In presence of CDHA, such calcium deposition was severely delayed and only to be observed at the very end of the culture period (i.e. day 21).
   The reason(s) for the suppressed and delayed cell-induced calcium deposition in the extracellular matrix in presence of CDHA was tested:

   (a) The rate of cell-induced deposition of calcium in the extracellular matrix in absence of CDHA was comparable to the sorption rate of calcium induced by CDHA when cells were highly mature. Thus, when combined in the same culture environment, mature cells and CDHA could in prinicple compete for the same calcium under fair conditions.

   (b) When growing SAOS-2 cells during five days in presence of CDHA, and thereafter during another four days in absence of CDHA, cell-induced calcium deposition was perfectly comparable to calcium deposition induced by cells grown in absence of CDHA throughout the full period of nine days. That observation indirectly indicated that cells initially grown in presence of CDHA resided in a well-developed extracellular matrix.

   (c) Cellular ALP activity was reduced only at day 3 and day 9 compared to cells grown in absence of CDHA if using normal medium.

   (d) Osteogenic medium in general increased cellular ALP activity. Maximum ALP activity was very similar both in presence and absence of CDHA, but it occurred at different time points. In presence of CDHA, maximum ALP activity was delayed until day 15. However, even at that time point still insignificant calcium deposition was observed in presence of CDHA. Therefore, absent calcium deposition in the extracellular matrix ought not to be entirely ascribed to delayed cellular ALP activity.

   (e) The ionic extracellular environment determined by CDHA must have played an important role in the delayed cell-induced calcium

deposition. Since material-induced sorption of calcium was constant throughout the full length of the experiment, it is tempting to speculate that the main suppresser for cell-induced calcium deposition was the extracellular concentration of P_i which in contrast to calcium gradually became less affected by CDHA over time.

8.1.4 Ion Sensors for Online Monitoring (Chapter 6)

1. An instrumentation for multi-channel potentiometric measurements was fabricated and successfully tested and used for various types of ion electrodes.

2. Miniaturised Ag/AgCl electrodes were successfully produced in house from electro-oxidation of Ag wires. The Ag/AgCl electrodes (in shape of both wire and disk electrodes) responded to chloride activity according to the Nernst equation and they maintained their sensitivity during several weeks. The electrode potential demonstrated insignificant drift at constant concentration and temperature. The fabricated Ag/AgCl electrodes held promise to be useful both as internal reference electrodes for potentiometric ion-selective electrodes as well as for direct measurements of chloride activity.

3. Ag/AgCl disk electrodes were used to measure chloride activity in real-time at the direct solid/aqueous interface between hydrolysing α-TCP and Ringer's solution. The electrode signal revealed a fast, non-linear sorption of chloride ions onto the material. The sorption could be perfectly described by second-order sorption models.

4. Calcium-selective electrodes were elaborated from a traditional calcium-selective polymeric membrane and a Ag/AgCl wire electrode which was housed in an internal electrolyte of constant concentration. That configuration allowed for fast and cheap fabrication of numerous Ca^{2+}-electrodes of small dimensions, suitable for incorporation in tissue engineering bioreactors or similar cell culture environments. The same design can be used to elaborate electrodes for other ions than calcium by only changing the polymeric membrane and the internal electrolyte solution.

5. The calcium-selective electrodes responded to changes in calcium concentration within reasonable time frames (31.4 ± 4.9 seconds) and according to the Nernst equation (30.3 ± 2.4 mV decade^{-1}). The sensitivity was preserved for at least four weeks when used with simple

salt solutions. The electrodes further demonstrated superior selectivity towards calcium ions compared to other major extracellular cations.

6. Characterisation of calcium-selective electrodes in more complex solutions revealed that the fabricated electrodes withstood well both UV irradiation (for sterilisation purposes) and prolonged exposure of protein-containing culture medium (up to 96 hours). The intrinsic drift of potential in protein-containing culture medium was small (0.095 mV h^{-1}), and could be well described by a linear function.

7. Introduction of calcium-selective electrodes into osteoblast-like cell cultures did not influence the cellular proliferation.

8. The calcium-selective electrodes were used to measure sorption of calcium onto CDHA in real-time during 24 hours and in protein-containing culture medium at standard *in vitro* conditions. The obtained data fitted the predicted sorption behaviour, and initial and final potential readings were in agreement with reference measurements.

9. Regarding cell-induced calcium deposition in osteoblast-like cultures it was first observed that calcium deposition occured in SAOS-2 cultures provided either low or high concentration of β-glycerophosphate (3 or 10 mM, respectively). In both cases, the calcium deposition was monitored in real-time, indicating a clear cellular influence on extracellular calcium during the measurement.

8.1.5 Sensors for Local Measurements (Chapter 7)

1. Solid-state Au microelectrodes were fabricated in house, and were made sensitive to pH using well-known protocols for electrodeposition of iridium oxide onto the metal electrode surfaces. The IrO_2-modified electrodes were confirmed to have a super-Nernstian response (-64.9 $\pm$ 2.4) mV $decade^{-1}$ at room temperature, and it changed little over several weeks if stored in salt buffer solution.

2. IrO_2 pH microelectrodes were located inside curing α-TCP cement that was prepared with a clinically relevant liquid-to-powder ratio (0.65 mL/g). Continuous potentiometric readings during 24 hours revealed a strong alkalinisation of the cement paste during the first couple of hours from mixture, reaching a minimum pH around 10 units. Thereafter the mix acidified until the end of the experiment but without reaching steady-state. A similar pH evolution was observed when pH microelectrodes were located at the immediate cement/liquid interface.

3. Finally, IrO_2 pH microelectrodes were located at the immediate solid/liquid interface of cured α-TCP (i.e. CDHA) and protein-containing cell culture medium. Online measurements during 24 hours revealed non-linear acidification of culture medium due to presence of CDHA.

8.2 Perspectives

As demonstrated, the ionic concentrations of mainly calcium and phosphorus in osteogenic culture medium were significantly influenced by presence of cells that expressed high alkaline phosphatase activity. Real-time (or strategic discrete) measurements of the ionic extracellular environment could therefore to some extent be used to estimate bone tissue development without affecting the sample. Such measurements would be highly beneficial during large-scale production of mineralised bone, or during elaboration of new protocols related to bone mineralisation events.

The different behaviour of SAOS-2, rMSC, and MG63 cells with respect to both ALP activity and calcium deposition highlights the general importance of choosing an appropriate cell model when studying cellular response mechanisms to a certain biomaterial *in vitro*. And it becomes even more important if the biomaterial is biochemically active with respect to calcium and phosphorus, as was the case with for example CDHA. The situation is further complicated by the fact that ion reactivity of CDHA was dependent on both the chemical composition of the aqueous phase and accumulated time of exposure to fresh culture medium. Therefore, meaningful extrapolation of cellular response mechanisms to calcium phosphate compounds obtained from studies performed *in vitro* will minimally require a perfect understanding of all components of the TE envrionment: i.e. cells, scaffold material, and culture medium. The application of ion sensors as enabling tools in TE have in Chapters 3 and 4 been clearly demonstrated to possess a key role in trying to achieve such knowledge.

Although difficult to interpret and extrapolate, attempts to learn something concrete about cellular response to CDHA from *in vitro* studies are far from useless. One such attempt was presented in Chapter 5 of this thesis. It was revealed that the capacity of cells to reinforce the extracellular matrix with calcium phosphate was severly decreased in presence of CDHA. Yet, as the material's sorption of phosphorus decreased with time, conditions for calcium deposition were slowly created, and by the end of the three-week long experiment significant amounts of calcium was detected in the extracellular matrix of cells cultured in presence of CDHA. That observation proposes that it is phosphorus rather than calcium that initially prevent osteoblastic

mineralisation to occur in presence of CDHA. As the conditions of the performed experiments were created as a 'worst-case' scenario by using the culture medium subject to highest CDHA reactivity with respect to phosphorus, different cellular response may be obtained using a different culture medium (e.g DMEM which releases P_i to its environment and therefore should promote calcium deposition rather than prevent). Still, the determining role of phosphorus over calcium should likely be independent of the medium used.

Given that ionic interactions provoked by cells and/or biomaterials (like CDHA, but also most other calcium phosphate compounds) at instances can be indirectly indicative of the tissue development process or the conditions for it, it was desired to develop instruments that allowed for real-time monitoring of ions in standard *in vitro* conditions. For that purpose it was fabricated easy-to-make, cheap, miniaturised ion-selective electrodes, and as a proof-of-concept these electrodes were successfully applied to measure calcium activity in global environments of small-volume containing mineralising osteoblasts and CDHA, respectively. Further miniaturisation of sensors (here as all-solid-state pH microelectrodes) makes it possible to approach traditionally inaccessible TE environments, such as the cell-biomaterial interface. The benefits of the developed system include being able to work with biologically and volumetrically relevant environments, as well as simultaneously obtain data from different ions. Such measurements will prove extremely useful for improved characterisation of ion reactive biomaterials, which in the end also will favour correct extrapolation of its *in vivo* performance.

8.3 Future Work

Looking back at the presented work, there are naturally several aspects of it that could have been done or approached differently, as well as there are many ways to continue developing the discussed topics.

One major issue in bone tissue engineering is to produce high quality mineralised bone, but as discussed in Section 3.5.4, the protocols used to induce such bone formation *in vitro* are highly debated. Although care was taken to include different osteoblast-like cell models and work with to low concentration of β-glycerophosphate (down to 3 mM), an additional cell model which induce characteristic nodule formation would have been highly beneficial in order to compare such mineralisation both quantitatively and qualitatively with the massive calcium deposition provoked by SAOS-2 and rMSC cells. One such cell model is the MC3T3-E1 line derived from mouse (Balint *et al.*, 2001).

The characterisation of CDHA ion reactivity presented in Chapter 4 was initiated with the objective to determine the biochemical capacity of CDHA to influence cellular behaviour. Therefore, all ionic interactions were monitored in complex protein-containing solutions. Obviously, the ionic interactions would be better characterised if working with simpler ionic solutions, as well as with more precisely specified surface area. Therefore, sorption studies with ion reactive biomaterials are suggested to be complemented with single ionic solutions of varying concentrations in order to establish sorption isotherms of each ion, and from which can be determined the maximal sorption capacity of the material. It is also suggested that the characterisation includes sorption of carbonate. Moreover, as long-term experiments revealed that sorption is a function of material maturity, it would be informative to perform short-term sorption studies with material of different maturity to more carefully determine how ageing of the material influences the ionic interactions with the aqueous surrounding. The material's capacity to respond differently to small changes in the ionic composition of its aqueous surrounding further suggests that future characterisation of CDHA (or similar materials) should be made in biological relevant solutions (e.g. blood or serum) and be sampled from a big pool.

With respect to the developed ion sensors, there are many things to improve and also to further characterise in order to classify them as true enabling tools for certain tissue engineering processes. The intention of this work was only to establish a general platform for potentiometric measurements and to produce a few proof-of-concept measurements. From there on, future modifications of the system are numerous. To begin with, sensors selective to other ions than calcium could be easily achieved only by changing the composition of the polymeric membrane according to well-established protocols in literature. One tempting modification is the development of phosphate-selective sensors for simultaneous detection of Ca^{2+} and P_i in osteoblast cultures and other TE environments that hold chemically active biomaterials such as CDHA. Although not as common as cation-membranes (no commercial alternatives exist), phosphate-selective membranes are indeed possible to develop if using an appropriate ionophore (Ganjali *et al.*, 2006; Kivlehan *et al.*, 2007).

Any ion-selective membrane developed for application in standard *in vitro* environments should withstand the harsh conditions (mainly protein fouling and ionic interference) that it inevitably will be exposed to. In the scope of this work, the calcium-sensor withstood well such conditions during periods at least up to 48 hours. Since longer incubation times possibly will have deteriorating effects on the sensor properties, it could be necessary to evaluate

different anti-fouling strategies (Gavalas *et al.*, 2006). For example, physically protective coatings or incorporation of poly(ethylene glycol), PEG, into the polymeric membrane have both shown very promising results and are worth exploring (Trouillon *et al.*, 2009; Radomska *et al.*, 2008).

In addition to the electrochemical properties of the sensor, also its shape can be greatly modified. In this work was used the conventional design of ion-selective electrodes with an internal electrolyte and reference electrode. Although the size of such sensor design can be further reduced, an all-solid-state design similar to the Ag/AgCl disk electrode or the pH microelectrode would allow for much greater miniaturisation. However, extra care then has to be taken that the polymeric membrane attaches well to the electrode surface. This can be achieved through coating of the electrode with a thin film of conducting polypyrrole that promotes adhesion of the polymeric ion-selective membrane and establishes a well defined electrode interface (Zine *et al.*, 2006). Reducing the size of the indicator electrode is however useless if not also the reference electrode can be miniaturised. Different approaches based on Ag/AgX reference electrodes embedded in hydrogels to reduce its sensitivity to chloride ions and pH have been reported (Ciobanu *et al.*, 2002, 2004), and may be interesting for application in small environments.

Miniaturised sensors that can perform measurements in small tissue engineering environments can provide a different perspective on how cells and materials integrate with each other, and how local microenvironments may arise at the cell-material interface. One such example is the growth of osteoblast cells directly onto CDHA. As seen in Figure 8.3a, presence of MG63 cells onto CDHA decreases the material-induced uptake of calcium with time. This indicates that those cells and their extracellular matrix act as a partly isolating biofilm to produce a local microenvironment at the material interface (recall Figure 2.4). The same isolating effect could not be observed with SAOS-2 cells which created a more heterogenous biofilm onto the surface of CDHA than MG63 cells (Figure 8.1). Application of sensors in the material interface can therefore be useful to learn more about the local chemical environments created around these biofilms in which cells reside. Chapter 7 includes the initial efforts to develop a system for pH sensing in similar microenvironments, and future work with that system could include the separation of the biofilm from the material through the use of cell culture inserts (Figure 8.2a). The insert can then be perfectly incorporated with the culture chamber used in Chapter 7, creating a minimal space between material and biofilm, in which pH measurements (or other ions if the microelectrode is further modified) can be realised (Figure 8.2b).

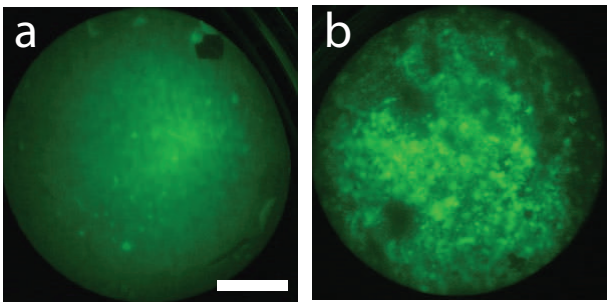

Figure 8.1: MG63 (a) and SAOS-2 (b) cells grown directly onto CDHA for 15 days, and then stained with fluorescein diacetate. Scalebar 35 mm.

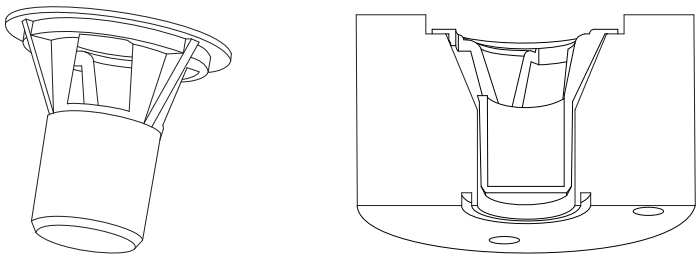

(a) Cell culture insert.

(b) Cross-section of chamber.

Figure 8.2: Suggested setup for measurements in local microenvironments.

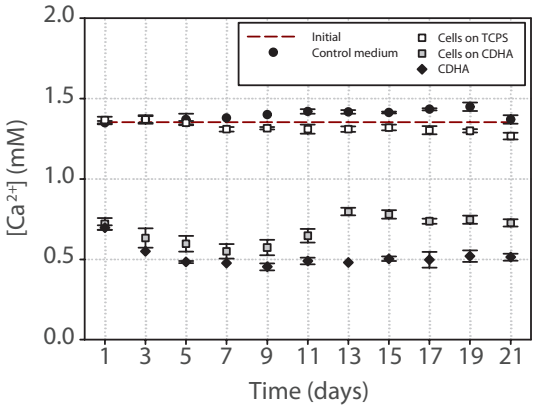

(a) MG63 cells

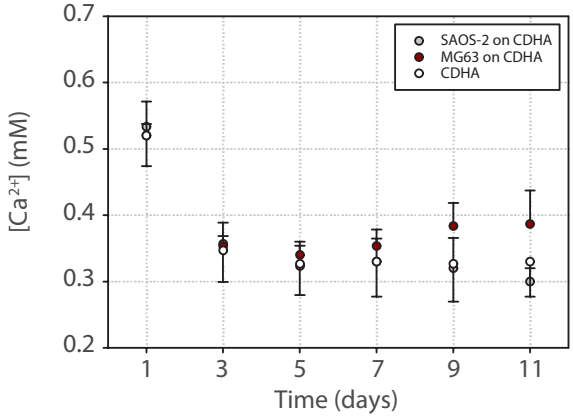

(b) MG63 and SAOS-2 cells.

Figure 8.3: Calcium concentration of DMEM medium in presence of CDHA onto which MG63 (a,b) and SAOS-2 (b) cells were grown.

Bibliography

Balint, E., Szabo, P., Marshall, F., & Sprague, S. (2001). *Bone,* **28** (1), 21–28.

Ciobanu, M., Wilburn, J. P., Buss, N. I., Ditavong, P., & Lowy, D. A. (2002). *Electroanalysis,* **14** (14), 989–997.

Ciobanu, M., Wilburn, J. P., & Lowy, D. A. (2004). *Electroanalysis,* **16** (16), 1351–1358.

Ganjali, M. R., Norouzi, P., Hatambeygi, N., & Salavati-Niasari, M. (2006). *Journal of the Brazilian Chemical Society,* **17** (5), 859–865.

Gavalas, V. G., Berrocal, M. J., & Bachas, L. G. (2006). *Analytical and Bioanalytical Chemistry,* **384**, 65–72.

Kivlehan, F., Mace, W. J., Moynihan, H. A., & Arrigan, D. W. (2007). *Analytica Chimica Acta,* **585**, 154–160.

Radomska, A., Singhal, S., Ye, H., Lim, M., Mantalaris, A., Yue, X., Drakakis, E. M., Toumazou, C., & Cass, A. E. (2008). *Biosensors and Bioelectronics,* **24**, 435–441.

Trouillon, R., Combs, Z., Patel, B. A., & OHare, D. (2009). *Electrochemistry Communications,* **11**, 1409–1413.

Zine, N., Bausells, J., Vocanson, F., Lamartine, R., Asfar, Z., Teixidor, F., Crespo, E., de Oliveira, I. M., & ad A. Errachid, J. S. (2006). *Electrochimica Acta,* **51**, 5075–5079.